

# FINAL REPORT

Characterizing and Quantifying Emissions and Transport of  
Fugitive Dust Emissions Due to Department of Defense Activities

SERDP Project RC-1729

SEPTEMBER 2015

John Gillies  
Vic Etyemezian  
Dongzi Zhu  
George Nikolich  
Johann Engelbrecht  
**Desert Research Institute**

William Shaw  
Larry Berg  
Elaine Chapman  
Samuel Clopton  
Mikhail. Pekour  
James Rishell  
Frederick Rutz  
**Pacific Northwest National Laboratory**

*Distribution Statement A*

*This document has been cleared for public release*



This report was prepared under contract to the Department of Defense Strategic Environmental Research and Development Program (SERDP). The publication of this report does not indicate endorsement by the Department of Defense, nor should the contents be construed as reflecting the official policy or position of the Department of Defense. Reference herein to any specific commercial product, process, or service by trade name, trademark, manufacturer, or otherwise, does not necessarily constitute or imply its endorsement, recommendation, or favoring by the Department of Defense.



## **Table of Contents**

<b>Abstract</b>	<b>1</b>
<b>1 Objectives</b>	<b>3</b>
<b>2 Background</b>	<b>6</b>
<b>3 Materials and Methods</b>	<b>12</b>
3.1 Vehicle characteristics that influence dust emissions	12
3.2 Transfer Standards: TRAKER™ and PI-SWERL®	14
3.2.1 TRAKER™	14
3.2.2 PI-SWERL®	16
3.3 Moisture and suppressant effects on road dust emissions	19
3.4 Attenuation of emissions by near-field deposition processes	21
3.4.1 Instrument set up, inter-comparison and measurement uncertainty	21
3.4.2 Sampling array at the different sites	22
3.4.3 Horizontal gradient method to infer deposition velocity	24
3.5 DUSTRAN	27
3.5.1 Conversion to Open-Source GIS	27
3.5.2 Incorporation of AERMOD into DUSTRAN	27
3.5.3 Incorporation of project-developed deposition velocities	28
<b>4 Results and Discussion</b>	<b>29</b>
4.1 Vehicle characteristics that influence dust emissions	29
4.2 Transfer standards: TRAKER™ and PI-SWERL®	32
4.2.1 TRAKER™ Development	32
4.2.2 PI-SWERL® Development	35
4.3 Spatial variability of road dust emission potential	38
4.3.1 Road dust emission potential Dugway Proving Ground, UT	38
4.3.2 Road dust emission potential Ft. Riley, KS	44
4.4 Moisture and Suppressant effects on road dust emissions	47
4.4.1 Moisture effects on road dust emissions at Ft. Riley and the Dugway Proving Ground	47
4.4.2 Long-term use of Magnesium Chloride on the Mannix Road, Ft. Irwin, CA	53
4.4.3 Total PM <sub>10</sub> emissions from Mannix Road based on vehicle travel inventory data	55

4.4.4	Potential Contributions of PM <sub>10</sub> from Military vehicles travelling the Mannix Road	58
4.5	Attenuation of emissions by near-field deposition processes	60
4.5.1	PM <sub>10</sub> attenuation downwind of the source	60
4.5.2	Size specific PM deposition velocities	62
4.5.3	Changes in particle size distribution with downwind distance	64
4.5.4	PM number changes in the vertical and the mass median diameter	66
4.6	DUSTRAN	68
4.6.1	AERMOD Modeling System	68
	4.6.1.1 AERMET	70
	4.6.1.2 Wind Speed/Direction	71
	4.6.1.3 Temperature	71
	4.6.1.4 Pressure	72
4.6.2	AERMAP	72
4.6.3	AERMOD	72
	4.6.3.1 Source Emissions: AERMOD	73
	4.6.3.2 Source Emissions: AERMOD-DRI	74
4.6.4	Example Simulation of Dust Dispersion from Active Source Emissions Using AERMOD	75
	4.6.4.1 Starting DUSTRAN	75
	4.6.4.2 Selecting a Site	76
	4.6.4.3 Creating a Domain	77
	4.6.4.4 Setting the Release Period	78
	4.6.4.5 Setting the simulation scenario	78
	4.6.4.6 Setting the Model Species	79
	4.6.4.7 Creating a point source	80
	4.6.4.8 Creating an area source	81
	4.6.4.9 Entering Meteorological Data and Surface Characteristics	83
4.6.5	Running DUSTRAN	85
	4.6.5.1 Displaying Model Output	85
	4.6.5.2 Viewing Model Results	86

<b>5 Conclusions and Implications for Future Research/Implementation</b>	<b>89</b>
5.1 General Conclusions	89
5.2 Implementation	93
5.3 Implications for Future Research	94
<b>6 Literature Cited</b>	<b>96</b>
<b>Appendix A List of Scientific/Technical Publications</b>	<b>102</b>
<b>Appendix B DUSTRAN Version 2 Users Guide</b>	<b>103</b>

### List of Tables

Table 1. Summary of calibration factors for TRAKER™ II and III from tests at DPG, UT	34
Table 2. The mean per segment emission factors based on TRAKER™ measurements for the three measurement periods	54
Table 3. Estimates of total PM <sub>10</sub> emitted for each rotation vehicle inventory based on scaling the TRAKER™ per segment emission factor	56
Table 4. PM <sub>10</sub> produced by vehicles traveling the Mannix Road for the emission conditions measured during the three sampling periods	59
Table 5. Mean surface aerodynamic roughness length, friction velocity, and stability class for the five different surface sites during particle deposition testing	61
Table 6. AERMOD Model Components and Version Numbers Implemented in DUSTRAN	69
Table 7. CALPUFF/CALGRID Model Components and Version Numbers Implemented in DUSTRAN	70
Table 8. AERMET meteorological input requirements	71

### List of Figures

Figure 1. Relationships between project research components	4
Figure 2. Flux tower and medium volume PM <sub>10</sub> and PM <sub>2.5</sub> samplers	13
Figure 3. TRAKER™ III	14
Figure 4. TRAKER™ II	15
Figure 5. PI-SWERL®	17
Figure 6. Experimental setup for measuring PI-SWERL® induced surface shear-stress	17
Figure 7. The dust deposition instrument enclosures	22

Figure 8. The eight-channel PM particle number concentrations during a co-location test	23
Figure 9. Schematic of the near-field dust deposition model	25
Figure 10. Relationship between emission factor and vehicle momentum for tracked vehicles	29
Figure 11. Relationship between emission factor and vehicle momentum for tracked military vehicles measured at the Yakima Proving Ground, WA and four other test locations	30
Figure 12. Average emission factors ( $\text{g-PM}_{10} \text{ VKT}^{-1}$ ) and average TRAKER™ II signals from left and right inlets as well as average of both inlets	33
Figure 13. Average emission factors ( $\text{g PM}_{10} \text{ VKT}^{-1}$ ) and average TRAKER™ III signals from the reference and supplemental inlets	33
Figure 14. Relationship between TRAKER™ III reference and supplemental inlet $\text{PM}_{10}$ concentrations	35
Figure 15. Characteristics of $\tau$ and emissions in radial cross section in the PI-SWERL®	37
Figure 16. Spatial survey of approximately 110 km of DPG roads conducted by TRAKER™ II	39
Figure 17. Spatial survey of approximately 93 km of DPG roads conducted by TRAKER™ III	40
Figure 18. Delineation of road segments for TRAKER™ II survey path within DPG	41
Figure 19. Delineation of road segments for TRAKER™ III survey path within DPG	42
Figure 20. Comparison of segment averaged emission factors as estimated by TRAKER™ II and TRAKER™ III	43
Figure 21. Scatterplot of TRAKER™ III versus TRAKER™ II segment averaged emission factors ( $\text{g-PM}_{10} \text{ VKT}^{-1}$ )	43
Figure 22. Spatial survey of Ft. Riley roads conducted by TRAKER™ II	45
Figure 23. Spatial survey of Ft. Riley roads conducted by TRAKER™ II zoomed into southeast quadrant	46
Figure 24. Relationships between duration of time after application of water, dust emissions as measured by TRAKER™ II and water content of the test road at Ft. Riley, KS	48
Figure 25. Relationships between duration of time after application of water, dust emissions as measured by TRAKER™ III and water content of the Lima-P test road at Dugway Proving Ground, UT	48
Figure 26. Relationships between duration of time after application of water, dust emissions as measured by TRAKER™ III and water content of the Lima test road at Dugway Proving Ground, UT	49

Figure 27. Relationships between duration of time after application of water, dust emissions as measured by TRAKER™ III and water content of the X-ray test road at Dugway Proving Ground, UT	49
Figure 28. Relationship between normalized TRAKER signal (measured using TRAKER™ II) and moisture for the test road at Ft. Riley, KS	51
Figure 29. Relationship between normalized TRAKER signal (measured using TRAKER™ III) and moisture for the Lima-P test road, Dugway Proving Ground, UT	51
Figure 30. Relationship between normalized TRAKER signal (measured using TRAKER™ III) and moisture for the Lima test road, Dugway Proving Ground, UT	52
Figure 31. Relationship between normalized TRAKER signal (measured using TRAKER™ III) and moisture for the X-ray test road, Dugway Proving Ground, UT	52
Figure 32. Relationship between TRAKER™ signal (measured using TRAKER™ II and III) and moisture content for the four test roads	53
Figure 33. Mannix Road segments used for segregating data	54
Figure 34. Frequency distributions of vehicle weight for the three rotations at Ft. Irwin	57
Figure 35. Change in downwind PM <sub>10</sub> concentration referenced to near source PM <sub>10</sub> concentration	62
Figure 36. Particle deposition velocity based on box model for five surface types	63
Figure 37. Deposition velocities for particles measured during a single plume passage	64
Figure 38. An example of re-suspended dust number size distribution and mass size distribution	65
Figure 39. AERMOD Modeling Components within DUSTAN	69
Figure 40. CALPUFF/CALGRID Modeling Components within DUSTAN	69
Figure 41. MapWindow Toolbar	75
Figure 42. DUSTAN User Interface	76
Figure 43. Available DUSTAN sites	76
Figure 44. Yakima site displayed in DUSTAN	77
Figure 45. Domain panel	78
Figure 46. Release period panel	78
Figure 47. Simulation scenario panel	79
Figure 48. Species tab – “Available Species” list	79
Figure 49. Point source input form – “Release Parameters” tab	80
Figure 50. Area source input form – “Release Parameters” tab	81

Figure 51. Area source input form – “Vehicle Parameters” tab	82
Figure 52. Sources tab – “Sources” list	83
Figure 53. Specify meteorological data form – “Hourly Observations” tab	83
Figure 54. Specify meteorology data form – “Surface Characteristics” tab	84
Figure 55. “Run Simulation” button for running DUSTRAN simulation	85
Figure 56. Display options tab – “Contours” options	86
Figure 57. Contours tab - “Contour Types” listbox	87
Figure 58. Display of deposition contours for the hour from 9-10 AM	88

### **List of Acronyms**

AERMOD	Air Module
CALGRID	California Grid Model
CALPUFF	California Puff Model
DoD	Department of Defense
DPG	Dugway Proving Ground
DRI	Desert Research Institute
DUSTRAN	Dust Transport Model
EF	Emission Factor
EI	Emission Inventory
GIS	Geographic Information System
NAAQS	National Ambient Air Quality Standards
PI-SWERL <sup>®</sup>	Portable In Situ Wind Erosion Laboratory
PNNL	Pacific Northwest National Laboratory
SERDP	Strategic Environmental Research and Development Program
TRAKER <sup>™</sup>	Testing Re-Entrained Aerosol Kinetic Emissions from Roads
US EPA	US Environmental Protection Agency
YTC	Yakima Training Center

### **Keywords**

Dust, PM<sub>10</sub>, dust transport, dust deposition, dust modeling, vehicle emissions

## **Acknowledgments**

We gratefully acknowledge the support of SERDP as we carried out this project and the opportunities they provided for increasing our scientific understanding of dust processes and the roles of military activities and the environment in affecting these processes. We also acknowledge the roles of our colleagues in projects RC-1730 and RC-1776 who aided in the development of ideas related to dust emission and transport processes. We are grateful to Dr. R. Kirgan, US Army Environmental Command, Ft. Hood TX, for facilitating access to Ft. Irwin and Mr. J. Pace and D. Storwold, Dugway Proving Ground, UT, for supporting our work at their installation. Finally, we would like to thank all the personnel at the various military installations and the Hanford Site that helped us to execute the work and provided important logistical support during the field campaigns.

## **Abstract: RC-1729**

**Objectives.** This project's objectives were to: (1) develop new understanding of dust emission processes related to Department of Defense (DoD) testing and training activities, (2) identify the fate of those emissions as the dust interacts with the landscape (on the scale of several hundred meters), and (3) further develop and refine a comprehensive dust modeling system known as the Dust Transport Model (DUSTRAN).

**Technical Approach.** Measurement systems and methods were further-developed to quantify actual emissions (e.g., the flux tower method), as well as potential emissions using the transfer standard approach (TRAKER™ and PI-SWERL®). These developed methods have been accepted by the US Environmental Protection Agency as designated Other Test Methods (OTM). DUSTRAN's code was restructured to operate using open-source GIS and incorporate the US EPA AEROMOD dispersion model to facilitate its meeting regulatory applications.

**Results.** Measurements of dust emissions from vehicles (wheeled and tracked) indicated that they conform to general relationships between vehicle weight and speed developed earlier and represent a robust means to estimate emissions. Some areas, however, can produce much higher emissions for vehicles of similar weight and speed that can, in part, be explained by the specific mineralogical and textural attributes of roads. TRAKER™ and PI-SWERL® also were used to evaluate the spatial variability of road dust emission potential, and effectiveness of water spray to reduce emissions on un-paved roads, and longer term effectiveness of the dust palliative Magnesium Chloride used at Fort Irwin. Watering is essentially a short-term control method, on the order of hours. Magnesium Chloride, in the case of Fort Irwin, was used effectively to suppress dust emissions. TRAKER™ data clearly indicated, however, that over-use of this suppressant and cost and material usage has occurred and could have been curtailed, thus demonstrating that adopting the use of TRAKER™ can lead to developing more effective management strategies to meet air quality regulations and reduce costs.

Dust deposition in the near field (i.e., within 200 m of the source) and the role that the surface plays in affecting the deposition process was clearly demonstrated as part of this research. Based on field measurements it was observed that the deposition velocities increased with particle size and surface roughness under similar moderate wind speed conditions and were greater than predicted by application of the Stokes settling velocity equation. Although the effect of the surface on deposition was observed, and quantified for the range of test surfaces, the limited range of surface types and meteorological conditions did not allow for the development of general relationships that would explain this effect across a wider range of surface types. The developed relationships must still be used carefully and applied only for surfaces that are quite similar to those tested as part of this project.

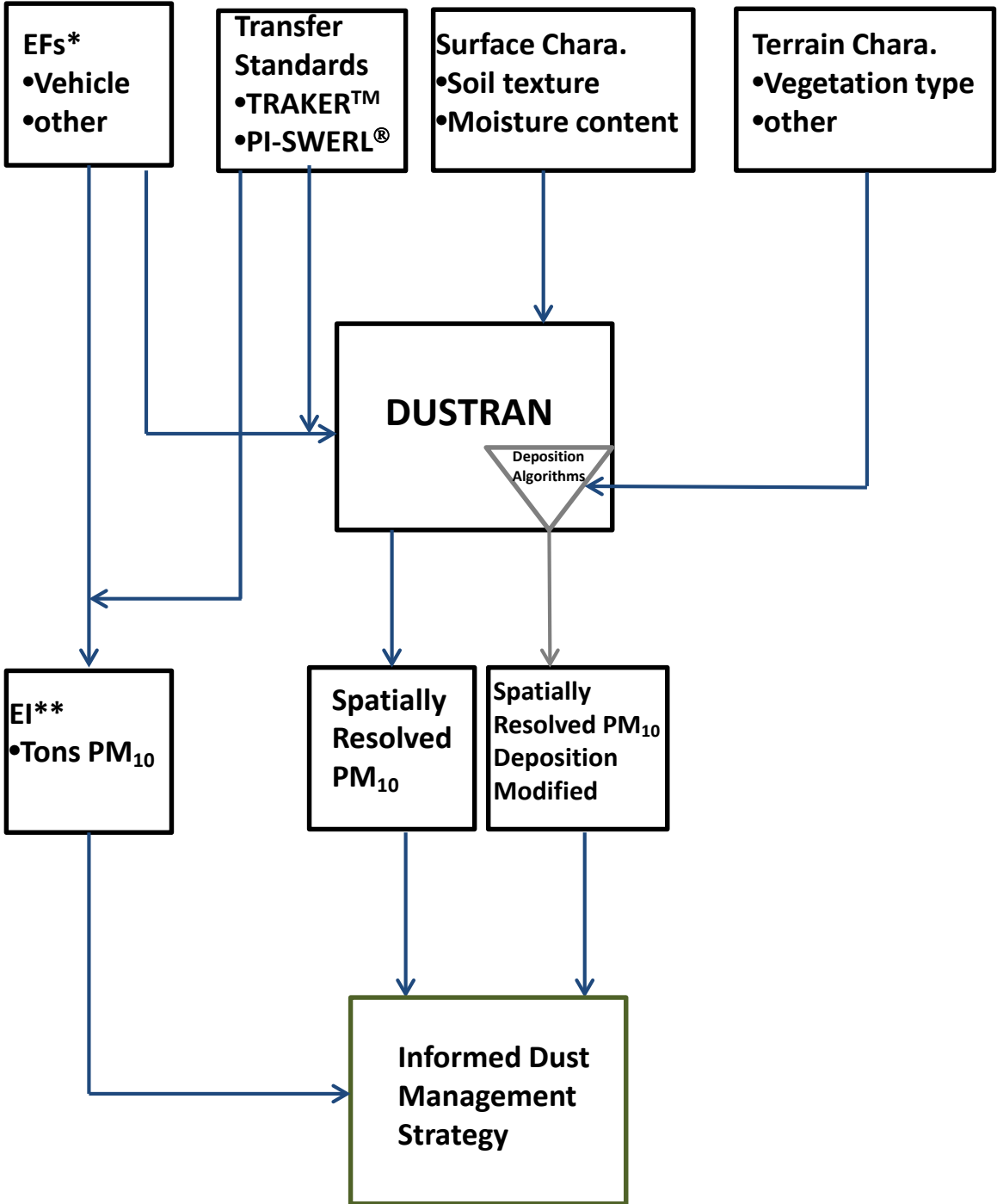
**Benefits.** New formulations of emission factors and measurement methods that allow for the extension of the specific results to areas and installations where measurements were not acquired can provide more defensible estimates of contributions of dust from testing and training activities

than was previously available to DoD installations. Characterization of terrain effects that modulate dust emission and transport may also lead to more accurate estimates of these contributions. DUSTRAN was modified significantly through the replacement of Esri®'s ArcMap Geographic Information System (GIS) with the open-source MapWindow GIS, which should contribute to making DUSTRAN much more widely used. The dispersion model component within DUSTRAN now includes AERMOD, the US EPA's preferred model. This fully restores DUSTRAN's ability to make dispersion calculations for regulatory use. For DUSTRAN users who prefer, the option to use CALPUFF is still available. DUSTRAN now offers the option to calculate dispersion using deposition velocities developed as part of this project linked to specific vegetation/roughness environments. Both the EPA regulatory distribution of AERMOD and the modified version (AERMOD-DRI) are included in DUSTRAN Version 2 (Both produce exactly the same results when AERMOD-DRI is run using the resistance-method option for deposition.). DUSTRAN Version 2 represents a major update to the modeling system that is far more easily distributable, is again consistent with US EPA's preferences for regulatory models, and is capable of calculating, with the incorporation of the new algorithm system, deposition effects in the near-field zone ( $\approx 0$  to 200 m).

## 1 Objectives:

The Desert Research Institute (DRI) and Pacific Northwest National Laboratory (PNNL) combined their resources and personnel to carry out this project to develop new understanding of dust emission processes related to Department of Defense (DoD) testing and training activities, the fate of those emissions as the dust interacts with the landscape (on the scale of several hundred meters) and to further develop and refine a comprehensive dust modeling system known as the Dust Transport Model (DUSTRAN) developed by PNNL. The dust emission and deposition research component was framed within an empirically-based study to: 1) provide additional information on key vehicle characteristics that influence dust emissions, 2) define transfer standards that enable effective and efficient modification of available emission factors to represent wider geographic areas using available dust emission potential measurement systems (Testing Re-Entrained Aerosol Kinetic Emissions from Roads [TRAKER<sup>TM</sup>] and Portable In Situ Wind Erosion Laboratory [PI-SWERL<sup>®</sup>]), 3) identify practically quantifiable surface properties that are most useful for estimating dust emission strength as a function of soil moisture and disturbance level, 4) identify and quantify terrain properties that are most useful for estimating attenuation of emissions by near-field deposition processes. A chart is provided in Fig.1 that illustrates the relationships between the component elements of the research and indicates how they relate to each other and provide information to inform a dust management strategy for installations.

A major goal for objectives one through four was to provide a means by which the DoD can more accurately quantify the amount of dust that testing and training, and other dust raising activities has on local and regional air quality, and therefore reduce the uncertainty associated with the reporting of this amount. This can be achieved by incorporating instrumentation to measure the property of interest directly (e.g., particulate matter  $\leq 10 \mu\text{m}$  aerodynamic diameter [PM<sub>10</sub>]) and characterize the environmental properties that influence the strength of the emissions (e.g., soil [or roadbed] texture), the transport of particles (e.g., surface conditions [e.g. vegetation cover]), and how these properties change over space and through time. In addition to direct measurement techniques, it is equally important to have a means to extend the results to areas where measurements were not made and generate similar results with a high degree of confidence. To fulfill this objective TRAKER<sup>TM</sup> and PI-SWERL<sup>®</sup> were further developed as part of this project to provide robust means to acquire data on emission characteristics that allow extension of results from the more detailed process-based measurements. The improvements for characterization and quantification of dust emissions, as undertaken by this project, offer the opportunity for improved management and remediation of dust emissions based on a more thorough understanding of emission processes and the scale of the process.



**Figure 1.** Relationships between the research components of project RC-1729 with the final goal being to provide information to better inform a dust management strategy depending on the conditions at individual installations. \*EF is Emission Factor. \*\*EI is Emission Inventory.

An important part of this project was to unify the results of the empirically-based research with a dust emission and transport model. Such a model would enable estimation of the potential impacts to air quality by the dust PM over a broad spatial scale for defined testing and training activities at any military installation, provided the input data are available (e.g., meteorological, dust source types, vehicle inventories, etc.). The model that provides this synthesis is called DUSTRAN. The objective for this part of the project was to advance this model for use by the military by ensuring that it remained flexible for meeting regulatory applications, and to modify DUSTRAN to incorporate the US Environmental Protection Agency's (EPA) regulatory dispersion model AERMOD. The objectives of this modification of DUSTRAN were: (1) to provide the user the option of using either CALPUFF or AERMOD for dispersion calculations; (2) to preserve as much as possible the interface experience for the user irrespective of the choice of model; and (3) to make the meteorological inputs required of the user as similar as possible. Dust emissions from the source-term modules are fully available to both CALPUFF and AERMOD within DUSTRAN. A second major component for the development of DUSTRAN was to replace the proprietary Esri® ArcMap Geographic Information System (GIS) that formed the basis of the user interface for DUSTRAN with open-source GIS software. Since the original development of DUSTRAN, open-source GIS software has advanced dramatically in capability, making it practical to replace ArcMap with an open-source GIS integrated directly into the DUSTRAN software while preserving the look, feel, and functionality of the original system. The final objective associated with DUSTRAN for this project has been to integrate new information gained from the field studies into DUSTRAN. This objective was specifically to determine a functional form that captured the new deposition results and to appropriately incorporate it into both the CALPUFF and AERMOD modules of DUSTRAN.

## 2 Background:

Fugitive emissions of mineral dusts created by testing and training activities on military ranges are an important environmental issue for the DoD. Dust generated by military activities and wind erosion on military lands can contribute to local exceedances of the limits allowed by the National Ambient Air Quality Standards (NAAQS) for PM<sub>10</sub> and PM<sub>2.5</sub>, particulate matter with aerodynamic diameter  $\leq 10 \mu\text{m}$  and  $\leq 2.5 \mu\text{m}$ , respectively. NAAQS exceedances require state and local governments to develop strategies for mitigation methods to reduce ambient particulate matter concentrations in order to achieve NAAQS compliance. Such actions could create conditions whereby testing and training activities must be modified or curtailed to reduce dust emissions. The principal off-site impact of dust-raising activities on military installations would likely be that the particulate matter from these activities contributes to ambient levels of PM<sub>10</sub> and PM<sub>2.5</sub> at downwind locations. This is most consequential when this contribution may result in exceedance of the 24-hour and annual average Federal at monitoring locations that report to the US EPA via local air quality management entities or to State Agencies (e.g., California Air Resources Board) in the case of State air quality standards.

Ensuring military readiness and the sustainability of testing and training ranges will require that the research community contribute knowledge that can be used to develop an effective understanding of fugitive emission processes, accurately simulate these processes with models, and combine this information to develop effective management practices that reduce environmental impacts caused by DoD-generated dust entering the atmosphere.

Currently 44 DoD installations have regulatory drivers for dust control for vehicle-derived and other process operations (Mr. P. Josephson, US Army IMCOM AEC, pers. comm., 8-31-2015). There is, however, no broad requirement for reporting of PM emissions from training activities or dust control on training lands to state or federal agencies. There are reporting requirements for selected unpaved roads. In the case of US Army installations the Army has a responsibility to report dust emissions that align with three standards: 1) conformity, 2) opacity, and 3) visibility. Conformity requires that an installation keep dust emissions below a set amount for a specified source (e.g., an identified length of unpaved road). The opacity standard requires that the opacity of observed dust emissions must be less than 20%. The visibility standard requires that an identified dust source, for example a tank trail, does not impair the visibility of an adjacent major thoroughfare (e.g., an Interstate Highway) when it is emitting dust either by mechanical disturbance (e.g., vehicle travel) or by a high wind event causing suspension and transport of dust from the source.

Fugitive dust emissions are considered to be derived from area sources, as opposed to point sources such as smokestacks. Prior to the research initiated by SERDP through a series of projects related to characterization and quantification of fugitive dust from DoD activities, the primary method to determine dust levels originating from DoD activities was evaluating dust plume opacity using trained human observers. This method is still applied at military installations. In the case of evaluating a conformity standard, the estimation relies on methods

using an emission factor for the activity based on application of available factors in US EPA's AP-42 Compilation of Air Pollutant Emission Factors, Volume 1: Stationary Point and Area Sources (US EPA, 1995) and knowledge of the activity rate. Visibility impairment is also judged to be in conformity using opacity determination methods. The use of opacity as a means to quantify dust emissions creates a large degree of uncertainty in estimates of its frequency and magnitude as opacity, which is an optical property of the dust plume, does not relate simply or directly to a mass concentration of dust. It is also affected by the position where the measurement is taken, time of day when the observation is made, distance between observer and the plume and the background conditions behind the plume. In addition this property is typically estimated by a trained observer, which incorporates subjectivity into its determination. To reduce some of the uncertainty in quantification digital camera based techniques have been developed (e.g., Du et al., 2007), but this does not overcome the fundamental weakness of opacity to quantify dust emission strength.

SERDP recognized that developing measurement methods that better-quantified emission factors was an important step forward to allow for better estimation of contributions of dust created by DoD testing and training activities. Emission factors available from AP-42 have been used to represent military vehicles or activities, but there was little scientific justification or corroboration that emission factors from AP-42 are adequately representative of actual emissions of dust created by DoD vehicles or other military activities that raised dust plumes. The characterization of the strength of emissions by wheeled and tracked DoD vehicles has been an important area of research (e.g., Gillies et al., 2005, Kuhns et al., 2010), because of the frequency they are used both on-and off-road by testing, training, and other on-base activities (e.g., convoys to move materiel). Sources such as the dust raised by artillery backblast (Gillies et al., 2007) and rotary-winged aircraft traveling close to the surface have been demonstrated to be of lesser importance for affecting regional air quality (Gillies et al., 2010; McAlpine et al., 2010).

The studies cited above were undertaken to characterize fugitive dust emission factors and their spatial and temporal variability, but confined to a relatively small geographic area (up to a few tens of kilometers). Extending the results beyond the specific location they represent has been challenging, and confidence in using measured emission factors to evaluate dust emission potential for areas where no measurements are available remains subject to further scrutiny. There is good understanding of which critical surface properties influence the processes of wind erosion and dust emissions (Shao, 2000), for example, soil moisture (Cornelis et al., 2004a, 2004b; Fécan et al., 1999), texture (Alfaro et al., 2004; Gillette, 1978, 1999; Engelbrecht et al., 2012), mineralogy (Engelbrecht et al., 2012), roughness (Gillette, 1999, Gillies et al., 2006, 2007; Gillies and Lancaster, 2013; Gillies et al., 2015), and crusting (Belnap and Gillette, 1997; Houser and Nickling, 2001a, 2001b; Rice and McEwan, 2001). These properties also influence the fugitive dust emission processes caused by vehicular or other activities. We do not, however, have a full understanding of how to modify emission factors based on changing surface conditions. Absent from the literature are complete datasets, obtained with a common standard of measurement, that can be queried to determine the combined effects of variations in soil

moisture, texture, roughness, crusting, and other relevant parameters. One reason for this dearth of information is that there is a large combination of these different parameters and measuring the dust emissions under the range of conditions represented has been prohibitively difficult.

One approach that has been developing to overcome the difficulties described above for characterizing emission potential in different environments and surface conditions is the transfer standard. This approach allows extension of location-specific, empirical results to different areas. Rather than directly measuring dust emissions at an area of concern, a transfer standard for dust emission prediction is based on measurement of a property that is correlated with dust emission factors. The relationship between emissions measured with a primary standard and the transfer standard measurement may or may not be linear, but can be established empirically once, and then utilized to conduct a multitude of measurements that would simply not be possible with the primary standard.

DRI has developed two measurement systems, as part of their SERDP-supported research, that can serve as transfer standards for estimating dust emission potential, one for vehicle travel on unpaved and off-road surfaces, the Testing Re-Entrained Aerosol Kinetic Emissions from Roads (TRAKER™) (Etyemezian et al., 2003b, 2003c, 2006) and the other for wind-generated dust emissions, the Portable In-Situ Wind Erosion Laboratory (PI-SWERL®) (Etyemezian et al., 2007). TRAKER™ can be used to estimate emissions from unpaved roads for a range of types of wheeled vehicles due to the essentially linear nature of the relationship between dust emissions and vehicle weight and speed (Gillies et al., 2005). The PI-SWERL® device is being used increasingly in research to characterize dust emission potential from susceptible surfaces (e.g., Sweeney et al., 2008, 2011, 2013; Buck et al., 2009; King et al., 2011) and the effectiveness of dust suppressants (e.g., Kavouras et al., 2009; Bacon et al., 2014). The PI-SWERL® system has advanced technologically and increased understanding of key influences such as surface roughness on its operation have been gained (Etyemezian et al., 2014) as a result of support from SERDP.

Military testing and training activities may also indirectly contribute to fugitive dust emissions. Soil surfaces that are mechanically disturbed tend to be much more prone to wind erosion than the original undisturbed surface, frequently with order of magnitude higher emissions for comparable wind conditions (Gillies, 2013). Dust emissions generated during high wind events from disturbed military lands are likely to be a significant contributor to local and regional PM emissions. The amount of PM generated, however, by these episodic events is not yet well-bounded for DoD installations.

Another outstanding fugitive dust research problem is the role of deposition of particulate matter to ground-level surfaces and vegetation in the immediate (order  $\approx$ 100-200 m) downwind region of the source of the dust. The contribution of mineral dust measured at air quality monitoring sites, often attributed to fugitive emission processes, does not reconcile well with the amount attributed to regional particulate matter levels using an emission inventory approach. Two hypotheses can be developed to explain this discrepancy: either the emission factors are not

characterizing the source term adequately or only a fraction of the initially suspended dust is transported to the receptor sites. Computer simulations based on a model developed by Pardyjak et al. (2008) have demonstrated that near source deposition of emitted particulate matter is consistent with established aerosol and fluid flow theory and can explain the observed difference between air quality measurements of fugitive dust contributions to regional PM levels and emission inventory-derived simulation methods.

Veranth et al. (2009) argue that classical deposition formulations do not apply in the near-source region, where vertical profiles of particle concentration are quite variable with downwind distance. A limited number of studies have provided measurements as model inputs for studies such as Veranth et al. (2003) and Etyemezian et al. (2004), but they lack critical data to fully evaluate the role of the surface features identified by Pardyjak et al. (2008), such as vegetation characteristics (e.g., height and density) and boundary layer conditions (e.g., atmospheric stability), which affect the dust deposition and removal process. Recent wind tunnel studies have presented results that suggest particle deposition is increased by increasing turbulence intensity, which increases particle interception (Moran et al., 2013; Zhang et al., 2014; Zhang and Shao, 2014) by surfaces that interact with the mean wind flow, for example plant leaves, leaf hairs, stems, etc. Zhang and Shao (2014) also present evidence that macro-roughness (e.g., shrubs) also affects the deposition process by a process similar to shear stress partitioning (Raupach et al., 1993; Gillies et al., 2007) by affecting the overall resistance of the surface to “collecting” particles. This resistance, according to Zhang and Shao (2014), scales as a function of the roughness density,  $\lambda$  ( $\lambda = n b h / S$ , where  $n$  is the number of roughness elements occupying the test area  $S$  ( $m^2$ ),  $b$  is element breadth (m), and  $h$  is element height (m)), with resistance decreasing as roughness density increases to a minimum, then increasing as the roughness elements reach a condition where the air flow begins to skim over them as opposed to going in and around them ( $\lambda > 0.2$ ). Both these effects could aid in explaining observed depositional losses for surfaces with increased roughness such as vegetation as the roughness will enhance turbulent motion in the flow and present more surface area for removal by impaction processes.

Models are needed to integrate theoretical and empirical relationships that can, in part, be used to understand how the outcome of events may impact an environment of concern. In the context of modeling the emissions, dispersion, and deposition of dust raised by military testing and activities it may be useful to know, for example, how the emissions impact local and regional air quality. Models offer the opportunity to guide management decisions on how best to potentially lessen the impact of these emissions on the environment, but to be effective they need to be based on the best-available scientific understanding of the processes they are intended to replicate, be able to be used and operated effectively and efficiently by personnel requiring the information they produce, and be held to a standard, in the case for air pollutants, that is acceptable to regulatory agencies (i.e., US Environmental Protection Agency [EPA]). Models that have been available (e.g., Industrial Source Complex 3 ISC3 [US EPA, 1995a], AP-42 [US EPA, 1995b], DUSTCON [Parrett, 1992]) are difficult to implement for military purposes as they lack sufficient information to effectively account for military-specific emission sources, the

capability to characterize testing and training scenarios, and representation of particle deposition processes in the near-source region.

The response to this lack of adequate modeling tools for military purposes was the development of the Dust Transport model (DUSTRAN) developed by PNNL. PNNL's DUSTRAN (Allwine et al., 2006; Shaw et al., 2008) calculates atmospheric dust concentrations that result from both natural and human activity. From January 2001 through August 2006, PNNL carried out a multi-year research project funded primarily by SERDP to develop an atmospheric dispersion modeling system to assist the DoD in addressing particulate air quality issues at military training and testing ranges. The culmination of that work was the development of the DUST TRANsport, or DUSTRAN, modeling system V1.0 (Allwine et al., 2006). DUSTRAN V1.0 functioned as a console application within the ArcMap Geographic Information system (GIS) and included the U.S. Environmental Protection Agency (US EPA)-approved CALPUFF dispersion model for modeling active sources of dust emissions from military vehicular activities and the widely used CALGRID dispersion model for modeling wind-blown dust generation. Source terms for vehicular and wind-blown dust are both native to the DUSTRAN modeling system.

When DUSTRAN was originally developed, CALPUFF was a recommended US EPA regulatory model for both short range (i.e., source-to-receptor distances less than 50 km) and long range (greater than 50 km) applications. Since that time, US EPA has reclassified CALPUFF as preferred only for long range regulatory applications, with the Gaussian-plume model AERMOD now the preferred US EPA regulatory model for short range applications. The CALPUFF system is technically advanced, however, and recent evaluation (Dresser and Huizer, 2011; Brode, 2012) shows that it can perform very well in short range applications. For regulatory use, it can still be used in special circumstances with prior US EPA approval.

Originally, the DUSTRAN modeling system was integrated with the Esri® ArcMap application as a means to supply the modeling system with a GIS base for handling geographic inputs as well as providing a method to geographically view the results generated by each simulation. At the time, ArcMap was the premier GIS system, and integration with ArcMap allowed the DUSTRAN modeling system to make use of the extensive geospatial capabilities found within the ArcMap application, reducing the amount of required code development. A significant issue has become evident since the initial development of DUSTRAN, which is that new versions of ArcMap that Esri® releases are commonly not fully backward compatible. For the DUSTRAN modeling system, this meant that each time Esri® upgraded its software, DUSTRAN needed to also be upgraded in order to be used with the latest version of ArcMap. This lack of backward compatibility and the propriety nature of the Esri® software make it difficult to provide users with the modeling software and substantially increases the maintenance costs for DUSTRAN. Since the original development of DUSTRAN, open-source GIS software has advanced dramatically in capability, making it practical to replace ArcMap with an open-source GIS

integrated directly into the DUSTRAN software while preserving the look, feel, and functionality of the original system.

Available dispersion models such as CALPUFF and AERMOD estimate depositional losses by assigning a deposition velocity as a function of particle size and meteorology. For CALPUFF, the deposition velocity can be provided as an input values. AERMOD determines deposition velocity via a resistance model. With the recognition that deposition in the near field (<200 m) may have a considerable impact on particle removal, efforts have been undertaken to improve understanding of the physics of this process (e.g., Pardyjak et al., 2008, Moran et al., 2013, and this project) with the goal being to determine functional forms that better-capture the deposition process that can be incorporated it into both the CALPUFF and AERMOD modules of DUSTRAN.

### 3 Materials and Methods:

The research carried out in this project was largely field-based and hence required that sites be selected that provided both the necessary features and reasonable opportunity to collect data that would serve to answer the science objectives. The final choice of sites where the experiments were carried out reflected a balance between optimal characteristics for experimentation and pragmatism, taking into account access and on-site infrastructural support for helping to achieve the science goals. The military bases Ft. Riley, Kansas and Ft. Irwin, California, also represented areas with acknowledged dust issues and hence provided areas with conditions known to produce dust that can be problematic for these installations. Dugway Proving Ground (DPG), Utah and the Hanford Site, Washington, offered the opportunity to generate dust for study due to the dry nature of the environment and multiple locations with different vegetation covers, but also infrastructural resources to support the complex field set-up of instrumentation for the dust deposition measurements along with a safe and secure environment. In addition these locations offered established meteorological networks to provide data to characterize the regional state of the atmosphere. Although by necessity the number of testing sites was small, the approach of utilizing robust transfer standards was developed to overcome the limitation of a restricted range of measurement locations.

#### 3.1 Vehicle characteristics that influence dust emissions

Dust emission measurements for vehicles travelling on unpaved roads were made using our established tower-based methodology (Gillies et al., 2005, 2007, 2010) (Fig. 1). Measurements were made at Ft. Riley, KS and the DPG, UT. Briefly, dust emissions were created by having a vehicle travel back and forth along the test surface for a number of passes over a sequence of driving speeds (15 – 40 km hr<sup>-1</sup>, within the limits of safety). The dust plume PM<sub>10</sub> characteristics (i.e., vertical concentration gradient) that is generated by the vehicles is measured immediately downwind of the source and used in conjunction with wind speed, wind direction, and vehicle characteristics to define its emission factor (g-PM<sub>10</sub> produced per unit distance of travel).

DRI's flux tower technology (Fig. 2) employs a vertical array of light scattering particle sensors, anemometers, and a wind vane mounted on a portable 9 m tower (Gillies et al. 2005, 2007, 2010). Prior work has shown excellent agreement (<5% difference in PM flux) between collocated towers and to be in general agreement with measurements using optically-based instrumentation (e.g., Du et al., 2011). PM<sub>10</sub> and PM<sub>2.5</sub> emission fluxes are calculated using the following equation:

$$EF = \sum_{\text{start of peak}}^{\text{end of peak}} \left\{ \cos(\theta) \sum_{i=1}^5 u_i C_i \Delta z_i \Delta t \right\} \quad (1)$$

where the outer summation is over the period of plume impact, EF is the estimated emissions factor of PM in grams per vehicle kilometer traveled (g-PM vkt<sup>-1</sup>),  $\theta$  is the angle of the 5-min.



**Figure 2.** Flux tower (right side of frame) and medium volume PM<sub>10</sub> and PM<sub>2.5</sub> samplers deployed to measure dust plumes characteristics generated by vehicles traveling on an unpaved road.

average wind direction relative to the flux plane,  $i$  is monitor position on the tower,  $u_i$  is the 1 second wind speed ( $\text{m s}^{-1}$ ) over the height interval represented by the  $i^{\text{th}}$  monitor,  $C_i$  is 1-s PM concentration ( $\text{mg m}^{-3}$ ) as measured by the  $i^{\text{th}}$  monitor,  $\Delta z$  (m) is the vertical interval represented by the  $i^{\text{th}}$  monitor, and  $\Delta t$  (s) is the duration that the plume impacts the tower. For all emission factor calculations, only the concentration data associated with wind approach angles  $\leq 45^\circ$  to travel surfaces and towers are used.

Ft. Riley, KS had initially offered access to tracked military vehicles at their disposal, however, due to unforeseen circumstances these resources were withdrawn and a commercially available tracked vehicle used for agriculture was substituted. In addition, emission measurements were made of the TRAKER<sup>TM</sup> II vehicle (Mercedes-Benz Sprinter Van) at Ft. Riley and on a playa surface at Jean Lake in Nevada. A final set of vehicle emission data were collected at the DPG during the testing of TRAKER<sup>TM</sup> III (1/2 ton pickup truck).

## 3.2 Transfer Standards: TRAKER™ and PI-SWERL®

### 3.2.1 TRAKER™

As part of this project TRAKER™ was redesigned to more effectively measure emissions from unpaved and off-road surfaces. The new TRAKER™ III (Fig. 3) overcomes the problem of high particulate matter concentration levels associated with travel on unpaved and off-road surfaces that caused flow problems through the TRAKER™ II measurement system (Fig. 4). This reduced the operation time for TRAKER™ II as the sampling lines became plugged requiring extensive maintenance.

The TRAKER™ III takes a different approach to measuring road dust emissions by moving the measurements of dust concentrations from behind the front wheels, as in previous versions, to the wake zone in the immediate lee of the vehicle that forms behind a custom-designed baffle (Fig. 3). Following extensive characterization of the flow and dust concentration distribution in this wake zone, TRAKER™ III was performance-tested at the DPG, UT by calibrating its emission signal against TRAKER™ II and also the DRI flux tower emission flux measurement system.



**Figure 3.** TRAKER™ III. Instrumentation is held within the bed of a standard pickup truck and dust concentrations created by vehicle travel are measured in the lee of the custom-designed baffle mounted to the truck's rear bumper.



**Figure 4.** TRAKER™ II. Instrumentation is within the van and dust concentrations resulting from vehicle travel are measured behind both front tires.

For TRAKER™ II and III the method to determine emission potential is similar, with the main difference being the position where the PM emitted from the test surface is measured. This vehicle-based system is equipped with inlet lines that sample PM either behind the front tires or in the wake of the vehicle and deliver the dust laden air to photometers (Model 8520 DustTrak, TSI, Inc.). There are four photometers in use, two that are equipped with inlets that allow measurement of PM<sub>10</sub> and two that have inlets that allow measurement of PM<sub>2,5</sub>, and in the case of TRAKER™ II a background measurement is made with a sampling line at the front of the vehicle. These instruments provide a measure of the concentration of PM dust in units of milligrams per cubic meter ( $\text{mg m}^{-3}$ ). The concentration measurements are geo-referenced using an onboard GPS to a location and travel speed. Additional instrumentation is used to determine the influence of ambient winds on the measurement quality. Data are flagged as invalid if ambient wind speed exceeds  $8 \text{ m s}^{-1}$  as the cross-wind component to the direction of travel would adversely affect the zone of the vehicle where the sampling inlets are positioned to measure the dust plume. All data are collected in real-time by an onboard computer. The measured concentrations are converted to g-PM<sub>10</sub> produced per vehicle kilometer travelled by application of the calibration relationship developed using our flux-tower method (Gillies et al., 2005) from measurements made at the DPG, UT, as part of this project.

TRAKER™ II was used at Ft. Riley, KS, and TRAKER™ II and III at the DPG, UT, to characterize the spatial variability of road dust emission potential at these installations to evaluate the range of potential emissions for comparison with other military installations

measured previously, and to evaluate if emission potential can be linked to specific conditions of the roads. TRAKER™ III was used to characterize the emission potential of a specific unpaved road, the Mannix Rd., at Ft. Irwin, CA, which serves as the route for convoys of vehicles moving materiel between the post and Barstow, CA. The Mannix Rd. at Ft. Irwin was traversed between four and six times during each of three sampling campaigns.

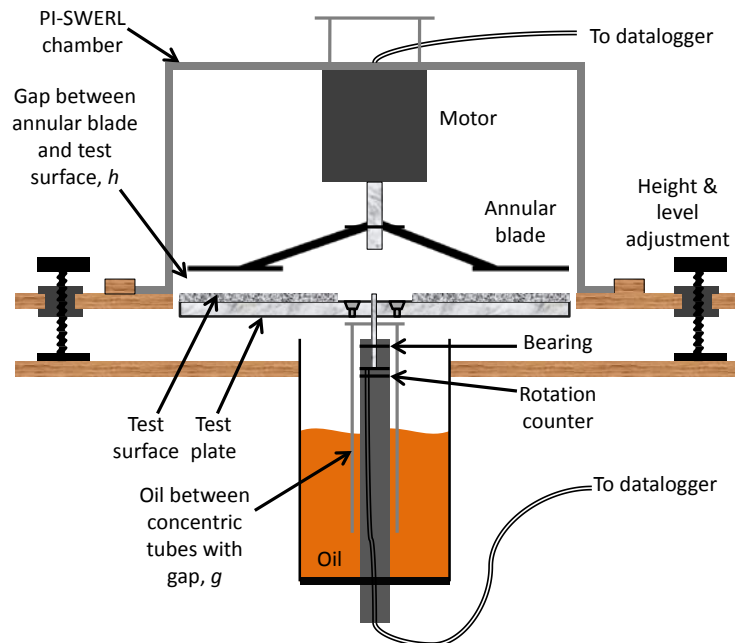
### 3.2.2 PI-SWERL®

To improve the accuracy when quantifying the dust emission potential as a function of applied shear stress relationship using PI-SWERL®, new information on parameterizing roughness effects on shear stress generation was developed using a unique viscometer-like instrument to quantify applied shear stress generated by the PI-SWERL® on test surfaces. Figure 5 illustrates PI-SWERL® in a field test situation. Figure 6 is a schematic representation of the PI-SWERL® depicting how it was operated over a synthetic test surface that was center-mounted onto a bearing and coupled to a fluid friction source. As the test surface rotates in response to shear stress ( $\tau$ ,  $\text{N m}^{-2}$ ) induced by the PI-SWERL®, the viscosity of the fluid exerts a torque ( $\text{N m}^{-1}$ ) that eventually balances with  $\tau$ . The amount of torque exerted by the fluid at varying rates of rotation of the test surface can be calculated accurately using Newtonian mechanics. In this manner, the magnitude of  $\tau$ , measured in terms of the torque that the PI-SWERL® exerts onto surfaces of varying roughness can be measured at multiple rates of rotation of the PI-SWERL® annular blade. Forty-one roughness configurations were fitted to the viscometer-device to evaluate the relationship between PI-SWERL® revolutions per minute (RPM), which generate  $\tau$  as calculated from the measurement of torque and the roughness characteristics of the surface.

Five types of roughness were tested. The first and simplest types of rough surfaces were sand paper of grit that varied from very rough (#12) to very smooth (#120). The second type of roughness was achieved by gluing small dome-shaped forms to a test surface in varying surface densities defined as the percentage of the plan view area covered by the domes. Two sizes of domes were used: 1) 7 mm diameter and 2.9 mm height, and 2) 4 mm diameter and 2.5 mm height. Five different patterns of roughness were created, which resulted in densities of domes that varied from sparse to nearly packed. The third type of roughness consisted of toothpicks (average diameter = 2 mm). The toothpick patterns included the same five patterns used with dome-forms as well as a pattern that emulated clumped blades of grass. The fourth set of roughness type examined was wave-like. Three wave-like surfaces with different amplitude and frequency were tested. These were intended to emulate the small ripples that are sometimes encountered when using the PI-SWERL® on very sandy soils. The fifth type of surface was made using gravel of two different sizes.



**Figure 5.** The PI-SWERL<sup>®</sup> instrument on a test surface for measuring PM<sub>10</sub> dust emission potential in situ.



**Figure 6.** Experimental setup for measuring the effect of roughness on shear stress.

The roughness was parameterized two ways. The first was a simple classification based on five arbitrary categories of element height range and pattern. The second was a photogrammetric method that involved illumination of the surface at a set angle through  $22.5^\circ$  increments over a  $90^\circ$  range. Digital images of the surfaces were taken for each of the five angles. The processing of photographs was based on the analysis of shadows cast by roughness elements when they are illuminated at an oblique angle. A MatLab<sup>®</sup> program was written to automatically estimate the height of individual roughness elements based on the geometry of the shadows cast by the roughness.

### 3.3 Moisture and suppressant effects on road dust emissions

The TRAKER<sup>TM</sup> vehicles (II and III) were used to quantify the effect of moisture content on dust emissions from unpaved roads at Ft. Riley, KS, and DPG, UT. Straight test sections of roads >600 m were selected at these installations and baseline measurements of the road dust PM<sub>10</sub> emission potential for test roads were obtained prior to any application of water. Water was applied with spray-dispersing nozzles at the rear of tanker vehicles over the width of the road and a length that included an additional 150 m buffer at each end of the test sections. These buffer sections were needed to avoid edge effects at the wet/dry interface during the TRAKER<sup>TM</sup> measurements.

The water truck operator was instructed to quantify the amount of water in the truck, maintain constant water application rate, maintain constant truck speed, and note the time it took for the water truck to empty. Using this information, it was estimated that the test roads received the equivalent of 0.5 millimeters of rain at the time of water application. Starting within a few minutes after water application, TRAKER<sup>TM</sup> II or III traversed the test sections. The procedure was to transit the section, turn around, wait for a few minutes and then transit the test section in the opposite direction. This frequency of travel was maintained for several hours. For the DPG experiments additional traverses were completed up to seven hours after application of the water. At intervals between vehicle passes samples of the road material ( $\approx 250$  g) were removed and placed in air-tight containers. These samples were weighed as soon as possible after collection, and then again following drying to estimate the percent water content in the road surface through time. The time of collection of the samples were linked to the times of the TRAKER<sup>TM</sup> passes, which allowed for a comparison between emission strength and moisture content of the road surface.

The opportunity to evaluate the effectiveness of long-term application of the dust suppressant Magnesium Chloride (MgCl<sub>2</sub>) arose during this project based on a request from U.S. Army Environmental Command (Ft. Sam Houston, TX), which fit well with the overall objectives of this project. The objective was to evaluate the effectiveness of long-term applications of the dust suppressant Magnesium Chloride to the Mannix Rd. located in Ft. Irwin, CA, and determine whether the current schedule for application of this suppressant was justified in terms of cost and need to control emissions below the allowable limit of 100 tons of PM<sub>10</sub> released on an annual basis.

At Ft. Irwin, the Mannix Road was traversed between four and six times during each of three sampling campaigns: 1) just prior to application of MgCl<sub>2</sub> in June 2014, 2) approximately one week following application of MgCl<sub>2</sub> (July 2, 2014), and 3) just prior to (September 11, 2014) the application of MgCl<sub>2</sub> in September 2014. In order to facilitate data analysis, the road was divided into ten segments based on natural breaks in geography and principal travel direction. Each one second data point from TRAKER<sup>TM</sup> III was associated with a road segment and a nominal travel direction, either “NB” for northbound or “SB” for southbound. Segment 10 data were not segregated by travel direction (labeled “NSB”). Each one second data point was

checked for validity based on speed, acceleration, and wheel angle characteristics. Additionally, data associated with high ambient winds or moderate winds at angles oblique to the travel direction were considered not valid. All one second data points associated with any single NB or SB pass were averaged together. If there were not sufficient data for a reliable average (fewer than 20% data recovery for road segment), that particular pass was considered invalid for the entire length of the segment.

### **3.4 Attenuation of emissions by near-field deposition processes**

To contribute to improved understanding of the near field deposition process, a series of field measurement campaigns was undertaken to measure in real-time the change in atmospheric concentration and size distribution of PM in dust plumes advecting downwind following emission from unpaved road sources. The measurements were carried out over one non-vegetated surface at Jean Lake, NV, and four differently vegetated surfaces at Ft. Riley, KS and the Hanford Site, WA and under a restricted range of wind speeds and atmospheric stability conditions. Use of near real-time instruments allowed for the characterization of multiple individual dust plumes at each study location. The objective of these field studies was to quantify the size-segregated deposition velocities of suspended PM for different surface roughness and assess the effect of vegetation type (long grass, short grass, sagebrush, steppe grass, and no vegetation) on the attenuation of emissions by near-field deposition processes. We used a refined box model (Zhu et al., 2011) to calculate PM deposition velocities of different sized particles based on dust concentration measured in downwind locations.

#### **3.4.1 Instrument set up, inter-comparison and measurement uncertainty**

To evaluate the precision of the instruments used to measure particle diameter, the instruments were collocated near the roadside at each site prior to the formal field testing. Instruments used for measuring particle number concentration and mass concentration were encased in weatherproof enclosures (Fig. 7). Instrumentation in each enclosure consisted of: two DustTraks, one each equipped with PM<sub>10</sub> and PM<sub>2.5</sub> inlets (Model 8520, TSI, Shoreview, MN), one Aerosol Profiler (AP) (Model 212-2 MetOne, Grants Pass, OR), one MiniVol sampler (Airmetric, Eugene, OR) collecting PM<sub>10</sub> on a 47 mm Teflon filter for gravimetric and chemical analysis, and two deep cycle gel cell batteries (Fig. 7). Particle size cut points for the MetOne AP instrument were programmed at 0.3 μm, 0.5 μm, 0.7 μm, 1 μm, 2 μm, 2.5 μm, 5 μm and 10 μm. MetOne TSP inlets were placed on the sampling tubes for each of the five aerosol samplers. Each enclosure also had one MetOne Model 014A anemometer with a 024A wind vane attached to it on an exterior mast. When an enclosure was resting on the ground, the wind sensors and aerosol inlets were located ≈2.2 m above ground level (a.g.l.). Each deposition box is capable of operating for approximately 20 hours on a battery charge and all environmental data were recorded by a laptop computer inside the enclosure.

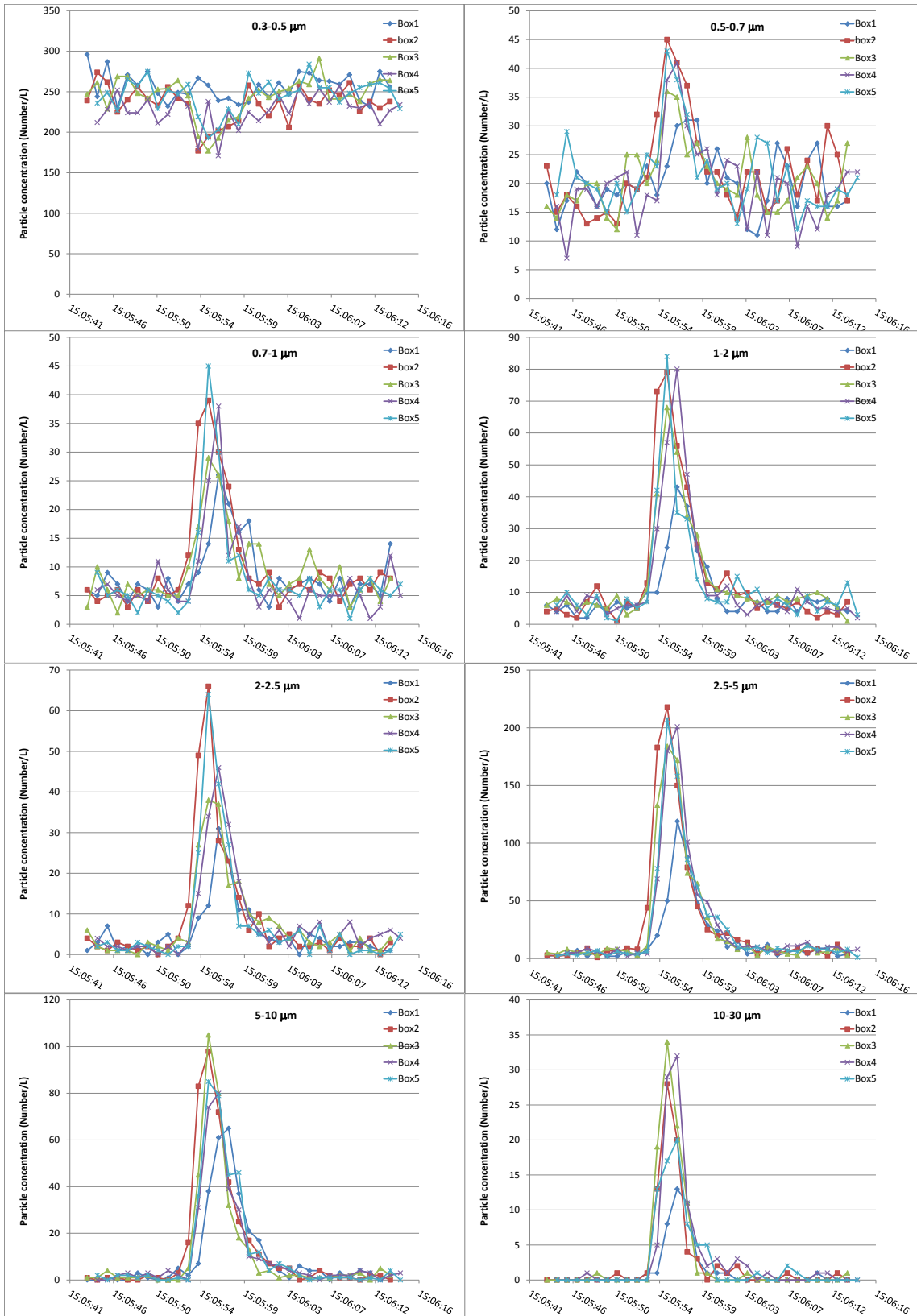


**Figure 7.** The four dust deposition instrument enclosures set up for the initial collocated precision measurements (left panel) and the instrumentation inside (right panel). Note the anemometer and wind vane are not at the height used during field measurements, which matched the height of the PM inlets.

Figure 8 illustrates the eight-channel PM concentrations during a co-location test that consisted of 20 vehicle passes. Regression analyses were performed to reference all measurements to one unit (i.e., Unit 1). The standard error of the slope and intercept for each regression were calculated and propagated as the uncertainty for all particle count concentrations (Zhu et al., 2011). The slope and intercept correction factors were applied to the measurements from the other four APs (Units 2 to 5) to standardize the readings relative to Profiler Unit 1. The average standard error of the regression was applied to each reading from each particle size bin to infer the precision of the measurements.

### 3.4.2 Sampling array at the different sites

The plume-by-plume dispersion and deposition during vehicle passes at each test site were observed using the measurement system described above, but configured differently than that used during the co-location tests. The array of samplers downwind of the source was placed along a line perpendicular to the road beginning with a near source position (10 or 20 m) with low level inlet (2.2 m a.g.l.), one sampler with low level inlet (2.2 m) and one sampler with a high level inlet (6.1 m) at  $\approx 110$  m downwind of the road, one sampler with a low level inlet (2.2 m) and one sampler with a high level inlet (6.1 m) at  $\approx 210$  m downwind of the road. The array of samplers was designed to resolve changes in the particle size distribution of the suspended dust in the horizontal and vertical directions as the plume advected downwind. A 10



**Figure 8.** The eight-channel PM particle number concentrations during a co-location test.

m high tower configured with five anemometers, one wind vane, five PM<sub>10</sub> and three PM<sub>2.5</sub> monitors was also placed 10 m downwind of the road to measure the vertical wind speed profile and calculate the mass flux of dust using the method of Gillies et al. (2005). At the Hanford site, a nearby 120 m meteorological tower also provided data for estimating atmospheric stability. Measurement of PM deposition for each surface type at each site was conducted over a minimum of two days. On each day, the test vehicle ran multiple passes (typically 50-70 per day) when the wind was within  $\pm 45^\circ$  of perpendicular to the road.

The surfaces at four sites used to generate the dust plumes were unpaved roads and in all cases the vehicle used to generate the plumes was a 2005 Dodge Sprinter van (weight  $\approx 2250$  kg). At the Ft. Riley, KS test sites the vegetation downwind of the roadway was initially a continuous cover of dense long grass ( $\approx 1.2$  m high) and then that grass was mowed to a height of  $\approx 0.2$  m to provide a second, different vegetative cover. At the Hanford, WA site PM measurements were made for a sagebrush community ( $\approx 1.5$  m high) and over a steppe grass community ( $\approx 0.4$  m high). At the Jean Lake, NV site PM measurements were made of dust plumes as they advected over a smooth and flat dry lakebed surface devoid of vegetation. Only at the long grass site at Ft. Riley (the first site tested), one deposition box was placed at upwind of the source (to measure background conditions) with four downwind locations (10 m, 55 m, 105 m, and 155 m) from the unpaved road dust source. To improve spatial resolution in the downwind direction the array was reconfigured for the other sites by moving the upwind sampler to a position downwind and calculating background conditions during periods when there were no dust emissions from the unpaved road.

### 3.4.3 Horizontal gradient method to infer deposition velocity

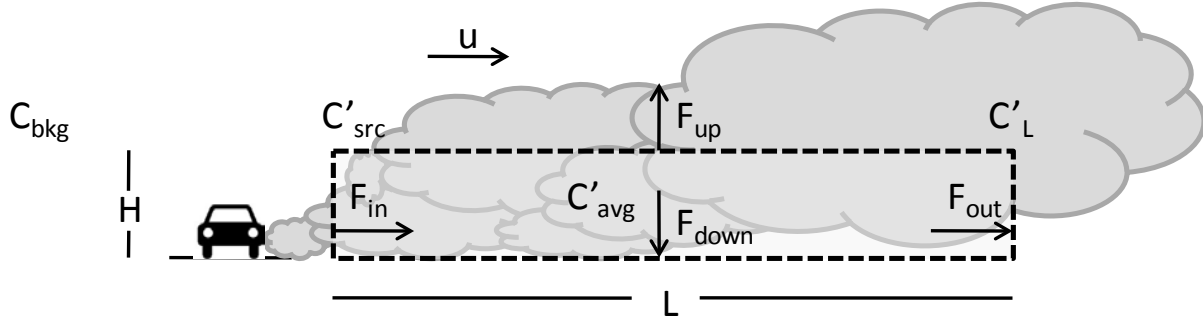
For this study deposition velocities for particles  $>1 \mu\text{m}$  were calculated using the particle size concentration measurements (# particles/liter) of the background air (background,  $C_{bkg}$ ) in the periods prior to the presence of a generated dust plume, and then of the dust plume generated by the source ( $C'_{src}$ ) at a distance  $L$  downwind of the source ( $C'_L$ ). The two dimensional model ( $z$  is vertical,  $x$  is horizontal) shown in Fig. 9 depicts a road dust plume transported from left to right at wind speed  $u$  ( $\text{m s}^{-1}$ ) through a control volume ( $CV$ ) of height  $H$  (m) and length  $L$  (m). For the flux calculation, the vertical unit area (cross section of the  $CV$ ) was assumed to be unit width times  $H$  and the horizontal unit area (cross section) was assumed to be unit width times  $L$ .

$C_{src} = C'_{src} - C_{bkg}$ ,  $C_L = C'_L - C_{bkg}$ , and  $C_{avg} = C'_{avg} - C_{bkg}$ . The mass balance for the particle concentration in the control volume (i.e., the sum of the fluxes is 0) is:

$$0 = F_{in} - F_{out} - F_{up} - F_{down} = uHC_{src} - uHC_L - LF_{up} - v_d LC_{avg} \quad (2)$$

where,  $F_{up}$  is the gross particle upward flux and  $v_d$  is the deposition velocity ( $\text{m s}^{-1}$ ).

The model is based on first principles but makes the following three assumptions:



**Figure 9.** Schematic of the near-field dust deposition model.

- Particles less than  $0.3 \mu\text{m}$  have a  $v_d$  that is negligible with respect to particles greater than  $1 \mu\text{m}$  (i.e.,  $v_d|_{<0.3\mu\text{m}} \ll v_d|_{>1\mu\text{m}}$ ). Submicron particles are slow to deposit by interception, impaction and/or gravitation compared to particles  $>1 \mu\text{m}$  and deposit primarily by Brownian diffusion (Seinfeld and Pandis, 1998).
- As observed by Zhu et al. (2011), the PM deposition can be approximated by  $C = C_o e^{-kx}$ . The average concentration in the control volume is determined by integrating  $C_o e^{-kx}$  over the beginning and ending horizontal points of the CV (i.e.,  $x_1$  and  $x_2$ ) and dividing by the

distance ( $x_1 - x_2$ ) as follows: 
$$C_{avg} = \frac{e^{-kx_1} - e^{-kx_2}}{k(x_1 - x_2)}$$
. Since the horizontal concentration change ( $dC/dx$ ) is not constant, an exponential approximation is a better representation of a real world deposition scenario than the assumption  $C_{avg} = (C_{src} + C_L)/2$  made previously by Zhu et al. (2011).

- The vertical diffusion velocity (upward flux  $F_{up}$  divided by  $C_{avg}$ ) is invariant with particle size since the turbulent diffusion coefficient  $K$  is much greater than the Brownian diffusion coefficient,  $D$ , for dust particles between  $0.3 \mu\text{m}$  and  $20 \mu\text{m}$  and the particle relaxation times are much shorter than the timescale for turbulent eddies (Seinfeld and Pandis, 1998). That is:

$$\left. \frac{F_{up}}{C_{avg}} \right|_{<0.3\mu\text{m}} = \left. \frac{F_{up}}{C_{avg}} \right|_{>1.0\mu\text{m}} \quad (3)$$

Solving Eq. 2 for  $v_d$  for particles  $>1 \mu\text{m}$  yields:

$$v_d|_{>1.0\mu\text{m}} = \frac{uH}{L} \frac{C_{src} - C_L}{C_{avg}|_{>1.0\mu\text{m}}} - \left. \frac{F_{up}}{C_{avg}} \right|_{>1.0\mu\text{m}} \quad (4)$$

Similarly, solving Eq. 2 for  $v_d$  for particles  $<0.3 \mu\text{m}$  and subtracting this from Eq. 2 yields:

$$v_d|_{>1.0\mu m} - v_d|_{<0.3\mu m} = \left( \frac{uH}{L} \frac{C_{src} - C_L}{C_{avg}} \Big|_{>1.0\mu m} - \frac{F_{up}}{C_{avg}} \Big|_{>1.0\mu m} \right) - \left( \frac{uH}{L} \frac{C_{src} - C_L}{C_{avg}} \Big|_{<0.3\mu m} - \frac{F_{up}}{C_{avg}} \Big|_{<0.3\mu m} \right) \quad (5)$$

Applying the first assumption and Eq. 3 produces the following equation for  $v_d$  as a function of particle diameter:

$$v_d|_{>1.0\mu m} - v_d|_{<0.3\mu m} \approx v_d|_{>1.0\mu m} = \frac{uH}{L} \left( \frac{C_{src} - C_L}{C_{avg}} \Big|_{>1.0\mu m} - \frac{C_{src} - C_L}{C_{avg}} \Big|_{<0.3\mu m} \right) \quad (6)$$

## **3.5 DUSTRAN**

The objective for developing DUSTRAN originally was to create a user-friendly console application that would optimize ease of use and flexibility for running the CALMET/CALGRID/CALPUFF software to calculate dispersion of dust arising particularly from military activities. The method for doing this was to create a framework to seamlessly create required inputs and display outputs for user-defined scenarios while leaving the regulatory code unmodified. With one exception, which is the incorporation of near-field deposition velocity into AERMOD, this approach has been carried forward in this work. This will be discussed further below.

### **3.5.1 Conversion to Open-Source GIS**

After a review of available open-source GISs, MapWindow was selected as a fully effective replacement for ArcMap in DUSTRAN. To implement the GIS change in the DUSTRAN software, the following modifications were performed. The connections to the ArcObjects API for ArcMap were severed, and the DUSTRAN user interface modified to make use of the new GIS control. Previously, the DUSTRAN modeling software was in the form of a dynamic link library that had to be registered with the ArcMap application. Severing the connections to the ArcMap application allows the software to be a stand-alone application. The ArcObjects API calls controlling the creation, deletion, and display of the GIS features were also replaced with the appropriate calls to the new GIS control.

### **3.5.2 Incorporation of AERMOD into DUSTRAN**

The AERMOD dispersion modeling system consists of the AERMOD Gaussian plume dispersion model, the AERMET meteorological pre-processor, and the AERMAP terrain pre-processor. The model was developed jointly under the American Meteorological Society/Environmental Protection Agency Regulatory Improvement Committee (AERMIC) and in December 2006 became the EPA's preferred system for modeling near-field dispersion. AERMOD includes state-of-the-science boundary layer theory and advanced algorithms for treating complex terrain.

Integrating the AERMOD model with the DUSTRAN modeling system required the development of data converters for the input and output data used and generated by the AERMOD model. Input parameters required by the AERMOD model are pulled from the DUSTRAN interface and the GIS control. These input data are then translated into the appropriate data file format required by the AERMOD model. Output data generated by the AERMOD model is also be translated to the appropriate file formats used by the post-processors previously developed for DUSTRAN in order for the system to generate the desired output products. Changes to DUSTRAN's interface were implemented to allow the input of parameters specific to the AERMOD model. Additionally, modifications to the model selection and execution portions of the DUSTRAN modeling system were performed to allow users the ability to select AERMOD, CALPUFF, or CALGRID as the atmospheric model to be used in the

simulation. The new models added to DUSTRAN were validated by demonstrating the ability of DUSTRAN to reproduce results of test cases supplied with the component regulatory models.

### **3.5.3 Incorporation of project-developed deposition velocities**

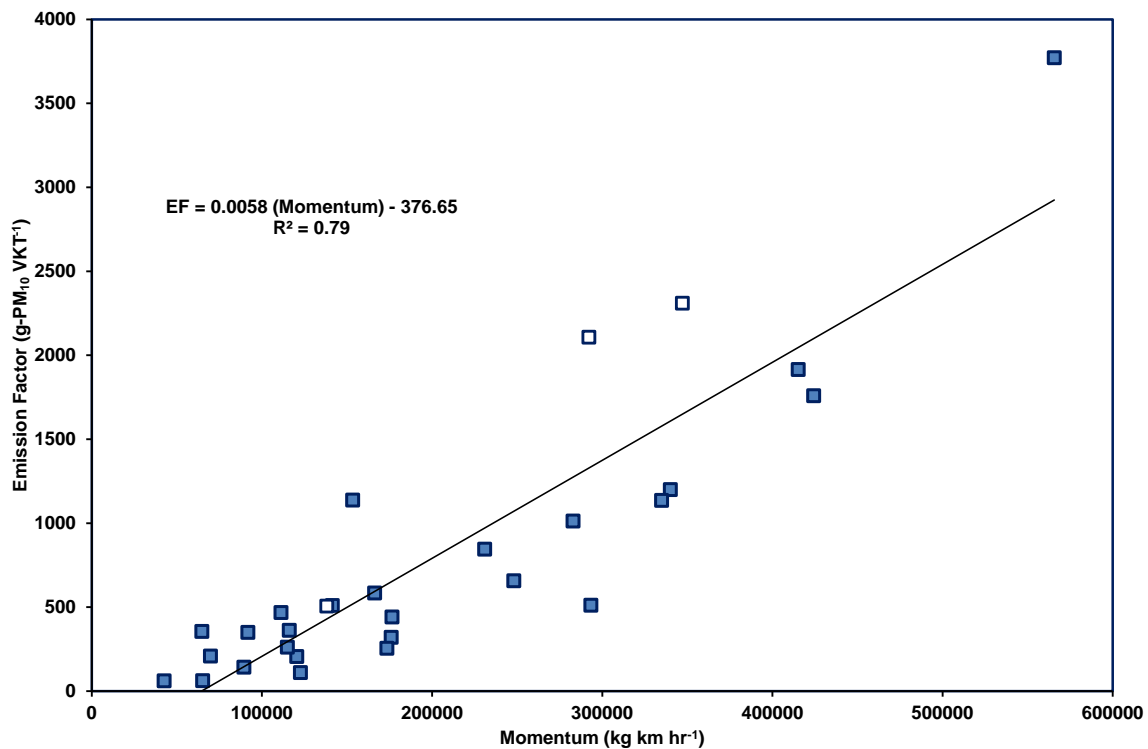
One additional objective of this study was to make available to DUSTRAN the results of the new, near-field deposition measurements made during this study. At the same time, a continuing requirement for DUSTRAN is that it be built on distributed, regulatory versions of dispersion code. For CALPUFF, adding the option to use the newly-developed deposition velocity functions was straightforward, since deposition velocities can be supplied as input to the model runs. For AERMOD the solution was more complicated because deposition is calculated using a resistance model that is integral to the compiled code for AERMOD. This was solved by including two versions of AERMOD within DUSTRAN: (1) AERMOD (EPA version) and (2) AERMOD–DRI (version including the dry deposition function derived from project-acquired measurements). AERMOD is the unmodified code as distributed by EPA. AERMOD–DRI has the option to run using either the conventional resistance model for dry deposition or the functional formulation using DRI results. The user can verify that the resistance option in AERMOD–DRI produces identical results to those of the unmodified AERMOD. This preserves the utility of DUSTRAN for situations in which the formal regulatory code is required.

## 4 Results and Discussion:

### 4.1 Vehicle characteristics that influence dust emissions

Although not a direct result of this project alone, the method developed through this and previous SERDP-supported projects to quantify emissions and emission factors for vehicles raising dust by travel on paved and unpaved roads has now been formally acknowledged as US EPA Other Test Method (OTM) 32 (<http://www.epa.gov/ttn/emc/prelim/otm32.pdf>).

As mentioned in Section 3.1, our plan to measure emissions from tracked vehicles was limited due to the lack of access to this type of vehicle. However, while at Ft. Riley access to one large tracked civilian vehicle was provided and the comparison between the emission factor as a function of vehicle momentum (i.e., vehicle weight  $\times$  speed) shown in Fig. 10 indicates that the measured emissions fit well with the general relationship for military-tracked vehicles based on a sample of three vehicles from a previous project (Gillies et al., 2006). This provides confidence that for tracked vehicles travelling on unpaved roadways similar to those found on Ft. Riley, KS, Ft. Collins, CO., and Ft. Bliss, TX, the general relationship shown in Fig. 10 can be used. The exception to this is the Yakima Proving Ground, WA where emission factors for tracked vehicles

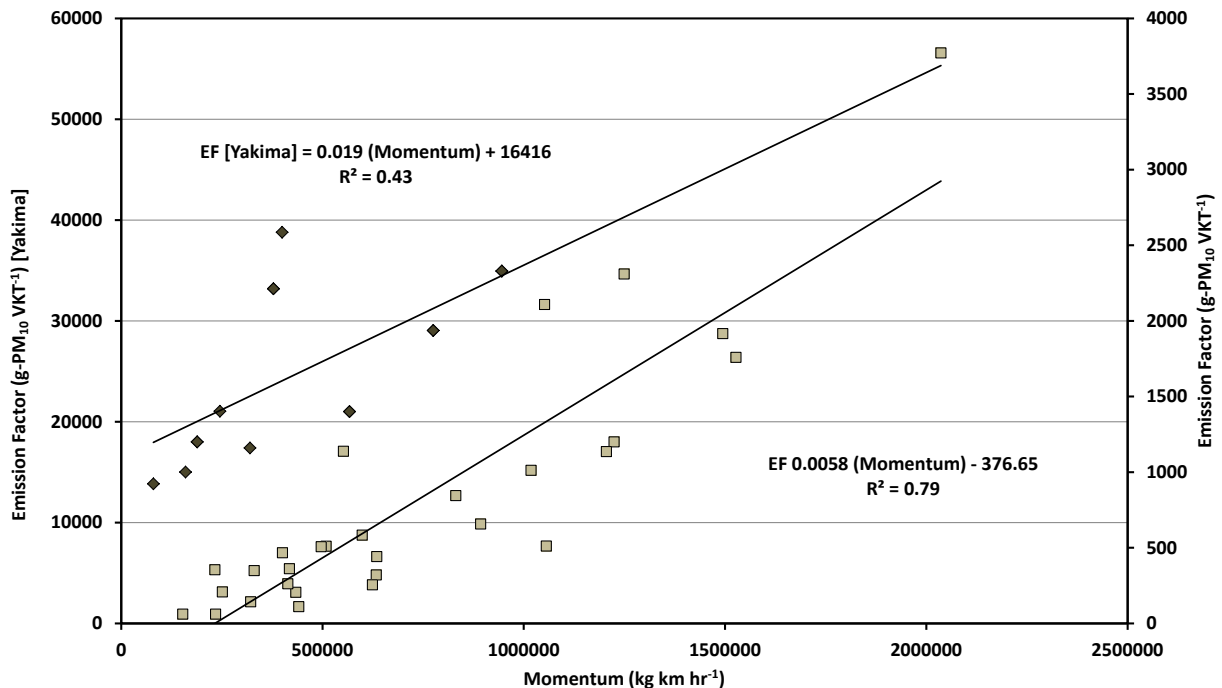


**Figure 10.** The relationship between emission factor (g-PM<sub>10</sub> VKT<sup>-1</sup>) and vehicle momentum for tracked military vehicles (blue squares) and one civilian tracked vehicle (white squares).

were approximately two orders of magnitude great than were observed at the other identified sites (Fig. 11).

Engelbrecht et al. (2012) examined the controls on emissions of mineral dust at four locations in the western US using data collected for a previous SERDP project (Gillies et al., 2006) and concluded that particle size distribution and mineralogy differences contribute to the emission properties of the surface, providing an explanation for the observed differences in emission factors between samples from Yakima (YTC), and the other test sites. They suggest that emission factors can, in part, be predicted from the measurement of particle size distributions, together with the mineralogical content of the surface soils.

At YTC, the high silt content of the surface sediment (>50%), which is predominantly glacial loess and the different suite of minerals present, which are mostly non-weathered igneous minerals including plagioclase, amphibole, and pyroxene, together with trace amounts of carbonate (calcite, dolomite), help to explain its increased emission potential. Engelbrecht et al. (2012) from CCSEM measurements, report that these silicate mineral particles are largely coated by a veneer of clay minerals and fine hematite. They suggest that this veneer of fine particles are removed, and thus enhance the dust concentration, through abrasion processes between the vehicle tracks and the surface and perhaps during collision as the tracks spew the material from the surface into the air behind the vehicle.



**Figure 11.** The relationship between emission factor ( $\text{g-PM}_{10} \text{ VKT}^{-1}$ ) and vehicle momentum for tracked military vehicles measured at the YTC, WA (dark diamonds) and four other test locations (beige squares).

Engelbrecht et al. (2012) observed that high silt content does not, by itself, contribute to the high emissions observed at YTC. The presence of high clay content can constrain the emissions by providing cohesive forces that bind the particles together more effectively. This situation was observed in Ft. Carson, CO. At the driest desert sites for which data were available (i.e., Yuma Proving Ground, CA), Engelbrecht et al. (2012) attributed cementation of grains to minerals formed during weathering (e.g., calcite, dolomite) together with evaporate minerals (including artificially added potassium sulfate) serve to cement the silicate and other particles, thereby lowering the dust emission factors.

## 4.2 Transfer standards: TRAKER™ and PI-SWERL®

TRAKER™ and PI-SWERL® both underwent additional development during this project. In the case of TRAKER™ a new instrument configuration was undertaken to allow it to more efficiently measure PM<sub>10</sub> and PM<sub>2.5</sub> (if warranted) emissions from unpaved surface that can create quite high concentrations of particulate matter that was problematic for TRAKER™ II in terms of affecting the inlet nozzles (clogging issues). PI-SWERL® was not modified in any of its design parameters, but prior to the work undertaken as part of this project there was uncertainty as to how to accurately quantify the shearing stress created under the rotating blade for surfaces of varying roughness. As part of this project we undertook a controlled experiment to characterize the effect of surface roughness on shear stress (Etyemezian et al., 2014), which will allow PI-SWERL® users to collect data with more constrained values of measured shear stress and dust emissions.

### 4.2.1 TRAKER™ Development

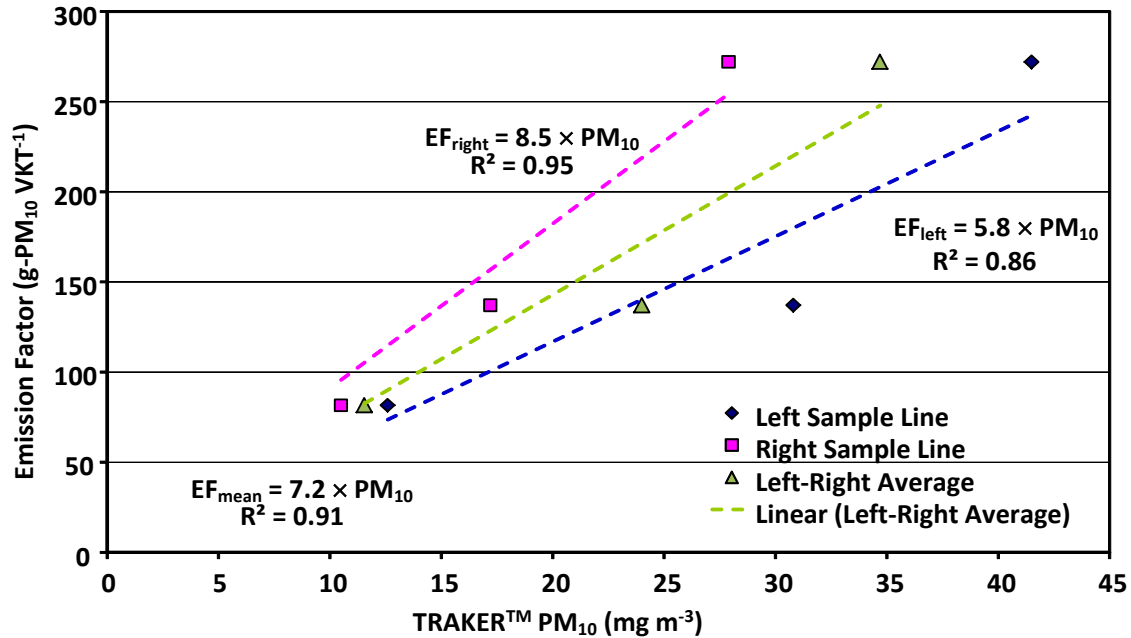
The TRAKER™ system was re-designed as part of this project to make it more functional and efficient to measure the high emission potential for unpaved and off-road vehicle travel. As part of this development the two versions were tested for comparability and calibrated against flux tower measurements to convert the measured TRAKER™ PM<sub>10</sub> signal (mg m<sup>-3</sup>) to emission factor (kg-PM<sub>10</sub> VKT<sup>-1</sup>) following the method of Gillies et al. (2005) at the DPG, UT.

Based on the 20 passes when both the individual tower flux measurements associated with the passage of the TRAKER™ II vehicle and the measurements simultaneously collected by TRAKER™ II were considered valid, a relationship between TRAKER™ II raw signal measurements and the emission factor from an equivalently sized vehicle were obtained. This relationship is shown in Fig. 12 and was based on four measurements when the TRAKER™ II was operated at a nominal speed of 16 km h<sup>-1</sup>, eight measurements at a nominal speed of 24 km h<sup>-1</sup>, and eight measurements at a nominal speed of 40 km h<sup>-1</sup>. As with previous, recent work (e.g., Langston et al., 2008) the relationship between TRAKER™ II signal and measured emission factors appears to be well represented by a linear model. The following simple relationship was used:

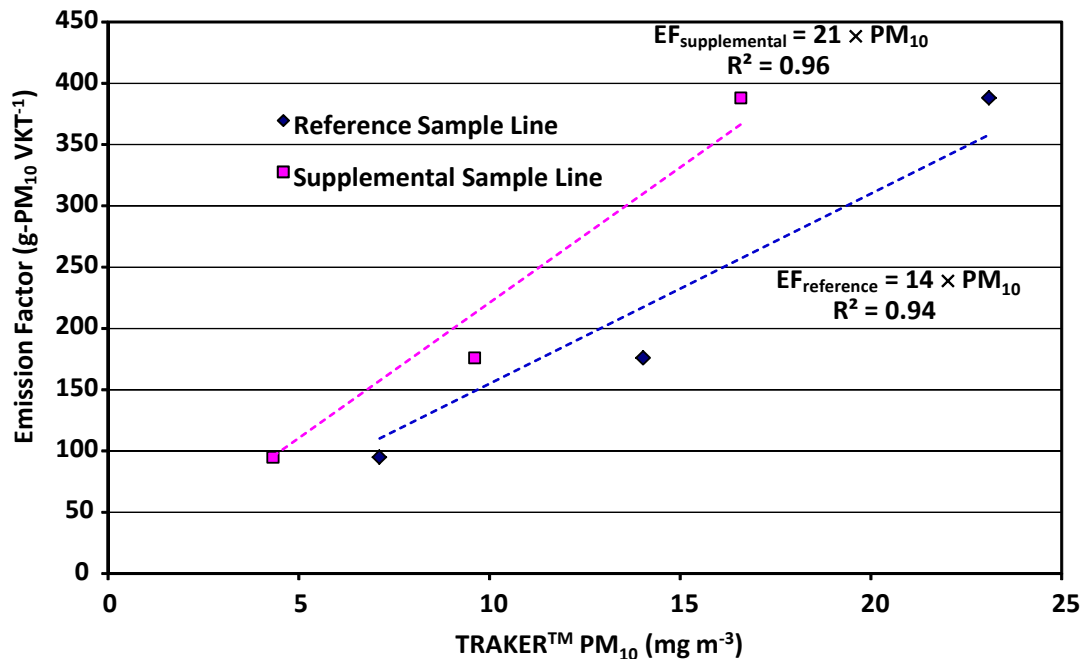
$$EF_{II} = A_{II} T_{II,Ave} \quad (7)$$

Here,  $EF$  is the emission factor in grams of PM<sub>10</sub> emitted per vehicle kilometer traveled, the subscript “ $II$ ” indicates that the emission factor is specific to the TRAKER II™ vehicle (i.e., Dodge Sprinter van),  $A$  is a simple constant derived from an empirical fit to the data, and  $T_{Ave}$  is the average of the concentrations of PM<sub>10</sub> from the left and right inlets in mg m<sup>-3</sup> of PM<sub>10</sub>.

Similarly, valid data from TRAKER™ III passes were examined by nominal travel speed (Fig. 13). There were a total of 10 passes where both TRAKER™ III measurements and the tower based emission factor measurement were considered valid. As with TRAKER™ II, it is expected that within the range of measured emission factors, a linear relationship like the one shown in Eq. 7 would adequately describe the relationship between TRAKER™ III



**Figure 12.** Illustration of measured average emission factors (g-PM<sub>10</sub> VKT<sup>-1</sup>) and average TRAKER<sup>TM</sup> II raw signals from left and right inlets as well as average of both inlets. Data are shown for nominal speeds of 16 km h<sup>-1</sup> (n=4), 24 km h<sup>-1</sup> (n=8), and 40 km h<sup>-1</sup> (n=8).



**Figure 13.** Illustration of measured average emission factors (g PM<sub>10</sub> VKT<sup>-1</sup>) and average TRAKER<sup>TM</sup> III raw signals from the reference and supplemental inlets. Data are shown for nominal speeds of 16 km h<sup>-1</sup> (n=1), 24 km h<sup>-1</sup> (n=4), and 40 km h<sup>-1</sup> (n=5).

measurements and the emission factors of the TRAKER™ III vehicle. That is, we assume that the following equation holds true:

$$EF_{III} = A_{III} T_{III,Ref} \quad (8)$$

In Eq. 8, the Reference inlet PM<sub>10</sub> concentration is used to estimate the emission factor (as indicated by the subscript, “Ref”), but we note that the reference and supplemental inlet concentrations are well correlated so that the latter could also be used if necessary (Fig. 14).

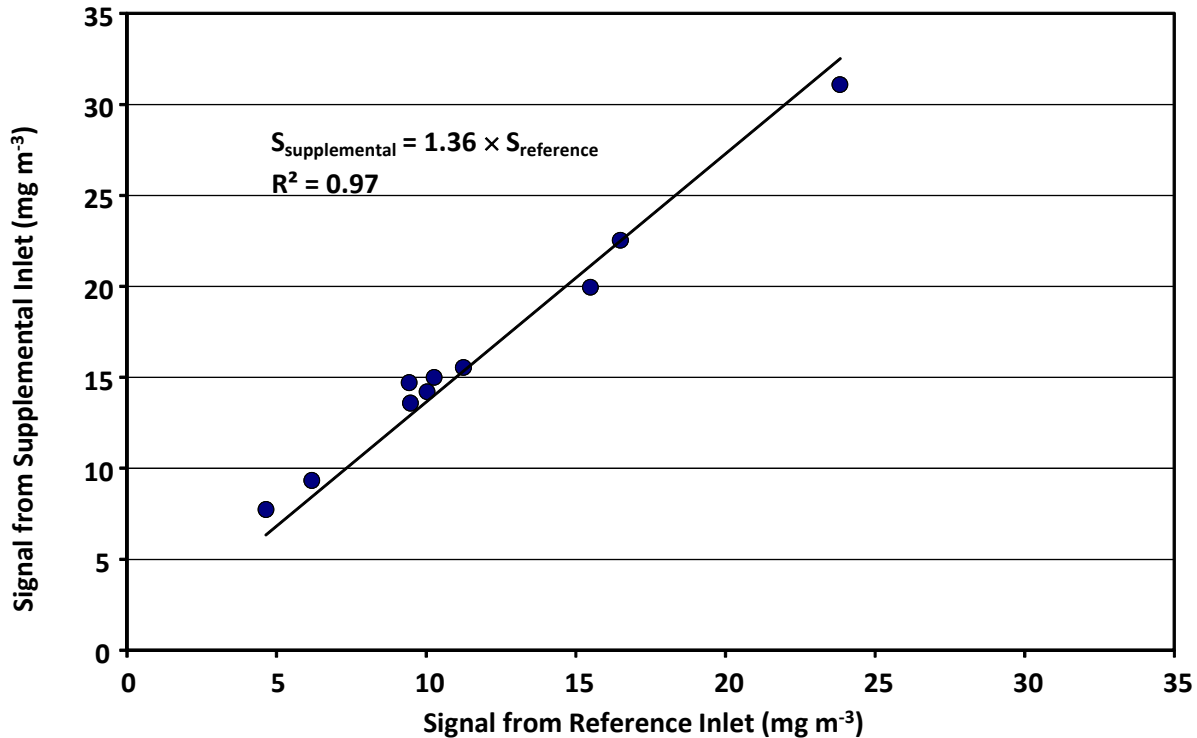
Assuming that vehicle travel speed does not impact the value of *A* in Eqs. 7 and 8, all of the respective data for TRAKER™ II and TRAKER™ III calibration passes can be aggregated to arrive at the calibration coefficients shown in Table 1.

SERDP support has been instrumental in the development of the TRAKER™ technology and the culmination of this support is twofold. This technology has now matured sufficiently to the point that we feel that it can become commercialized and provided to military installations under a service contract. This has been demonstrated, in part, by its use to address a specific DoD problem identified by the US Army Environmental Command at Ft. Irwin, CA (see Section 4.3.2) concerning the long term effectiveness of dust suppressant application and its effect on unpaved road dust emissions. According to Dr. Robert Kirgan (US Army Environmental Command, pers. comm.) there is interest from other military installations to use TRAKER™ to characterize road network emission potential and use this information to guide dust management strategies for specific installations to decrease costs and increase effectiveness of dust management strategies.

The second major achievement related to the maturation of the TRAKER™ technology is that the principles of measurement employed by TRAKER™ are now codified within US EPA Other Test Method (OTM) 34 (<http://www.epa.gov/ttn/emc/prelim/otm34.pdf>). The acceptance of the TRAKER™ method to quantify road dust particulate matter emissions from vehicular travel on paved and unpaved roads as an OTM allows TRAKER™-based measurements that follow the OTM guidelines to be accepted as reasonable means to represent the emission process and of a quality that meets regulatory standards. This provides users of TRAKER™ with confidence that the data obtained will provide an acceptable quantification of the magnitude of the emissions for air quality inventory purposes.

**Table 1.** Summary of calibration factors for TRAKER™ II and III from tests at DPG, UT.

$A_{II} [\text{g-PM}_{10} \text{ VKT}^{-1}]/[\text{mg m}^{-3}]$	TRAKER™ II total Vehicle mass (lbs/kg)	$A_{III} [\text{g-PM}_{10} \text{ VKT}^{-1}]/[\text{mg m}^{-3}]$	TRAKER™ III total Vehicle mass (lbs/kg)
7.2 (±1.1)	5,500/2,500	21 (±3)	6,000/2,730



**Figure 14.** Relationship between TRAKER™ III reference and supplemental inlet PM<sub>10</sub> concentrations for the 10 valid passes used to estimate the value of  $A$  in Eq. 8.

#### 4.2.2 PI-SWERL® Development

Support from SERDP has contributed substantially to the development of the PI-SWERL® as a tool for characterizing and quantifying PM emission strength from surfaces susceptible to windblown emissions of PM<sub>10</sub>. As part of this SERDP project we undertook a study to address a number of outstanding questions regarding the interpretation of PI-SWERL® measurements. Principal among these questions was the effective area underneath the rotating blade from which the PM emissions are generated and the role of surface roughness to influence the estimated shearing stress developed under the blade.

The importance of knowing the effective area is that it allows for recasting absolute emissions measured with the PI-SWERL® (units of mass of dust per unit time) as emission factors expressed on a per ground area basis (units of mass of dust per unit time per unit ground area). The effective area is arrived at by considering that the distribution of shear stress underneath the PI-SWERL® annular blade and the nonlinear relationship between shear stress and dust emissions work together so that on the test surface, a contiguous area in the shape of an annular ring is overwhelmingly the main contributor to measured emissions at any given time. In prior work, Etyemezian et al. (2007) described how the shear stress distribution under a larger version of the PI-SWERL® (D=0.57 m) was estimated using a series of profiling measurements with an

Irwin-type sensor (Irwin, 1981). The Irwin sensor uses characteristics of the boundary layer to infer the magnitude of  $\tau$ .

Figure 15 illustrates that there is an annular region that corresponds roughly to the PI-SWERL<sup>®</sup> annular blade location and centered on a normalized radial distance ( $r/R$ ) of 0.8 where the value of  $u^*$  is relatively constant. Etyemezian et al. (2014) demonstrated that the active region for wind erosion measurement and the effective area for calculating PI-SWERL<sup>®</sup> emissions  $A_{eff}$  is given by:

$$A_{eff} = 0.875 \times \pi(0.15 \text{ m}^2 - 0.10 \text{ m}^2) = 0.035 \text{ m}^2 \quad (9)$$

Etyemezian et al. (2014) show that the error in the emissions estimate resulting from a defined  $A_{eff}$  is 12%. By defining  $A_{eff}$  an acceptable uncertainty in the knowledge of the value of  $u^*$  that is causing the emissions minimizes the uncertainty associated with this dimensional aspect of the PI-SWERL<sup>®</sup>.

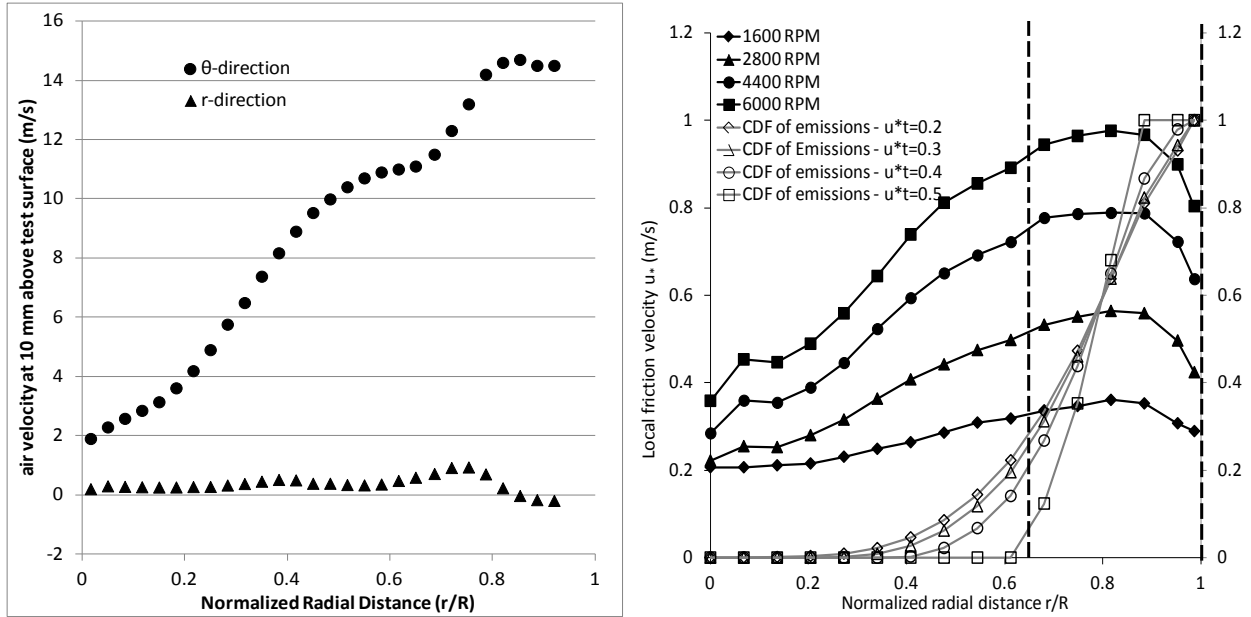
It was found by Etyemezian et al. (2014) that a single parameter  $\alpha$  could be used to describe the effect of roughness on  $u^*$  ( $\text{m s}^{-1}$ ) versus PI-SWERL<sup>®</sup> RPM curves through the equation:

$$u_{*,eff}(RPM) = C_1 \cdot \alpha^4 \cdot RPM^{C_2/\alpha} \quad (10)$$

where  $C_1$  is a constant equal to 0.000683 and  $C_2$  is a constant equal to 0.832. Fitting values of  $\alpha$  to the different test surfaces described in Section 3.2.2 resulted in a median RMSE of 0.028  $\text{m s}^{-1}$  and a 95-percentile value of 0.085  $\text{m s}^{-1}$ .

The relationship between PI-SWERL<sup>®</sup> rate of rotation (expressed as RPM) and  $u_{*,eff}$  was, as expected, found to be dependent on the roughness of the surface. A series of measurements using a device similar to a viscometer indicated that  $\alpha$  ranged between a high value of unity for smooth surfaces and a low value of 0.85 for the roughest surfaces tested. The same measurement technique was used to investigate the effect of small variations in the distance between the PI-SWERL<sup>®</sup> annular blade and the test surface. Such variations may be encountered in field settings as a result of the observed change in compressibility of the elastomeric foam used to seal the PI-SWERL<sup>®</sup> to the test surface or due to unevenness in the test surface. It was found that there were no statistically significant differences for changes on the order of 0.01 m in the distance between the blade and the surface.

Two techniques for accounting for surface roughness in estimating the equivalent  $u_{*,eff}$  exerted at a particular PI-SWERL<sup>®</sup> RPM were investigated. In the first method, it was assumed that an experienced field scientist would be able to compare a test surface of interest to a gallery of surfaces that were tested and summarized in Etyemezian et al. (2014). It was assumed without formal justification that the error in estimating the parameter  $\alpha$  would be less than 0.04, which is roughly equivalent to 20% at 3,000 RPM. The second method used a simple photogrammetric technique to relate physical roughness parameters to the parameter  $\alpha$ . Although a number of simplifying assumptions were invoked and only a limited combination of surface roughness



**Figure 15.** Characteristics of  $\tau$  and emissions in radial cross section. (left panel) wind velocity distribution measured with 2-axis hot wire anemometer probe at a height of 10 mm above the test surface and PI-SWERL<sup>®</sup> RPM of 4000; (right panel) profiling measurements with Irwin-type sensor. Solid markers show the distribution of  $u_*$  at varying RPM. Open markers show the cumulative emissions up to a normalized radial distance  $r/R$  as a fraction of total emissions within the PI-SWERL<sup>®</sup> for 2800 RPM and varying  $u_*t$ . The dashed vertical lines indicate the region considered to be active in simulating wind erosion ( $0.67 \leq r/R < 1$ ).

geometries were examined, the method did appear to reduce the uncertainty in estimating  $\alpha$  by  $\approx 50\%$  as compared to the first method.

### 4.3 Spatial variability of road dust emission potential

Using the calibration relationships presented in Section 4.2.1, road segments surveyed at Ft. Riley, KS and DPG, UT can be translated into spatial surveys of emission factors. Moreover, since two different TRAKER™ technologies were used to survey many of the same road segments during the same periods of time, results obtained with TRAKER™ II and III can be compared to each another.

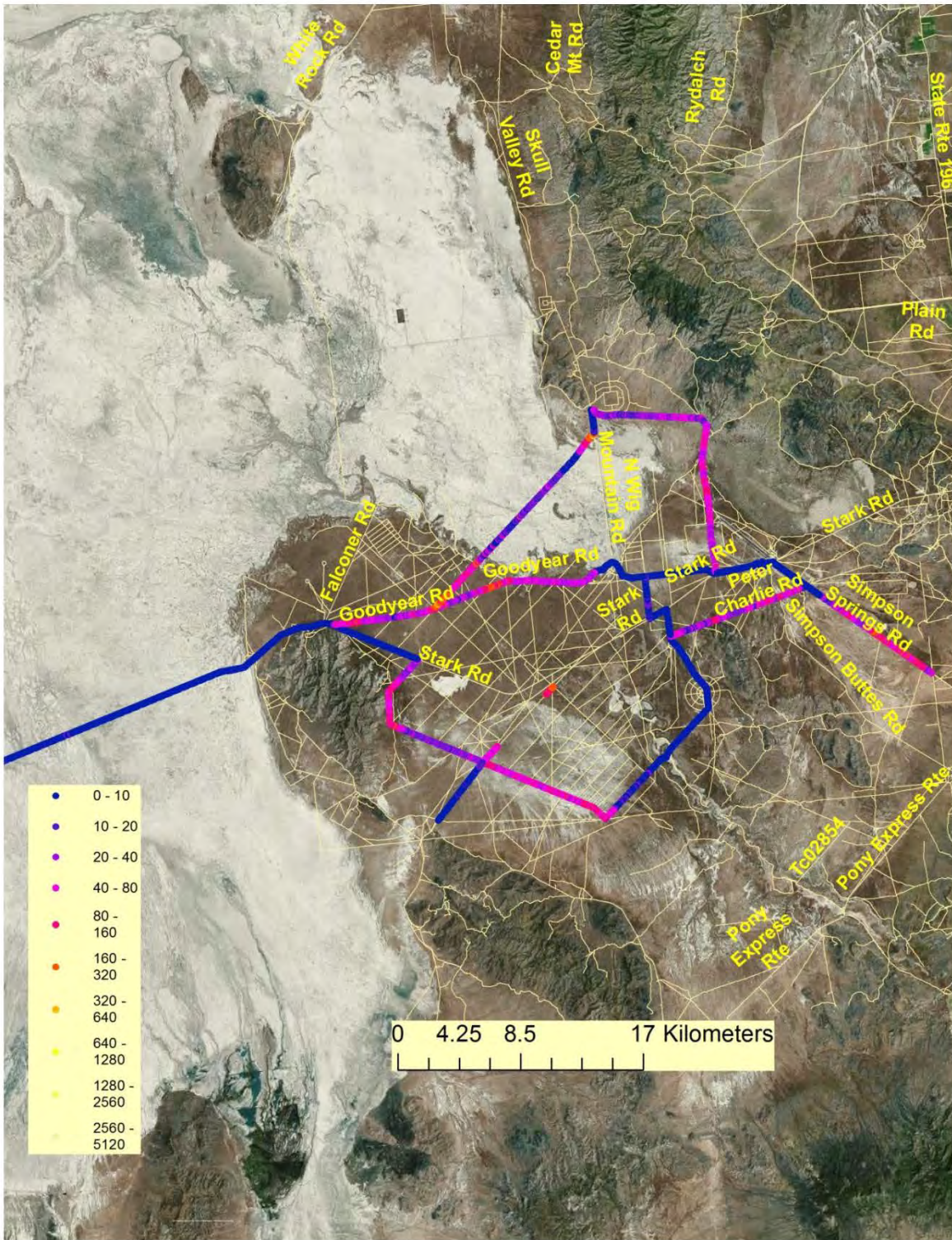
#### 4.3.1 Road dust emission potential Dugway Proving Ground, UT

Figure 16 shows the results of approximately 110 km of roads surveyed by TRAKER™ II and Fig. 17 shows the same information for 93 km of roads surveyed by TRAKER™ III. The two figures use the same scale for ease of comparison. It is clear from visual comparison that TRAKER™ II and III capture the same gross spatial variations in PM<sub>10</sub> road dust emission factors. For a more rigorous comparison, the routes shown in Figs. 16 and Fig. 17 were segmented as shown in Figs. 18 and 19, respectively. The segment start/end locations were chosen somewhat arbitrarily, but are shared between TRAKER™ II and III.

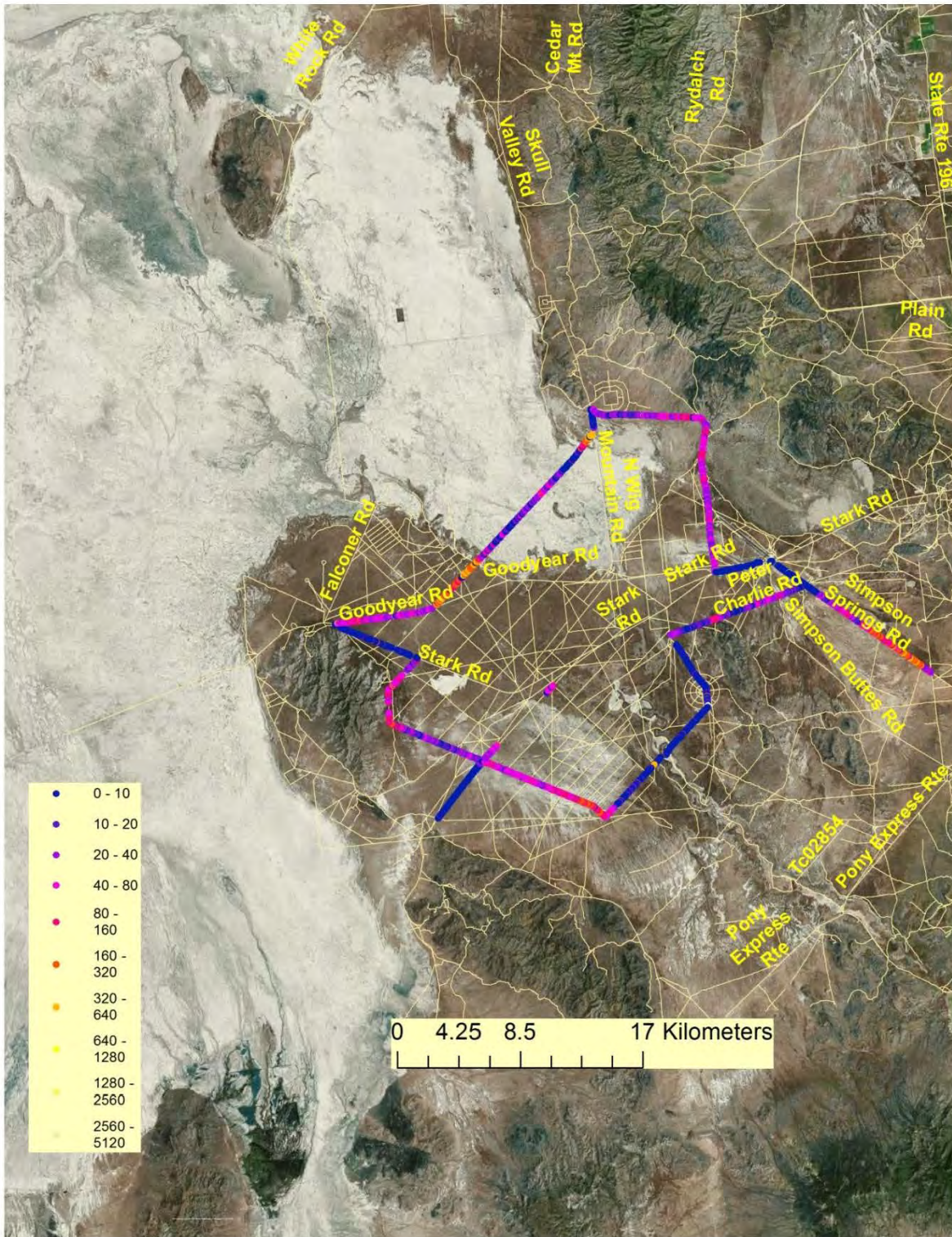
Figure 20 provides a segment by segment comparison between the TRAKER™ II and TRAKER™ III based segment-averaged emission factors. There are some readily seen differences between emission factors on different segments of road. For example, Segment B, which corresponds to the roads in and around the cantonment exhibits relatively low EF values. Segments F2 and F3 are on the same road, but F2 travels through a salt-crusted dry lake bed while F3 travels through the lake bed fringe and onto the alluvial fan.

Although the road bed is raised above the lakebed surface, it appears that F2 is significantly less emissive than F3. Also interesting is the difference in EF between G and H, the former an unpaved road that intersects the latter, a paved road. Noting that there are several different ways to arrive at the same location, these observations suggest that it may be possible to consider and map out travel routes that minimize PM<sub>10</sub> emissions from unpaved road travel at facilities such as DPG when such route modifications do not substantially interfere with the operations of the facility.

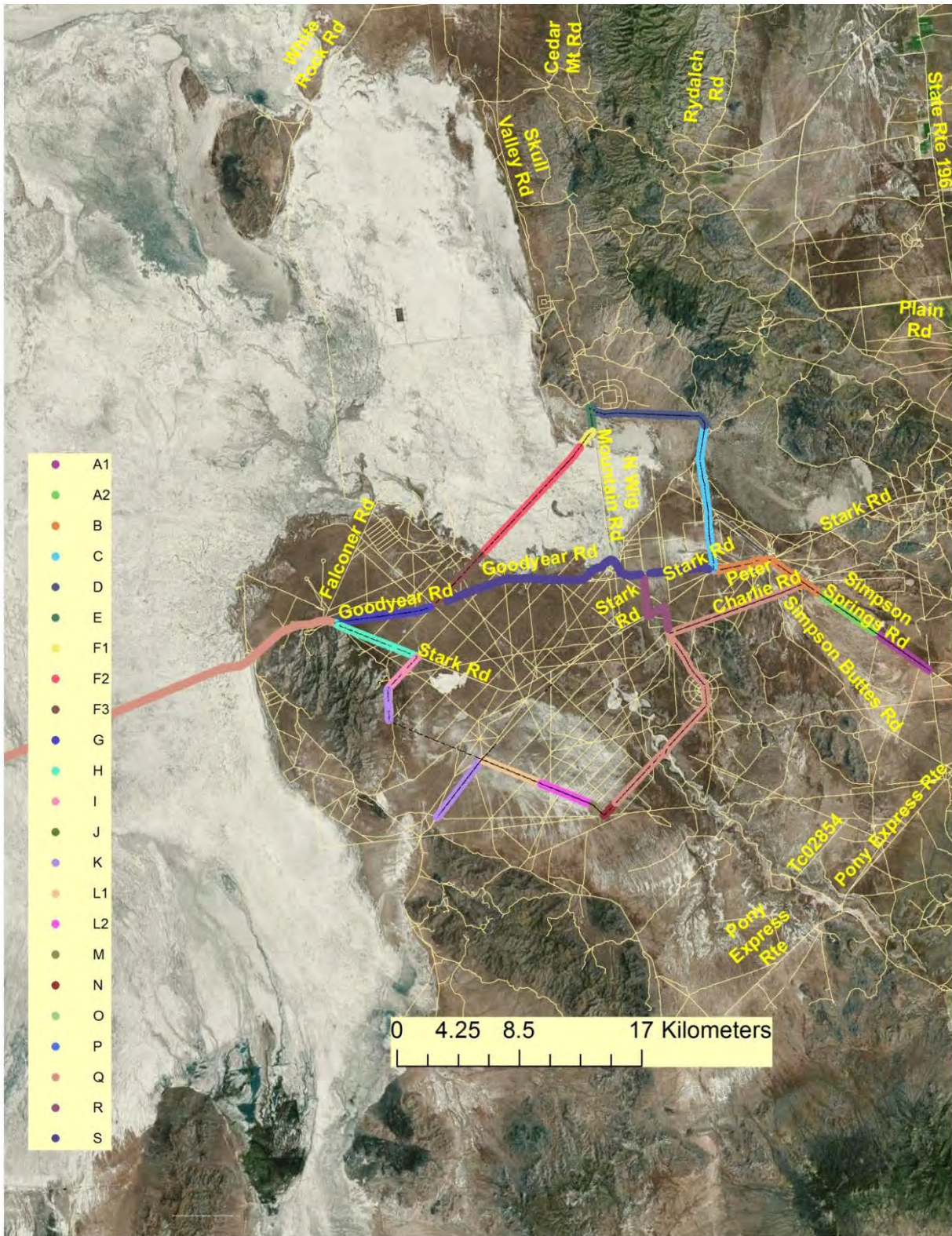
Figure 21 shows the same information as Fig. 20 in a scatterplot format. A least squares regression between TRAKER™ II and III segment averaged emission factors suggests that TRAKER™ III emission factors are about 37% higher than those measure by TRAKER™ II, although the two estimates are well correlated as indicated by a good R<sup>2</sup> value (0.93). This difference can be partially explained by the fact that the mass of the TRAKER™ III vehicle is about 10% greater than that of TRAKER™ II (see Table 1); Gillies et al. (2005) suggest that if all other factors are held equal, then emission factors scale with vehicle momentum, which is the product of the speed and the vehicle mass. Speed was held constant for all of these survey routes (40 km hr<sup>-1</sup>). However, the approximately 10% difference in mass between TRAKER™ III and II would suggest that emission factors for TRAKER™ III would be about 10% higher. The difference between the two technologies is closer to 37%. This is perhaps attributable to other



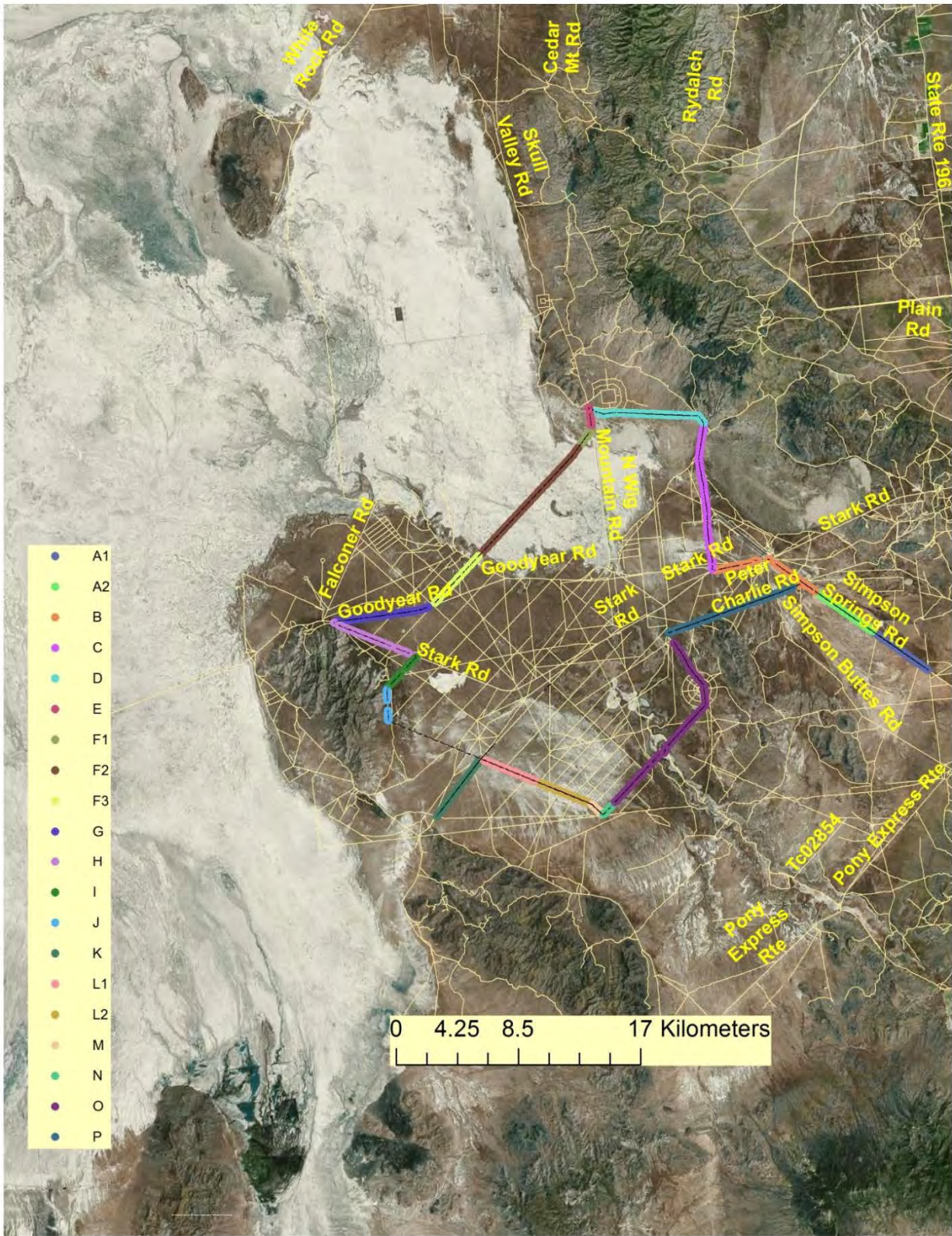
**Figure 16.** Spatial survey of approximately 110 km of DPG roads conducted by TRAKER™ II. Individual one-second TRAKER™ II measurements have been converted into estimates of emission factors using the constants in Table 1. Numbers in color-coded legend correspond to emission factors in units of  $\text{g-PM}_{10} \text{ VKT}^{-1}$ .



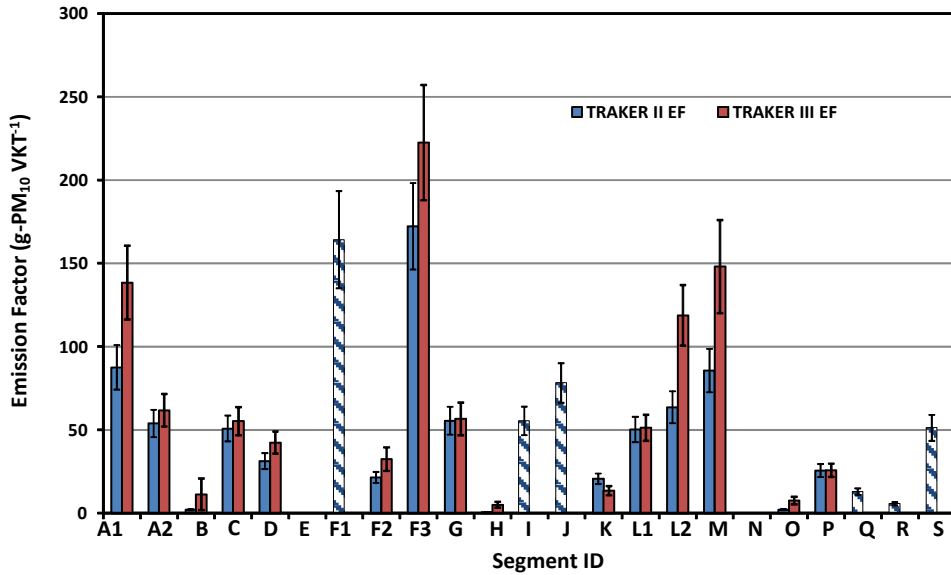
**Figure 17.** Spatial survey of approximately 93 km of DPG roads conducted by TRAKER™ III. Individual one-second TRAKER™ III measurements have been converted into estimates of emission factors using the constants in Table 1. Numbers in color-coded legend correspond to emission factors in units of  $\text{g-PM}_{10} \text{ VKT}^{-1}$ .



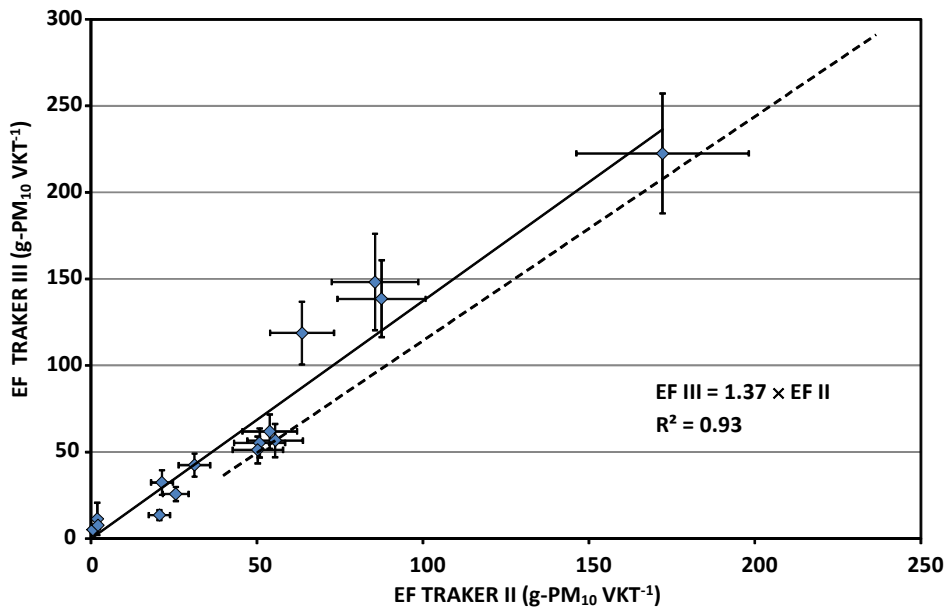
**Figure 18.** Delineation of road segments for TRAKER™ II survey path within DPG.



**Figure 19.** Delineation of road segments for TRAKER™ III survey path within DPG.



**Figure 20.** Comparison of segment averaged emission factors as estimated by TRAKER<sup>TM</sup> II and TRAKER<sup>TM</sup> III. Striped bars correspond to segments where TRAKER<sup>TM</sup> III data are unavailable. The vertical bars represent the propagated uncertainty of the emission factor relationship with the respective TRAKER<sup>TM</sup> signal in combination with the standard error of the average of the signal over the indicated segment.



**Figure 21.** Scatterplot of TRAKER<sup>TM</sup> III versus TRAKER<sup>TM</sup> II segment averaged emission factors (g-PM<sub>10</sub> VKT<sup>-1</sup>) for segments shown in Figs. 17 and 18. The thick dashed line has a slope of 1 and intercept of zero. Vertical and horizontal bars represent the propagated uncertainty of the emission factor relationship with the respective TRAKER<sup>TM</sup> signal in combination with the standard error of the average of the signal over the indicated segment.

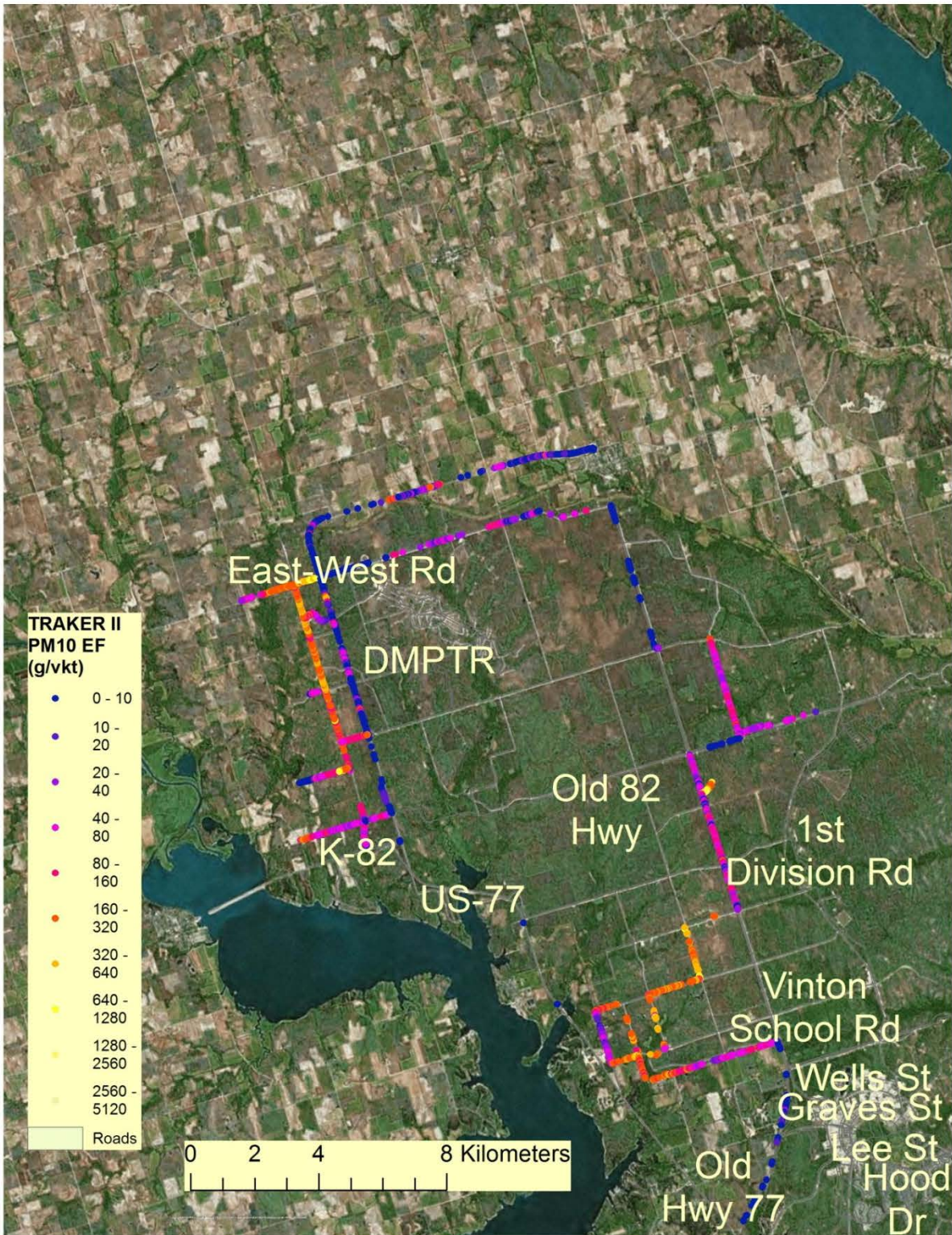
small differences between the vehicles' potentials to emit dust (e.g., tire types and pressures, form factor) or else due to the uncertainty of measurements. Figure 21 shows that the measurement uncertainties are of the same order as the apparent difference between the two TRAKER vehicles.

#### **4.3.2 Road dust emission potential Ft. Riley, KS**

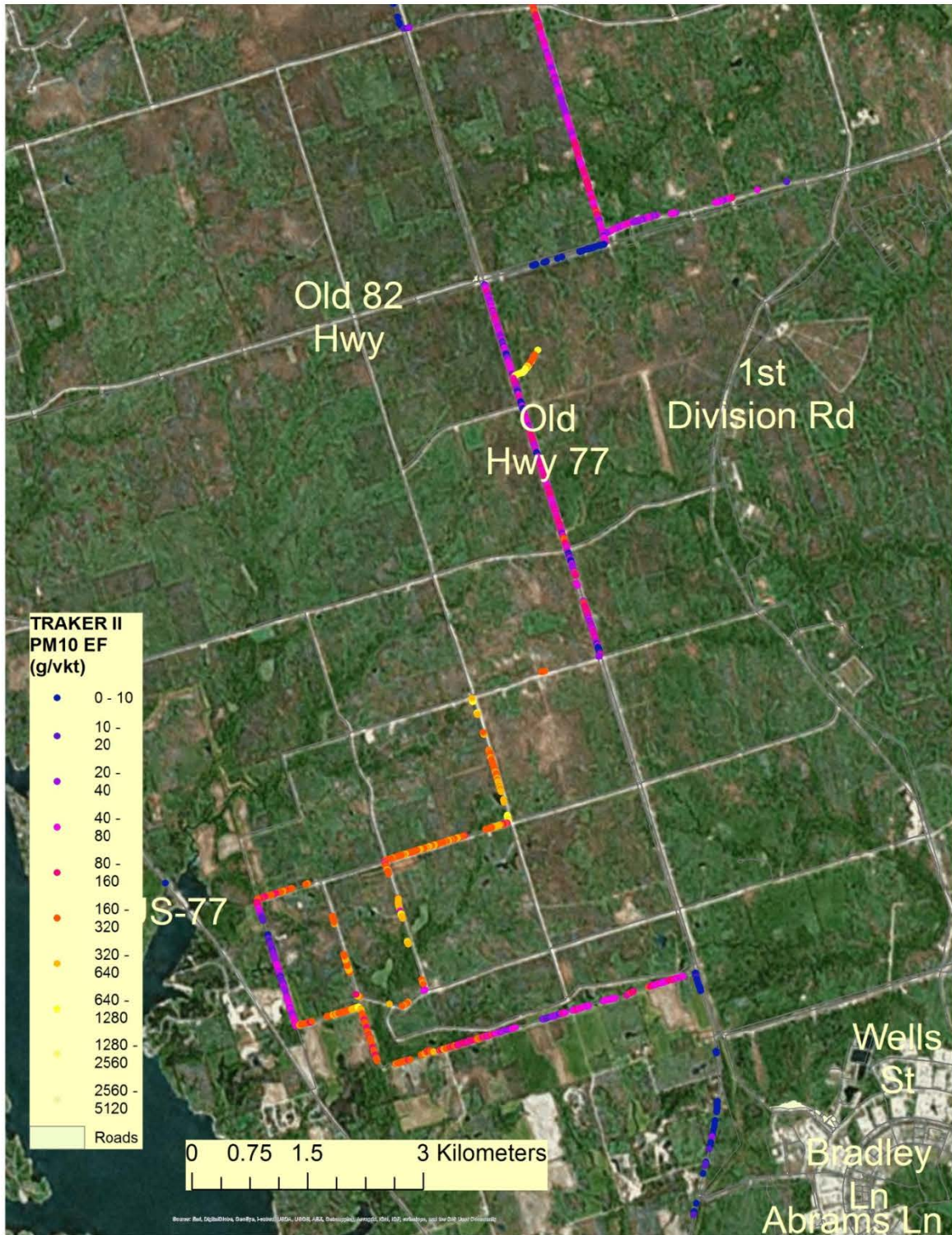
Data recovery from the TRAKER™ II measurements at Ft. Riley was not as complete as at DPG. The main reason for this was a series of TRAKER™ II equipment failures that could not be corrected in the field. The greatest difficulty was encountered with the onboard GPS system, which was unable to obtain and maintain a satellite lock for long periods of time. Consequently, critical information such as vehicle speed, location, and other parameters were often lost during the measurements. A backup GPS system was employed; however, that unit also did not function properly. It is unknown why these GPS units were not working properly at Ft. Riley as no specific malfunction was discovered. In any case, significant amounts of data were recovered and gross comparisons between Ft. Riley and DPG can be drawn.

Figure 22 shows the TRAKER™ II spatial survey results from Ft. Riley. The figure uses the same color scale as the ones used in Figs. 16 and 17 to facilitate direct comparison. In the case of Ft. Riley, all of the traces that show emission factors less than  $20 \text{ g-PM}_{10} \text{ VKT}^{-1}$  (blue dots) correspond to paved access roads. Unpaved roads are those that are orange and red.

Interestingly, emission factors from unpaved roads at Ft. Riley appear to be much greater on average than those from DPG. This is perhaps because almost all unpaved DPG roads were graded and covered with gravel whereas at the time of measurements, many of the unpaved roads at Ft. Riley had been heavily degraded – possibly by recent exercises that had been conducted there. Some of the Ft. Riley roads where chipping techniques had been used intermittently exhibited emission factors between those for paved and unpaved roads (see purple dots in close-up section of Fig. 23).



**Figure 22.** Spatial survey of Ft. Riley roads conducted by TRAKER™ II. Individual one-second TRAKER™ II measurements have been converted into estimates of emission factors using the constants in Table 1. Numbers in color-coded legend correspond to emission factors in units of g-PM<sub>10</sub> VKT<sup>-1</sup>.



**Figure 23.** Spatial survey of Ft. Riley roads conducted by TRAKER™ II zoomed into southeast quadrant. Numbers in color-coded legend correspond to emission factors in units of g-PM<sub>10</sub> VKT<sup>-1</sup>.

## 4.4 Moisture and suppressant effects on road dust emissions

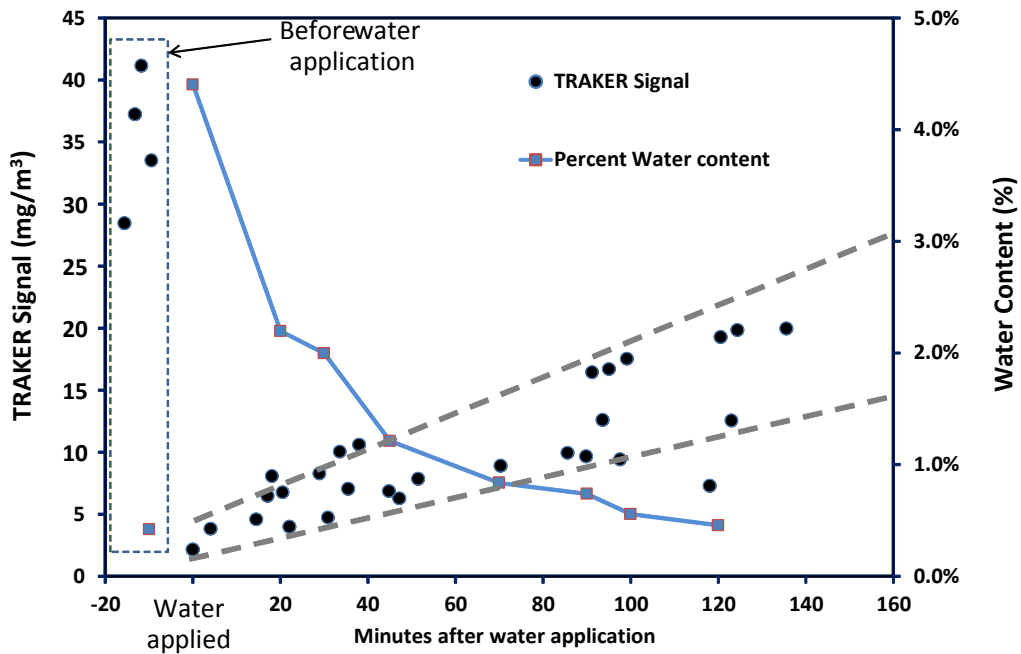
### 4.4.1 Moisture effects on road dust emissions at Ft. Riley, KS and the Dugway Proving Ground, UT

Moisture effects on dust emission measurement campaigns were carried out at Ft. Riley, KS in 2010 on one road and at the DPG, UT in 2012, on three different roads (codenamed Lima, an unnamed road perpendicular to Lima [named here Lima-P], and X-Ray). In both locations the initial moisture content of the roads was less than 0.5%. The moisture content was raised to over 3.5% for all test roads immediately after application of water to the road surfaces over the length of the test segments.

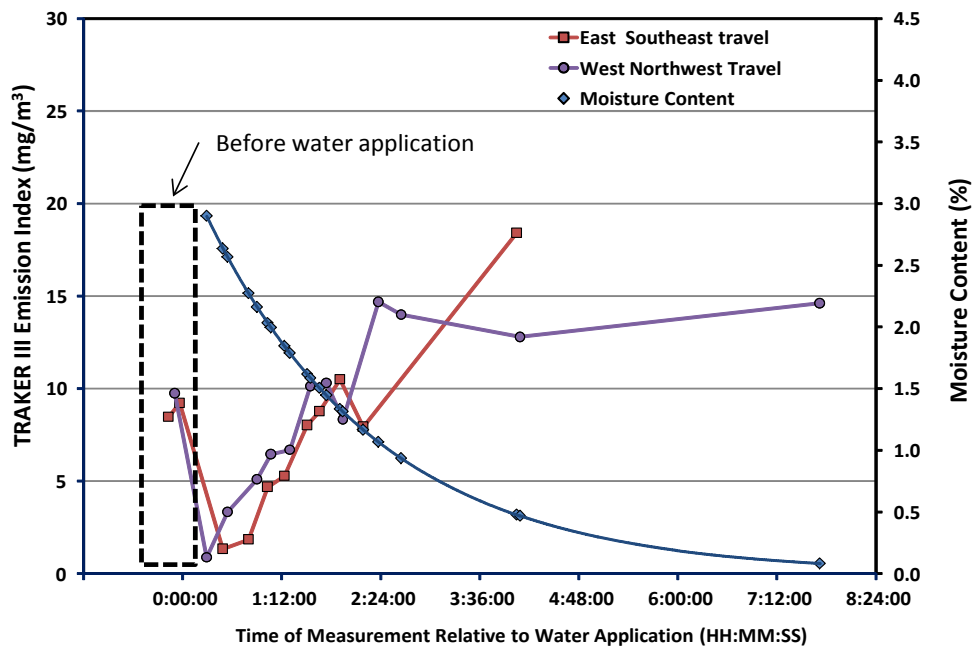
It is important to note that the application of water is not a well-controlled process. Typically, several sprayers are used at the back of the water truck to disperse the water onto the road. However, the flow visibly varies between one sprayer and the next. The application rate of the water is controlled by a valve setting for the water sprayers as well as by the rate at which the truck is moving. Neither of these parameters can be controlled precisely. Therefore, the amount of water applied to the road surface will vary substantially on small spatial scales (order 0.1 – 1 m) due to heterogeneity in sprayer effectiveness and on larger spatial scales (10 – 100 m) due to variations in water delivery rate through the sprayers and water truck travel speed. Related to this, the collection of soil samples for moisture analysis is essentially a point measurement on a long road. Although an effort was made to obtain samples from up to three different areas within a few meters of one another to mitigate some of the small-scale heterogeneity, it was not possible to capture the distribution of soil moisture over larger spatial scales. Thus, while we expect that the entire road surface was qualitatively undergoing the same drying over the course of the experiment, the absolute amounts of soil moisture are likely to vary significantly from one location to the next.

Prior to water application, the TRAKER™ (II at Ft Riley and III at DPG) was operated over the test road segment several times to provide a PM<sub>10</sub> dust emission signal prior to treatment. After water application, the TRAKER™ traversed the test road segments every two to three minutes in alternating directions. There were periods when the time between traversals was longer than a few minutes and as long as twenty minutes in one case. These corresponded to periods when there was an instrument malfunction that required user intervention. For each test road segment traversal when TRAKER™ II (Fig. 4) was used (i.e., at Ft. Riley, KS), the TRAKER™ signals from the left and right inlet lines were averaged together and then averaged over the time it took to traverse the segment. This was not necessary when using TRAKER™ III (Fig. 3) at DPG due to its different design.

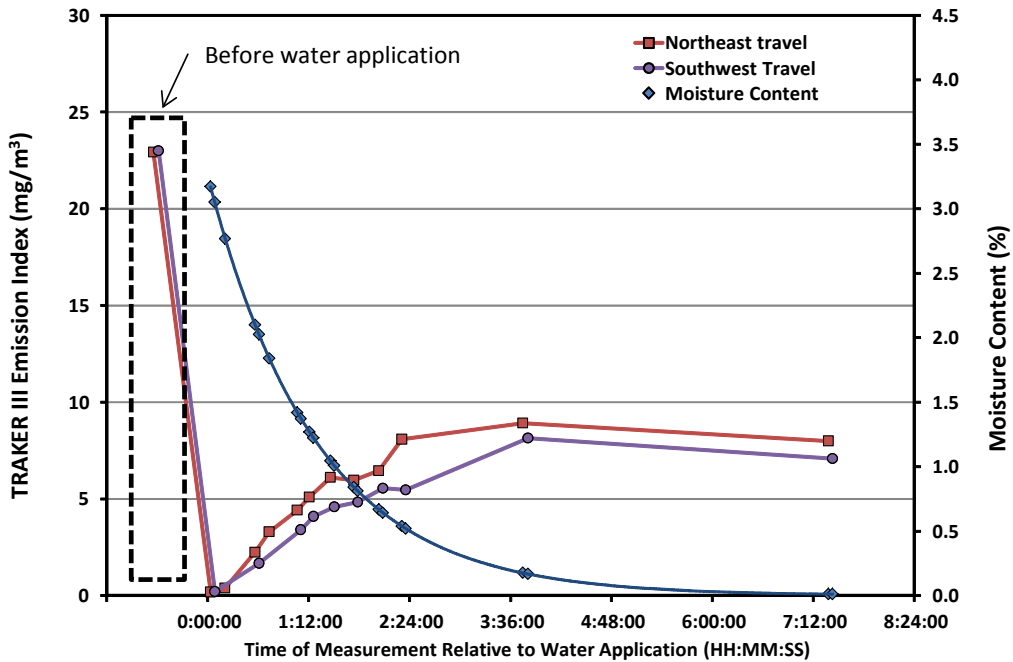
TRAKER™ results, along with the soil moisture content are plotted as a function of time before and after road watering for each of the four test roads, in Fig. 24 for Ft. Riley, and Figs. 25 to 27 for DPG. Moisture content in these figures is represented by the best-fit regression line based on the moisture content of samples collected and the time elapsed between collection



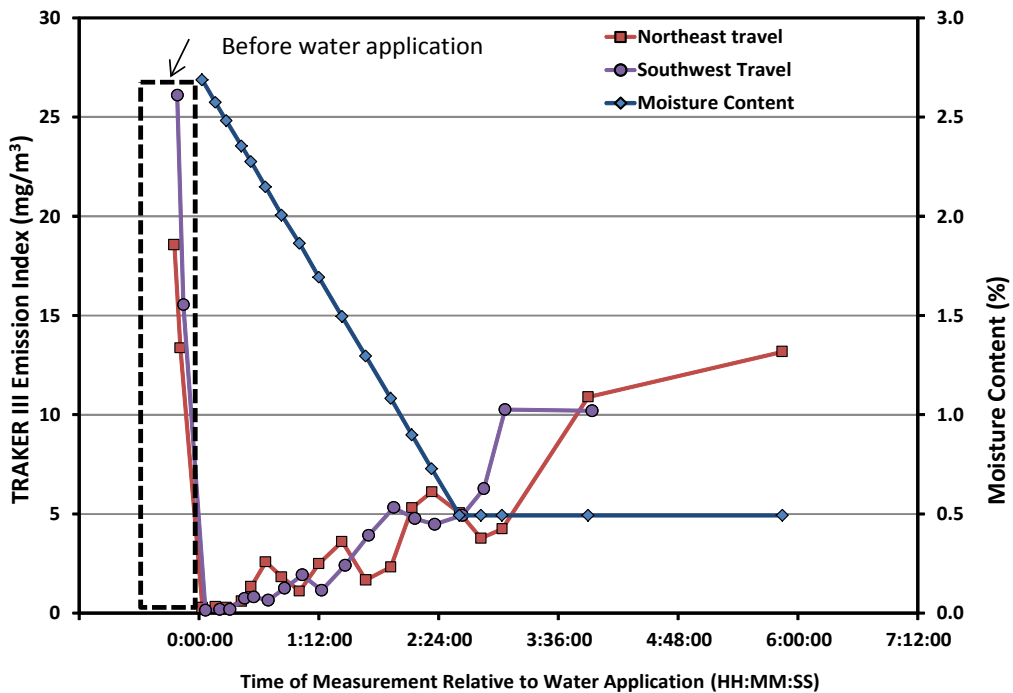
**Figure 24.** The relationships between duration of time after application of water, dust emissions as measured by TRAKER™ II and water content of the test road at Ft. Riley, KS.



**Figure 25.** The relationships between duration of time after application of water, dust emissions as measured by TRAKER™ III and water content of the Lima-P test road at DPG, UT, 10-30-2012.



**Figure 26.** The relationships between duration of time after application of water, dust emissions as measured by TRAKER™ III and water content of the Lima test road at DPG, UT, 10-30-2012.

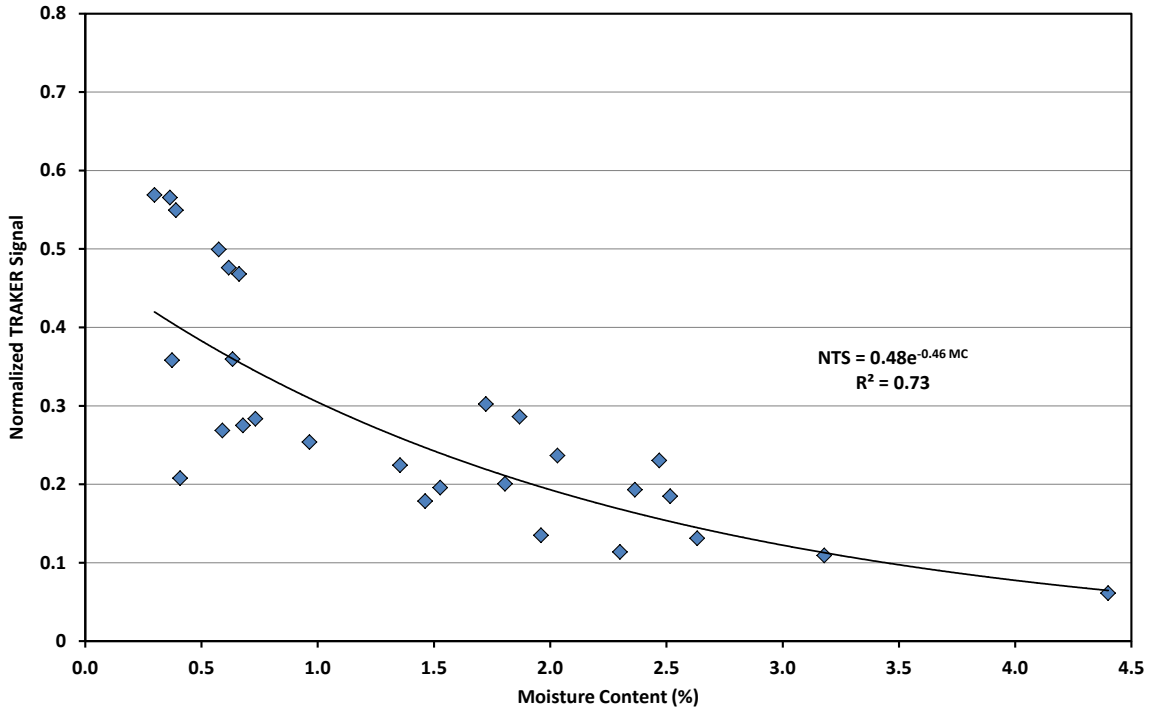


**Figure 27.** The relationships between duration of time after application of water, dust emissions as measured by TRAKER™ III and water content of the X-Ray test road at DPG, UT, 11-1-2012.

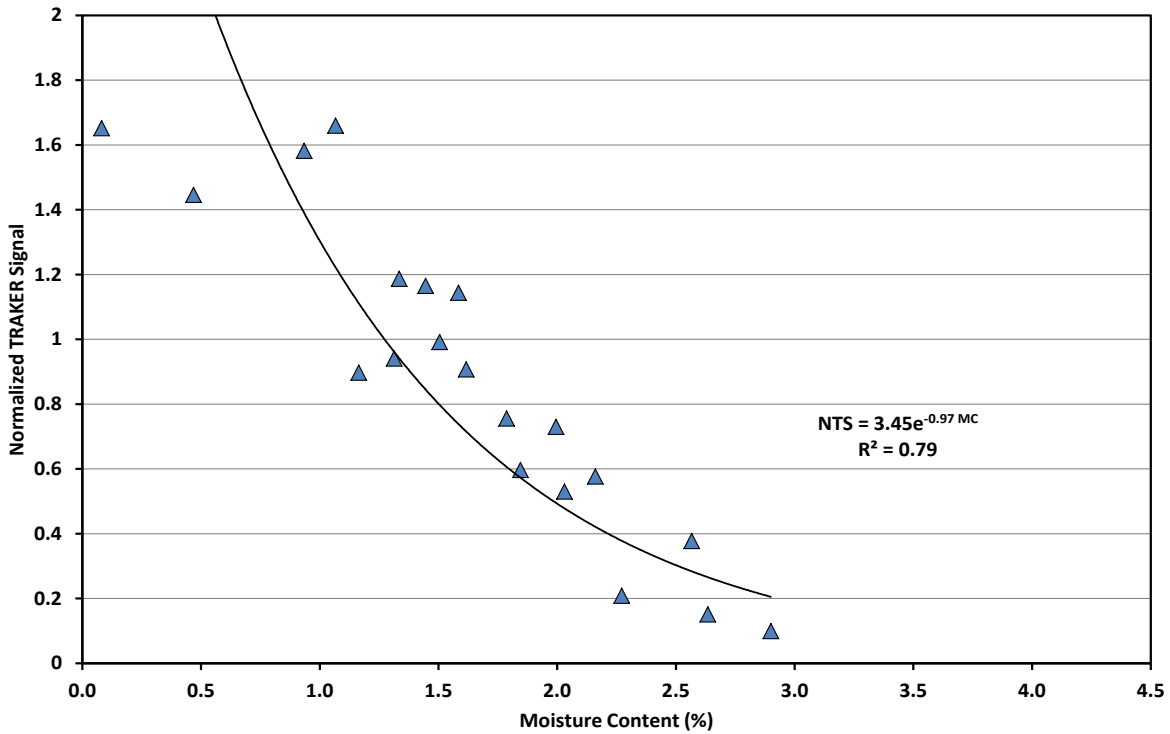
periods after the water was applied. This was done so that TRAKER™ signal could be compared with moisture content interpolated between collection periods. The TRAKER™ measurements clearly indicate that the emission potential changes dramatically after application of water. There is significant variation in TRAKER™ signal values from one measurement to the next, indicating perhaps that small variations where the vehicle tires contact the road can greatly affect the average emissions for any given traverse. However, on the whole, these data indicate that the effect of watering begins to diminish within as little as 10 – 20 minutes after application and continues to do so for at least two hours. This will be influenced by the ambient drying conditions (air temperature, relative humidity, and wind speed), as well as the vehicle traffic levels.

The relationship between PM<sub>10</sub> emissions and moisture content of the road material is evident in Figs. 28-31. In these figures the TRAKER™ signal in each case is normalized by dividing the measured signal by the mean TRAKER™ signal prior to wetting to allow comparison among the sites. The data are averaged based on multiple passes in both directions. These figures all show that this relationship, regardless of the differences in the test road characteristics (i.e., its textural characteristics [% gravel, sand, silt, and clay]), is best-described by an exponential function. Considering all four data sets, PM<sub>10</sub> emissions are reduced between 88% and 99% from their pre-wetted condition if moisture content reaches 3.5%. The absolute TRAKER™ signal is plotted against moisture content for the four test roads in Fig. 32 to illustrate that the test roads are not equally emissive for the same moisture content. This suggests that the textural characteristics of the road bed material also influence the strength of the emissions.

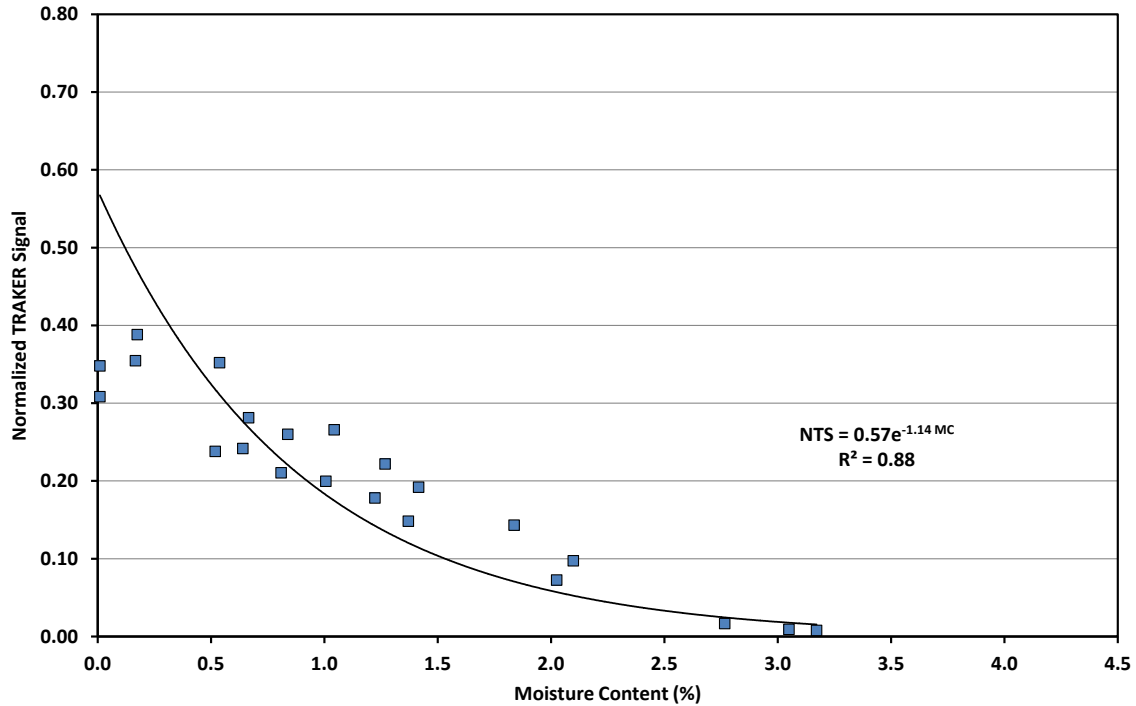
After 120 minutes, soil moisture levels had nearly returned to pre-wetted values in all four test cases. In contrast, dust emission potential had only returned to 19%, 28%, and 55% of the pre-wetted values for, respectively X-Ray, Lima, and Ft. Riley test roads over the same time period. The exception to this was the Lima-P test road that returned to its pre-wetted emission potential in 120 minutes. This was not evident at the time of testing since the TRAKER™ and moisture content data are post-processed and such information is not available in the field. These data may indicate that some parts of the test road were still wet while other parts, such as the section where soil moisture samples were collected, were dry. Alternatively, it may be that the application of water has a modest longer-term dust-suppressing effect in addition to the dramatic short-term effect. It would be important in future measurements to measure soil moisture at a sufficient number of locations to determine which of these two possibilities is more likely. It is unclear at this time if the road dust emission potential would have continued to increase past 120 minutes or at what rate such an increase might have occurred. We simply note here that a least-squares linear fit to the data sets collected in the first 120 minutes suggests that these roads regain, on average, 6.7% ( $\pm 3.1\%$ ) of their dust emission potential every minute after water application.



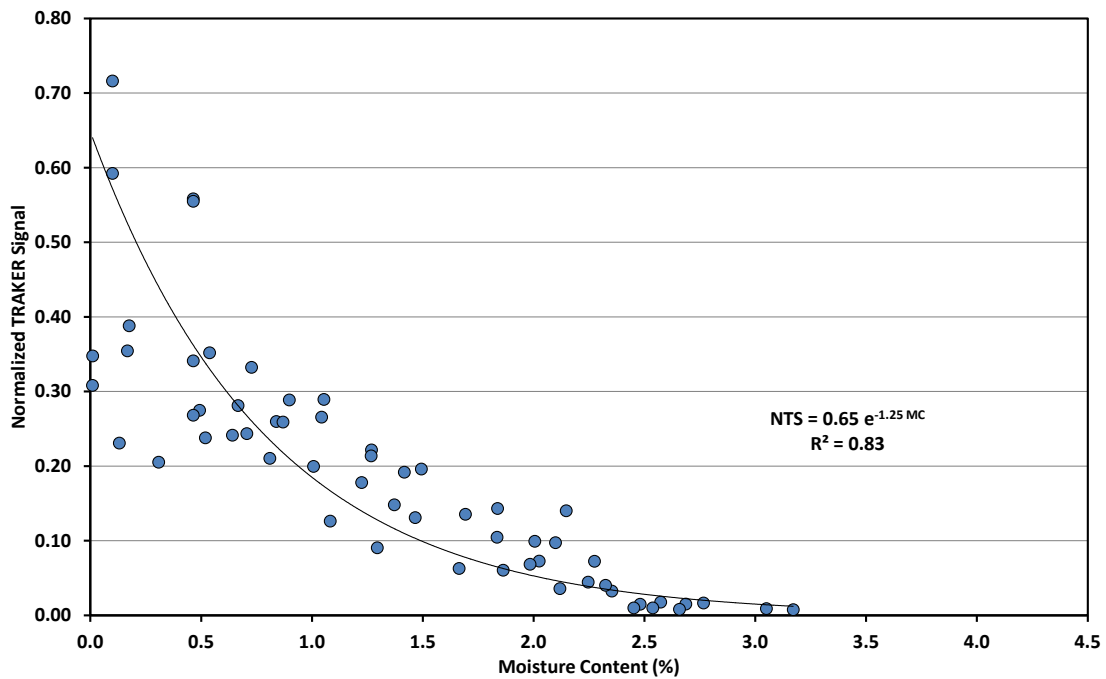
**Figure 28.** The relationship between normalized TRAKER™ signal (measured using TRAKER™ II) and moisture for the test road at Ft. Riley, KS.



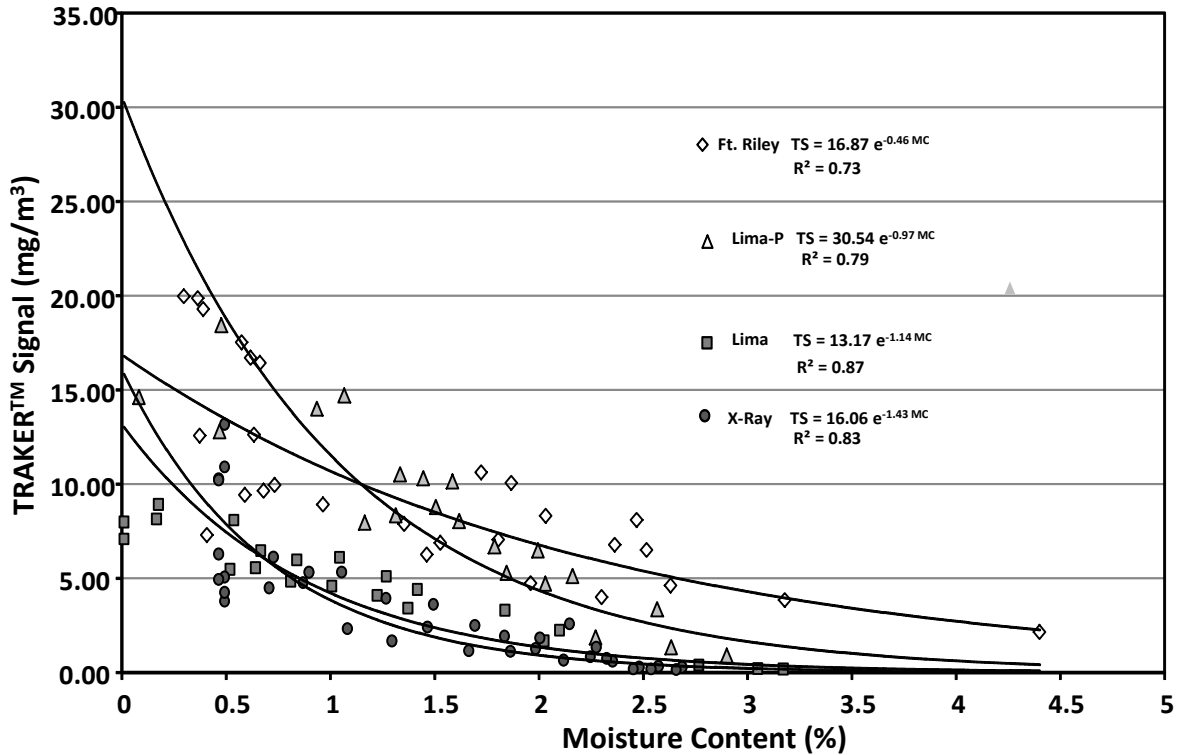
**Figure 29.** The relationship between normalized TRAKER™ signal (measured using TRAKER™ III) and moisture content for the Lima-P test road at DPG, UT, 10-30-2012.



**Figure 30.** The relationship between normalized TRAKER<sup>TM</sup> signal (measured using TRAKER<sup>TM</sup> III) and moisture content for the Lima test road at DPG, UT, 10-30-2012.



**Figure 31.** The relationship between normalized TRAKER<sup>TM</sup> signal (measured using TRAKER<sup>TM</sup> III) and moisture content for the X-Ray test road at DPG, UT, 11-01-2012.



**Figure 32.** The relationship between TRAKER™ signal (measured using TRAKER™ II and III) and moisture content for the four test roads.

#### 4.4.2 Long-term use of Magnesium Chloride on the Mannix Road, Ft. Irwin CA

The Mannix Road is part of an access route between Ft. Irwin and Barstow, CA, and routinely receives magnesium chloride ( $MgCl_2$ ) dust suppressant treatment on a quarterly basis. The DRI TRAKER™ III was deployed in June, July, and September 2014 to characterize its  $PM_{10}$  dust emission factor (g of  $PM_{10}$  released per kilometer of vehicle travel). The acquired data from TRAKER™ was used to provide estimates of total  $PM_{10}$  emissions (tons) based on knowledge of emission factors for wheeled and tracked military vehicles, and the known vehicle traffic inventory in June, July, and August 2014.

Emission potential estimates for each of the 10 segments (Fig. 33) of the Mannix Road for the three measurement periods for TRAKER™ are provide in Table 2. The  $PM_{10}$  mass concentrations measured in the vehicle wake were converted to g- $PM_{10}$  produced per vehicle



**Figure 33.** Mannix Road segments used for segregating data.

**Table 2.** The mean per segment emission factors based on TRAKER™ measurements (TRAKER™ mass is 2738 kg) for the three measurement periods.

Segment ID*	Segment Length (km)	Emission Factor (g-PM10/vehicle km travelled)		
		June 12 & 13, 2014	July 2, 2014	September 11, 2014
1	1.8	22.5	24.7	35.3
2	3	244.2	232.0	278.5
3	1.6	42.5	28.2	5.5
4	4.3	56.3	39.7	5.1
5	5.6	258.0	112.7	6.4
6	5.7	129.8	63.9	5.9
7	6.5	90.5	75.8	6.2
8	6.4	56.4	67.5	11.8
9	3.2	29.2	27.0	3.1
10	2.9	80.6	86.3	8.9
Weighted Average (sum of EF/total length of road)		24.6	18.5	8.9

\*refer to Fig. 2 for segment location on Mannix Rd.

kilometer travelled by application of the calibration relationship developed using our flux-tower method (Gillies et al., 2005) from measurements made at the DPG, UT.

Emission potentials are somewhat low for an unpaved road both before and after  $MgCl_2$  treatment with a mean value of  $PM_{10}$  mass concentration for all measurement periods and segments of  $1.12 \text{ mg m}^{-3}$  ( $\pm 1.13 \text{ mg m}^{-3}$ ) (corresponding to a range of 19 to 39  $\text{g-PM}_{10} \text{ VKT}^{-1}$  for a vehicle the size of a pickup truck). This is much lower than previously measured for unpaved roads at other military installations for a similar sized vehicle. For example at a speed of  $40 \text{ km hr}^{-1}$  (same as maintained for the Mannix Road testing) the emission factors for TRAKER™ at DPG, UT was approximately  $418 \text{ g-PM}_{10} \text{ VKT}^{-1}$  and Ft. Riley, KS,  $533.4 \text{ g-PM}_{10} \text{ VKT}^{-1}$  (TRAKER™ used at Ft. Riley was a slightly lighter weight version).

There are too few data for formal statistical analysis, but it is clear that there is no order-of-magnitude (factor of 10) or even factor of three improvements in emission potential after treatment compared to before treatment for any of the segments in either travel direction. Data collected on 9/11/2014 indicate that recent rainfall events had significantly impacted the potential for road dust emissions. Whereas segments 1 and 2 showed comparable emissions to prior measurements, emissions from segments 3 – 10 were clearly lower by several-fold. In examining the elevation profile, it appears that the low-lying portions of Mannix Road were wet at the time of sampling in September. Puddles of water on the road were observed to be present in the segments closer to Highway I-15 and removing the hard surface crust on segments 3-10 revealed damp road material underneath.

The TRAKER™ data suggest that the Mannix Road in the condition that existed from June through the beginning of September 2014, emits very low amounts of  $PM_{10}$  as a function of this (heavy pickup truck) size vehicle travelling at  $40 \text{ km hr}^{-1}$  ( $\approx 25 \text{ m.p.h.}$ ). To reach the limit of 100 tons of  $PM_{10}$  emitted in one year would require 90,016, 41 km long trips based on the June 2014 mean weighted emission factor, 119,997 trips for the July 2014 mean weighted emission factor, and 248,010 trips for the September 2014 mean weighted emission factor. This amounts to approximately, for the low (September) and high (July) mean weighted emission factors, 689 trips per day and 250 trips per day, respectively.

#### **4.4.3 Total $PM_{10}$ emissions from Mannix Road based on vehicle travel inventory data**

Data detailing vehicle type, weight, and number of trips for three rotations (January, April, and June 2014) at Ft. Irwin were received from U.S. Army Environmental Command, which allow for the estimation of total  $PM_{10}$  emitted by vehicles that travelled the Mannix Road based on several assumptions. These assumptions are: 1) the vehicles travel at the posted speed limit (25 mph [ $40 \text{ km hr}^{-1}$ ], 2) the emissions scale as a function of the product of vehicle weight and speed (Gillies et al., 2005; Kuhns et al., 2010), and 3) the emissions for each vehicle type scale linearly with the TRAKER™-measured emissions.

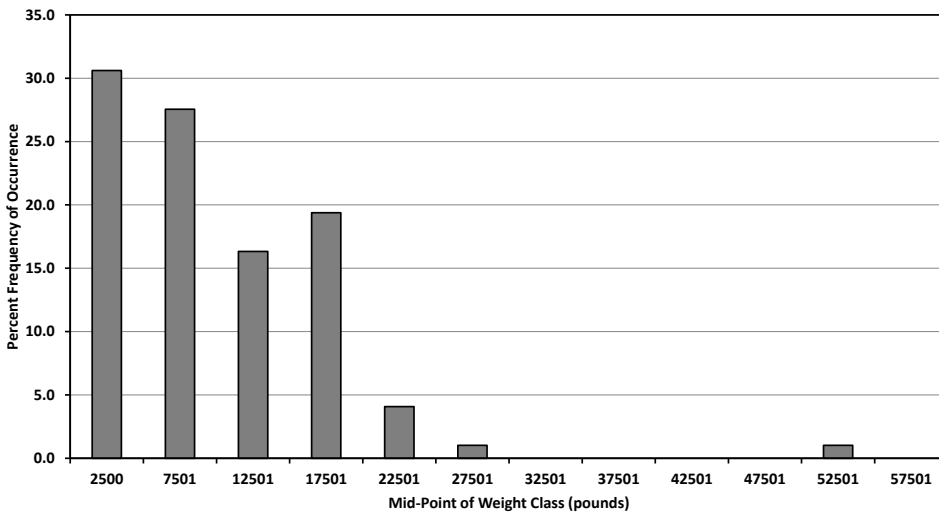
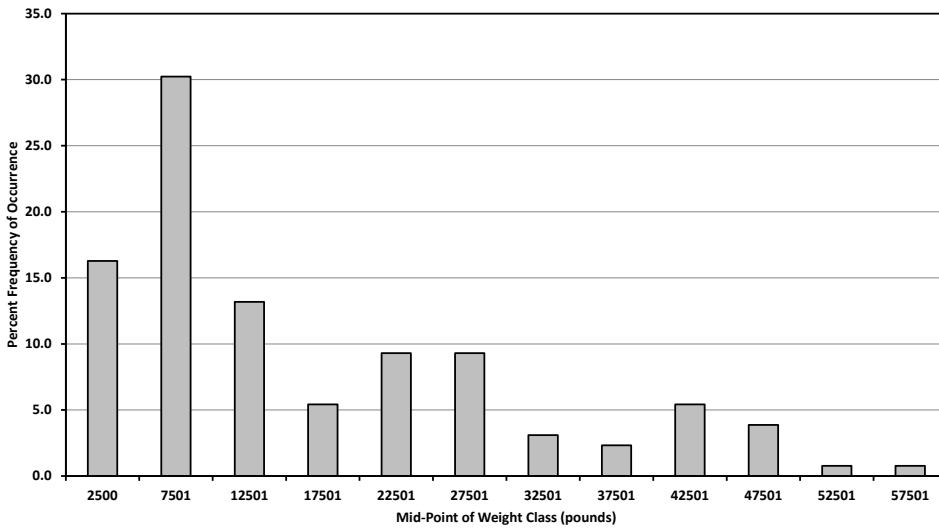
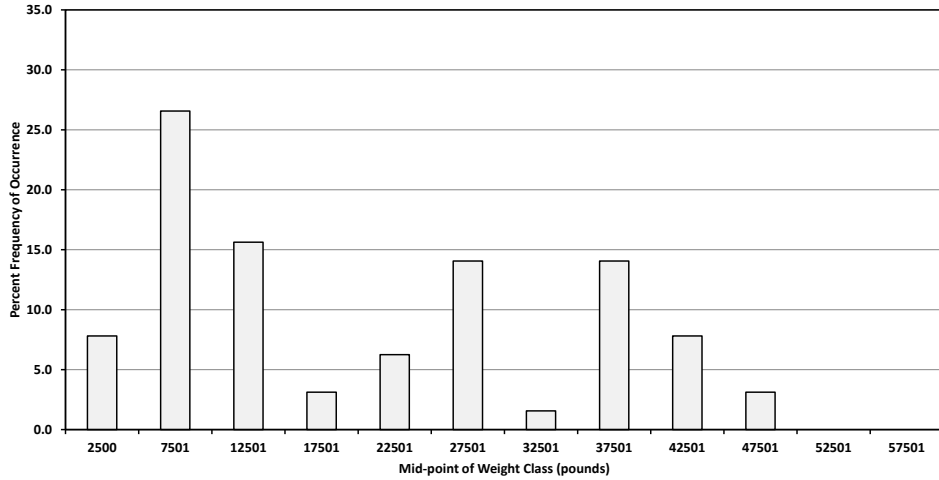
Estimates of the total  $PM_{10}$  for each rotation based on scaling up the TRAKER™ data for each vehicle type (i.e., vehicle weight) and each rotation are shown in Table 3. The change in the

total emitted PM<sub>10</sub> is a function of the vehicle numbers and different distributions of vehicle weights between the three rotations. The differences in vehicle weight distribution by rotation are shown as percent frequency of occurrence histograms of vehicle weight classes (5000 pound intervals) in Fig. 34. Rotations 3 and 6 have a higher percentage of heavy vehicles than rotation 8, but there were more vehicles travelling the Mannix Road during rotation 8.

For comparison purposes the total PM<sub>10</sub> mass emitted by the vehicles during a rotation period was calculated based on the emission potential measured in each of the ten defined segments for each of the three measurement periods (June, July and September 2014). The far right column in Table 3 represents total emissions of PM<sub>10</sub> if the Mannix Road was emitting similarly to unpaved (and non-dust suppressant treated) roads at Ft. Bliss, TX and Ft. Collins, CO. These estimates indicate that the Mannix Road is producing PM<sub>10</sub> as a function of vehicle traffic at much lower amounts than the Ft. Bliss and Ft. Carson unpaved roads and that for the three rotation periods the sum of all the emitted PM<sub>10</sub> is approximately ten times less than the allowable limit of 100 tons. By using the percent variation in PM<sub>10</sub> emissions in each segment as quantified by TRAKER™, an upper-bound of these total PM<sub>10</sub> emission values can be estimated. For the 10 segments in the three measurement periods the in-segment variation in emissions ranged from a low of 6% (June period, segment 8) to a high of 113% (September, segment 2). Applying the observed individual variance in each increases emissions by 86% to 228%, however, the total emissions increase by between 1.32 tons and 3.62 tons, which still results in total emissions well below the 100 ton limit. Only if the Mannix Road had an emission potential similar to roads at

**Table 3.** Estimates of total PM<sub>10</sub> emitted for each rotation vehicle inventory based on scaling the TRAKER™ per segment emission factor as a function of vehicle weight for the inventoried vehicles. The total emissions if the Mannix Road was emitting similarly to roads at Ft. Bliss, TX and Ft. Collins, CO, are shown in the far-right column. Vehicle speed is assumed to be 40 km hr<sup>-1</sup>.

Rotation #	Month	Total # Vehicles	Tons of PM <sub>10</sub> Emitted				FT. Bliss/Ft. Carson EF Levels
			Sum of 10 Segments, Pre MgCl <sub>2</sub> (June)	Sum of 10 Segments, Post 1 MgCl <sub>2</sub> (July)	Sum of 10 Segments, Post 2 MgCl <sub>2</sub> (September)		
3	January	1477	3.27	2.43	1.10	36.77	
6	April	951	1.78	1.33	0.63	3.66	
8	June	1624	4.22	3.16	1.53	46.37	
Sum for Rotations		4052	9.26	6.92	3.25	86.81	
Mean of 3 Rotations		1351	3.09	2.31	1.08		



**Figure 34.** Frequency distributions of vehicle weight for the three rotations at Ft. Irwin: top panel rotation 1, middle panel rotation 2, and bottom panel rotation 3.

Ft. Bliss and Ft. Carson would the amount of PM<sub>10</sub> released by all three rotations combined (≈87 tons) be close to the limit allowed.

For the inventory data from the three rotations, the mean number of vehicles was 1351.

Assuming this represents a typical number of vehicles in a rotation, one rotation each month, applying the low and high total (mean) emissions, based on data presented in Table 3, the annual total emissions would be between 13 (1.08 tons per month × 12 months) and 37 (3.09 tons per month × 12 months) tons of PM<sub>10</sub>, which is well below the limit of 100 tons.

#### **4.4.4 Potential Contributions of PM<sub>10</sub> from Military vehicles traveling the Mannix Road**

Based on our previous research to characterize the emission factors of PM<sub>10</sub> produced by wheeled and tracked military vehicles (Gillies et al., 2005; Gillies et al., 2010; Kuhns et al., 2010) estimates of the emissions from specific types of vehicles travelling on the Mannix Road can be made. We have observed that the magnitude of vehicle emissions, wheeled and tracked, is strongly related to its speed and its weight (Gillies et al., 2005; Kuhns et al., 2010) and that this is best-described by a linear relationship. Because these relationships are linear in nature, measurements made with one type of vehicle (i.e., TRAKER™) can be scaled to represent the emissions from vehicles that are heavier or travelling at a different speed. Based on the known scaling relationships for emission between TRAKER™ and other military vehicles, the emissions for four military-type wheeled vehicles and six tracked vehicles for one 41 km long trip on the Mannix Road and the total number of passes required to reach the 100 ton limit for PM<sub>10</sub> emissions are shown in Table 4.

As Table 4 shows the numbers of vehicles, regardless of vehicle type, required to make trips over the 41 km length of the Mannix Road to reach the allowable limit are quite high. It would require for the lowest emitting vehicle (TRAKER™ for September conditions), 689 trips per day every day for one year, and for the highest emitting vehicle (M1A1, for June conditions), 30 trips per day every day for one year. It is clear from the data presented in Tables 3 and 4 that the Mannix Road currently produces very limited amounts of PM<sub>10</sub> as function of vehicle traffic with the assumption of travel at the posted speed limit. The estimated emissions are conservative because it is highly likely that the mean vehicle speed is less than the posted speed limit as the larger vehicles probably cannot reach that limit due to the grade over parts of the road, and the presence of a sufficient number of curves that require reduced speeds.

These data suggest that a strong case can be made for reducing the use of MgCl<sub>2</sub> dust suppressant on the Mannix Road. The application could be curtailed or reduced until the road surface degrades, due to vehicle travel and physical/chemical weathering, to a level where vehicle-created emissions threaten to reach the 100 ton limit for the projected vehicle emission inventory if that is known, or a typical inventory based on long-term inventory records. Although the rate of degradation of the road surface and the resulting increase in emissions is not currently well-defined, we do know that from July through to September 2014, the emission

**Table 4.** PM<sub>10</sub> produced by vehicles traveling the Mannix Road for the emission conditions measured during the three sampling periods (June, July, and September 2014) and the number of vehicle trips it would take for each vehicle to make to reach the 100 ton limit for PM<sub>10</sub> emissions, assuming a travel speed of 40 km hr<sup>-1</sup> (≈25 mph, the posted speed limit).

Vehicle	kg-PM <sub>10</sub> from one 41 km trip			Tons of PM <sub>10</sub> from one 41 km trip			# passes to reach 100 tons		
	June	July	September	June	July	September	June	July	September
<b>Wheeled</b>									
TRAKER III	1.01	0.76	0.37	0.001	0.001	0.0004	90016	119979	248010
HUMVEE	1.41	1.06	0.51	0.002	0.001	0.001	64297	85699	177150
LMTV	2.83	2.12	1.03	0.003	0.002	0.001	32148	42850	88575
5-ton	7.27	5.46	2.64	0.008	0.006	0.003	12502	16664	34446
HEMTT	7.37	5.53	2.68	0.008	0.006	0.003	12331	16436	33974
<b>Tracked</b>									
M1A1	8.48	6.36	3.08	0.009	0.007	0.003	10716	14283	29525
BFV	3.94	2.96	1.43	0.004	0.003	0.002	23081	30764	63592
M113A3	1.31	0.99	0.48	0.001	0.001	0.001	69243	92292	190777
M577	2.42	1.82	0.88	0.003	0.002	0.001	37506	49991	103338
M88	4.28	3.21	1.55	0.005	0.004	0.002	21230	28297	58493
M270	3.43	2.58	1.25	0.004	0.003	0.001	26475	35288	72944

potential of the road remained relatively unchanged, suggesting the vehicle traffic during that period did not adversely affect the road.

To determine how the degradation is occurring through time we recommend that the potential roadway emissions be measured regularly using the TRAKER™ monitoring approach. Regular monitoring (e.g., once per quarter) should provide a clear indication if the emission potential is approaching a critical level that requires re-application of the MgCl<sub>2</sub> dust suppressant. For example, a change in the mean weighted emission factor as measured by TRAKER™ to values observed at Ft. Bliss and Ft. Carson (≈500 g-PM<sub>10</sub> VKT<sup>-1</sup>) would reduce the number of trips for HUMVEEs to 3,168 (9 per day) and M1A1 tanks to 528 (1 per day). Using a projected vehicle travel inventory, a better approximation of when to next apply dust suppressant could be obtained. Having the information as to when the Mannix Road requires dust suppressant treatment, based on knowing its actual emission characteristics would provide the opportunity to develop a more cost-effective management plan for controlling emissions, which has the potential to greatly reduce the cost and material usage (e.g. dust suppressants, water) compared with the current level of expenditure.

## 4.5 Attenuation of emissions by near-field deposition processes

### 4.5.1 PM<sub>10</sub> attenuation downwind of the source

The deposition of particles from dust plumes will be dependent on the state of the atmosphere at the time of the emission as well as the aerodynamic and physical attributes of the surface that the dust plumes interact with. The state of the atmosphere as described by the friction velocity ( $u^*$ ,  $\text{m s}^{-1}$ ), the aerodynamic roughness of the surfaces, and the stability class for the different test surfaces are provided in Table 5. The long grass vegetation had the highest surface aerodynamic roughness ( $z_0$ ) at 0.206 m. Sagebrush had second highest aerodynamic roughness of 0.188 m, the mowed grass ( $z_0 = 0.025$  m) had less rough surface than the steppe grass site ( $z_0 = 0.027$  m), the bare soil had the lowest surface roughness ( $z_0 = 0.007$  m).

As not all winds came from the direction perpendicular to the road source, the angle of wind approach (AOA) was used to calculate the actual transport distances from source to the sampling positions. If the distance between two measurement positions is  $D$ , then the actual plume transport distance under an AOA ( $\theta$ ) would be  $D/\cos\theta$ . Particles in all size classes generally show an exponential decay in particle number concentration with increasing downwind distance (Fig. 35). A non-linear least squares regression (no forcings were used) was used to fit a function to the data and the coefficients of determination,  $R^2$  all  $>0.95$  indicate the exponential regression is a reasonable representation of the data. The largest fractional decrease in particle concentration decay was observed at the 50 to 100 m position downwind of the source. The exponential decay in number concentration is reflective of the removal of particles from the plume and proportional to plume concentration as previously observed by Johnson et al. (1992). However, for the dense, long grass site (Ft. Riley, KS), the decay is better fit by a power function due to the very rapid change of particle number concentration for all sizes measured in the initial  $\approx 100$  m downwind.

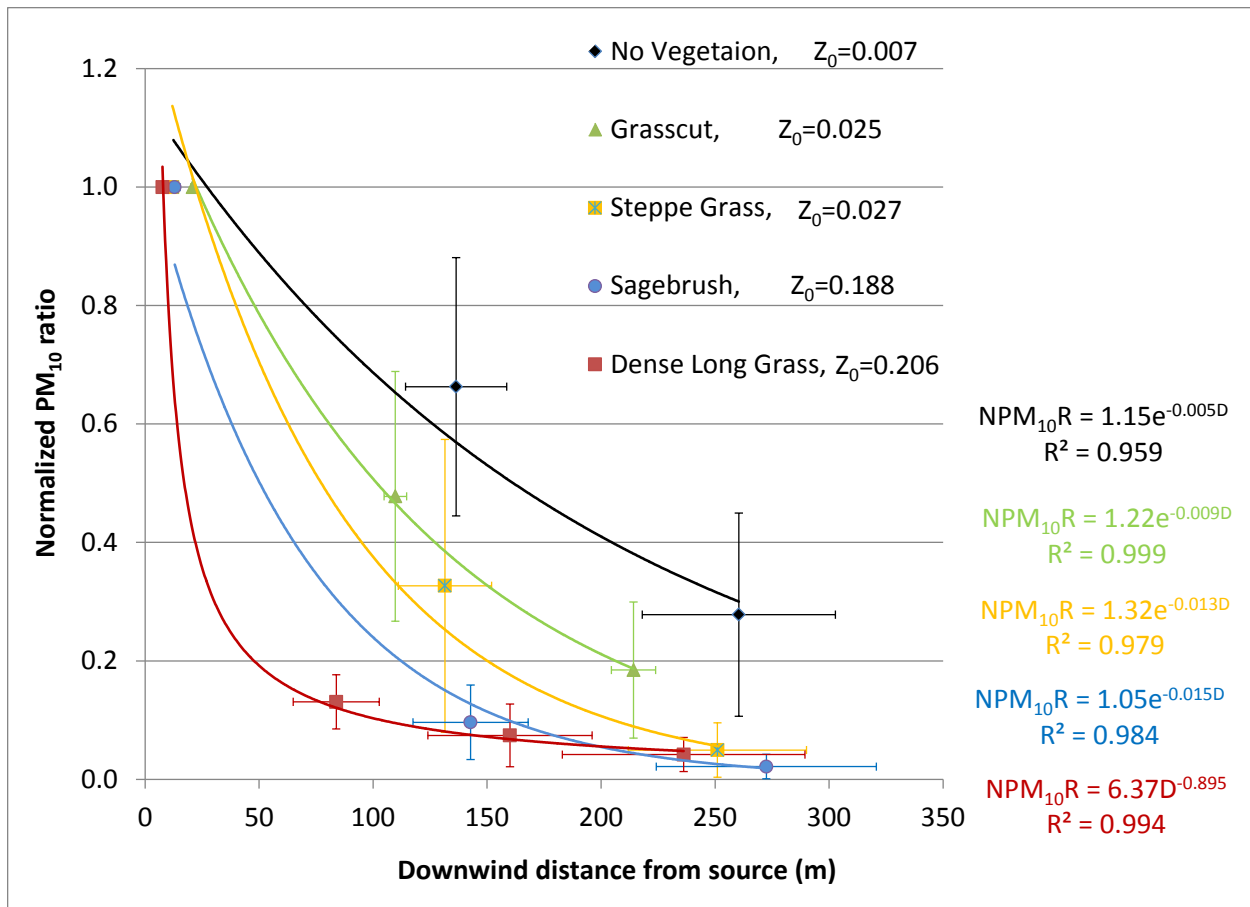
Two causal, and complimentary, mechanisms are proposed that could explain this very rapid change of particle number concentration for the long grass surface. First, this surface has the highest aerodynamic roughness length,  $z_0$  (0.206 m). Numerical modeling and measurement of channel flow indicate roughness increases turbulence intensity (Bhaganagar et al., 2004; Kussin and Sommerfeld, 2002). Roth (2000) summarizes several mechanisms how roughness elements influence turbulence. Roth (2000) notes an intense shear layer is formed near the top of the roughness elements, resulting in higher turbulence intensities; the mixing generated by turbulent wakes behind individual roughness elements, efficiently mix and diffuse momentum or any scalar quantity; the pressure difference across individual roughness elements augments the transport of momentum to the surfaces. For particles in turbulent flow, turbulence will spread the particles and enhance the deposition rate (Li and Ahmadi, 1992). Moran et al. (2013) report experimental evidence and modeling results that indicate that turbulence enhances particle deposition onto all surfaces of vegetation even for small particle sizes (e.g., PM<sub>10</sub>) in near source transport. A second mechanism that may be enhancing deposition in the long grass, more than the other vegetation types, are interception/impaction processes that affect deposition via contact

**Table 5.** Mean surface aerodynamic roughness length, friction velocity, and stability class for the five different surface sites during testing. The standard deviation of the mean value is provided in parentheses.

<b>Vegetation Type</b>	<b><math>z_0</math> (m)</b>	<b><math>u^*</math> (m s<sup>-1</sup>)</b>	<b>Avg. <math>U</math> at 2.2 m (m s<sup>-1</sup>)</b>	<b>Avg. <math>U</math> at 10 m (m s<sup>-1</sup>)</b>	<b>Stability Class</b>
No Vegetation (Jean Lake, NV)	0.007 (±0.003)	0.31 (±0.03)	2.94 (±1.08)	4.08 (±1.04)	Neutral
Cut Grass (Ft Riley, KS)	0.025 (±0.007)	0.37 (±0.03)	4.19 (±0.57)	4.85 (±0.51)	Mostly Neutral
Steppe Grass (Hanford, WA)	0.027 (±0.014)	0.31 (±0.06)	2.71 (±0.53)	3.15 (±0.75)	Unstable
Sagebrush (Hanford, WA)	0.188 (±0.045)	0.34 (±0.04)	3.07 (±1.32)	3.38 (±1.50)	Unstable
Dense Long Grass (Ft Riley, KS)	0.206 (±0.022)	0.33 (±0.04)	3.21 (±0.49)	3.64 (±0.61)	Unstable to Slightly Unstable

of the particles in the dust plume with the grass blades. Belot and Gauthier (1975) report from wind tunnel experimental results, roughness elements with more surface area have better particle collection efficiency, e.g., blades of grass collect more particles than broad leaf vegetation types. This also can be invoked to explain why the long grass site shows enhanced particle losses compared to the sagebrush site even though their aerodynamic roughness lengths are similar (Table 5).

With particle density assumed to be 2.65 g cm<sup>-3</sup> (with minerals like silica abundant in soil dust, Tegen et al., 2002), the particle number concentration was converted to a PM<sub>10</sub> mass concentration by summing all particles in the size bins less than 10 μm. PM<sub>10</sub> mass concentrations were found to decrease at faster rates as a function of downwind distance with increased surface roughness for the five surface types tested in the first ≈100 m from the source, again taking into account the actual fetch length depending on the AOA of the wind (Fig. 35). For the long grass site at Ft. Riley, PM<sub>10</sub> decayed to 13% of the near road concentration at 84 m downwind. For the short grass (mowed long grass), PM<sub>10</sub> diminished to 48% of the near road concentration at 130 m downwind. For bare soil without vegetation at the Jean Lake, NV site, PM<sub>10</sub> reduced to 67% of the near road concentration at 136 m downwind. Further downwind, the rate of decrease (dC/dx) reversed (decreased) with increased surface roughness.

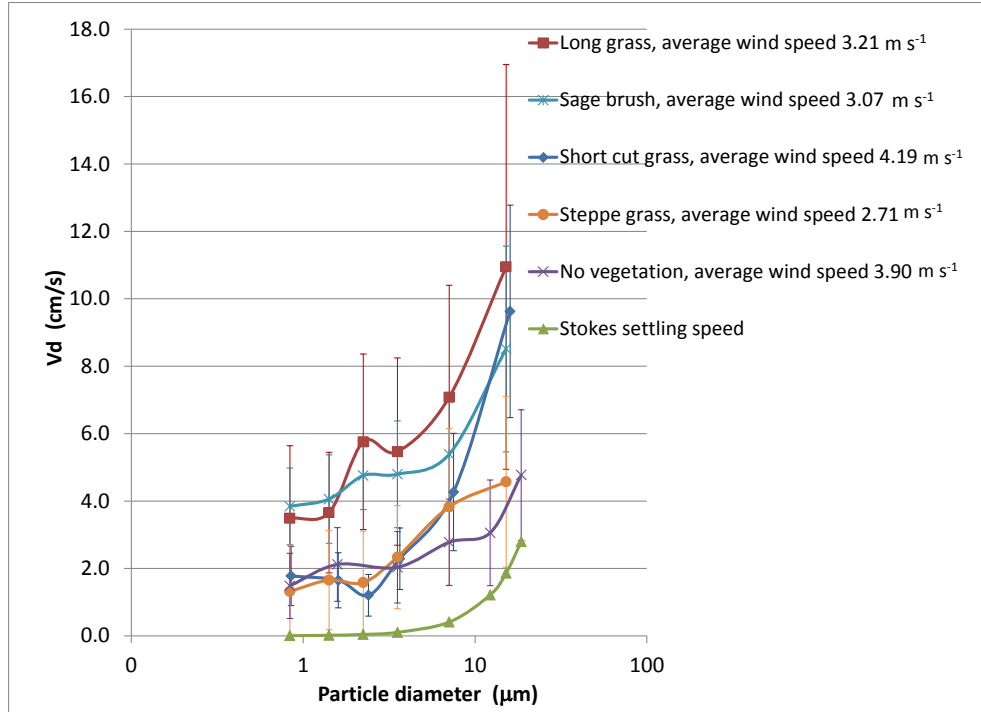


**Figure 35.** The change in downwind  $PM_{10}$  concentration referenced to near source  $PM_{10}$  concentration for the different test surfaces measured at 2 m a.g.l. The Y axis is  $PM_{10}$  concentration normalized to the sampler nearest the source.

As aforementioned, the removal of particles is proportional to the concentration along the downwind ( $x$ ) direction. Due to increased turbulence caused by the higher roughness and increased impaction losses associated with the grass blades the long grass site has the lowest normalized  $PM_{10}$  concentration after 100 m of transport. At distances  $>100$  m the rate of decrease of particle number concentration for the long grass site was the lowest observed, while  $dC/dx$  was highest for the non-vegetated lakebed surface. For the dry lakebed site after 100 m of transport, the normalized  $PM_{10}$  concentration was highest compared with all the other sites.

#### 4.5.2 Size specific PM deposition velocities

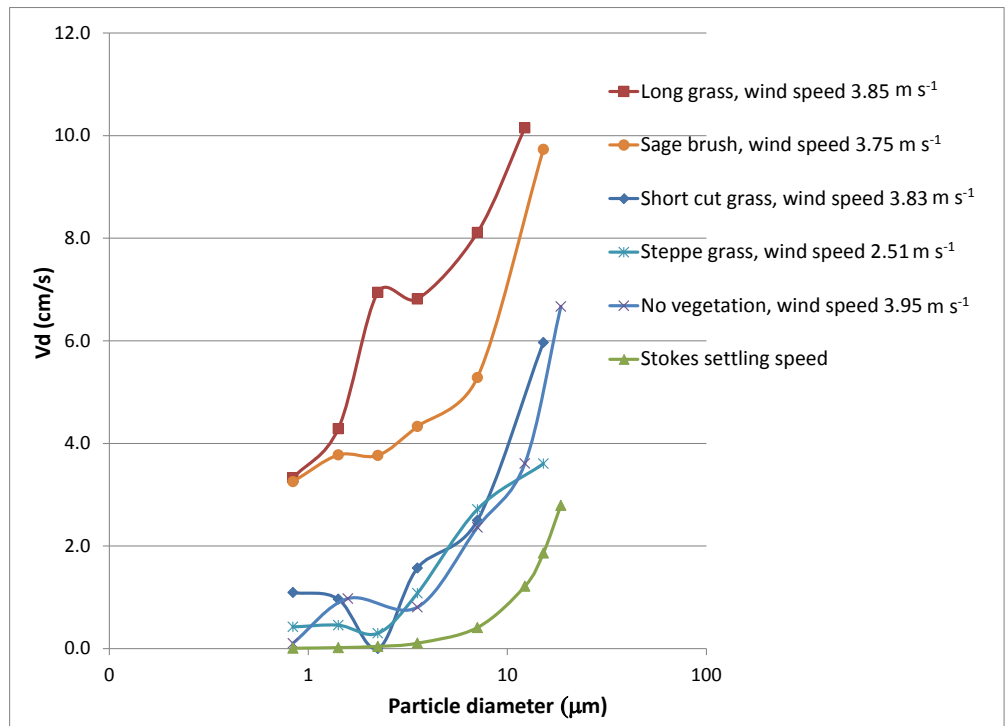
Size-specific PM deposition velocities inferred from the box model were calculated and are presented in Fig. 36. For comparison, the terminal settling velocity  $v_t$  was also calculated for the same sized particles using the Stokes Eq.:



**Figure 36.** Particle deposition velocity based on box model for five surface types. Error bars represent the standard deviation of the mean particle diameter from multiple plume measurements.

$$v_t = \frac{1}{18} \frac{D_p^2 \rho_p g C_c}{\mu} \quad (11)$$

Where  $D_p$  is the particle diameter,  $\rho_p$  is the particle density,  $g$  is the gravitational constant ( $9.8 \text{ m s}^{-2}$ ),  $C_c$  is the Cunningham Slip Correction factor, and  $\mu$  is the dynamic viscosity of the atmosphere ( $1.7 \times 10^{-5} \text{ kg m}^{-1} \text{ s}^{-1}$ ). Figure 36 illustrates that the particle deposition velocity increases with particle size, as expected. As shown by Eq. 6 in the box model, the deposition velocity ( $v_d$ ) is linearly related to horizontal wind speed  $U$  (that scales with  $u_*$ ). The deposition velocity is generally higher for long grass vegetation with greater roughness even though the average wind speed was higher for the short grass testing. It seems that the particle concentration difference in the control volume has a higher magnitude impact on the deposition velocity. This is due to higher surface roughness causing greater reduction in the number (or mass) concentration of PM, which then results in higher deposition velocities ( $v_d$ ). Figure 37 compares the deposition velocity from a single pass for five vegetation types with similar wind speeds. Under similar horizontal wind speeds, deposition velocity for equivalent diameter particles is higher for vegetation with greater surface roughness. The deposition velocities calculated for particles in the turbulent surface layer is higher than the Stokes setting velocities for same-sized particles, which may be due to the higher Reynolds numbers in the airflow

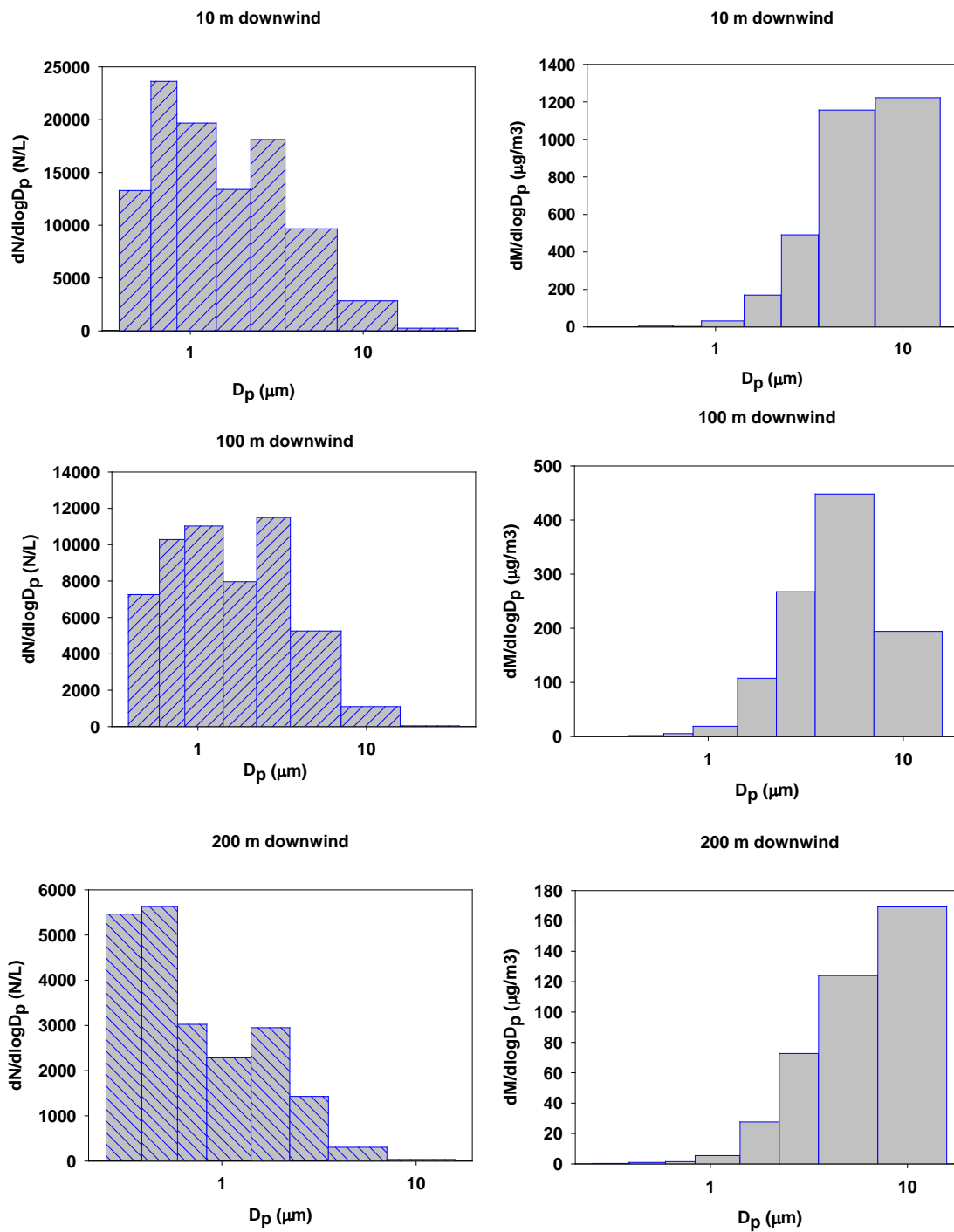


**Figure 37.** Deposition velocities for particles measured during a single plume passage with similar wind speed for the five test surfaces and the Stokes-predicted deposition velocities.

resulting in increased deposition velocities due to a combination of turbulent transfer and Stokes settling. Zufall et al. (1998) similarly reported larger than Stokes deposition velocities for particles in turbulent boundary-layer flow over the waters of Lake Michigan. In that study, deposition velocities for  $\approx 2.5 \mu\text{m}$  Ca-rich particles was  $\approx 3.5 \text{ cm s}^{-1}$  compared with a Stokes settling velocity of  $0.04 \text{ cm s}^{-1}$ .

#### 4.5.3 Changes in particle size distribution with downwind distance

Examples of the downwind particle number and mass size distribution for a single test run on the long grass surface are shown in Fig. 38. The coarse particles (between  $2.5$  and  $10 \mu\text{m}$ ) accounted for  $\approx 20\%$  of the  $\text{PM}_{10}$  number concentration at the three downwind measurement locations at Ft. Riley, but accounted for  $\approx 95\%$  of the  $\text{PM}_{10}$  mass concentration at the three downwind distances for the other sites. The coarse PM mass dominance was observed at all surface types. This indicates coarse particles dominate resuspended dust mass created by the vehicle travel on the unpaved test roads. Compared with mass size distribution from an urban roadside environment (i.e., a paved road) in Greece (Samara et al., 2005), submicron particles accounted for 52% of the total mass, and coarse PM just 20% of the total mass. Generally high proportions (40–80%) of aerosol mass in the submicron size range have been reported for urban sites (Chan and Kwok, 2000). The difference of the mass size distribution reflects different



**Figure 38.** An example of re-suspended dust number size distribution (left column) and mass size distribution (right column) from samplers at 10 m, 100 m, and 200 m downwind of a road source.

dominant source types with resuspended soil dust in the rural settings and combustion particles in the urban environment.

#### **4.5.4 PM number changes in the vertical and the mass median diameter**

The concentration measurements made at the lower inlet height (2.2 m) at the 100 m and 200 m downwind positions, compared with number concentrations at the same size bin from the sampler with the low elevation inlet at the near road position (i.e., 10 m downwind of the source), show that larger particles decrease at a faster rate not only in the horizontal, but also in the vertical directions as measured at the 6.1 m high inlet. For example, under the short grass condition, normalized to the corresponding size-bin number concentration at the 20 m downwind site, the ratio value or survival rate of  $PM_{0.5-0.7}$  at 105 m is 0.85. The ratio decreases with increasing particle size, reaching 0.65 for  $PM_{2.5-5}$ , 0.47 for  $PM_{5-10}$ , and 0.22 for  $PM_{>10}$ . When the dust reaches 205 m downwind, survival rate for  $PM_{0.5-0.7}$  at 205 m is 0.12, decreasing as a function of increasing particle size, reaching 0.08 for  $PM_{2.5-5}$ , 0.065 for  $PM_{5-10}$ , and 0.025 for  $PM_{>10}$ . In the vertical direction, particle concentration normalized by the corresponding size-bin concentration from the 20 m sampler low elevation inlet measurement, the survival ratio for  $PM_{0.5-0.7}$  at 6.2 m a.g.l., 105 m downwind is 0.80, 0.35 for  $PM_{2.5-5}$ , 0.116 for  $PM_{5-10}$ , and 0.042 for  $PM_{>10}$ . The survival ratios at 6.2 m high, 205 m downwind are 0.05 for  $PM_{0.5-0.7}$ , 0.03 for  $PM_{2.5-5}$ , 0.02 for  $PM_{5-10}$ , and 0.01 for  $PM_{>10}$ .

The mass median diameter (MMD) is a useful statistically-derived parameter for characterizing a distribution of suspended particles to compare and contrast differences between the distributions resulting from changes due to aging of the plume mass as it is transported. For example, an MMD of 10  $\mu\text{m}$  means that 50% of the total sample mass will be present in particles having diameters  $<10 \mu\text{m}$ , and 50 % of the total sample mass will be present in particles having a diameter  $>10 \mu\text{m}$ . Analysis of MMD at different locations of the dust plume also indicates the change of the MMD in both the horizontal and vertical directions. For the Ft. Riley cut grass surface, the MMDs of the dust plume were 11  $\mu\text{m}$ , 9.6  $\mu\text{m}$ , and 9.0  $\mu\text{m}$  measured at the low sampler inlets at 20 m, 105 m, and 205 m downwind, respectively, and 9  $\mu\text{m}$  and 7.5  $\mu\text{m}$  at the high sampler inlet at 105 m and 205 m downwind. At the bare, smooth Jean Lake site the MMDs were 16  $\mu\text{m}$ , 16  $\mu\text{m}$ , and 15.2  $\mu\text{m}$  at the low sampler inlets at 10 m, 110 m, and 210 m downwind, respectively, and 13.2 and 13  $\mu\text{m}$  from the high inlet at 110 m and 210 m downwind. The difference of MMD at the first downwind sampler between the two sites (Ft. Riley vs. Jean Lake) is due to the different particle size distribution of the source material at each site. The trend of MMD decreasing as a function of downwind distance however is similar for the different surface conditions, which indicates the larger particles were deposited and removed from the dust plume at a faster rate than small particles during downwind transport. Similar findings were reported by researchers studying the transportation of African dust over the Mediterranean Sea (Dulac et al., 1989). Dulac et al. (1989) reported MMDs of  $>3.5 \mu\text{m}$  (for aluminum-rich particles) were generally obtained close to the African coast. The MMDs observed in Corsica ( $\approx 1000 \text{ km}$  of transport distance from the African coast) during the same

period were 2.0 to 2.3  $\mu\text{m}$ , which suggests a decrease of the MMD during the transport of mineral aerosol from Africa over the Mediterranean Sea. Dulac et al. (1989) estimated this change is due to gravitational settling (en route) of the coarse particle fraction of the aerosol.

To sum up this component of the research, near source PM reduction for different vegetation types and deposition velocities were studied using measurements and application of a horizontal gradient box model. The dust plumes were created by wheeled vehicles traveling at a constant speed on unpaved roads at test sites in Kansas and Washington, and a playa surface in Nevada. These three locations provided five different surfaces, one barren and four with various types and covers of vegetation to estimate the impact of the roughness/vegetation on PM deposition. The estimated particle deposition velocities were found to increase with particle size and surface roughness under similar moderate wind speed conditions and were greater than predicted by application of the Stokes settling velocity equation. Coarse particles accounted for  $\approx 95\%$  of the  $\text{PM}_{10}$  mass concentration at three downwind locations extending to 200 m downwind.  $\text{PM}_{10}$  removal increased with increasing surface and aerodynamic roughness. The dense, high grass surface had the highest reduction of  $\text{PM}_{10}$ , which is attributed to increased deposition due to increased turbulence induced by the rougher surface and by enhanced particle impaction/interception effects with the blades of grass. These data also suggest that the type of vegetation also exerts some control on the depositional process as the long grass site had higher PM losses than the sagebrush site even though their aerodynamic roughness, and hence drag characteristics, were not that dissimilar.

Larger particle mass concentrations were observed to decrease at a faster rate not only in horizontal direction, but also in the vertical dimension as the dust plume was transported downwind. The mass median diameter of the dust plume also decreased along both the horizontal and vertical dimensions, which further supports our contention that the larger particles were being deposited and removed from the dust plume at a faster rate than small particles during downwind transportation.

These results also suggest a reason for the poor reconciliation between emission inventory estimates of unpaved road dust and the amount of mineral dust observed in samples collected in air quality sampling networks. The inventory approach may be over-estimating contributions because it is based on only near source emission fluxes that do not take into account the depositional losses in the near field that were clearly affected to a significant degree by the type of surface the dust plumes interacted with as they advected downwind.

## 4.6 DUSTRAN

The new version of DUSTRAN is a comprehensive dispersion modeling system consisting of a dust-emissions module, a diagnostic meteorological model, and dispersion models that are now integrated seamlessly into the MapWindow open-source GIS. DUSTRAN functions as a console application within MapWindow and allows the user to interactively create a release scenario and run the underlying models. Through the process of data layering, the model domain, sources, and results—including the calculated wind vector field and plume contours—can be displayed with other spatial and geophysical data sources to aid in analyzing and interpreting a scenario.

In this second version of DUSTRAN, dust transport, diffusion, and deposition are simulated using one of three dispersion models—AERMOD, CALPUFF, or CALGRID. Three dispersion models are used according to their frames of reference in calculating plume transport, allowing DUSTRAN users to take advantage of each model's inherent strengths in simulating different source types and transport distances. These models are:

AERMOD (US EPA, 2014a). A steady-state plume model for short-range (<50 km) dispersion and particle deposition from active-source emissions (i.e., point, area, or line). AERMOD incorporates planetary boundary layer turbulence structure and scaling concepts, including treatment of surface and elevated sources and simple and complex terrains.

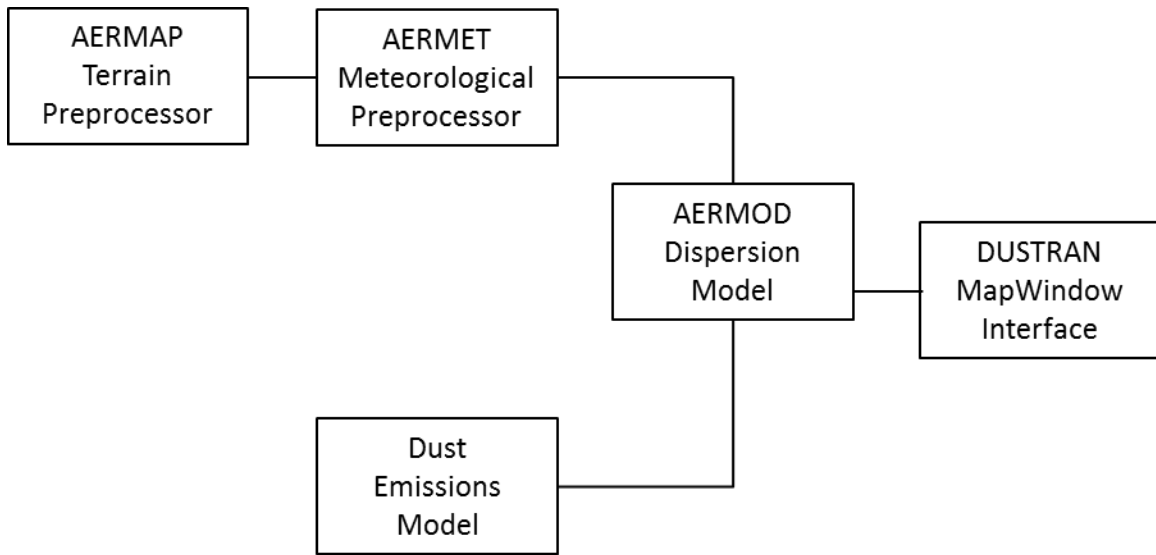
CALPUFF (Scire et al., 2000). A non-steady-state puff dispersion model with regulatory approval for long-range (>50 km) dispersion and particle deposition from active-source emissions (i.e., point, area, or line). CALPUFF simulates the effects of time- and space-varying meteorological conditions on pollution transport, transformation, and removal in both simple and complex terrains.

CALGRID (Scire et al., 1989). An Eulerian dispersion model used for wind-blown dust emissions, where the entire model domain is a potential emission source.

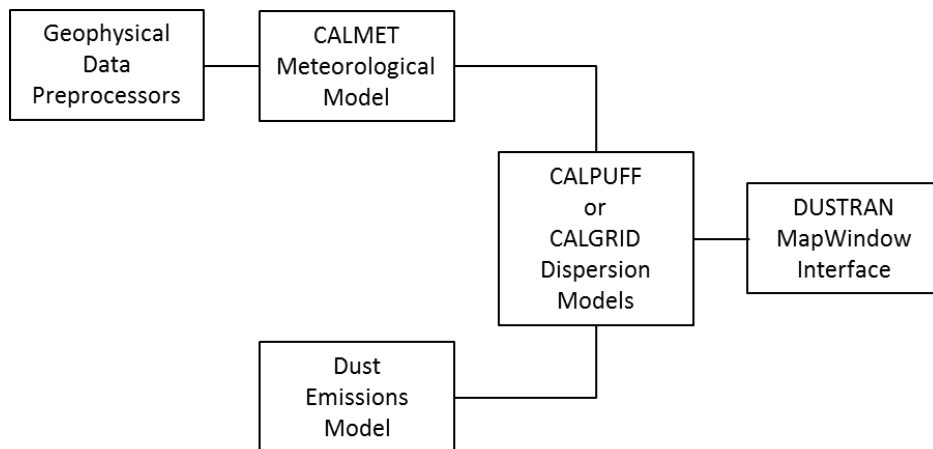
Figures 39 and 40 illustrate the parallel approach to the implementation of both AERMOD and CALPUFF/CALGRID. Because DUSTRAN was built on the CALPUFF/CALGRID dispersion models as part of the previous work, the remainder of the discussion of DUSTRAN will focus on the new implementation of AERMOD into DUSTRAN. For comparison, Tables 6 and 7 list the current version numbers of each model component.

### 4.6.1 AERMOD Modeling System

The AERMOD modeling system (US EPA, 2014a, 2014b) is used to model short range (<50 km) dispersion from active-source emissions (i.e., point, area, or line). The following sections describe the AERMOD modeling system components and their implementation within DUSTRAN.



**Figure 39.** AERMOD Modeling Components within DUSTAN.



**Figure 40.** CALPUFF/CALGRID Modeling Components within DUSTAN.

**Table 6.** AERMOD Model Components and Version Numbers Implemented in DUSTAN

Component	Purpose	Version Number
AERMOD	Dispersion model	14134
AERMET	Meteorological Model	14134
AERMAP	Terrain Preprocessor	11103

**Table 7.** CALPUFF/CALGRID Model Components and Version Numbers Implemented in DUSTRAN.

Component	Purpose	Version Number
CALPUFF	Dispersion model	5.5
CALGRID	Dispersion Model	1.6
CALMET	Meteorological Model	5.2
CALPOST	Post-processing Program	5.2
TERREL	Terrain Preprocessor	2.1
CTGPROC	Land Use Preprocessor	1.2
MAKEGEO	Merges Terrain/Land Use Datasets	1.1
READ62	Meteorological Preprocessor for Extracting Standard Upper-Air Formats	4.0

#### 4.6.1.1 AERMET

AERMET (US EPA, 2014b) is a meteorological preprocessor that uses hourly meteorological observations to calculate certain boundary-layer parameters (e.g., mixing height and friction velocity [ $u^*$ ]) for use in AERMOD. AERMET requires surface and upper-air meteorological observations as well as certain surface characteristics (i.e., albedo, Bowen ratio, and surface roughness). These data are supplied through the “Meteorology” tab within DUSTRAN. In addition, lookup tables for typical values of albedo, Bowen ratio, and surface roughness are included in DUSTRAN. These values are based on various surface characteristics tables from Appendix A of the EPA’s AERSURFACE User’s Guide (US EPA, 2008).

Table 8 lists meteorological observations required by AERMET. Surface data are hourly observations, whereas upper-air vertical profiles are required less frequently, normally twice daily (00Z and 12Z). A single surface and upper-air station must be used. The input meteorological data are written to formatted surface and upper-air files by the DUSTRAN interface for use in AERMET.

Since upper-air data can be difficult to obtain, profiling equations have been incorporated into DUSTRAN as an alternative to approximate upper-air soundings. Using the single observation data entered by the user, and certain parameters listed in the Cal.par file, DUSTRAN automatically generates an upper-air sounding file, which is used by the AERMET model. The sounding data consist of wind speed/direction, temperature, and pressure at several heights above the ground, where the lower and upper heights and the number of heights are specified in an input file called “Cal.par”. The height spacing is logarithmic to allow narrower spacing close to the surface. The DUSTRAN profiling equations are described in the following sections.

**Table 8.** AERMET meteorological input requirements.

Surface Data (Hourly)	Upper-Air Data (Usually Twice Daily)
Wind Speed and Direction	Wind Speed and Direction
Temperature	Temperature
Relative Humidity	Pressure
Station Pressure	Measurement Height
Total Sky Cover	
Ceiling Height	
Measurement Height	

#### 4.6.1.2 Wind Speed/Direction

For simplicity, the wind direction is assumed constant with height, and the wind speed is assumed to increase with height using the power-law relationship:

$$U_n = U_1 \left( \frac{Z_n}{Z_1} \right)^P \quad (12)$$

- where  $U_n$  = wind speed at sounding height “n” ( $\text{m s}^{-1}$ )  
 $U_1$  = wind speed at lowest sounding height ( $\text{m s}^{-1}$ )  
 $Z_n$  = sounding height “n” (m)  
 $Z_1$  = lowest sounding height (m)  
 $P$  = power-law exponent depending on atmospheric stability

The power-law exponents in Eq. 12 follow from Table 4.6 of Turner (1994) and are listed in the Cal.par file for application of DUSTRAN in either “rural” or “urban” areas.

#### 4.6.1.3 Temperature

The temperature sounding is developed from temperature lapse rates specified as a function of stability in the Cal.par file and the surface temperature specified in the user-input window. Consequently, the temperature sounding is determined as:

$$T_n = T_1 + T_{LR}(Z_n - Z_1) \quad (13)$$

- where  $T_n$  = temperature at sounding height “n” (K),  
 $T_1$  = temperature at lowest sounding height (K),  
 $T_{LR}$  = temperature lapse rate depending on stability (K/m)

$Z_n$  = “n” sounding height (m)  
 $Z_1$  = lowest sounding height (m).

#### 4.6.1.4 Pressure

The atmospheric pressure as a function of sounding height is determined from the hydrostatic relationship as:

$$P_n = P_1 \text{ EXP} \left[ - \frac{a(Z_n - Z_1)}{(T_n + T_1)/2} \right] \quad (14)$$

where  $P_n$  = pressure at sounding height “n” (mb),  
 $P_1$  = pressure at lowest sounding height (mb),  
 $a$  = 0.0342 K m<sup>-1</sup>.

#### 4.6.2 AERMAP

AERMAP (US EPA, 2011) is a terrain preprocessor that uses publicly available terrain data to extract elevations for sources and receptors as well as calculate the receptor “hill-height scale” for AERMOD dispersion calculations. DUSTRAN utilizes the U.S. Geological Survey’s (USGS) Global Multi-resolution Terrain Elevation Data 2010 (GMTED2010) data files for use within AERMAP. These files provide global coverage at a resolution around 7.5 arc seconds (150 m). The GMTED2010 terrain files are clipped as part of the site creation process within DUSTRAN’s “Add Site” utility. This results in a smaller terrain file for use within a given AERMAP domain. This also eliminates the need for users to define or supply multiple DEM files, which may not completely cover the AERMOD model domain.

#### 4.6.3 AERMOD

AERMOD is the US EPA’s preferred regulatory dispersion model (see 40 CFR Part 51, Appendix W) for most modeling applications. The model is useful for simulating short-range dispersion (<50 km) from discrete source-type configurations (e.g., point, line, and area sources). Within DUSTRAN, area and line sources are integrated using AERMOD to simulate particle dispersion and deposition from paved or unpaved roadways due to various vehicle types.

AERMOD is a steady-state plume model; meteorological conditions can be updated hourly and are assumed to be spatially homogenous across the entire model domain. In the stable boundary layer, the plume concentration is assumed to be Gaussian. In the convective boundary layer, the horizontal plume concentration is assumed to be Gaussian, but the vertical plume concentration is described by a bi-Gaussian probability density function. The model calculates average plume concentration and deposition-flux values at defined receptor locations. The receptor field is automatically defined and created by DUSTRAN based upon the model domain size and source input configuration.

The AERMOD input file (Aermod.inp) defines the “Control,” “Source,” “Meteorology,” “Receptor,” and “Output” options for a given run. Every site in DUSTRAN has a “StaticData” directory that stores a template Aermod.inp to be used for that site. The template file is merged with user input from the DUSTRAN interface before running the model. Unlike CALPUFF, the AERMOD input file does not contain multiple options for controlling transport and diffusion; rather, a single, regulatory method is implemented within the model. A complete description of AERMOD’s scientific basis is described in the model formulation’s document (US EPA, 2004a).

In AERMOD, the dry-deposition flux,  $F_d$ , is calculated as the product of the concentration,  $\chi_d$ , and a dry-deposition velocity,  $V_d$ , computed at a reference height,  $z_r$ :

$$F_d = \chi_d \cdot V_d \quad (15)$$

where  $F_d$  = the dry-deposition flux onto the ground ( $\mu\text{g m}^{-2} \text{s}^{-1}$ ),  
 $\chi_d$  = the air concentration ( $\mu\text{g m}^{-3}$ ) calculated at reference height  $z_r$ ,  
 $V_d$  = the particle dry-deposition velocity ( $\text{m s}^{-1}$ ),  
 $z_r$  = the dry-deposition reference height (m) =  $z_o + 1$ , and  
 $z_o$  = the site surface roughness length (m) from the meteorological file

AERMOD and AERMOD–DRI differ only in their method for estimating  $V_d$ . The following sections discuss how  $V_d$  is estimated in the US EPA and DRI versions of AERMOD; all other model formulations are the same.

#### 4.6.3.1 Source Emissions: AERMOD

The US EPA version of AERMOD computes a particle dry-deposition velocity to estimate the dry-deposition flux of particles onto the ground. The dry-deposition velocity is estimated using a resistance model, whereby the atmosphere is treated as a series of resistance layers to the depositing particles. The method is analogous to electrical resistance and is expressed as the inverse sum of a series of resistance layers near the ground, plus a gravitational settling velocity (US EPA, 2004b):

$$V_d = \frac{1}{R_a + R_b + R_a R_b V_g} + V_g \quad (16)$$

where  $V_d$  = the dry-deposition velocity ( $\text{m s}^{-1}$ ),  
 $R_a$  = the aerodynamic layer resistance ( $\text{s m}^{-1}$ ),  
 $R_b$  = the quasi-laminar layer resistance ( $\text{s m}^{-1}$ ), and  
 $V_g$  = the gravitational settling velocity ( $\text{m s}^{-1}$ ).

The aerodynamic layer resistance ( $R_a$ ) occurs in the shallow layer (~10 m) next to the ground and depends on several meteorological parameters (e.g., wind speed, atmospheric stability, and surface roughness); the more turbulent the atmosphere, the smaller the aerodynamic resistance.

The quasi-laminar layer resistance occurs in the thin, non-turbulent layer just above the depositing surface and depends on molecular, rather than turbulent properties. US EPA (2004b) summarizes formulations for  $R_a$  and  $R_b$ ; these formulations are used in the US EPA's version of AERMOD to estimate dry-deposition velocities for various particle sizes.

#### 4.6.3.2 Source Emissions: AERMOD–DRI

The DRI version of AERMOD also computes a particle dry-deposition velocity to estimate the dry-deposition flux of particles onto the ground. The dry-deposition velocity is estimated from an empirical function derived from experimental data collected during this project. Data were collected over five different surface types (i.e., short grass, long grass, steppe, sage, and bare) with five different surface roughness lengths (refer to Section 4.5 for details). For each surface type, a mean deposition velocity with its standard deviation in six size bins centered in a range from approximately 0.7 to 18  $\mu\text{m}$  was estimated. The roughness values for each measurement site ranged from approximately 0.01 to 0.20 m. Further, the minimum deposition velocity did not drop below 1  $\text{cm s}^{-1}$ . Therefore, in the curve fitting described below, 1  $\text{cm s}^{-1}$  was adopted as a lower bound for deposition velocity.

Visual inspection of the data suggested that while a linear fit in surface roughness was sufficient, some curvature was suggested in the deposition velocity dependence on particle aerodynamic diameter. Because the derived function is entirely empirical, a curve-fitting routine was applied to the general quadratic function:

$$V_d(D_p, Z_0) = aZ_0^2 + bD_pZ_0 + cD_p^2 + dZ_0 + eD_p + f \quad (17)$$

where  $V_d$  = the dry-deposition velocity ( $\text{cm s}^{-1}$ ),  
 $D_p$  = the aerodynamic particle diameter ( $\mu\text{m}$ ),  
 $Z_0$  = the surface roughness length (m),

$a, b, c, d, e,$  and  $f$  are determined by regression.

An initial fit using this general quadratic form yielded large uncertainty and near zero values for coefficients  $a$  and  $c$ , while explaining approximately 80 percent of the variance. The terms including  $a$  and  $c$  were dropped, and the fit was repeated with:

$$V_d(D_p, Z_0) = bD_pZ_0 + dZ_0 + eD_p + f \quad (18)$$

The fit using this form also explained approximately 80 percent of the variance, confirming that the dropped terms were not useful in the fit.

On further inspection, a datum for deposition velocity at 15  $\mu\text{m}$  over the bare surface appeared to be anomalously large. Dropping this point reduced the number of observations available from 30 to 29 and increased the variance explained to 93 percent. This fit was adopted for use in DUSTRAN. The resulting coefficients are:

$b = 1.43, d = 12.4, e = 0.128,$  and  $f = 1.16.$

These coefficients and the above function apply in the region  $\{0 \leq D_p < 18, 0 \leq Z_0 < 0.21\}$ . Outside this fitted domain, the following forms are used:

$$\{0 \leq D_p < 18, Z_0 \geq 0.21\} \quad V_d = V_d(D_p, 0.21) = bD_p \times 0.21 + d \times 0.21 + eD_p + f \quad (19)$$

$$\{D_p \geq 18, 0 \leq Z_0 < 0.21\} \quad V_d = V_d(18, Z_0) = b \times 18 \times Z_0 + dZ_0 + e \times 18 + f \quad (20)$$

$$\{D_p \geq 18, Z_0 \geq 0.21\} \quad V_d = V_d(18, 0.21) = 11.5 \quad (21)$$

#### 4.6.4 Example Simulation of Dust Dispersion from Active Source Emissions Using AERMOD

This example steps through setting up and running a dust-dispersion scenario from active source emissions for the “Yakima” site using the newly incorporated AERMOD dispersion model in DUSTRAN. In this example, a point source is used to represent particle emissions from a stack, and the emissions are defined explicitly. An area source is created and it represents a region of dust emissions from vehicular activity. These emissions are calculated automatically by the DUSTRAN vehicular dust-emissions module. Both sources are set to run for the same duration, and the downwind air-concentration and ground deposition are simulated.

##### 4.6.4.1 Starting DUSTRAN

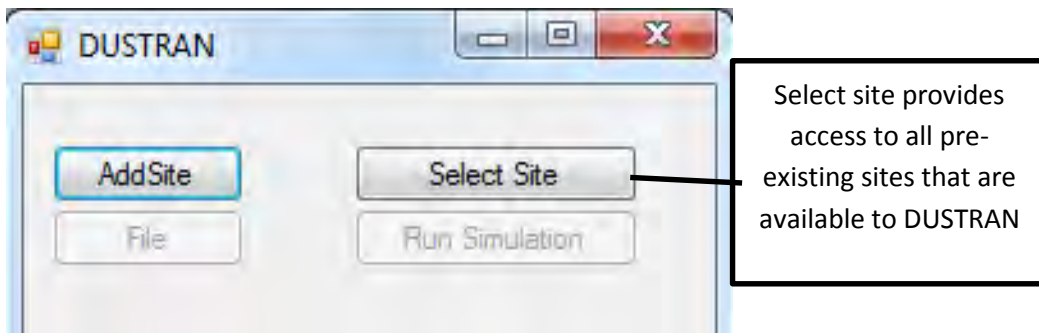
To begin a DUSTRAN simulation, one needs to open MapWindow and then click on the “D” button on the MapWindow toolbar (far right in Fig. 41).



**Figure 41.** MapWindow Toolbar.

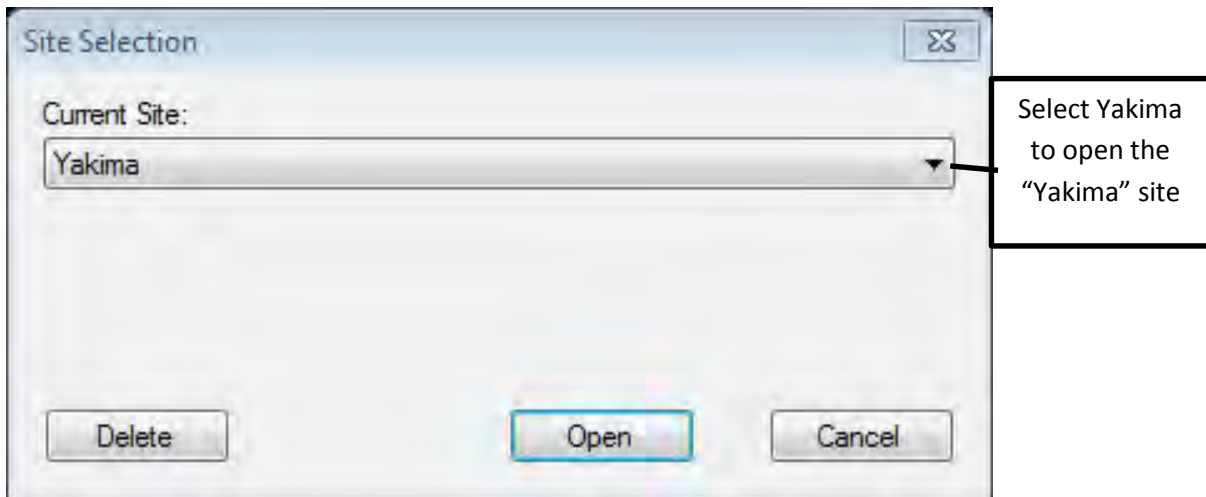
#### 4.6.4.2 Selecting a Site

The user interface to the DUSTRAN model appears alongside the MapWindow GIS application (Fig. 42). The “Select Site...” button opens a dialog box that allows the user to select an existing site.



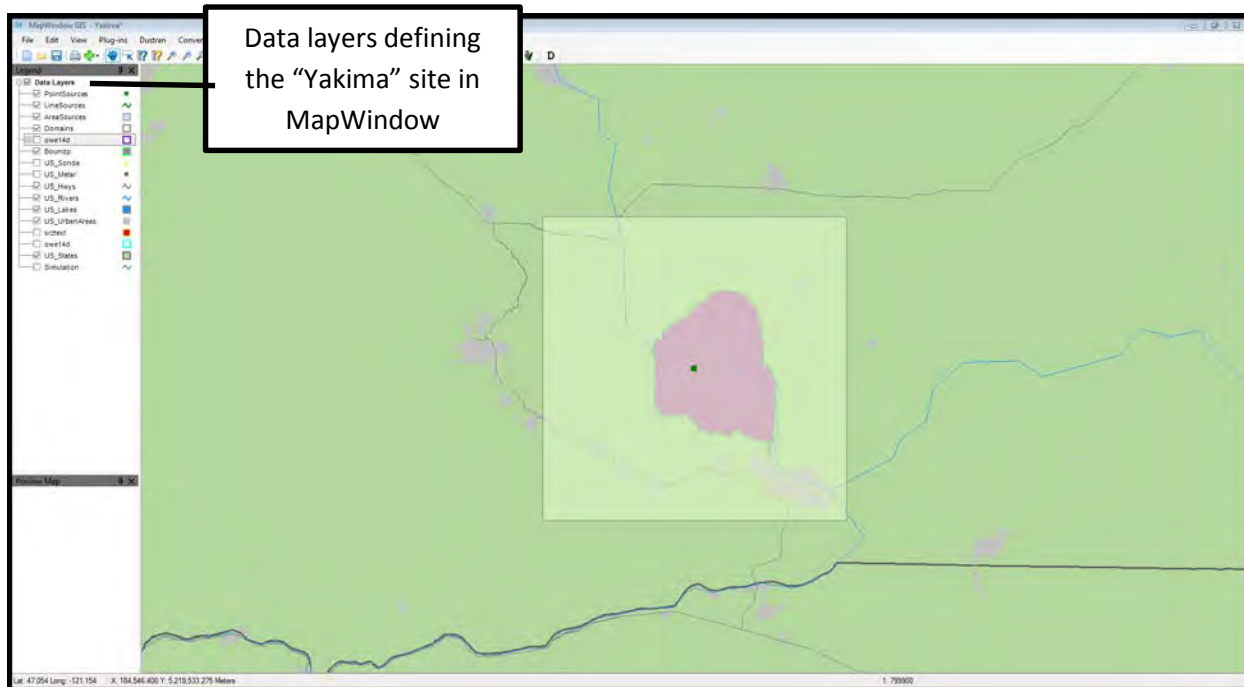
**Figure 42.** DUSTRAN user interface.

This example shows “Yakima” on the drop-down list of available model sites (Fig. 43). The “Yakima” site is then selected by clicking “Open” (Note: The process for creating a site is identical to the previous version of DUSTRAN and is not described here.).



**Figure 43.** Available DUSTRAN sites.

At this point, the “Yakima” site opens within MapWindow. A list of available GIS data layers appears in the left frame, and DUSTAN-specific input parameters appear in the DUSTAN frame (Fig. 44).

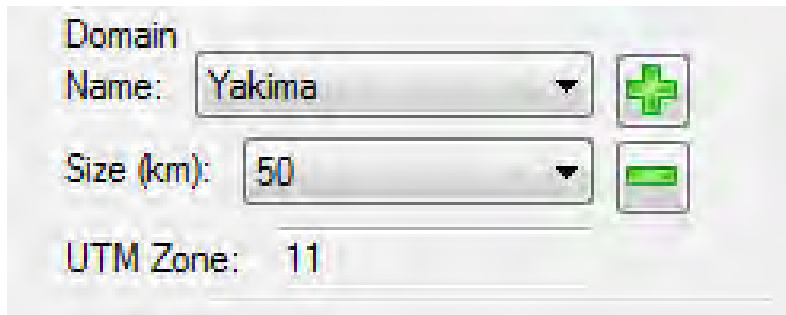


**Figure 44.** Yakima site displayed in DUSTAN.

#### 4.6.4.3 Creating a Domain

To set up a scenario in DUSTAN it is necessary to select a domain and set the domain size. A domain is a user-specified area where both meteorological and dispersion model calculations are performed.

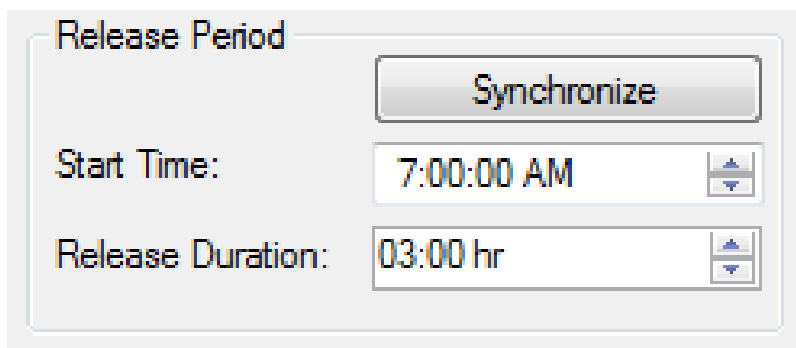
Since AERMOD is a plume model, it should only be used to model short-range dispersion (i.e., out to approximately 50 km). In this example, a domain size of 50 km is specified by setting the size from the “Size” listbox in the “Domain” panel to 50 km (Fig. 45). The domain appears as a shaded, rectangular region within Mapwindow:



**Figure 45.** Domain panel.

#### 4.6.4.4 Setting the Release Period

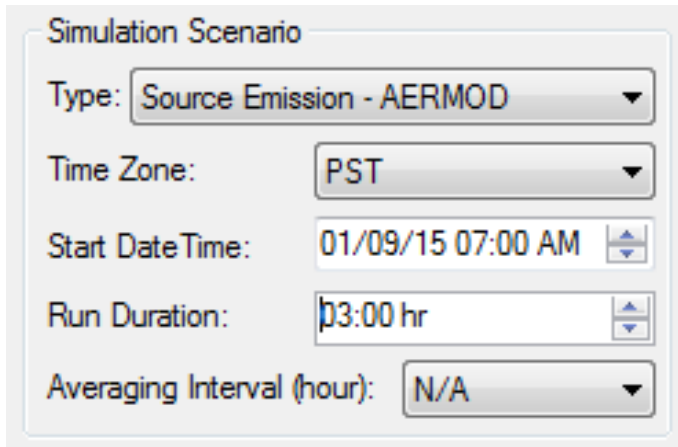
The example simulates an early-morning release. The “Release Period” start time is set to 7 a.m., and the “Release Duration” to 3 hours (Fig. 46).



**Figure 46.** Release period panel.


#### 4.6.4.5 Setting the simulation scenario

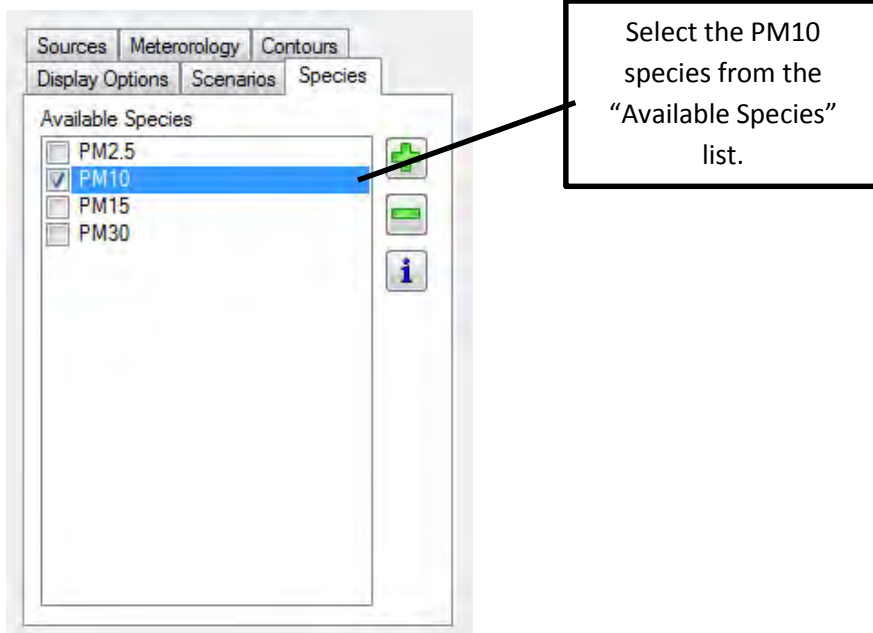
The “Simulation Scenario” dialog is where the dispersion model is selected. Since this example is using AERMOD, the simulation type is “Source Emission – AERMOD”. Appropriate to the “Yakima” domain, the time zone is set to PST. The start date is set to the date of the run and the start time to 7 a.m. Finally, the model run duration is set to 3 hours (Fig. 47).



**Figure 47.** Simulation scenario panel.

#### 4.6.4.6 Setting the Model Species

By default, there are four particulate matter (PM) species available to model in DUSTAN (Fig. 48). For this example, the 10  $\mu\text{m}$  ( $\text{PM}_{10}$ ) species is checked and  $\text{PM}_{2.5}$ ,  $\text{PM}_{15}$ , and  $\text{PM}_{30}$  are unchecked. Additional species (particles and gases) can be added using the “Add Species”  button on the “Species” tab.



**Figure 48.** Species tab – “Available Species” list.

#### 4.6.4.7 Creating a point source

The “Sources” tab in Fig. 49 is used to create a point source. Note that there is already a point source called “Yakima” that would be listed under “Point Sources”. This corresponds to the point that is used by DUSTAN to mark the center of the model domain. If that name is unchecked, the point disappears from the center of the domain in the MapWindow map display.

To create a new point source, one would click on the “Point Source” button on the “Sources” tab. Clicking on a location within the domain places the point source. In this example the source has been named “Stack”. When “OK” is clicked in the “Sources” tab, a “Source Input” form for the point source appears (Fig. 49). Example “Release Parameters” are shown in Fig. 49.

The screenshot shows a dialog box titled "Source Input - Stack" with two tabs: "Release Parameters" (selected) and "Coordinates". The main content area is titled "Stack Source Parameters".

Parameters and their values:

- Height of release: 15 m
- Enable Stack Release Parameters
- Stack gas exit velocity: 2 m/s
- Stack gas exit temperature: 25 C
- Stack diameter: 1 m
- Building cross section: 5 m<sup>2</sup>
- Initial horizontal plume size: 1 m
- Initial vertical plume size: 1 m
- Start DateTime: 01/09/2015, 07:00 AM
- Duration: 3 Hours

Emission rates (g/s) table:


Specie	Emission Rate
PM2.5	0
PM10	1
PM15	0
PM30	0

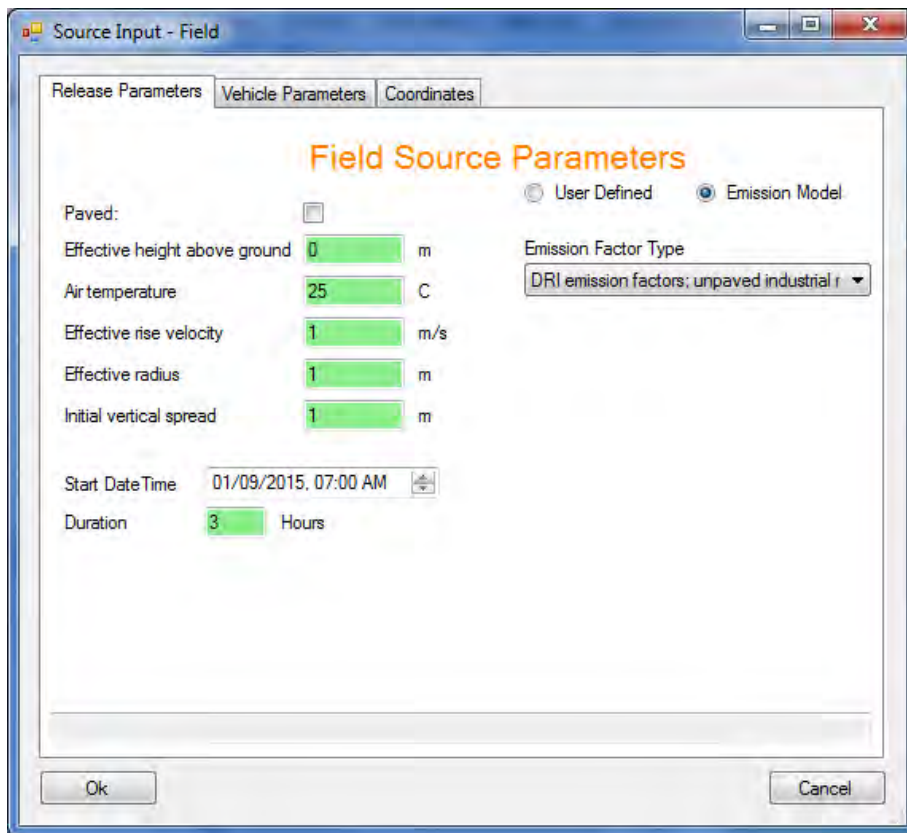
Buttons: Ok, Cancel

Figure 49. Point source input form – “Release Parameters” tab.

The new source will show up as a point in the MapWindow display and also appear in the “Point Source” list on the “Sources” tab.

#### 4.6.4.8 Creating an area source

An area source is created by clicking on the “Area Source”  button on the “Sources” tab (not shown). An area source can be a triangle or four-sided polygon. It is created by clicking on three or four locations in the MapWindow map display. The polygon is completed by right-clicking the final corner. In this example, the area source was created by drawing  $\approx 1$  km square polygon near the center of the domain and given the name “Field”. The “Source Input” form for the area source is shown in Fig. 50.



The screenshot shows a window titled "Source Input - Field" with three tabs: "Release Parameters", "Vehicle Parameters", and "Coordinates". The "Release Parameters" tab is active, displaying "Field Source Parameters". The parameters are as follows:

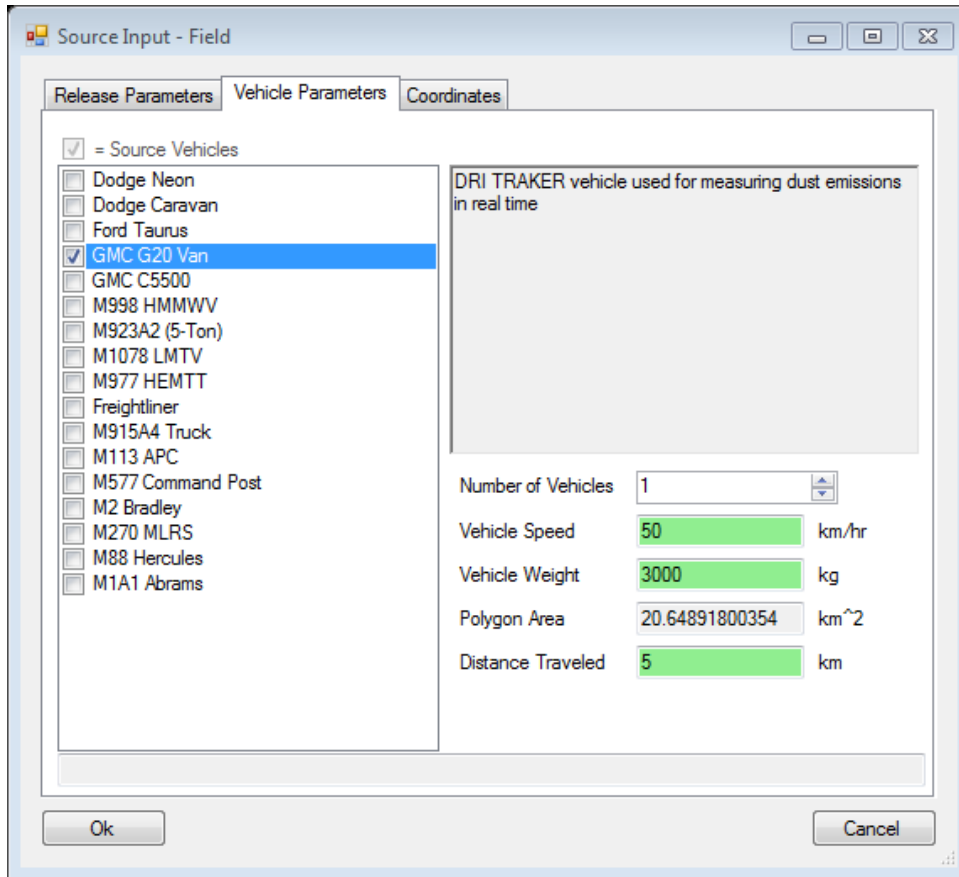
Parameter	Value	Unit
Paved:	<input type="checkbox"/>	
Effective height above ground	0	m
Air temperature	25	C
Effective rise velocity	1	m/s
Effective radius	1	m
Initial vertical spread	1	m
Start DateTime	01/09/2015, 07:00 AM	
Duration	3	Hours

Additional settings include "User Defined" and "Emission Model" radio buttons, with "Emission Model" selected. The "Emission Factor Type" dropdown menu is set to "DRI emission factors; unpaved industrial". "Ok" and "Cancel" buttons are at the bottom.

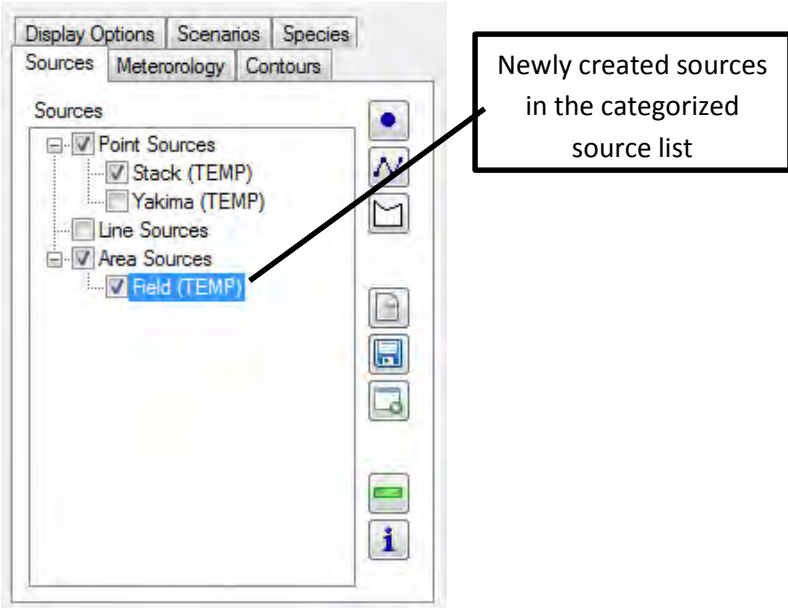
**Figure 50.** Area source input form – “Release Parameters” tab.

For the area source, the example uses the “Emission Model” selection to calculate dust emissions using previously developed emission factors (e.g., Gillies et al., 2005). Vehicular dust emissions are a function of vehicle parameters, such as weight and speed. Clicking “OK” at this point set the selections.

The “Vehicle Parameters” allow selection of specific vehicle combinations from documented emission factors (Gillies et al., 2005) (Fig. 51). For this scenario a single GMC G20 Van is selected. The specified vehicle model determines the vehicular weight used in the emission calculation. The “Distance Traveled” is the total distance traveled by the vehicle within the area, set to 5 km for this case. The emissions are assumed to be uniformly distributed over the area and constant for the duration of the release. Clicking “OK” causes the area source to appear in the MapWindow map display and also under “Area Sources” of the “Sources” tab (Fig. 52).



**Figure 51.** Area source input form – “Vehicle Parameters” tab.



**Figure 52.** Sources tab – “Sources” list.

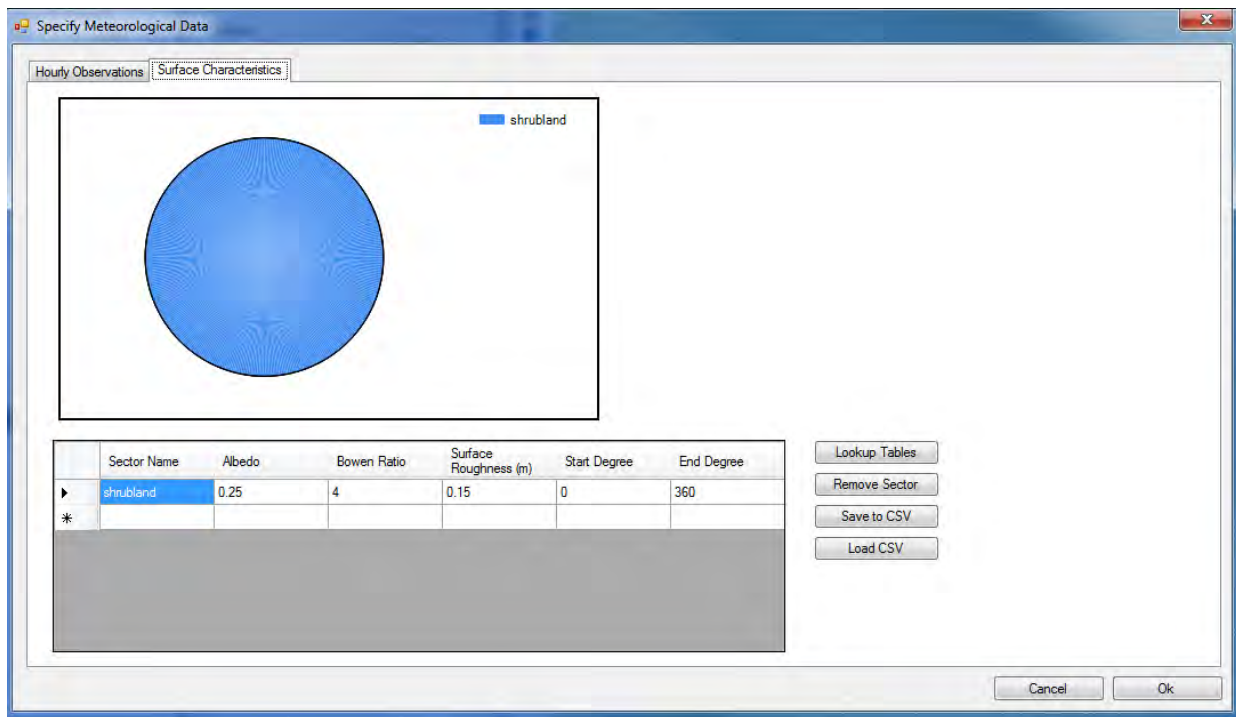
#### 4.6.4.9 Entering Meteorological Data and Surface Characteristics

Meteorological information is entered via the “Meteorology” tab within DUSTAN. For this example “Single Observation” was selected from the listbox (not shown). This causes the “Specify Meteorological Data” form to appear. Meteorological observations can then be entered as shown in Fig. 53.

Simulation Hour	Year	Month	Day	Hour	Wind Direction (deg)	Wind Speed (m/s)	Temperature (C)	Relative Humidity (%)	Station Pressure (mb)	Total Sky Cover (#enths)	Measurement Height (m)	Ceiling Height (ft)
1	2015	1	9	8	255	2.3	20	20	1003	0	10	1000
2	2015	1	9	9	180	4	19	15	1000	0	10	1000
3	2015	1	9	10	160	4.5	22	45	1005	0	10	1000

**Figure 53.** Specify meteorological data form – “Hourly Observations” tab.

AERMOD’s meteorological preprocessor AERMET also requires information about the underlying model domain’s surface characteristics. Clicking on the “Surface Characteristics” tab allows the user to specify directional sectors and associated with varying surface characteristics (i.e., albedo, Bowen ratio, surface roughness). Multiple sectors can be specified, and the resulting sectors should cover the entire model domain (i.e., 360°). In this example, a single “Shrubland” sector is specified (0° to 360°). Values for “Albedo”, “Bowen Ratio”, and “Surface Roughness” can be selected by right-clicking in a given cell and selecting a value or by using the “Lookup” button to list tables of common values. Figure 54 shows the uniform (over 360°) information entered for this case.



**Figure 54.** Specify meteorology data form – “Surface Characteristics” tab.

#### 4.6.5 Running DUSTRAN

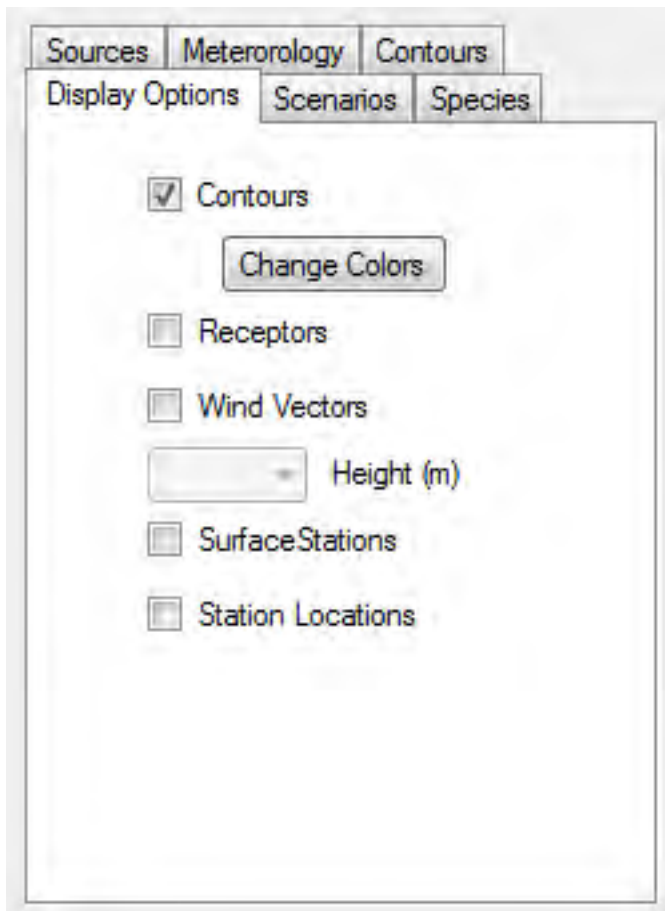
After the sources, meteorology, and release duration information have been entered, a DUSTRAN simulation can be made. This is accomplished by clicking on the “Run Simulation” button (Fig. 55).



**Figure 55.** “Run Simulation” button for running DUSTRAN simulation.

##### 4.6.5.1 Displaying Model Output

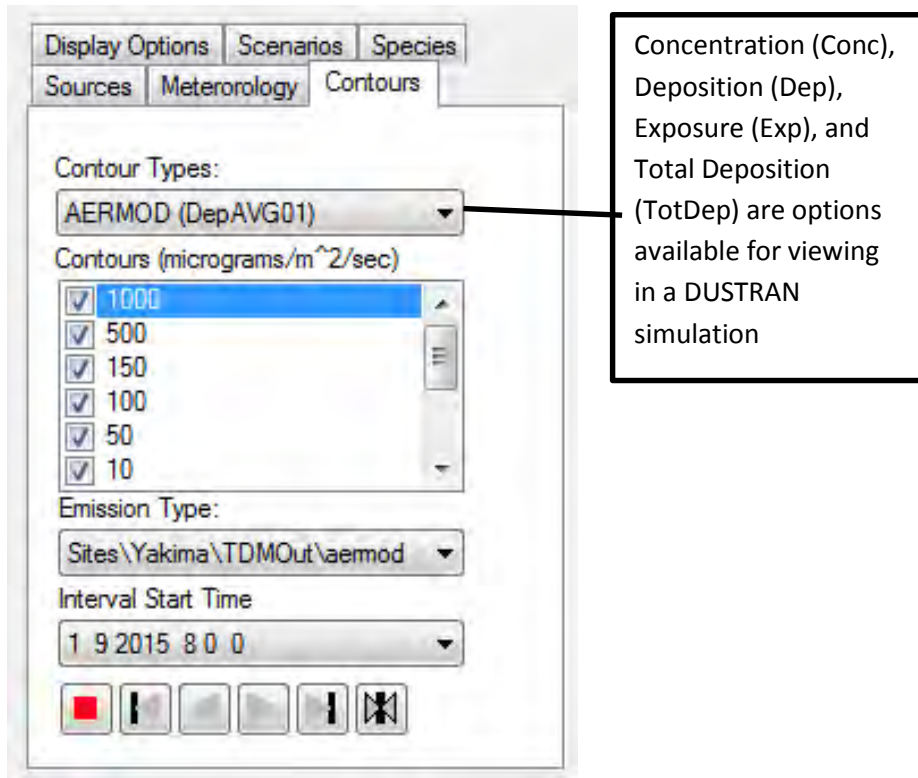
After the models finish running, the “Display Options” tab allows for configuration of the graphical display. To display concentration or deposition contours in the MapWindow map display, “Contours” needs to be checked (Fig. 56). Note that since AERMOD is a plume model that uses a single, hourly wind direction to transport the plume, there is no wind vector field to display within AERMOD.



**Figure 56.** Display options tab – “Contours” options.

#### 4.6.5.2 Viewing Model Results

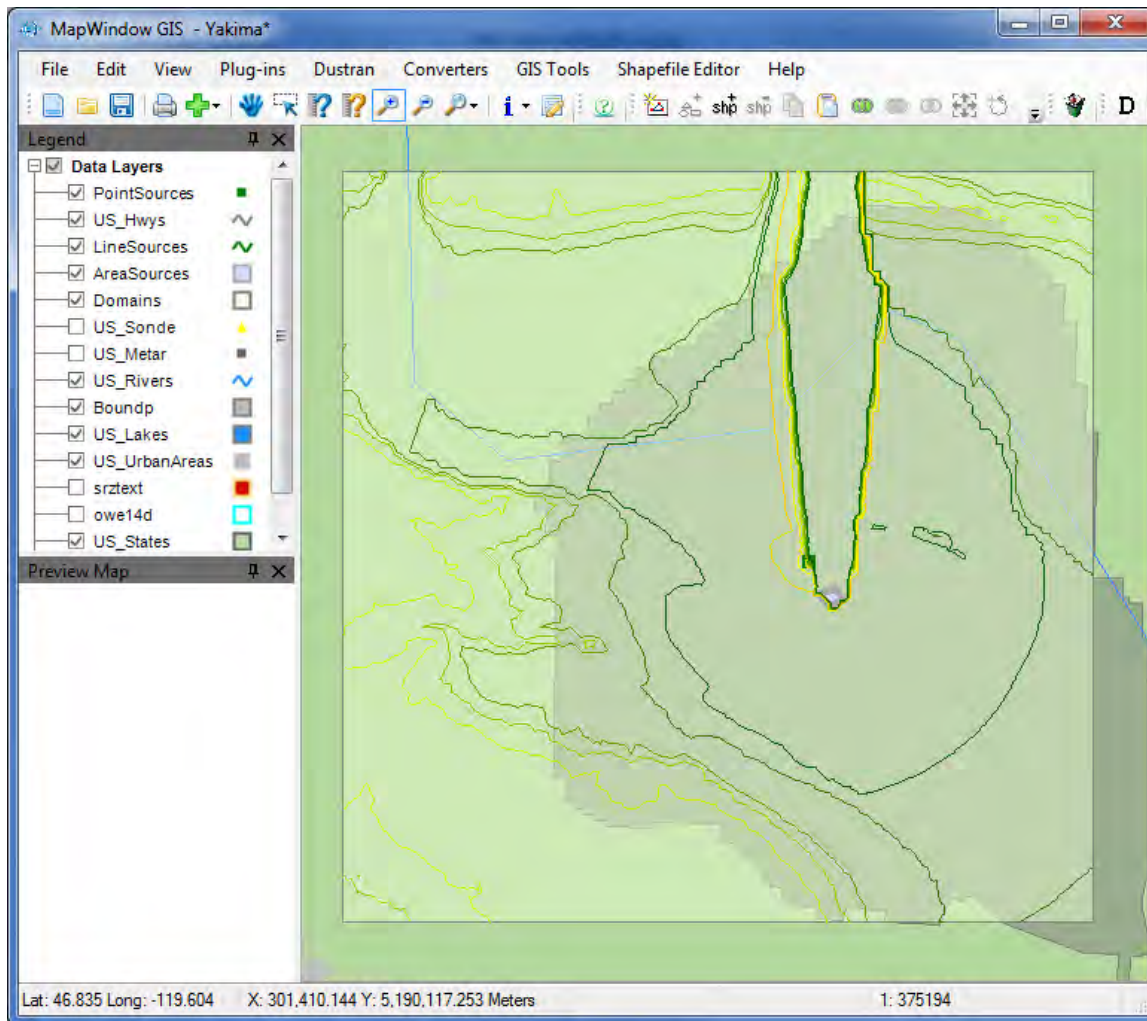
For each model time step, DUSTRAN calculates plume concentration and exposure as well as deposition and total deposition. To view a particular contour, click on the “Contours” tab and choose from the “Contour Types” listbox (Fig. 57). In this example, “Dep” is selected to display hourly surface deposition values within MapWindow.



**Figure 57.** Contours tab - “Contour Types” listbox.

For a given contour type, numerous “Contours” are available for displaying. Particular contour intervals are selected by checking the box next to the contour value. The default selection is normally adequate for displaying the maximum extent of the plume envelope.

To view a particular time step, one selects an interval from the “Interval Start Time” listbox. In this example, hourly time steps are available from the start of the release (7:00 a.m. local time) until the end of the run. Figure 58 shows the 9:00 a.m. time step, which corresponds to the one hour (9:00 a.m. till 10:00 a.m.) average concentration and surface deposition. Based on the above selections, the deposition pattern represents a combination of the two plumes (point and area-sources).



**Figure 58.** Display of deposition contours for the hour from 9-10 AM.

## 5 Conclusions and Implications for Future Research/Implementation

### 5.1 General Conclusions

This project was designed to increase understanding of dust emission processes related to testing and training activities on DoD installations and how those emissions are influenced by the physical characteristics of the vehicles generating the emissions as well as the influence of the surface conditions from which the dust originates. It also examined how the created dust plumes interact with the environment, both its physical form and the state of the atmosphere transporting the dust. This newly-acquired understanding has been incorporated into a state-of-the-art model (DUSTRAN) that can be used to better estimate how dust emissions impact the local and regional air quality environment as a result of testing, training, or the day-to-day operations on military installations that generate dust by vehicle travel.

Dust deposition in the near field and the role that the surface plays in affecting the deposition process was clearly demonstrated as part of this research. Based on field measurements it was observed that the deposition velocities increased with particle size and surface roughness under similar moderate wind speed conditions and were greater than predicted by application of the Stokes settling velocity equation. This was observed for four broad categories of surface type: bare, short grass, long grass, and open shrub community (approx. 1 m high plants).

The results from the near field deposition experiments are complemented by the results of SERDP Project RC-1730 (Pardyjak et al., 2013), which focused in detail on the physics of PM removal from suspension to deposition on idealized and real surfaces. They report deposition effects on dust plumes measured at the Hanford site (during the same field campaign of RC-1729) that also indicate that the fraction of dust plume mass flux that transfers through a near source vegetation layer is reduced in 56 m by  $\approx 26\%$  ( $\pm 13\%$ ), which is in fair agreement with our results for a reduction in mass concentration of  $\approx 20\%$ . RC-1730 (Pardyjak et al., 2013, their Fig. 42) also show that deposition increases as vegetation canopy height and density increase, which also matches with our observations that the dense, long-grass prairie site in Kansas produced the greatest removal of  $PM_{10}$  as the plumes moved downwind due to its very high density and leaf surface area. The conclusion of both projects was that the enhancement of particle deposition is due to turbulent effects within the canopy that also increase loss of particles by impaction.

The data sets on the deposition process from both RC-1729 and RC-1730 have clearly demonstrated that the removal of PM in the near field can be significant for some conditions (i.e., combination of vegetation canopy height and density) and thus needs to be accounted for in emission estimates and air quality models that are concerned with regional PM concentrations that are potentially significantly impacted by dust-raising activities. Although the effect of the surface on deposition was observed and quantified for the range of test surfaces, the limited range of surface types and meteorological conditions did not allow for the development of general relationships that would explain this effect across a wider range of surface types. The implementation of the developed relationships must still be exercised carefully and only for

surfaces that are quite similar to those tested as part of this project. If applied generally without regard to the limitations of the data set or additional information, the uncertainties introduced on the estimates of PM concentration may be regarded as unknown.

Further research is needed, both empirical and theoretical to better quantify the physics of particle deposition in the near-field and evaluate how these effects translate to measured PM concentrations over short- (<50 km) and long-range (>50 km) transport distances. Verification of these relationships and demonstrable effect on PM concentrations with increasing downwind distance may be necessary for application within the regulatory environment. An opportunity that could present itself in the future to, in part, advance towards verification of the effect of deposition is the use of the eye-safe Light Detection and Ranging (LIDAR) instrument developed as part of RC-1767. This type of instrument could be used to estimate PM concentrations across relatively long horizontal pathways downwind of emitted dust, which will be necessary to capture the dispersing dust plume and afford an opportunity to reconcile measurements with model predictions.

In addition to gaining understanding of the generation, transport, and deposition of the dust, measurement systems and methods were further developed to quantify actual emissions (e.g., the flux tower method), as well as potential emissions using transfer standards (TRAKER™ and PISWERL®). During the execution of this project, and with contributions of results from this and prior research, the methods developed have been accepted by the US EPA as designated Other Test Methods (OTM). These OTMs are the upwind-downwind flux measurement and the vehicle based method to estimate road dust emissions (i.e., TRAKER™). These designations for SERDP-developed measurement methods represent a major advancement for using them to characterize and quantify dust emissions on military installations with confidence that they are acceptable by the US EPA as a means for so doing. This has been a major concern of SERDP with respect to emission estimates made prior to the OTM designations. These instruments and methods can be used to generate data on dust emissions that can, for example, be used to develop a more accurate PM<sub>10</sub> emission inventory for a military installation that is reported for regulatory purposes.

These measurement methods were used in this project to evaluate the spatial variability of road dust emission potential, and evaluate the effectiveness of water spray to reduce emission on unpaved roads and the longer term effectiveness of the dust palliative Magnesium Chloride used at Ft. Irwin. Watering is essentially a very short term control method, on the order of hours. Magnesium Chloride, in the case of Ft. Irwin, has been used effectively to suppress dust emissions. However, the need to achieve a margin of safety and the absence of a means to estimate emissions may have led to over-use of Magnesium Chloride. The cost and material usage could have been curtailed if a tool like TRAKER™ had been available earlier to provide accurate feedback on dust suppression effectiveness. The use of TRAKER™ clearly demonstrated that the test road was not in need of quarterly treatment with the suppressant and that by adopting the use of TRAKER™, a more effective management strategy could be

developed to meet air quality regulations and reduce costs incurred by Ft. Irwin to control this dust source. US Army Environmental Command has reported that the information from TRAKER™ has been used to guide the decision to reduce treatment schedule to twice a year on the Mannix Road with a saving of ≈\$200K to the installation (Paul Josephson, US Army Environmental Command, pers. comm., 2-18-2015).

The development of the TRAKER™ and PI-SWERL® offers means to evaluate emission potential for key PM dust sources without the need to measure emissions from the sources characterized as part of this work for every combination of installation and specific source. For example, TRAKER™ can be used to estimate PM dust emissions for an assemblage of vehicle types at any installation for which TRAKER™ measurements are available through application of the known scaling relationships between vehicle weight and speed. TRAKER™ can provide a baseline measurement of actual emission potential as a function of its specific weight and speed characteristics. Using the known scaling relationship and the known, or projected, vehicle inventory that would traverse the roads measured with the TRAKER™ obviates the need to make dust emission measurements for specific vehicles everywhere. Because TRAKER™ is easily deployed and capable of evaluating hundreds of kilometers of roadway emissions in a short period of time, efficient and timely emission potential characterization is now possible. This represents a much less resource intensive methodology than was previously available for assessing dust emission potential at multiple installations allowing comprehensive characterization without the complexity associated with multiple vehicle-specific measurements. In much the same way PI-SWERL® offers an efficient and effective method to evaluate the emission potential of surfaces that can be sources of PM dust caused by wind erosion. Both TRAKER™ and PI-SWERL® have been used in this manner in the civilian environment for both State (e.g., California State Parks [TRAKER™ and PI-SWERL®]) and private sectors (e.g., British Columbia Hydro [PI-SWERL®]).

The research contributions of RC-1767 concerning measurement and modeling of fugitive dust from off-road activities complements the research of RC-1729 by providing additional insight into the impact of disturbance on dust emissions from specific military vehicle activities. These effects could be accounted for in future modifications to emission factors or evaluation of emission potential at the spatial scale mapped by TRAKER™ and PI-SWERL®.

Recognizing shortcomings in the original DUSTRAN Version 1 substantial changes and enhancements to the model were undertaken as part of this project. DUSTRAN was originally developed under SERDP Project RC-1195 as a comprehensive dispersion modeling system that integrated a dust-emissions model, a diagnostic meteorological model, and dispersion models into a console application that could run on a desktop computer within Esri®'s ArcMap GIS. A primary motivation of DUSTRAN Version 1 was to develop a tool that could easily be used to evaluate the impact of military operations against both Federal Class I area impacts and National Ambient Air Quality Standards. In order to accomplish this without the need for extensive independent validation, DUSTRAN was built on the EPA-approved CALPUFF system.

Since the completion of the original DUSTRAN, several changes have occurred that necessitated the development of Version 2. One was that in 2006 AERMOD became the EPA-sanctioned model for short-range (<50 km) dispersion calculations for regulatory purposes. Over the same period, it became apparent that Esri®'s sequential updates of the ArcMap GIS were not fully backward-compatible, which greatly limited the effective distribution of DUSTRAN. Finally, there is increasing interest in representing the deposition of suspended dust that occurs very close to sources of active emission, and a revision of DUSTRAN provided an opportunity to incorporate deposition calculations based on research also undertaken as part of this project. Thus, the major accomplishments of this revision of DUSTRAN are as follows:

- *Replacement of Esri®'s ArcMap GIS with the open-source MapWindow GIS.* There is little visual difference to the DUSTRAN user who is familiar with Version 1. MapWindow is fully capable as the GIS for DUSTRAN, and since it is open-source, the current version can always be freely distributed as part of the DUSTRAN installation package. This should make DUSTRAN much more widely used than previously.
- *Addition of AERMOD to DUSTRAN.* The AERMOD modeling system has been fully incorporated into the new version of DUSTRAN. The look and feel of the AERMOD interface is as similar as possible to that for CALPUFF so that users already familiar with the system should have little trouble navigating the new option. This fully restores DUSTRAN's ability to make dispersion calculations for regulatory use. For DUSTRAN users who prefer, there is still the option to use CALPUFF for the near-field.
- *Near-field deposition calculations.* DUSTRAN now offers the option to calculate dispersion using deposition velocities developed as part of this project linked to specific vegetation environments. Because of the way that deposition is handled in AERMOD, the new functions needed to be compiled into a modified version of AERMOD (This is not needed for CALPUFF). Both the EPA regulatory distribution of AERMOD and the modified version (AERMOD-DRI) are included in DUSTRAN Version 2 (Both produce exactly the same results when AERMOD-DRI is run using the resistance-method option for deposition.).

In summary, DUSTRAN Version 2 represents a major update to the modeling system that is far more easily distributable, is again consistent with US EPA's preferences for regulatory models, and is capable of calculating near-field deposition based on recent research findings.

## 5.2 Implementation

Results and the DUSTRAN Version 2 developed as part of this research are able to be implemented for use by the DoD with the release of this Final Report.

The code and User's Guide to DUSTRAN Version 2 are available by request from PNNL at: [http://dustran.pnnl.gov/download\\_dustran\\_beta.asp](http://dustran.pnnl.gov/download_dustran_beta.asp). The link to DUSTRAN V2 and the User's Guide are also available at the SERDP/ESTCP Tools and Training page of their website (<https://www.serdp-estcp.org/Tools-and-Training>). This freely-available, comprehensive dispersion modeling system, consisting of a dust-emissions module, a diagnostic meteorological model, and dispersion models allows the user to interactively create a release scenario and run the underlying models. Through the process of data layering, the model domain, sources, and results--including the calculated wind vector field and plume contours--can be displayed with other spatial and geophysical data sources to aid in analyzing and interpreting the scenario. This can provide a valuable tool for range or environmental managers to better evaluate how testing and training scenarios can affect local and regional air quality as it is impacted by the released particulate matter.

The two dust potential measurement systems TRAKER™ and PI-SWERL® are available via a service contract from Dust-Solve, LLC (both technologies are licensed from DRI), and in the case of PI-SWERL, can be purchased directly from Dust-Quant, LLC. These measurement systems can be used by DoD installations to evaluate dust emission potential of their testing and training facilities across a range of scales and emission scenarios. Using TRAKER™ to carry out PM<sub>10</sub> or PM<sub>2.5</sub> emission measurements for paved/unpaved/off-road surface generated by vehicle travel will provide a robust means to develop emission inventories for these major dust sources that can be reported to the US EPA and local air quality management organizations. In addition, TRAKER™ can be used to evaluate, guide, and optimize dust emission management strategies that involve the use of water or applied dust palliatives. In addition to saving costs to DoD, this can provide a detailed database on total emissions from roadway or off-road sources.

### 5.3 Implications for Future Research

The tools that have been developed in support of this project can now enable efficient research that directly benefits DoD. These research efforts can span the range from answering targeted lines of inquiry to advanced decision support tools. An example of targeted work would be the use of TRAKER™ to systematically identify the most cost effective surface treatment products for a range of road conditions. Several unpaved roads can be sampled with TRAKER™ and then treated with different products. The effectiveness of specific products over time can be evaluated with TRAKER™. Specific soil, meteorological, and road use conditions may favor one type of product over another. At DoD facilities where windblown dust is of concern, similar work can be completed with PI-SWERL®. Kavouras et al. (2009) showed convincingly that the performance of a surface treatment product depends on the properties of the soil and the exposure to ambient conditions. Additional parameters such as the effect of precipitation, breaking of crust, and freeze/thaw cycling can be investigated either systematically or in-situ at an appropriate facility. Another example of targeted studies would be to use the TRAKER™ or PI-SWERL® to collect representative suspendable dust for the purpose of assessing potential health impacts to exposed personnel. This can be done on training facilities or at any number of DoD bases worldwide.

Another avenue where research ought to be pursued is the validation of the estimates that are provided by the TRAKER™/DUSTRAN combination of tools. DUSTRAN is built on an EPA dispersion model, but the ability of that model to represent the suspension of dust and its transport to a receptor of interest has not been demonstrated. There are several means for accomplishing such validation. In one example, TRAKER™ would be used to characterize unpaved roads at a facility prior to conducting some scheduled activity or exercise (preferably of duration of several days or more). Using real activity data from the exercise, DUSTRAN simulations would be compared with PM<sub>10</sub> measured at key receptors. This would help determine which model parameters (and at what spatial and temporal scales) are most useful and accurate.

Although the effect of the surface on particulate matter deposition in the near-field zone was observed, and quantified for the range of test surfaces, the limited range of surface types and meteorological conditions did not allow for the development of general relationships that would explain this effect across a wider range of surface types. Further research is needed, both empirical and theoretical to better quantify the physics of particle deposition in the near-field.

Although not strictly a research enterprise, it would be useful to invest resources in making the TRAKER™ and DUSTRAN more “turnkey”, both individually and when used in conjunction with one another. TRAKER™ has advanced considerably in terms of reliability and data quality. However, it is still a research-level tool that has quirks both during operation and in subsequent data analysis. These quirks make it essentially impossible for anyone other than DRI (or other very technically proficient) personnel to operate. Automating the instrument to a greater degree, including real-time quality assurance and error reporting, would enable its use by a

broader range of personnel, including environmental management staff and others on DoD facilities. This would also enable standardization of the instrument so that there could be numerous identical units that operate identically. Related to this, the analysis of data from TRAKER™ remains very labor intensive and requires the capabilities of someone who is familiar with its quirks of operation. This too can be automated so that there is relatively little input needed from the operator. Finally, the import and updating of TRAKER™ information into DUSTRAN can be streamlined so that the DSUTRAN model can be equipped with the latest field data. The further development of TRAKER to achieve operability for DoD personnel and achieve wider use could be proposed for an ESTCP project.

The ultimate purpose of an emissions information and management system is to economically assemble emission inventories, identify means for reducing emissions where necessary, and to optimize resources. If PM dust emissions are considered as a type of currency or limited resource, then the DoD can use a planning tool to determine how to make maximal use of its resource. At the highest level then, the TRAKER™/DUSTRAN system can be used to assist in planning (timing, location, extent of activities) and optimization of training activities in the context of dust emissions within the constraints of testing and training needs. Understanding how such a decision support tool can be best constructed for maximal utility by DoD is a forward-looking, but attainable research goal.

## Literature Cited

- Alfaro, S.C., J.L. Rajot, and W.G. Nickling (2004), Estimation of PM<sub>20</sub> emissions by wind erosion: main sources of uncertainties, *Geomorphology*, 59 (1-4), 63-74.
- Allwine, Jr., K.J., F.C. Rutz, W.J. Shaw, J.P. Rishel, B.G. Fritz, E.G. Chapman, B.L. Hoopes, and T.E. Seiple (2006), DUSTRAN 1.0 User's Guide: A GIS-Based Atmospheric Dust Dispersion Modeling System, PNNL-16055, Pacific Northwest National Laboratory, Richland, WA.
- Bacon, S.N., E.V. McDonald, G.K. Dalldorf, W. Lucas, and G. Nikolich (2014), Recommendations for the development of a dust-suppressant test operations procedure (TOP) for U.S. Army materiel testing, in *Military Geosciences in the Twenty-First Century*, edited by R.S. Harmon, S.E. Baker and E.V. McDonald, pp. 83-100, The Geological Society of America, Inc., Boulder, CO.
- Belnap, J., and D.A. Gillette (1997), Disturbance of biological soil crusts: Impacts on potential wind erodibility of sandy desert soils in southeastern Utah, *Land Degradation and Development*, 8 (4), 355-362.
- Belot, Y., and D. Gauthier (1975), Transport of micronic particles from atmosphere to foliar surfaces, in *Heat and Mass Transport in the Biosphere*, edited, p. 31, Scripta Book Co., Washington, DC.
- Bhaganagar, K., J. Kim, and G. Coleman (2004), Effect of roughness on wall-bounded turbulence, *Flow Turbulence and Combustion*, 72 (2-4), 463-492.
- Brode, R. W. (2012), CALPUFF Near-field Validation, paper presented at 10<sup>th</sup> Conference on Air Quality Modeling, American Meteorological Society, Research Triangle Park, NC.
- Buck, B.J., J. King, V. Etyemezian, J. Morton, and M. Howell (2009), Effects of salt mineralogy on surface characteristics: Implications for dust emissions, Salton Sea California, USA, in *7th International Conference on Geomorphology (ANZIAG)*, Melbourne, Australia.
- Chan, L.Y., and W.S. Kwok (2000), Vertical dispersion of suspended particulates in urban area of Hong Kong, *Atmospheric Environment*, 34, 4403-4412.
- Cornelis, W.M., and D. Gabriels (2004), A simple model for the prediction of the deflation threshold shear velocity of dry loose particles, *Sedimentology*, 51 (1), 39-51.
- Cornelis, W.M., D. Gabriels, and R. Hartmann (2004), A conceptual model to predict the deflation threshold shear velocity as affected by near-surface soil water: I. Theory, *Soil Science Society of America Journal*, 68, 1154-1161.
- Dresser, A.L., and R.D. Huizer (2011), CALPUFF and AERMOD Model Validation Study in the Near Field: Martins Creek Revisited, *Journal of the Air & Waste Management Association*, 61 (6), 647-659.

- Du, K., M.J Rood, B.J. Kim, M.R. Kemme, B. Franek and K. Mattison (2007). Quantification of plume opacity by digital photography. *Environmental Science and Technology*, 41, 928-935.
- Du, K., W. Yuen, W. Wang, M.J. Rood, R. Varma, R.A. Hashmonay, B.J. Kim, and M.R. Kemme (2011), Optical remote sensing to quantify fugitive particulate mass emissions from stationary short-term and mobile continuous sources: Part II. Field applications, *Environmental Science and Technology*, 45, 666-672.
- Dulac, F., P. Buat-Ménard, U. Ezat, S. Melki, and G. Bergametti (1989), Atmospheric input of trace metals to the western Mediterranean: uncertainties in modelling dry deposition from cascade impactor data, *Tellus B*, 41 (3), 362-378.
- Engelbrecht, J.P., J.A. Gillies, V. Etyemezian, H. Kuhns, S.E. Baker, D. Zhu, G. Nikolich, and S.D. Kohl (2012), Mineralogical controls on dust emissions at four arid locations in the western USA, *Aeolian Research*, 6, 41-54.
- Etyemezian, V., H.D. Kuhns, and G. Nikolich (2006), Precision and repeatability of the TRAKER vehicle-based paved road dust emission potential, *Atmospheric Environment*, 40, 2953-2958.
- Etyemezian, V., H. Kuhns, J.A. Gillies, M. Green, M. Pitchford, and J.G. Watson (2003a), Vehicle based road dust emissions measurement (I): methods and calibration, *Atmospheric Environment*, 37, 4559-4571.
- Etyemezian, V., J.A. Gillies, M. Shinoda, G. Nikolich, J. King, and A.R. Bardis (2014), Accounting for surface roughness on measurements conducted with PI-SWERL: Evaluation of a subjective visual approach and a photogrammetric technique, *Aeolian Research*, 13, 35-50
- Etyemezian, V., J. Gillies, H. Kuhns, D. Gillette, S. Ahonen, D. Nikolic, and J. Veranth (2004), Deposition and removal of fugitive dust in the arid southwestern United States: measurements and model results, *Journal of the Air & Waste Management Association*, 54, 1099-1111.
- Etyemezian, V., G. Nikolich, S. Ahonen, M. Pitchford, M. Sweeney, J. Gillies, and H.D. Kuhns (2007), The Portable In-Situ Wind Erosion Laboratory (PI-SWERL): a new method to measure PM<sub>10</sub> windblown dust properties and potential for emissions, *Atmospheric Environment*, 41, 3789-3796.
- Etyemezian, V., H. Kuhns, J.A. Gillies, J.C. Chow, M. Green, K. Hendrickson, M. McGowan, and M. Pitchford (2003b), Vehicle based road dust emissions measurement (III): effect of speed, traffic volume, location, and season on PM<sub>10</sub> road dust emissions, *Atmospheric Environment*, 37, 4583-4593.

- Fécan, F., B. Marticorena, and G. Bergametti (1999), Parametrization of the increase of the aeolian erosion thresholds wind friction velocity due to soil moisture for arid and semi-arid areas, *Annales Geophysicae*, 17(1), 149-157.
- Gillette, D.A. (1978), A wind tunnel simulation of the erosion of soil: effect of soil texture, sandblasting, wind speed, and soil consolidation on dust production, *Atmospheric Environment*, 12, 1735-1743.
- Gillette, D.A. (1999), A qualitative geophysical explanation for "hot spot" dust emitting source regions, *Contributions to Atmospheric Physics*, 72 (1), 67-77.
- Gillies, J.A. (2013), Fundamentals of aeolian sediment transport | Dust emissions and transport – near surface, in *Treatise on Geomorphology*, edited by J. Shroder and N. Lancaster, pp. 43-63, Academic Press, San Diego, CA.
- Gillies, J.A., H. Green, G. McCarley-Holder, S. Grimm, C. Howard, N. Barbieri, D. Ono, T. Schade (2015). Using solid element roughness to control sand movement: Keeler Dunes, Keeler, California, *Aeolian Research* 18, 35-46, doi: 10.1016/j.aeolia.2015.05.004.
- Gillies, J.A., and N. Lancaster (2013), Large roughness element effects on sand transport, Oceano Dunes, California, *Earth Surface Processes and Landforms*, 38 (8), 785-792.
- Gillies, J.A., W.G. Nickling, and J. King (2006), Aeolian sediment transport through large patches of roughness in the atmospheric inertial sublayer, *Journal of Geophysical Research - Earth Surface*, 111 (F02006), doi: 10.1029/2005JF000434.
- Gillies, J.A., W.G. Nickling, and J. King (2007), Shear stress partitioning in large patches of roughness in the atmospheric inertial sublayer, *Boundary-Layer Meteorology*, 122 (2), 367-396.
- Gillies, J.A., V. Etyemezian, H. Kuhns, D. Nikolic, and D.A. Gillette (2005), Effect of vehicle characteristics on unpaved road dust emissions, *Atmospheric Environment*, 39, 2341–2347.
- Gillies, J.A., H. Kuhns, J.P. Engelbrecht, S. Uppapalli, E. Etyemezian, and G. Nikolich (2007), Particulate emissions from U.S. Department of Defense artillery backblast testing, *Journal of the Air & Waste Management Association*, 57, 551-560.
- Gillies, J.A., V. Etyemezian, H. Kuhns, J.D. McAlpine, S. Uppapalli, G. Nikolich, and J. Engelbrecht (2010), Dust emissions created by low-level rotary-winged aircraft flight over desert surfaces, *Atmospheric Environment*, 44 (8), 1043-1053.
- Houser, C.A., and W.G. Nickling (2001a), The emission and vertical flux of particulate matter <10 micrometers from a disturbed clay-crust surface, *Sedimentology*, 48, 255-267.
- Houser, C.A., and W.G. Nickling (2001b), The factors influencing the abrasion efficiency of saltating grains on a clay-crust play, *Earth Surface Processes and Landforms*, 26, 491-505.

- Irwin, H.P.A.H. (1981), A simple omnidirectional sensor for wind tunnel studies of pedestrian level winds, *Journal of Wind Engineering and Industrial Aerodynamics*, 7, 219-239.
- Janhäll, S., P. Molnár, and M. Hallquist (2003), Vertical distribution of air pollutants at the Gustavii Cathedral in Göteborg, Sweden, *Atmospheric Environment*, 37(2), 209-217.
- Johnson, T.C., D.A. Gillette, and R.L. Schwiesow (1992), Fate of dust particles from unpaved roads under various atmospheric conditions, in *Precipitation Scavenging and Atmosphere-Surface Exchange, Volume 2-The Semonin Volume: Atmosphere-Surface Exchange Processes*, edited by S. E. Schwartz and W. G. N. Slinn, pp. 933-945.
- Kavouras, I.G., V. Etyemezian, G. Nikolich, J. Gillies, M. Young, and D. Shafer (2009), A new technique for characterizing the efficacy of fugitive dust suppressants, *Journal of the Air & Waste Management Association*, 59, 603-612.
- King, J., V. Etyemezian, M. Sweeney, B.J. Buck, and G. Nikolich (2011), Dust emission variability at the Salton Sea, California, USA, *Aeolian Research*, 3, 67-79.
- Kuhns, H., J.A. Gillies, V. Etyemezian, G. Nikolich, J. King, D. Zhu, S. Uppapalli, J. Engelbrecht, and S. Kohl (2010), Effect of soil types and momentum on unpaved road particulate matter emissions from wheeled and tracked vehicles, *Aerosol Science and Technology* 44, 193-202.
- Kussin, J., and M. Sommerfeld (2002), Experimental studies on particle behaviour and turbulence modification in horizontal channel flow with different wall roughness, *Experimental Fluids*, 33 (1), 143-159.
- Langston, R., R.S. Merle Jr., D. Hart, V. Etyemezian, H. Kuhns, J. Gillies, D. Zhu, D. Fitz, K. Bumiller, D.E. James, and H. Teng (2008). The preferred alternative method for measuring paved road dust emissions for emissions inventories: "Mobile technologies vs. the traditional AP-42 methodology. Prepared for EPA OAQPS, March, 2008, 110 pages.
- Li, A., and G. Ahmadi (1992), Dispersion and deposition of spherical particles from point sources in a turbulent channel flow, *Aerosol Science and Technology*, 16 (4), 209-226.
- McAlpine, J.D., D. Koracin, D. Boyle, J.A. Gillies, and E.V. McDonald (2010), Assessment of the applicability of a CFD method to simulate a rotorcraft dust emission source, *Environmental Fluid Mechanics*, 10, 691-710.
- Pardyjak, E.R., S.O. Speckart, F. Yin, and J.M. Veranth (2008), Near-source deposition of vehicle generated fugitive dust on vegetation and buildings. Part 1: Model development and theory, *Atmospheric Environment*, 42, 6442-6452.
- Pardyjak, E.R., J.M. Veranth, S.O. Speckart, S. Moran and T. Price (2013). *Development of a Windbreak Dust Predictive Model and Mitigation Planning Tool*. SERDP Project RC-1730 Final Report, 83 p.
- Parrett, F. W. (1992), *Dust Emissions: A Review*, Applied Environmetrics.

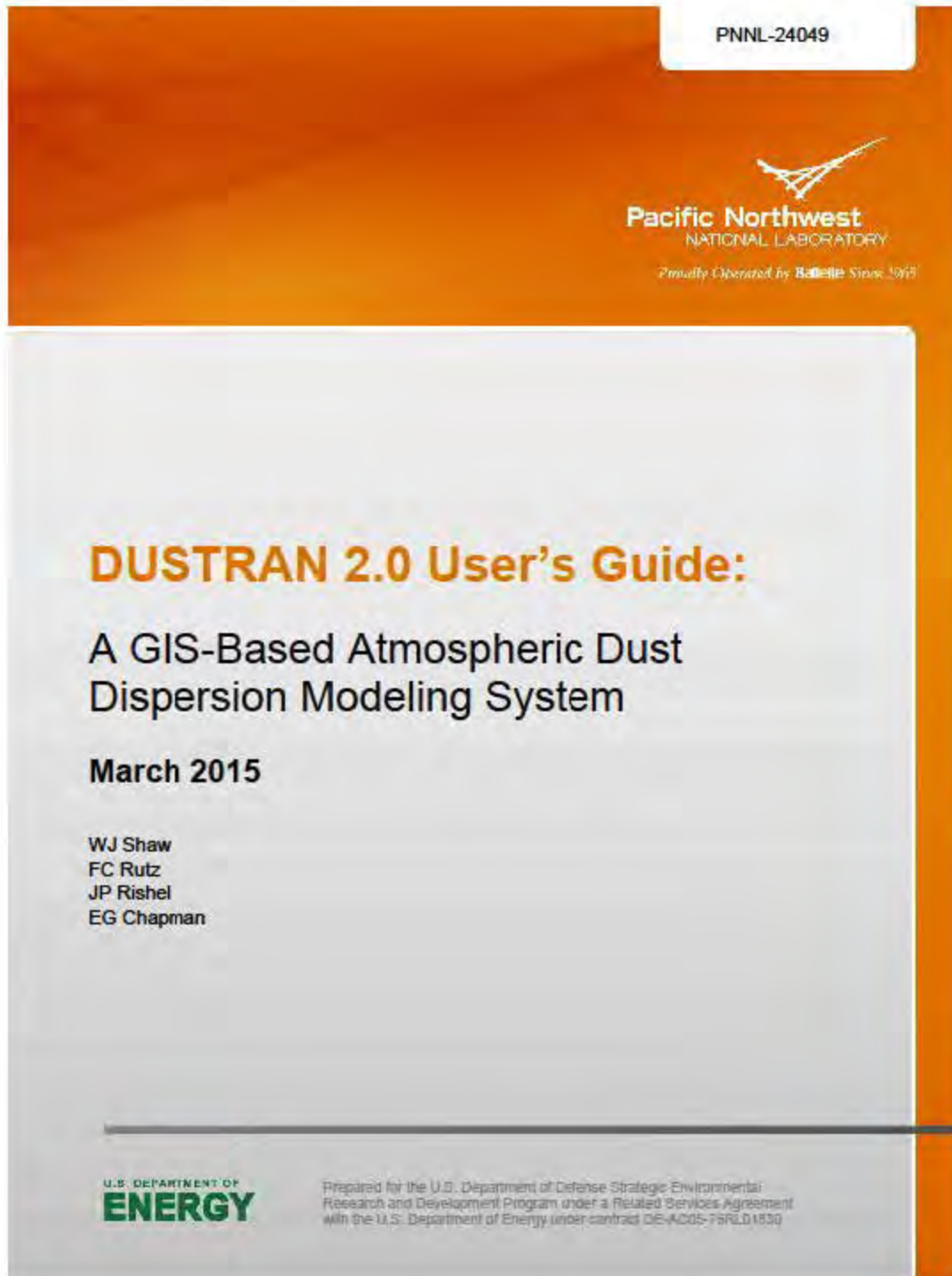
- Raupach, M.R., D.A. Gillette, and J.F. Leys (1993), The effect of roughness elements on wind erosion threshold, *Journal of Geophysical Research*, 98 (D2), 3023-3029.
- Rice, M.A., and I.K. McEwan (2001), Crust strength: a wind tunnel study of the effect of impact by saltating particles on cohesive soil surfaces, *Earth Surface Processes and Landforms*, 26, 721-733.
- Roth, M. (2000), Review of atmospheric turbulence over cities, *Quarterly Journal of the Royal Meteorological Society*, 126 (564), 941-990.
- Samara, C., and D. Voutsas (2005), Size distribution of airborne particulate matter and associated heavy metals in the roadside environment, *Chemosphere*, 59, 1197–1206.
- Scire, J.S., D.G. Strimaitis, and R.J. Yamartino (2000), A User's Guide for the CALPUFF Dispersion Model (Version 5), Earth Tech, Inc., Concord, MA.
- Scire, J.S., R.J. Yamartino, G.R. Carmichael, and Y.S. Chang (1989), CALGRID: A Mesoscale Photochemical Grid Model Volume II – User's Guide, California Air Resources Board, Sacramento, CA.
- Seinfeld, J.H., and S.N. Pandis (1998), *Atmospheric Chemistry and Physics: From Air Pollution to Climate Change*, Wiley Interscience, New York, NY.
- Shao, Y. (2000), *Physics and Modelling of Wind Erosion*, Kluwer Academic Publishers, Dordrecht.
- Shaw, W.J., K.J. Allwine, Jr., B.G. Fritz, F.C. Rutz, J.P. Rishel, and E.G. Chapman (2008), An evaluation of the wind erosion module in DUSTRAN, *Atmospheric Environment*, 42, 1907-1921.
- Sweeney, M., E.V. McDonald, and V. Etyemezian (2011), Quantifying dust emissions from desert landforms, *Geomorphology*, 135, 21-34.
- Sweeney, M., V. Etyemezian, T. Macpherson, W.G. Nickling, J. Gillies, G. Nikolich, and E. McDonald (2008), Comparison of PI-SWERL with dust emission measurements from a straight-line field wind tunnel, *Journal of Geophysical Research, Earth Surface*, 113, F01012, doi: 10.1029/2007JF000830.
- Sweeney, M.R., and A. Mason (2013), Mechanisms of dust emission from Pleistocene loess deposits, Nebraska, USA, *Journal of Geophysical Research, Earth Surface* 118, 1-12, doi: 10.1002/jgrf.20101.
- Tegen, I., S.P. Harrison, K. E. Kohfeld, S. Engelstaedter, and M. Werner (2002), Emission of soil dust aerosol: Anthropogenic contribution and future changes, *Geochimica Et Cosmochimica Acta*, 66 (15A), A766-A766.
- Turner, D. B. (1994), *Workbook of Atmospheric Dispersion Estimates: An Introduction to Dispersion Modeling*, Second ed., CRC Press, Inc., Boca Raton, FL.

- US EPA (2014a), ADDENDUM: User's Guide for the AERMOD Meteorological Preprocessor (AERMET), EPA-454/B-03-002, Research Triangle Park, NC.
- US EPA (2014b), ADDENDUM: User's Guide for the AMS/EPA Regulatory Model – AERMOD, EPA-454/B-03-001, Research Triangle Park, NC.
- US EPA (2004), AERMOD Deposition Algorithms – Science Document, [http://www.epa.gov/scram001/7thconf/aermod/aer\\_scid.pdf](http://www.epa.gov/scram001/7thconf/aermod/aer_scid.pdf).
- US, EPA (2004), AERMOD: Description of Model Formulation, EPA-454/R-03-004, Research Triangle Park, NC.
- US EPA (2008), AERSURFACE User's Guide, EPA-454/B-08-001, Research Triangle Park, SC.
- US EPA (1995a), Compilation of Air Pollutant Emission Factors Volume I: Stationary, Point and Area Sources, US EPA Office of Air Quality Planning and Standards, Research Triangle Park, NC.
- US EPA (2014), Other Test Method (OTM) 32: Determination of Emissions from Open Sources by Plume Profiling, <http://www.epa.gov/ttn/emc/prelim/otm32.pdf>.
- US EPA (2014), Other Test Method (OTM) 34: Method to Quantify Road Dust Particulate Matter Emissions (PM<sub>10</sub> and/or PM<sub>2.5</sub>) from Vehicular Travel on Paved and Unpaved Roads, (<http://www.epa.gov/ttn/emc/prelim/otm34.pdf>).
- US EPA (1995b), User's Guide for the Industrial Source Complex (ISC3) Dispersion Models Volume I: User Instructions; EPA-454/B-95-003a, Office of Air Quality Planning and Standards, Research Triangle Park, NC.
- Valiulis, D., D. Čeburnis, J. Šakalys, and K. Kvietkus (2002), Estimation of atmospheric trace metal emissions in Vilnius City, Lithuania, *Atmospheric Environment*, 36, 6001-6014.
- Zhang, J., and Y. Shao (2014), A new parameterization of dust dry deposition over rough surfaces, *Atmos. Chem. Phys. Discuss.*, 14 (6), 8063-8094.
- Zhang, J., Y. Shao, and N. Huang (2014), Measurements of dust deposition velocity in a wind-tunnel experiment, *Atmos. Chem. Phys.*, 14(17), 8869-8882.
- Zhu, D., H. Kuhns, J.A. Gillies, V. Etyemezian, A. Gertler, and S. Brown (2011), Inferring deposition velocities from changes in aerosol size distributions downwind of a roadway, *Atmospheric Environment*, 45, 957-966.
- Zufall, J. D., C.I. Davidson, P.F. Caffrey, and J.M. Ondov (1998), Airborne concentrations and dry deposition fluxes of particulate species to surrogate surfaces deployed in southern Lake Michigan, *Environmental Science and Technology*, 32 (11), 1623-1628.

## Appendix A: List of Scientific/Technical Publications

- Engelbrecht, J.P., J.A. Gillies, V. Etyemezian, H. Kuhns, S.E. Baker, D. Zhu, G. Nikolich and S.D. Kohl (2012). Mineralogical controls on dust emissions at four arid locations in the western USA. *Aeolian Research* **6**: 41-54, doi: 10.1016/j.aeolia.2012.07.003.
- Etyemezian, V., J.A. Gillies, M. Shinoda, G. Nikolich, J. King, and A.R. Bardis (2014). Accounting for surface roughness on measurements conducted with PI-SWERL: Evaluation of a subjective visual approach and a photogrammetric technique. *Aeolian Research*, **13**: 35-50, doi: 10.1016/j.aeolia.2014.003.002.
- Shaw, W.J., F.C. Rutz, J.P. Rishel, and E.G. Chapman (2011). DUSTRAN – History and Current Development of an Atmospheric Dust Transport Model. Presented at the *American Meteorological Society Special Symposium on Applications of Air Pollution Meteorology*, Seattle, Washington
- Shaw, W.J., F.C. Rutz, J.P. Rishel, and E.G. Chapman (2015). *DUSTRAN 2.0 User's Guide: A GIS-Based Atmospheric Dust Dispersion Modeling System*. Pacific Northwest National Laboratory Report (in final review).
- Zhu, D., J.A. Gillies, and V. Etyemezian (2014). Evaluating dust emissions under different moisture conditions using a mobile monitoring system. *3rd Road Dust Best Management Practices Conference*, Minneapolis MN, 3-5 February 2014.
- Zhu, D., J.A. Gillies, V. Etyemezian, G. Nikolich, and W.J. Shaw (2015). Evaluation of the surface roughness effect on suspended particle deposition near unpaved roads. *Atmospheric Environment* (under revision).

## Appendix B Other Supporting Materials: DUSTRAN Version 2 Users Guide.



## DISCLAIMER

This report was prepared as an account of work sponsored by an agency of the United States Government. Neither the United States Government nor any agency thereof, nor Battelle Memorial Institute, nor any of their employees, makes **any warranty, express or implied, or assumes any legal liability or responsibility for the accuracy, completeness, or usefulness of any information, apparatus, product, or process disclosed, or represents that its use would not infringe privately owned rights.** Reference herein to any specific commercial product, process, or service by trade name, trademark, manufacturer, or otherwise does not necessarily constitute or imply its endorsement, recommendation, or favoring by the United States Government or any agency thereof, or Battelle Memorial Institute. The views and opinions of authors expressed herein do not necessarily state or reflect those of the United States Government or any agency thereof.

PACIFIC NORTHWEST NATIONAL LABORATORY

*operated by*

BATTELLE

*for the*

UNITED STATES DEPARTMENT OF ENERGY

*under Contract DE-AC05-76RL01830*

Printed in the United States of America

Available to DOE and DOE contractors from the  
Office of Scientific and Technical Information,  
P.O. Box 62, Oak Ridge, TN 37831-0062;  
ph: (865) 576-8401  
fax: (865) 576-5728  
email: [reports@adonis.osti.gov](mailto:reports@adonis.osti.gov)

Available to the public from the National Technical Information Service  
5301 Shawnee Rd., Alexandria, VA 22312  
ph: (800) 553-NTIS (6847)  
email: [orders@ntis.gov](mailto:orders@ntis.gov) <<http://www.ntis.gov/about/form.aspx>>  
Online ordering: <http://www.ntis.gov>



This document was printed on recycled paper.

(8/2010)

## **DUSTRAN 2.0 User's Guide:**

### A GIS-Based Atmospheric Dust Dispersion Modeling System

WJ Shaw  
FC Rutz  
JP Rishel  
EG Chapman

March 2015

Prepared for the U.S. Department of Defense Strategic Environmental  
Research and Development Program under a Related Services Agreement  
with the U.S. Department of Energy under contract DE-AC05-76RL01830

Pacific Northwest National Laboratory  
Richland, Washington 99352

## Summary

The U.S. Department of Energy's Pacific Northwest National Laboratory (PNNL) completed a multi-year project to update the DUSTRAN atmospheric dispersion modeling system, which is being used to assist the U.S. Department of Defense (DoD) in addressing particulate air quality issues at military training and testing ranges. This version—DUSTRAN V2.0—includes (1) a complete replacement of the geographic information system (GIS) platform to include the utilization of open-source GIS software (MapWindow) (2) user profiles to allow multiple users to run individual simulations using separate sites (3) integration of the Environmental Protection Agency's (EPA's) AERMOD air-dispersion model for modeling near-field (less than 50 km) releases, including an option to use a formulation for near-field deposition derived from new work by the Desert Research Institute; and (4) updates to the dust source-term module for military vehicles to include additional vehicle and soil types, as well as enhanced formulations for particle deposition. The project was funded by DoD's Strategic Environmental Research and Development Program (SERDP).

DUSTRAN V2.0 includes widely used, scientifically defensible atmospheric dispersion models and model components that are coupled with state-of-science dust-emission formulations in one, easy-to-use interface. The DUSTRAN modeling platform is built on the MapWindow open-source GIS software, and includes the EPA-approved AERMOD and CALPUFF dispersion models for modeling active-source dust emissions, as well as the CALGRID dispersion model for modeling wind-blown dust from large areas. DUSTRAN includes the necessary terrain and meteorological preprocessors that are required to run the dispersion models. Execution and data transfer between the preprocessors and dispersion models is managed automatically by the interface at runtime. DUSTRAN also includes dust-emission modules for generating source terms from both tracked and wheeled military vehicle activities as well as wind-blown dust generation from larger areas. The primary features of DUSTRAN include:

- A modeling domain that is graphically specified and size-selectable (20 km to 400 km).
- Dispersion models for treating near-field (AERMOD) and far-field (CALPUFF) dispersion from active emission sources and a gridded dispersion model (CALGRID) for modeling passive, wind-blown dust emissions from large areas.
- An “Add Site” utility for creating new modeling sites and the supporting files and data structure needed for a simulation.
- Easily specified single- or multi-station meteorology.
- Multiple point, area, and line sources created graphically within a scenario.
- Easily specified simulation and release times (typically a few hours to a few days) within the user interface.
- Resulting concentrations and deposition contours that are viewable within the GIS interface and can be animated to view the time-progression of the plume.
- Simulations of multiple particle sizes and gaseous species in a single run.
- Treatment of dry deposition as well as complex terrain effects.

This manual documents DUSTRAN V2.0 and includes installation instructions, a description of the modeling system, and detailed example tutorials.

## Acknowledgments

This research was supported in part by the U.S. Department of Defense through the Strategic Environmental Research and Development Program (SERDP Project RC-1729) under a Related Services Agreement with the U.S. Department of Energy (DOE) under Contract DE-AC05-76RL01830. Pacific Northwest National Laboratory (PNNL) is operated for DOE by Battelle.

Dr. Jack Gillies of Desert Research Institute (DRI) provided emission-factor data for wheeled military vehicles as well as new observations of deposition velocity incorporated into DUSTRAN as part of this project. The emission factors were developed under a previous Strategic Environmental Research and Development Program project (CP-1191) with DRI.

Dr. John Hall, the SERDP program manager, provided valuable guidance and support during all phases of the development of DUSTRAN.

## Acronyms and Abbreviations

AMS	American Meteorological Society
AERMAP	AMS/EPA MAPping program
AERMET	AMS/EPA METeorological model
AERMOD	AMS/EPA Regulatory Model
CALGRID	CALifornia photochemical GRID model
CALMET	CALifornia METeorological model
CALPOST	CALifornia POST-processing program
CALPUFF	CALifornia PUFF model
CST	Central Standard Time
DEM	digital elevation model
DoD	U.S. Department of Defense
DOE	U.S. Department of Energy
DRI	Desert Research Institute
DUSTRAN	DUST TRANsport
EPA	U.S. Environmental Protection Agency
ESRI	Environmental System Research Institute
EST	Eastern Standard Time
FSL	Forecast Systems Laboratory
GIS	geographic information system
GLCC	global land-cover characteristics
M-O	Monin-Obukhov (similarity theory)
MST	Mountain Standard Time
NARCS	number of arc distances
NOAA	National Oceanic & Atmospheric Administration
NWS	National Weather Service
NTC	National Training Center
OWE	Olson World Ecosystem (database)
PGEMS	Pacific Gas and Electric Modeling System
PGT	Pasquill-Gifford-Turner specifications
PM	particulate matter
PNNL	Pacific Northwest National Laboratory
PST	Pacific Standard Time
SERDP	Strategic Environmental Research and Development Program
USGS	U.S. Geological Survey
UTM	Universal Transverse Mercator

# Contents

Summary .....	iii
Acknowledgments.....	v
Acronyms and Abbreviations .....	vii
1.0 Introduction .....	1.1
1.1 Background .....	1.1
1.2 Features .....	1.2
2.0 Technical Overview of the DUSTRAN Modeling System .....	2.1
2.1 AERMOD Modeling System .....	2.3
2.1.1 AERMET .....	2.3
2.1.2 AERMAP .....	2.5
2.1.3 AERMOD.....	2.5
2.2 CALPUFF/CALGRID Modeling Systems.....	2.8
2.2.1 CALMET .....	2.8
2.2.2 CALPUFF .....	2.12
2.2.3 CALGRID .....	2.15
2.2.4 CALPOST .....	2.16
2.3 Dust-Emission Modules .....	2.16
2.3.1 Emission by Vehicular Activity .....	2.16
2.3.2 Windblown Dust .....	2.18
3.0 DUSTRAN Installation Instructions.....	3.1
3.1 Installing DUSTRAN.....	3.1
3.2 Installing DUSTRAN and Setting Up Access to DUSTRAN from Within MapWindow.....	3.1
4.0 DUSTRAN User Interface.....	4.1
4.1 Starting DUSTRAN and Loading a Site .....	4.1
4.2 Domain Panel .....	4.1
4.2.1 Creating a New Domain .....	4.2
4.2.2 Selecting an Existing Domain .....	4.2
4.2.3 Deleting a Domain from a Site.....	4.2
4.3 Release Period Panel .....	4.3
4.3.1 Setting the Default Release Start Time and Duration .....	4.3
4.3.2 Synchronizing the Release Start Time and Duration for All Sources .....	4.3
4.4 Simulation Scenario Panel .....	4.4
4.4.1 Setting the Simulation Type.....	4.4
4.4.2 Setting the Time Zone .....	4.5
4.4.3 Setting the Start Date.....	4.5
4.4.4 Setting the Start Time.....	4.5

4.4.5	Setting the Run Duration.....	4.6
4.4.6	Setting the Averaging Interval .....	4.6
4.5	Species Tab .....	4.6
4.5.1	Selecting an Existing Species.....	4.6
4.5.2	Modifying an Existing Species .....	4.7
4.5.3	Adding a New Species .....	4.7
4.5.4	Deleting an Existing Species.....	4.8
4.6	Sources Tab.....	4.8
4.6.1	Adding a New Point Source .....	4.8
4.6.2	Adding a New Line Source .....	4.10
4.6.3	Adding a New Area Source.....	4.14
4.6.4	Selecting Existing Sources to Use in a Simulation .....	4.17
4.6.5	View and Edit Existing Source Information .....	4.17
4.6.6	Deleting an Existing Source .....	4.17
4.6.7	Clearing All Existing Sources .....	4.18
4.6.8	Saving Existing Sources as a Scenario.....	4.18
4.6.9	Adding Characteristic Files (Soil and Vegetation for Wind-blown Dust) .....	4.18
4.7	Scenarios Tab.....	4.19
4.7.1	Adding an Existing Scenario.....	4.19
4.7.2	Deleting an Existing Scenario .....	4.20
4.8	Meteorology Tab.....	4.20
4.8.1	Selecting Single Observation Meteorology.....	4.20
4.8.2	Selecting User-Defined Meteorology.....	4.23
4.9	Contours Tab.....	4.24
4.9.1	Setting the Contour Type .....	4.24
4.9.2	Selecting Contour Levels .....	4.25
4.9.3	Selecting Emission Type.....	4.25
4.9.4	Selecting Interval Start Time.....	4.25
4.9.5	Animating Contours .....	4.26
4.10	Display Options Tab.....	4.26
4.10.1	Displaying the Contour Results.....	4.27
4.10.2	Displaying the Receptor Network.....	4.28
4.10.3	Displaying the Calculated Wind Vector Field.....	4.28
4.10.4	Displaying Surface and Upper-Air Meteorological Station Locations .....	4.28
5.0	Polygon Layer Creator.....	5.1
5.1.1	Starting the Polygon Layer Creator.....	5.1
5.1.2	Loading a Shapefile.....	5.2
5.1.3	Importing Polygons from an Existing Shape File .....	5.3
5.1.4	Starting a New Polygon Set .....	5.3

5.1.5	Site Navigation Within Map Display Window .....	5.3
5.1.6	Working with Polygons.....	5.4
5.1.7	Setting the Resolution of the Output .csv File.....	5.7
5.1.8	Creating the Output Shape File and .csv File .....	5.7
6.0	Adding a New User Profile to DUSTRAN.....	6.1
7.0	Adding a New Site to DUSTRAN.....	7.1
8.0	DUSTRAN Example Tutorials.....	8.1
8.1	Creating the Yakima Tutorial Site .....	8.1
8.2	Simulating Dust Dispersion from Active Source Emissions Using CALPUFF.....	8.4
8.2.1	Starting DUSTRAN .....	8.4
8.2.2	Selecting a Site .....	8.5
8.2.3	Creating a Domain .....	8.6
8.2.4	Setting the Release Period.....	8.6
8.2.5	Setting the Simulation Scenario .....	8.7
8.2.6	Setting the Model Species .....	8.7
8.2.7	Creating a Point Source .....	8.8
8.2.8	Creating an Area Source .....	8.9
8.2.9	Entering Meteorological Data .....	8.12
8.2.10	Running DUSTRAN .....	8.12
8.2.11	Displaying Model Output.....	8.12
8.2.12	Viewing Model Results.....	8.13
8.3	Simulating Dust Dispersion from Active Source Emissions Using AERMOD.....	8.15
8.3.1	Starting DUSTRAN .....	8.15
8.3.2	Selecting a Site .....	8.15
8.3.3	Creating a Domain .....	8.16
8.3.4	Setting the Release Period.....	8.17
8.3.5	Setting the Simulation Scenario .....	8.17
8.3.6	Setting the Model Species .....	8.17
8.3.7	Creating a Point Source .....	8.18
8.3.8	Creating an Area Source .....	8.19
8.3.9	Entering Meteorological Data and Surface Characteristics.....	8.22
8.3.10	Running DUSTRAN .....	8.24
8.3.11	Displaying Model Output.....	8.24
8.3.12	Viewing Model Results.....	8.25
8.4	Simulating Wind-blown Dust Dispersion .....	8.26
8.4.1	Starting DUSTRAN .....	8.27
8.4.2	Selecting a Site .....	8.27
8.4.3	Defining the Domain .....	8.28
8.4.4	Setting the Simulation Scenario .....	8.29

8.4.5	Setting the Soil and Vegetation Characteristic Files .....	8.29
8.4.6	Viewing the Soil and Vegetation Characteristic Files.....	8.31
8.4.7	Entering Meteorological Data .....	8.33
8.4.8	Running DUSTRAN .....	8.33
8.4.9	Viewing Model Results.....	8.34
9.0	References .....	9.1
	Appendix A – DUSTRAN Directory and File Documentation .....	A.1

# Figures

Figure 1.1. Primary DUSTRAN components .....	1.2
Figure 2.1. AERMOD Modeling Components within DUSTRAN .....	2.2
Figure 2.2. CALPUFF/CALGRID Modeling Components within DUSTRAN .....	2.2
Figure 2.3. Data Flow and Geophysical Preprocessors for CALMET .....	2.9
Figure 2.4. Example of the Primary Cartesian Receptor Grid and a Polar and Cartesian Sub-Grid Used Within CALPUFF .....	2.14
Figure 2.5. Contour Plot of RMS Differences Between Equation (2.15) and Observations of Dust Flux G Discussed by Gillette and Passi (1988) .....	2.20
Figure 2.6. Observations of G Versus $u^*$ after Gillette and Passi (1988). The solid line is Equation (2.15) with $C = 1.0 \times 10^{-14} \text{ g cm}^{-6} \text{ s}^3$ and $u_{*t} = 20 \text{ cm s}^{-1}$ . .....	2.20
Figure 3.1. .NET Framework 4.5 Installation Start .....	3.1
Figure 3.2. .NET 4.5 Installation Progress .....	3.2
Figure 3.3. DUSTRAN Install Start .....	3.3
Figure 3.4. DUSTRAN Destination Select .....	3.3
Figure 3.5. Start DUSTRAN Installation .....	3.4
Figure 3.6. DUSTRAN Install Finished .....	3.4
Figure 3.7. Microsoft Chart Control Installation Start Window .....	3.5
Figure 3.8. Chart Control License Agreement .....	3.5
Figure 3.9. Chart Control Installation Progress Window .....	3.6
Figure 3.10. Chart Control Installation Complete Window .....	3.7
Figure 3.11. DUSTRAN Configuration Manager .....	3.7
Figure 3.12. Select MapWindow.exe File .....	3.8
Figure 3.13. .tif File Extraction Window .....	3.8
Figure 3.14. DUSTRAN Configuration Complete .....	3.9
Figure 3.15. MapWindow Desktop Icon .....	3.9
Figure 3.16. Selecting DUSTRAN Plug-in .....	3.10
Figure 3.17. MapWindow DUSTRAN Menu Items .....	3.10
Figure 3.18. DUSTRAN Startup .....	3.11
Figure 4.1. Site Loaded into the DUSTRAN Modeling System .....	4.1
Figure 4.2. Example Domain Panel with Controls Labeled .....	4.2
Figure 4.3. Example Release Period Panel with Controls Labeled .....	4.3
Figure 4.4. Example Simulation Scenario Panel with Controls Labeled .....	4.4
Figure 4.5. Example Species Tab .....	4.7
Figure 4.6. Example Sources Tab with Point, Line, and Area Sources Entered .....	4.8
Figure 4.7. Example Point-Source Input Window .....	4.9
Figure 4.8. Example Line-Source Input Window Using the User-Defined Emission Option .....	4.11
Figure 4.9. Example Vehicle Input Window for a Line Source .....	4.13

Figure 4.10. Example Area-Source Input Window Using the User-Defined Emission Option.....	4.15
Figure 4.11. Example Vehicle Input Window for an Area Source .....	4.16
Figure 4.12. Characteristics Priorities Dialog Box for Adding Files, such as Soil and Vegetation Classes, in DUSTRAN.....	4.19
Figure 4.13. Example Scenario Tab with Controls Labeled .....	4.20
Figure 4.14. Example Meteorological Data Input Form for a CALPUFF simulation .....	4.21
Figure 4.15. Example Meteorological Data Input Form for an AERMOD simulation .....	4.21
Figure 4.16. AERMOD Surface Characteristics Input Form.....	4.22
Figure 4.17. Surface Characteristics Lookup Table.....	4.23
Figure 4.18. Sample “Surface Stations” Tab for Specifying CALMET-Ready Station Locations in DUSTRAN .....	4.24
Figure 4.19. Example Contours Tab with Controls Labeled .....	4.25
Figure 4.20. Animation Control with Buttons Labeled.....	4.26
Figure 4.21. Display Options Tab.....	4.27
Figure 4.22. Contour Color Selection Form .....	4.27
Figure 5.1. Polygon Layer Creator Interface .....	5.1
Figure 5.2. Launching Polygon Layer Creator from Within DUSTRAN.....	5.2
Figure 5.3. Select Grid Code Field Window.....	5.3
Figure 5.4. Grid Code Input Window .....	5.5
Figure 5.5. Grid Code Color Selection Window.....	5.6
Figure 5.6. Polygon Grid Code Value Window.....	5.7
Figure 5.7. Specify Sampling Resolution Window.....	5.7
Figure 6.1. DUSTRAN’s “Add Site” Button.....	6.1
Figure 6.2. “Select Simulation Profile To Use” Window .....	6.1
Figure 7.1. The DUSTRAN “Add Site” Button.....	7.1
Figure 7.2. DUSTRAN’s Instructions for Selection of Site Location .....	7.2
Figure 7.3. Prompt for Geospatial Site Dimensions .....	7.2
Figure 7.4. Red Box Enclosing Clipping Envelope.....	7.3
Figure 7.5. Prompt for Site Name and UTM Zone .....	7.3
Figure 7.6. Prompt for Sampling Resolution .....	7.3
Figure 7.7. Notification for Accessing the New Site .....	7.4
Figure 8.1. Add Site Map.....	8.1
Figure 8.2. Add Site Map with Boundary and Point Data Loaded .....	8.2
Figure 8.3. Site Name and Zone Input Form .....	8.3
Figure 8.4. Points Layer Displayed.....	8.3
Figure 8.5. Completed Yakima Site.....	8.4
Figure 8.6. MapWindow Toolbar .....	8.5
Figure 8.7. DUSTRAN User Interface.....	8.5
Figure 8.8. Available DUSTRAN Sites .....	8.5

Figure 8.9. Yakima Site Displayed in DUSTRAN .....	8.6
Figure 8.10. Domain Panel .....	8.6
Figure 8.11. Release Period Panel .....	8.7
Figure 8.12. Simulation Scenario Panel.....	8.7
Figure 8.13. Species Tab – “Available Species” List .....	8.8
Figure 8.14. Point Source Input Form – “Release Parameters” Tab.....	8.9
Figure 8.15. Area Source Input Form – “Release Parameters” Tab .....	8.10
Figure 8.16. Area Source Input Form – “Vehicle Parameters” Tab .....	8.11
Figure 8.17. Sources Tab – “Sources” List.....	8.11
Figure 8.18. Specify Meteorological Data Form – “Hourly Observations” Tab .....	8.12
Figure 8.19. “Run Simulation” Button for Running DUSTRAN Simulation.....	8.12
Figure 8.20. Display Options Tab – “Contours” and “Wind Vectors” options .....	8.13
Figure 8.21. Contours Tab - “Contour Types” Listbox .....	8.13
Figure 8.22. Display of Concentration Contours and Wind Vectors for the Hour from 9-10 AM .....	8.14
Figure 8.23. MapWindow Toolbar .....	8.15
Figure 8.24. DUSTRAN User Interface.....	8.15
Figure 8.25. Available DUSTRAN Sites .....	8.16
Figure 8.26. Yakima Site Displayed in DUSTRAN .....	8.16
Figure 8.27. Domain Panel .....	8.17
Figure 8.28. Release Period Panel .....	8.17
Figure 8.29. Simulation Scenario Panel.....	8.17
Figure 8.30. Species Tab – “Available Species” List .....	8.18
Figure 8.31. Point Source Input Form – “Release Parameters” Tab.....	8.19
Figure 8.32. Area Source Input Form – “Release Parameters” Tab .....	8.20
Figure 8.33. Area Source Input Form – “Vehicle Parameters” Tab .....	8.21
Figure 8.34. Sources Tab – “Sources” List.....	8.22
Figure 8.35. Specify Meteorological Data Form – “Hourly Observations” Tab .....	8.23
Figure 8.36. Specify Meteorological Data Form – “Surface Characteristics” Tab.....	8.24
Figure 8.37. “Run Simulation” Button for Running DUSTRAN Simulation.....	8.24
Figure 8.38. Display Options Tab – “Contours” options .....	8.25
Figure 8.39. Contours Tab - “Contour Types” Listbox .....	8.25
Figure 8.40. Display of Deposition Contours for the Hour from 9-10 AM .....	8.26
Figure 8.41. MapWindow Toolbar .....	8.27
Figure 8.42. Portion of User Interface to the DUSTRAN Model .....	8.27
Figure 8.43. List of Available Model Sites.....	8.27
Figure 8.44. Display of Yakima Site.....	8.28
Figure 8.45. DUSTRAN Domain Panel Showing the Yakima Domain Selected with a 200 km Size            8.28	
Figure 8.46. Display of 200-km-Square Yakima Domain within Yakima Site .....	8.29

Figure 8.47. “Simulation Scenario” Panel .....	8.29
Figure 8.48. Adding Soil and Vegetation Files from DUSTRAN User Interface .....	8.30
Figure 8.49. “Characteristics Priorities” Form.....	8.31
Figure 8.50. Display Showing Choices for Soil and Vegetation Layers.....	8.32
Figure 8.51. Display of Olson Vegetation Layer for the Yakima Site.....	8.32
Figure 8.52. Completed “Specify Meteorological Data” Form .....	8.33
Figure 8.53. “Run Simulation” Button in DUSTRAN User Interface .....	8.33
Figure 8.54. “Contours Types” Listbox .....	8.34
Figure 8.55. Display of Concentration Contours for the Hour from 7-8 AM.....	8.35

## Tables

Table 2.1. AERMOD Model Components and Version Numbers Implemented in DUSTRAN.....	2.3
Table 2.2. CALPUFF/CALGRID Model Components and Version Numbers Implemented in DUSTRAN .....	2.3
Table 2.3. AERMET Meteorological Input Requirements .....	2.4
Table 2.4. Data used to calculate functional form for deposition. ....	2.7
Table 2.5. CALMET Meteorological Input Requirements in DUSTRAN .....	2.8
Table 2.6. Olson Vegetation Classes Used in the Wind-blown Dust-Emission Model .....	2.22
Table 2.7. Features of Typical Dust Particles (after Nickovic et al. 2001) .....	2.22
Table 2.8. Fractions, $\beta_{j,k}$ , of the Soil Texture Classes in each Zobler Soil Category .....	2.23

# 1.0 Introduction

## 1.1 Background

Activities at U.S. Department of Defense (DoD) training and testing ranges can be sources of dust into local and regional air sheds governed by air quality regulations. Activities that could disturb the soil surface, and thus generate dust, include vehicle and troop maneuvers, convoy movement, helicopter activities, munitions impacts, roadway preparations, and wind erosion. Other sources of particulates include smokes and obscurants, controlled burns, and engine operations.

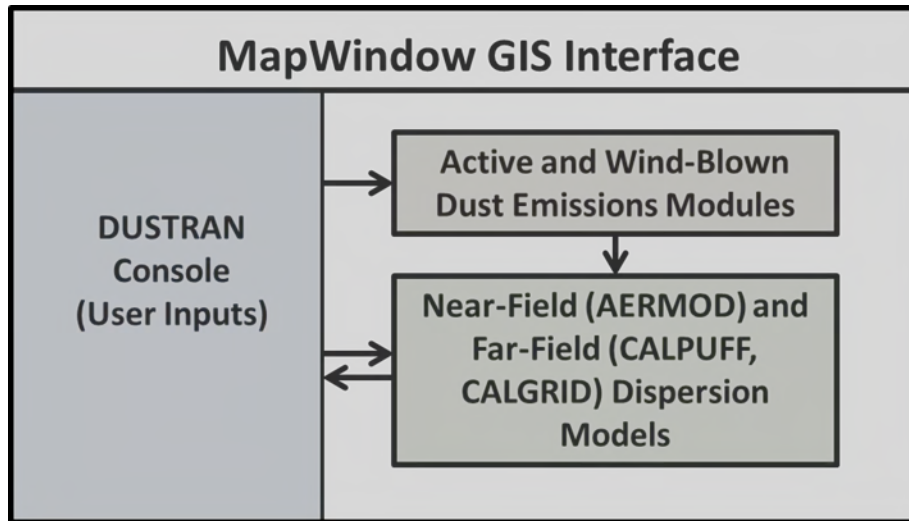
From January 2001 through August 2006, the Pacific Northwest National Laboratory (PNNL), operated by Battelle for the U.S. Department of Energy (DOE), carried out a multi-year research project funded primarily by DoD's Strategic Environmental Research and Development Program (SERDP) to develop an atmospheric dispersion modeling system to assist the DoD in addressing particulate air quality issues at military training and testing ranges. The culmination of that work was the development of the DUST TRANsport, or DUSTRAN, modeling system V1.0 (Allwine et al. 2006). DUSTRAN V1.0 functioned as a console application within the ArcMap Geographic Information system (GIS) and included the U.S. Environmental Protection Agency (EPA)-approved CALPUFF dispersion model for modeling active sources of dust emissions from military vehicular activities and the widely used CALGRID dispersion model for modeling wind-blown dust generation. Source terms for vehicular and wind-blown dust are both native to the DUSTRAN modeling system.

In 2010, SERDP funded additional development of DUSTRAN to 1) replace the GIS platform with open-source GIS software called MapWindow; 2) enable user profiles to allow multiple users to run individual simulations using separate sites; 3) add the EPA's AERMOD air-dispersion model for modeling near-field (less than 50 km) releases; and 4) update the vehicular dust source-term module to include additional vehicle and soil types, as well as enhanced formulations for particle deposition. The culmination of this work is the DUSTRAN V2.0 modeling system. Unless otherwise indicated, subsequent references to "DUSTRAN" in this document refer to DUSTRAN V2.0.

The primary objectives in formulating DUSTRAN have been to 1) identify and construct the system from widely available, scientifically defensible models and model components; 2) couple and integrate the models within a user-friendly, open-source GIS interface; 3) develop and implement an advanced dust-emission model into the modeling system; and 4) document the system through technical articles and a supporting user's guide. This user's guide supports that final objective.

Figure 1.1 identifies the primary components of DUSTRAN, which include the following:

- The MapWindow GIS interface, which allows the user to launch the DUSTRAN console application, view model data layers, and navigate (e.g., zoom, pan) the model domain.
- The DUSTRAN console for entering user inputs, including the model domain, release period, sources, and meteorology and selecting model output display options.
- The dust-emissions modules for estimating active and wind-blown dust-emission rates as a function of time and location.
- The atmospheric dispersion models for estimating near-field (AERMOD) or far-field (CALPUFF and CALGRID) dust concentrations and deposition patterns.



**Figure 1.1.** Primary DUSTRAN components.

## 1.2 Features

DUSTRAN V2.0 functions as a console application within the open-source MapWindow GIS software and includes near-field (AERMOD) and far-field (CALPUFF) dispersion models for simulating active dust emissions from vehicular sources. In addition, DUSTRAN includes the CALGRID dispersion model for wind-generated dust over the model domain. DUSTRAN includes the dust-emission modules for creating the necessary source-term factors from both the vehicular and wind-blown dust-generation activities. Dust-emission factors from wheeled and tracked military vehicles and from certain civilian vehicles were developed during SERDP projects CP-1191 and SI-1399 (Gillies et al. 2005a, 2005b; Gillies et al. 2010). DUSTRAN V2.0 also incorporates the widely used AP-42 emission factors (EPA 2005) for paved and unpaved roads using EPA online updates dated January 2011 and November 2006, respectively.

The EPA’s AERMOD (EPA 2014a) dispersion model is used to model near-field (within 50 km) air concentration and ground deposition from active sources of dust. DUSTRAN includes and automatically runs AERMOD’s terrain (AERMAP) and meteorological (AERMET) preprocessors. Data from the preprocessors are seamlessly merged with other user inputs prior to AERMOD’s execution. The EPA-approved CALPUFF dispersion model (Scire et al. 2000a) is used to model far-field (greater than 50 km) air concentration and ground deposition from active sources of dust. DUSTRAN includes and automatically runs the CALPUFF terrain (TERREL), land-use (CTGPROC), and meteorological (CALMET) preprocessors. The CALifornia photochemical GRID (CALGRID) dispersion model (Scire et al. 1989) is used to model wind-blown dust from large areas. The CALMET meteorological model (Scire et al. 2000b) provides the meteorological fields (e.g., winds and mixing height) for the CALPUFF and CALGRID dispersion models. The primary features of DUSTRAN include the following:

- The modeling domain is graphically specified and size-selectable (20 to 400 km).
- DUSTRAN operates at any U.S. geographic location and has an “Add Site” wizard that generates a new site’s supporting files and data structure for use in a simulation.
- Single-station or multiple-station meteorology can be used and easily specified.
- Multiple point, area, and line releases can be accommodated and specified graphically.
- Simulation and release times are easily specified in the user interface.

- The output concentrations and deposition contours can be viewed graphically, and the output can be animated to view the progression of the dust plume across the modeling domain.
- Multiple particle sizes can be simulated at one time.
- Simulation periods typically range from a few hours to 1 day.
- The atmospheric models process dry deposition using both native formulations and near-field formulations based on SERDP-funded experimental work carried out by DRI under this project..
- The atmospheric models process complex terrain effects.

The DUSTRAN interface allows the user to graphically create a model domain, which defines the area in which a simulation will be performed. For a wind-blown dust simulation, the domain defines the area of potential dust emissions. For source emissions, the domain contains specific emission locations defined by point-, area-, or line-source types. Area and line sources are integrated with a vehicular dust-emission module that allows the user to specify the type, speed, and number of vehicles. The DUSTRAN interface allows the user to specify the time and duration of the sources, size of the modeling domain, duration of the simulation, and source of the meteorological data. After running a simulation, the ground-level dust air concentrations and deposition fields are displayed graphically within the MapWindow GIS interface.

## 2.0 Technical Overview of the DUSTRAN Modeling System

DUSTRAN is a comprehensive dispersion modeling system, consisting of a dust-emissions module, a diagnostic meteorological model, and dispersion models that are integrated seamlessly into MapWindow's open-source GIS. DUSTRAN functions as a console application within MapWindow and allows the user to interactively create a release scenario and run the underlying models. Through the process of data layering, the model domain, sources, and results—including the calculated wind vector field and plume contours—can be displayed with other spatial and geophysical data sources to aid in analyzing and interpreting a scenario.

Fundamental to the DUSTRAN modeling system is a dust-emissions module that includes algorithms for calculating dust emissions from both active and natural sources. Active sources include vehicular dust generation from paved and unpaved roadway surfaces as well as emission factors for various wheeled and tracked military vehicles (Gillies et al. 2005a, 2005b; Kuhns et al. 2010) and the widely used AP-42 emission factors (EPA 2005). Natural sources include wind-blown dust generation from a user-specified domain and are a function of surface wind stress, soil type, and vegetation type. In either case, dust emissions are calculated for explicit particulate matter (PM) size classes, including PM<sub>2.5</sub>, PM<sub>10</sub>, PM<sub>15</sub>, and PM<sub>30</sub>.

In DUSTRAN, dust transport, diffusion, and deposition are simulated using one of three dispersion models—AERMOD, CALPUFF, or CALGRID. Three dispersion models are used due to their frames-of-reference in calculating plume transport, allowing DUSTRAN users to take advantage of each model's inherent strengths in simulating different source types and transport distances:

- AERMOD (EPA 2014a). A steady-state plume model for near-field (<50 km) dispersion and particle deposition from active-source emissions (i.e., point, area, or line). AERMOD incorporates planetary boundary layer turbulence structure and scaling concepts, including treatment of surface and elevated sources and simple and complex terrains.
- CALPUFF (Scire et al., 2000a). A non-steady-state puff dispersion model for long-range (>50 km) dispersion and particle deposition from active-source emissions (i.e., point, area, or line). CALPUFF simulates the effects of time- and space-varying meteorological conditions on pollution transport, transformation, and removal in both simple and complex terrains.
- CALGRID (Scire et al., 1989). An Eulerian dispersion model used for wind-blown dust emissions, where the entire model domain is a potential emission source.

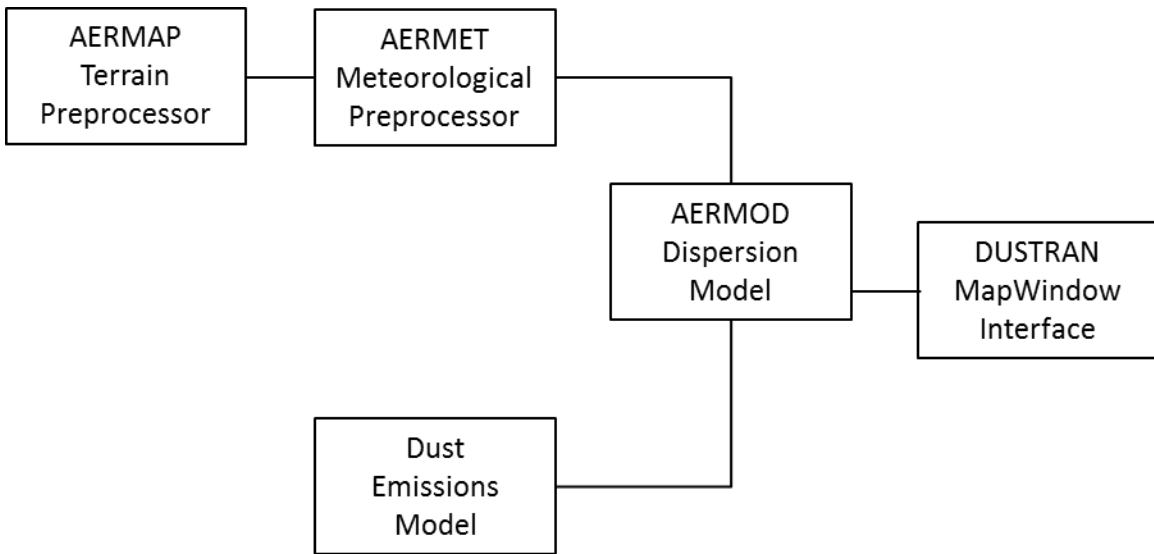
In addition to the AERMOD and CALPUFF regulatory versions, modified versions of both models have been included in DUSTRAN. The modified versions implement a dry-deposition algorithm based on experimental data from the Desert Research Institute (DRI), which is described further in Section 2.1.3.2.

Each dispersion model has a suite of preprocessors included in DUSTRAN for extracting terrain and meteorological data for use in the dispersion calculations. All the model components are dynamically linked by the DUSTRAN interface.

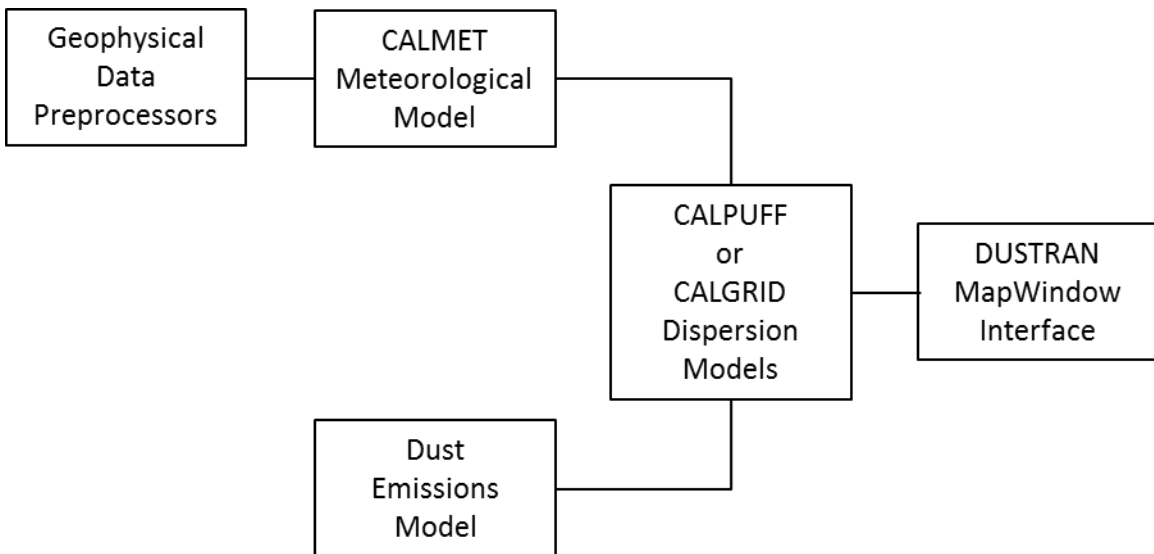
AERMOD utilizes two data preprocessors that are regulatory components of the modeling system: AERMET (EPA 2014b), a meteorological data preprocessor that incorporates planetary boundary layer turbulence structure and scaling concepts, and AERMAP (EPA 2011), a terrain data preprocessor that incorporates complex terrain using U.S. Geological Survey (USGS) Digital Elevation Model (DEM) data. CALPUFF and CALGRID utilize a suite of geophysical data preprocessors for extracting land-use and terrain data as well as CALMET (Scire et al., 2000b) for creating gridded fields of wind and boundary-

layer parameters from observed meteorological data. These gridded fields are then supplied to the CALPUFF and CALGRID dispersion models where they are used in plume dispersion and deposition calculations.

Figure 2.1 shows the primary components of the AERMOD modeling system as implemented within DUSTRAN. Similarly, Figure 2.2 shows the primary components of the CALPUFF and CALGRID modeling systems as implemented within DUSTRAN. Table 2.1 and Table 2.2 list the version numbers of each model component.



**Figure 2.1.** AERMOD Modeling Components within DUSTRAN



**Figure 2.2.** CALPUFF/CALGRID Modeling Components within DUSTRAN

**Table 2.1.** AERMOD Model Components and Version Numbers Implemented in DUSTRAN

Component	Purpose	Version Number
AERMOD	Dispersion Model	14134
AERMET	Meteorological Model	14134
AERMAP	Terrain Preprocessor	11103

**Table 2.2.** CALPUFF/CALGRID Model Components and Version Numbers Implemented in DUSTRAN

Component	Purpose	Version Number
CALPUFF	Dispersion Model	5.5
CALGRID	Dispersion Model	1.6
CALMET	Meteorological Model	5.2
CALPOST	Post-processing Program	5.2
TERREL	Terrain Preprocessor	2.1
CTGPROC	Land Use Preprocessor	1.2
MAKEGEO	Merges Terrain/Land Use Datasets	1.1
READ62	Meteorological Preprocessor for Extracting Standard Upper-Air Formats	4.0

The following sections provide a brief technical overview of the DUSTRAN model components. Numerous documents on the AERMOD (e.g., EPA 2004a, 2004b, 2004c, 2011, 2014a, 2014b) and CALPUFF/CALGRID (Scire et al. 1989, 2000a, 2000b) modeling systems discuss the theoretical and technical basis of the dispersion and meteorological models used within DUSTRAN; readers are referred to these documents for detailed information on each model component. This user's guide provides a cursory overview of the model components and their integration within the DUSTRAN framework. A more detailed discussion of the vehicular and wind-blown dust-emissions factor module is given in Section 2.5, and serves as the technical documentation and reference for this component.

## 2.1 AERMOD Modeling System

The AERMOD modeling system (EPA 2014a, 2014b) is used to model near-field (<50 km) dispersion from active-source emissions (i.e., point, area, or line). The following sections describe the AERMOD modeling system components and their implementation within DUSTRAN.

### 2.1.1 AERMET

AERMET (EPA 2014b) is a meteorological preprocessor that uses hourly meteorological observations to calculate certain boundary-layer parameters (e.g., mixing height and friction velocity) for use in AERMOD. AERMET requires surface and upper-air meteorological observations as well as certain surface characteristics (i.e., albedo, Bowen ratio, and surface roughness). These data are supplied through the "Meteorology" tab within DUSTRAN (see Section 4.8). In addition, lookup tables for typical values of albedo, Bowen ratio, and surface roughness are included in DUSTRAN. These values are based on various surface characteristics tables from Appendix A of the EPA's AERSURFACE User's Guide (EPA 2008).

Table 2.3 lists meteorological observations required by AERMET. Surface data are hourly observations, whereas upper-air vertical profiles are required less frequently, normally twice daily (00Z and 12Z). A single surface and upper-air station must be used. The input meteorological data are written to formatted surface and upper-air files by the DUSTRAN interface for use in AERMET.

**Table 2.3. AERMET Meteorological Input Requirements**

Surface Data (Hourly)	Upper-Air Data (Usually Twice Daily)
Wind Speed and Direction	Wind Speed and Direction
Temperature	Temperature
Relative Humidity	Pressure
Station Pressure	Measurement Height
Total Sky Cover	
Ceiling Height	
Measurement Height	

Since upper-air data can be difficult to obtain, profiling equations have been incorporated into DUSTRAN as an alternative to approximate upper-air soundings. Using the single observation data entered by the user, and certain parameters listed in the Cal.par file, DUSTRAN automatically generates an upper-air sounding file, which is used by the AERMET model. The sounding data consist of wind speed/direction, temperature, and pressure at several heights above the ground, where the lower and upper heights and the number of heights are specified in the Cal.par file (see Section A.2.1). The height spacing is logarithmic to allow narrower spacing close to the surface. The DUSTRAN profiling equations are described in the following sections.

### 2.1.1.1 Wind Speed/Direction Profile

For simplicity, the wind direction is assumed constant with height, and the wind speed is assumed to increase with height using the power-law relationship:

$$U_n = U_1 \left( \frac{Z_n}{Z_1} \right)^P \quad (2.1)$$

where

- $U_n$  = wind speed at sounding height “n” (m/s),
- $U_1$  = wind speed at lowest sounding height (m/s),
- $Z_n$  = sounding height “n” (m),
- $Z_1$  = lowest sounding height (m),
- $P$  = power-law exponent depending on atmospheric stability.

The power-law exponents in Equation 2.1 follow from Table 4.6 of Turner (1994) and are listed in the Cal.par file (Section A.2.1) for application of DUSTRAN in either “rural” or “urban” areas.

### 2.1.1.2 Temperature Profile

The temperature sounding is developed from temperature lapse rates specified as a function of stability in the Cal.par file and the surface temperature specified in the user-input window. Consequently, the temperature sounding is determined as:

$$T_n = T_1 + T_{LR}(Z_n - Z_1) \quad (2.2)$$

where

- $T_n$  = temperature at sounding height “n” (K),
- $T_1$  = temperature at lowest sounding height (K),
- $T_{LR}$  = temperature lapse rate depending on stability (K/m)
- $Z_n$  = “n” sounding height (m)
- $Z_1$  = lowest sounding height (m).

### 2.1.1.3 Pressure Profile

The atmospheric pressure as a function of sounding height is determined from the hydrostatic relationship as:

$$P_n = P_1 \text{ EXP} \left[ - \frac{a(Z_n - Z_1)}{(T_n + T_1)/2} \right] \quad (2.3)$$

where  $P_n$  = pressure at sounding height “n” (mb),  
 $P_1$  = pressure at lowest sounding height (mb),  
 $a$  = 0.0342 K/m.

### 2.1.2 AERMAP

AERMAP (EPA 2011) is a terrain preprocessor that uses publicly available terrain data to extract elevations for sources and receptors as well as calculate the receptor “hill-height scale” for AERMOD dispersion calculations. DUSTRAN utilizes the U.S. Geological Survey’s (USGS) Global Multi-resolution Terrain Elevation Data 2010 (GMTED2010) data files for use within AERMAP. These files provide global coverage at a resolution around 7.5 arc seconds (about 150 m). The GMTED2010 terrain files are clipped at site creation within DUSTRAN’s “Add Site” utility, resulting in a smaller terrain file for use within a given AERMAP domain. This eliminates the need for users to define or supply multiple DEM files, which may not completely cover the AERMOD model domain.

### 2.1.3 AERMOD

AERMOD is the EPA’s preferred regulatory dispersion model (see 40 CFR Part 51, Appendix W) for most modeling applications. The model is useful for simulating short-range dispersion (<50 km) from discrete source-type configurations (e.g., point, line, and area sources). Within DUSTRAN, area and line sources are integrated using AERMOD to simulate particle dispersion and deposition from paved or unpaved roadways due to various vehicle types.

AERMOD is a steady-state plume model; meteorological conditions can be updated hourly and are assumed to be spatially homogenous across the entire model domain. In the stable boundary layer, the plume concentration is assumed to be Gaussian. In the convective boundary layer, the horizontal plume concentration is assumed to be Gaussian, but the vertical plume concentration is described by a bi-Gaussian probability density function. The model calculates average plume concentration and deposition-flux values at defined receptor locations. The receptor field is automatically defined and created by DUSTRAN based upon the model domain size and source input configuration.

The AERMOD input file (Aermod.inp) defines the “Control,” “Source,” “Meteorology,” “Receptor,” and “Output” options for a given run. Every site in DUSTRAN has a “StaticData” directory that stores a template Aermod.inp to be used for that site. The template file is merged with user input from the DUSTRAN interface before running the model. Unlike CALPUFF (see Section 2.2.2), the AERMOD input file does not contain multiple options for controlling transport and diffusion; rather, a single, regulatory method is implemented within the model. A complete description of AERMOD’s scientific basis is described in the model formulation’s document (EPA 2004a).

Two versions of AERMOD have been implemented within DUSTRAN—“Source Emission – AERMOD” and “Source Emission – AERMOD (DRI).” The former version is the EPA’s regulatory version of AERMOD (EPA 2014); the latter version has been modified to implement a dry-deposition algorithm based on experimental data from DRI.

In both versions of AERMOD, the dry-deposition flux,  $F_d$ , is calculated as the product of the concentration,  $\chi_d$ , and a dry-deposition velocity,  $V_d$ , computed at a reference height,  $z_r$ :

$$F_d = \chi_d \cdot V_d \quad (2.4)$$

where

- $F_d$  = the dry-deposition flux onto the ground ( $\mu\text{g}/\text{m}^2/\text{s}$ ),
- $\chi_d$  = the air concentration ( $\mu\text{g}/\text{m}^3$ ) calculated at reference height  $z_r$ ,
- $V_d$  = the particle dry-deposition velocity (m/s),
- $z_r$  = the dry-deposition reference height (m) =  $z_o + 1$ , and
- $z_o$  = the site surface roughness length from the meteorological file.

The two versions only differ in their method for estimating  $V_d$ . The following sections discuss how  $V_d$  is estimated in the EPA and DRI versions of AERMOD; all other model formulations are the same.

### 2.1.3.1 Source Emissions – AERMOD

The EPA version of AERMOD (i.e., “Source Emissions – AERMOD) (EPA 2014) computes a particle dry-deposition velocity to estimate the dry-deposition flux of particles onto the ground. The dry-deposition velocity is estimated using a resistance model, whereby the atmosphere is treated as a series of resistance layers to the depositing particles. The method is analogous to electrical resistance and is expressed as the inverse sum of a series of resistance layers near the ground plus a gravitational settling velocity (EPA 2004d):

$$V_d = \frac{1}{R_a + R_b + R_a R_b V_g} + V_g \quad (2.5)$$

where

- $V_d$  = the dry-deposition velocity (m/s),
- $R_a$  = the aerodynamic layer resistance (s/m),
- $R_b$  = the quasi-laminar layer resistance (s/m), and
- $V_g$  = the gravitational settling velocity (m/s).

The aerodynamic layer resistance ( $R_a$ ) occurs in the shallow layer (~10 m) next to the ground and depends on several meteorological parameters (e.g., wind speed, atmospheric stability, and surface roughness); the more turbulent the atmosphere, the smaller the aerodynamic resistance. The quasi-laminar layer resistance occurs in the thin, non-turbulent layer just above the depositing surface and depends on molecular, rather than turbulent, properties. EPA (2004d) summarizes formulations for  $R_a$  and  $R_b$ ; these formulations are used in the EPA’s version of AERMOD to estimate dry-deposition velocities for various particle sizes.

### 2.1.3.2 Source Emissions – AERMOD (DRI)

The DRI version of AERMOD (i.e., “Source Emissions – AERMOD (DRI)) also computes a particle dry-deposition velocity to estimate the dry-deposition flux of particles onto the ground. The dry-deposition velocity is estimated from an empirical function derived from DRI experimental data. DRI collected data over five different surface types (i.e., short grass, long grass, steppe, sage, and bare) with five different

surface roughness lengths (Table 2.4). For each surface type, DRI provided a mean deposition velocity with its standard deviation in six size bins centered in a range from approximately 0.7 to 18  $\mu\text{m}$ . The roughness values for each measurement site ranged from approximately 0.01 to 0.20 m. Further, the minimum deposition velocity did not drop below 1 cm/s. Therefore, in the curve fitting described below, 1 cm/s was adopted as a lower bound for deposition velocity.

**Table 2.4.** Data used to calculate functional form for deposition.

Size Bin Range ( $\mu\text{m}$ )	0.7-1	1-2	2-2.5	2.5-5	5-10	>10	Avg Z0 (m)
<b>Dp (<math>\mu\text{m}</math>)</b>	0.837	1.414	2.236	3.536	7.071	15.166	
<b>Vd Short grass (cm/s)</b>	1.78	1.65	1.21	2.29	4.27	9.63	0.026
<b>Vd Long Grass (cm/s)</b>	3.49	3.66	5.76	5.47	7.08	10.95	0.206
<b>Vd Sagebrush (cm/s)</b>	3.84	4.06	4.75	4.80	5.39	8.51	0.188
<b>Vd Steppe grass (cm/s)</b>	1.49	1.81	1.78	2.51	3.98	4.76	0.039
<b>Vd No Vegetation (cm/s)</b>	1.07	1.59	1.60	2.14	2.38	3.61	0.012
Size Bin Range ( $\mu\text{m}$ )	0.7-1	1-2.5	2.5-5	5--10	10--15	>15	
<b>Dp (<math>\mu\text{m}</math>)</b>	0.837	1.581	3.536	7.071	12.247	18.574	

Visual inspection of the data suggested that while a linear fit in surface roughness was sufficient, some curvature was suggested in the deposition velocity dependence on particle aerodynamic diameter. Because the derived function is entirely empirical, a curve-fitting routine was applied to the general quadratic function:

$$V_d(D_p, Z_0) = aZ_0^2 + bD_pZ_0 + cD_p^2 + dZ_0 + eD_p + f \quad (2.6)$$

where  $V_d$  = the dry-deposition velocity (cm/s),  
 $D_p$  = the aerodynamic particle diameter ( $\mu\text{m}$ ),  
 $Z_0$  = the surface roughness length (m),  
 $a, b, c, d, e,$  and  $f$  are determined by regression.

An initial fit using this general quadratic form yielded large uncertainty and near-zero values for coefficients  $a$  and  $c$ , while explaining approximately 80 percent of the variance. The terms including  $a$  and  $c$  were dropped, and the fit was repeated with:

$$V_d(D_p, Z_0) = bD_pZ_0 + dZ_0 + eD_p + f \quad (2.7)$$

The fit using this form also explained approximately 80 percent of the variance, confirming that the dropped terms were not useful in the fit.

On further inspection, a datum for deposition velocity at 15  $\mu\text{m}$  over the bare surface appeared to be anomalously large. Dropping this point reduced the number of observations available from 30 to 29 and increased the variance explained to 93 percent. This fit was adopted for use in DUSTRAN. The resulting coefficients are:

$$b = 1.43$$

$$d = 12.4$$

$$e = 0.128$$

$$f = 1.16$$

These coefficients and the above function apply in the region  $\{0 \leq D_p < 18, 0 \leq Z_0 < 0.21\}$ . Outside this fitted domain, the following forms are used:

$$\{0 \leq D_p < 18, Z_0 \geq 0.21\} \quad V_d = V_d(D_p, 0.21) = bD_p \times 0.21 + d \times 0.21 + eD_p + f \quad (2.8)$$

$$\{D_p \geq 18, 0 \leq Z_0 < 0.21\} \quad V_d = V_d(18, Z_0) = b \times 18 \times Z_0 + dZ_0 + e \times 18 + f \quad (2.9)$$

$$\{D_p \geq 18, Z_0 \geq 0.21\} \quad V_d = V_d(18, 0.21) = 11.5 \quad (2.10)$$

## 2.2 CALPUFF/CALGRID Modeling Systems

The CALPUFF modeling system (Scire et al., 2000a) is a non-steady-state puff dispersion model used to model long-range (>50 km) dispersion and particle deposition from active-source emissions (i.e., point, area, or line). The CALGRID modeling system (Scire et al., 1989) is an Eulerian dispersion model used to model wind-blown dust emissions, where the entire model domain is a potential emission source. Both dispersion models utilize the same preprocessor components (e.g., CALMET and CALPOST). The following sections describe the models, their preprocessors, and how they are implemented within DUSTRAN.

### 2.2.1 CALMET

CALMET is a meteorological model that generates three-dimensional gridded wind fields and two-dimensional fields of boundary-layer parameters for the CALPUFF and CALGRID dispersion models. CALMET is a diagnostic meteorological model and therefore requires surface and upper-air observations to generate the gridded fields. These data are supplied through the “Meteorology” tab within DUSTRAN (see Section 4.8).

Table 2.5 lists required meteorological observations used by CALMET. The surface data are hourly observations whereas the upper-air vertical profiles are required less frequently, normally twice daily (i.e., 00Z and 12Z). Multiple surface and upper-air stations may be used, and the stations are not required to be on the DUSTRAN domain, as CALMET interpolates the data to the domain. These input meteorological data are written to formatted surface and upper-air files by the DUSTRAN interface for use in CALMET.

**Table 2.5.** CALMET Meteorological Input Requirements in DUSTRAN

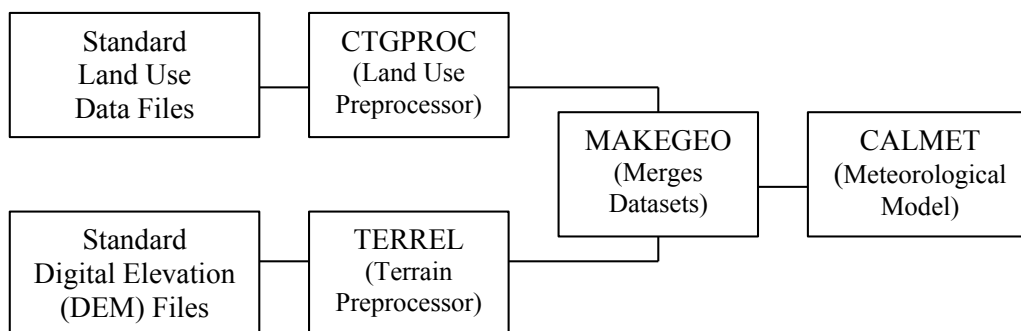
Surface Data (Hourly)	Upper-Air Data (Usually Twice Daily)
Wind Speed and Direction	Wind Speed and Direction
Temperature	Temperature
Cloud Cover	Pressure
Ceiling Height	Elevation
Surface Pressure	
Relative Humidity	

Geophysical data are also used by CALMET to derive the gridded meteorological fields. These data—terrain elevations and land use/land cover—are routinely available in datasets from the USGS with varying spatial resolution. In DUSTRAN, CALMET terrain data are supplied through GTOPO30 files, which are DEMs with a horizontal spacing of 30 arc seconds (approximately 1 km). Land-use/land-cover data are supplied through global land-cover characteristics (GLCC) files and are of similar resolution.

Preprocessing programs interface the geophysical datasets with the CALMET meteorological model. These preprocessors, shown in Figure 2.3, are implemented within DUSTRAN and automatically extract the required geophysical data based on the user’s domain size. The extracted data are used in the CALMET model formulations and written to the CALMET output file for use in the CALPUFF and CALGRID dispersion models.

The procedures that CALMET uses to derive the gridded meteorological fields are controlled largely by an input file called “Calmet.inp.” The input file is a text file with a series of keywords logically grouped based upon their overall function within CALMET. Every site in DUSTRAN has a “StaticData” directory that stores the template Calmet.inp to be used for that site. The template file is merged with user input from the DUSTRAN interface before running the model. The parameter settings within the template file are set to optimized values to produce the most realistic output (see Section A.2.2). Caution should be exercised if the user wishes to change any setting within the template file, as unrealistic results may be produced.

With the meteorological and geophysical input datasets defined, the following subsections provide an overview of the CALMET procedures for deriving gridded meteorological fields. Technical formulations are not provided here, as they are available in the CALMET User’s Guide (Scire et al. 2000b); instead, the CALMET processing and creation of gridded meteorological fields are described qualitatively.



**Figure 2.3.** Data Flow and Geophysical Preprocessors for CALMET

### 2.2.1.1 CALMET-derived Wind Field

CALMET uses a two-step process to create the three-dimensional wind field for each hourly time step. In step one, an “initial guess” wind field is modified for terrain effects. In step two, surface and upper-air observations are merged objectively with the step-one, terrain-adjusted winds to create the final flow field. Each step is briefly discussed below.

#### Step-One Wind Field Formulation

The step-one wind field formulation begins with an “initial guess” wind field. The “initial guess” wind field can be a spatially varying or a constant, domain-mean wind used throughout the grid. In DUSTRAN’s implementation of CALMET, the “initial guess” wind field is spatially varying and is based on surface and upper-air observations. The surface observations are extrapolated vertically using a power-law or Monin-Obukhov (M-O) similarity theory, assuming a neutral boundary layer, with M-O extrapolation used by default. The vertically extrapolated surface winds are then merged with the upper-air observations at each node on the grid using a  $1/r^2$  interpolation. During the merging, a bias can be applied at each vertical level in the domain, whereby the relative weighting of the surface and upper-air

data can be controlled. This level-by-level bias allows for surface data to more greatly influence the flow field in the lowest layers and the upper-air data to dominate the higher layers.

Once the “initial guess” wind field has been created, it is adjusted for terrain effects. CALMET has the option of adjusting the wind field for kinematic effects, slope flow, and flow blocking. Each option can be explicitly treated, and the cumulative effects are merged with the “initial guess” wind field to determine the step-one flow field.

1. Kinematic effects are calculated by assuming an initial zero vertical velocity in the “initial guess” wind field. The vertical velocity is then calculated because of topographic effects, and the horizontal velocity is adjusted using a divergence minimization scheme that iteratively adjusts the horizontal wind components until the three-dimensional divergence is less than a specified value.
2. Slope flow effects (e.g., upslope flows during the day and drainage flows at night) are based on an empirical scheme that is a function of the terrain slope, distance to the crest, and the sensible heat flux. A separate formulation for the sensible heat flux is used for the daytime and nighttime in CALMET and is performed for overland locations only.
3. Flow blocking, which is the result of stable stratification, is determined by calculating the Froude number for each grid node in CALMET. If a critical Froude number is not exceeded, then the flow is blocked by terrain and is adjusted tangent to the land feature (i.e., the flow is forced around the land feature).

Of the three terrain adjustment procedures, the kinematic effects can sometimes lead to unrealistically large horizontal velocities, particularly in complex terrain. Therefore, the kinematic adjustment is rarely implemented in DUSTAN.

## **Step-Two Wind Field Formulation**

The step-two formulation is an objective merging of the terrain-adjusted, step-one wind field with surface and upper-air observations. The objective analysis is performed level by level by first extrapolating the surface wind observations vertically using a constant power law or M-O as a function of stability. Then, for a given level, observations within a specified radius are weighted equally with the step-one wind field. All other observations at that level have a  $1/r^2$  weighting out to a specified radius of inclusion. The radii for equal weighting and inclusion can be specified separately for the surface and all other vertical levels.

Each level of the merged wind field is then smoothed, and the divergence at each grid cell is calculated to provide a new estimate of the vertical velocity. The vertical velocity for the top level of the domain can be set to zero (called the O’Brian adjustment procedure), and the horizontal wind components are readjusted to be mass consistent with the new vertical velocity field using a divergence minimization procedure. The resulting wind field is the final wind field output by CALMET for use in the CALPUFF or CALGRID dispersion calculations.

### **2.2.1.2 CALMET-Derived Boundary-Layer Parameters**

CALMET contains a micrometeorological model based upon an energy balance method, whereby the sensible heat flux is calculated at each grid node by parameterizing the unknown terms—latent heat flux, anthropogenic heat flux, ground storage/soil heat flux, and net radiation—in the surface energy balance equation. Once the sensible heat flux is calculated, gridded fields of other boundary-layer parameters that are functionally dependent on the sensible heat flux, such as the M-O length and surface-friction velocity, are computed.

CALMET has various formulations for calculating the mixing height based on time of day and stability classification. For unstable daytime conditions, the mixing height is thermally driven, and so it is a function of the surface heat flux and the vertical temperature profile from upper-air soundings. For stable nighttime conditions, the mixing height is mechanically driven and, thus, functionally dependent upon the friction velocity.

Because of the explicit use of the surface energy balance method in CALMET, all DUSTRAN simulation start times must be before sunrise. CALMET contains time-validation routines that mandate a start time of 5 a.m. local time, or earlier. So, if a noon-time or evening release is desired, the simulation start time must begin by 5 a.m. even though the source release time may not occur until much later in the day. Normally, this is of little consequence, as the model runtime is extremely fast and efficient.

### **2.2.1.3 Meteorological Data Input Options**

DUSTRAN allows the user to specify four sources of meteorological data to be used by CALMET (see Section 4.8). The four options include the following:

1. Available Data. Use available site-specific meteorological data where data format is known by DUSTRAN and data-ingest utilities are available in DUSTRAN. Currently, this feature applies to data from the DOE's Hanford site meteorological network and data from the DoD's Fort Irwin site meteorological network.
2. Single Observation. Use single-point meteorological observations specified in DUSTRAN through an input window. DUSTRAN creates one "surface" data file and one "upper-air" data file from the user input in the format needed by CALMET. The "dummy" stations are located at the center of the modeling domain and are assumed to persist for the duration of the simulation.
3. User Defined. Use surface and upper-air meteorological data files (surf.dat and up\_1.dat, up\_2.dat, ... up\_n.dat) that have already been prepared for being directly read by CALMET. These files were created outside of DUSTRAN using CALMET utilities.
4. National Oceanic & Atmospheric Administration (NOAA) Archived. Use meteorological data archived from web-site-accessible National Weather Service (NWS) surface and upper-air data stations.

Of the four methods, option two, "Single Observation," is the only method that relies on user input for defining basic meteorological conditions. These inputs are then used by DUSTRAN to construct all required inputs for use in the CALMET model. The other three options use actual data streams coming from defined sources. The methodology used within DUSTRAN to construct the necessary meteorological inputs for CALMET when using "Single Observation" is described in the following section.

### **Single Observation Methodology**

The Single Observation option provides the user with a very easy and convenient way to quickly view the effects of various configurations (e.g., multiple sources, long-rang transport, and nighttime stable flows) on resulting concentration and deposition fields. Even though the single-point meteorological observation persists and is used for the entire simulation, the model-derived meteorological grids will still vary spatially and temporally, as they are a function of land use, topography, and the surface-sensible heat flux (i.e., time of day). CALMET contains a solar model for use in determining sensible heat flux (which drives diffusion rates and mixing height growth) as a function of time.

The user specifies wind speed, wind direction, mixing height, ambient temperature, relative humidity, ambient pressure, and atmospheric stability through the DUSTRAN meteorological input window (see Section 4.8.2). CALMET also needs other surface quantities for completeness (i.e., ceiling height, opaque sky cover, and precipitation code), which are specified near the start of the Cal.par DUSTRAN setup file (see Section A.2.1). The Cal.par is a static text file used to initialize certain parameters in DUSTRAN. The file can be edited in a standard text editor; however, because it allows many features of DUSTRAN to be controlled, caution should be exercised if modifications to this file are desired. The default values in cal.par for ceiling height, opaque sky cover, and precipitation code are 100 (units are hundreds of feet), 0 (units are tenths of coverage), and 0 (no precipitation), respectively. The default values for the meteorological variables specified through the DUSTRAN user-input window are also given in the Cal.par file.

CALMET requires at least one upper-air sounding for operation. Using the single observation data entered by the user and parameters listed in the Cal.par file, DUSTRAN automatically generates an upper-air sounding file, which is used by the CALMET model. The sounding data consist of pressure, temperature, wind speed, and wind direction at several heights. Section 2.1.1 discusses the profiling methods used for AERMET; these same methods are used for generating vertical profiles for CALMET.

## **2.2.2 CALPUFF**

The CALPUFF dispersion model is ideal for simulating long-range dispersion (>50 km) from discrete source-type configurations (e.g., point, line, and area sources). The latter two sources—area and line—are integrated with a dust-emissions model and can simulate particle dispersion and deposition from paved or unpaved roadways due to various vehicle types.

As the name implies, CALPUFF is a puff model; it transports and diffuses source material as a series of discrete puffs using gridded meteorological fields from CALMET. The model calculates average plume concentration and deposition-flux values at defined receptor locations. The receptor field is automatically defined and created by DUSTRAN based on the model domain size and source input configuration.

The use of spatially varying meteorological fields makes CALPUFF ideal for medium- and long-range transport applications where domain sizes often exceed 50 km and the assumption of “spatially homogenous” meteorology used in straight-line plume models often fails. As a result, CALPUFF has gained widespread acceptance and has been approved by the EPA as a regulatory model (see 40 CFR Part 51, Appendix W) for applications involving long-range transport. Domain sizes in DUSTRAN can be up to 400 km; thus, CALPUFF is an appropriate selection for use in the modeling system.

The procedures that CALPUFF uses to define plume transport and dispersion are controlled largely by an input file called “Calpuff.inp.” The input file is a text file with a series of keywords that are logically grouped based upon their overall function within CALPUFF. Every site in DUSTRAN has a “StaticData” directory that stores the template Calpuff.inp to be used for that site. The template file is merged with user input from the DUSTRAN interface before running the model. The parameter settings within the template file are set to optimized values to produce the most realistic output (see Section A.2.3).

Two versions of CALPUFF have been implemented within DUSTRAN—“Source Emission – CALPUFF” and “Source Emission – CALPUFF (DRI).” The former version is the EPA’s regulatory version of CALPUFF (Scire 2000a) and the latter version has been modified to implement a dry-deposition algorithm based on experimental data from the DRI. The dry-deposition formulations in CALPUFF are the same as those described for the AERMOD dispersion model (see Section 2.1.3).

The sections that follow review some of the more important parameters used by CALPUFF to control puff transport and dispersion. Recommendations are made for the various parameter settings based on experience, guidance documents (e.g., Irwin 1998), and CALPUFF's specific implementation within the DUSTRAN system. Users should exercise extreme caution if changing any setting within the template file, as unrealistic results may be produced.

### **2.2.2.1 Near-Field Release Approximation**

Puff models are often computationally expensive when used for near-field applications involving continuous releases because the puffs are still relatively small, and so enough puffs must be released to approximate the source. In addition, sampling problems may arise near the source if too few puffs are released in a given time step, especially during rapidly varying meteorological conditions. To address these issues, CALPUFF can use an elongated puff, called a slug, to approximate the release. As the slug is transported downwind and its crosswind dimensions become larger because of dispersion, CALPUFF can transition the slug back to a puff. The slug method is an input parameter set in the CALPUFF input file and is recommended in most DUSTRAN applications.

### **2.2.2.2 Dispersion Coefficients**

CALPUFF is a Gaussian model and therefore approximates atmospheric diffusion through the specification of dispersion coefficients. The dispersion coefficients are a function of atmospheric stability and affect the vertical and lateral growth of a puff as it is transported downwind. CALPUFF provides many methods for defining the dispersion coefficients, including the following:

- direct measure of the horizontal and vertical velocity variances
- similarity theory formulations
- Pasquill-Gifford-Turner (PGT) specifications.

Of the listed methods, the similarity theory formulations are recommended and implemented in DUSTRAN, as the parameters used in their formulation are explicitly calculated by CALMET.

### **2.2.2.3 Plume Rise**

CALPUFF can account for plume rise, especially from point sources, which are often used to approximate releases from stacks. With stack-type releases, plume buoyancy (due to increased exhaust temperature) and momentum (from exhaust flows) can loft plumes into the air. Plume lofting can result in a phenomenon called partial plume penetration, whereby part of the plume is ejected into a stable layer (called an inversion) above the release. The overall effect of these parameters is to increase the release height and remove material from the initial plume, all of which act to reduce surface concentration and deposition-flux values downwind of the release, particularly near the source. Because DUSTRAN domain sizes tend to be large (e.g., >50 km), these effects play a smaller role and only act to increase computation time. They are not recommended for use unless near-field effects are of concern.

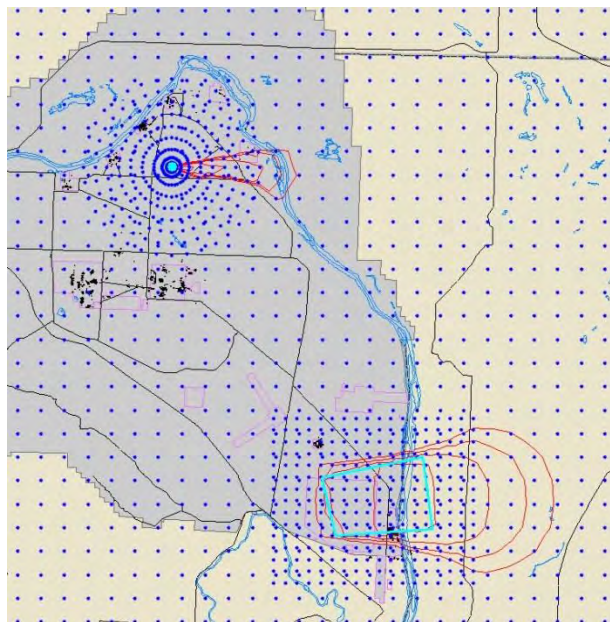
### **2.2.2.4 Receptor Grids**

Receptors are locations where the model performs concentration and deposition calculations. In CALPUFF, a primary receptor grid is used for calculating values across the entire domain. The grid is Cartesian and has uniformly spaced receptors in the X and Y directions. By default, 50 receptors are specified for both directions, so a 100-km domain, for example, has a receptor spacing of 2 km in the X

and Y directions. The number of receptors in the primary grid can be changed within the Cal.par file (see Appendix A.2.1).

In DUSTRAN, secondary receptor grids, or sub-grids, are automatically generated in and around sources to increase the resolution of the calculated concentration and/or deposition fields very near the source. These sub-grids are treated as discrete receptors in CALPUFF, and up to 4,000 discrete receptors are allowed. For each point source, a polar receptor sub-grid is used. For each area source, a rectangular receptor sub-grid is used. No sub-grid is currently implemented for a line source. The size and resolution of the receptor sub-grids are defined according to parameters set within the Cal.par file (see Section A.2.1).

Figure 2.4 presents an example of the various receptor grids implemented in DUSTRAN for a CALPUFF model simulation. Receptors are displayed as blue dots, with the primary Cartesian grid spaced uniformly across the domain and a polar and a rectangular sub-grid centered over their respective source types.



**Figure 2.4.** Example of the Primary Cartesian Receptor Grid and a Polar and Cartesian Sub-Grid Used Within CALPUFF

### 2.2.2.5 Representing Moving Vehicles as Line and Area Dust Sources

DUSTRAN does not treat the motion of individual vehicles, but rather takes a “bulk” approach to dust emissions from vehicle activities. That is, dust emissions from all vehicles active on a road segment or within a training area over a specified time are assumed to be released uniformly from the road or area at a constant rate throughout the duration of the activity. Therefore, the input fields on the DUSTRAN “Vehicle Parameters” window should not be interpreted as representing the specific motion of individual vehicles, but rather as a convenient approach for providing the vehicle information needed by DUSTRAN. Details of specifying the vehicle characteristics and activities for road segments and for training areas are given in Sections 4.6.2.2 and 4.6.3.2, respectively.

As described in Section 2.3.1, dust emissions from a moving vehicle are proportional to the vehicle momentum (i.e., vehicle weight  $\times$  vehicle speed). Therefore, if some vehicles of one type travel at significantly different speeds than other vehicles of the same type, another vehicle type will need to be

added to the DUSTRAN vehicle list such that the other speed(s) can be specified. Additional vehicles can be specified in DUSTRAN by editing the Cal.par file (see Section A.2.1).

### **2.2.3 CALGRID**

The CALGRID dispersion model has been implemented within DUSTRAN to simulate the dispersion of wind-generated dust; it is activated by setting the “Simulation Type” to “Wind-blown Dust” within the DUSTRAN interface (See Section 4.4). In the wind-blown dust mode, DUSTRAN creates gridded dust-emission factors for the entire model domain, which are then supplied to the CALGRID model to simulate the downwind dispersion and deposition. The dust-emission factors calculated by DUSTRAN are a function of wind stress, soil texture, and vegetation type across the domain and are discussed further in Section 2.3.2.

CALGRID is an Eulerian model and uses mass continuity to track material throughout a gridded volume. In DUSTRAN, the volume boundaries are defined by specifying a domain in which the user would like to simulate wind-blown dust dispersion. The amount of dust in a given volume is the sum of dust being generated by the wind or lost by deposition as well as the transfer of dust between volumes through wind transport and atmospheric diffusion. The gridded nature of the model makes it ideal for examining releases from large areas (e.g., wind-blown dust over a large domain).

The CALMET-derived spatially and temporally varying meteorological fields are used in CALGRID to transport and diffuse material throughout the domain. Horizontal transport requires the two-dimensional gridded fields of the velocity components (U and V) for each vertical layer. Terrain-following vertical velocities are used to determine the vertical transport through each of the vertical cell faces in CALGRID. Horizontal diffusion is a function of the CALMET-gridded PGT stability classification, modified for wind speed within each cell and distortion or shear between horizontal cells. Vertical diffusion is calculated from CALMET-gridded similarity fields and is functionally dependent upon the height above ground and stability.

Emissions are introduced into the CALGRID domain depending on the source type. For area sources, which include the model domain for wind-blown dust simulations, emissions are injected into CALGRID using emission layers, with each layer containing a fraction of the total emissions. In DUSTRAN’s implementation of CALGRID, area sources have one emission layer, bounded between the surface and 20 meters. For other source types, such as point sources, material is injected into one or more CALGRID layers based on the height of the stack, plume rise due to buoyancy and momentum, and the plume overlap with the model layers.

The procedures that CALGRID uses to define plume transport and dispersion are controlled largely by an input file called “Calgrid.inp.” The input file is a text file with a series of keywords that are logically grouped based upon their overall function within CALGRID. Every site in DUSTRAN has a “StaticData” directory that stores the template Calgrid.inp to be used for that site. The template file is merged with user input from the DUSTRAN interface before running the model. The parameter settings within the template file are set to optimized values to produce the most realistic output (see Section A.2.4). Users should exercise extreme caution if changing any setting within the template file, as unrealistic results may be produced.

#### **2.2.3.1 Receptor Grid**

In CALGRID, the primary receptor grid is Cartesian and has uniformly spaced nodes in the X and Y directions. The nodes serve to both define the horizontal extent of a given cell and specify receptor

locations where concentration and deposition values are calculated. Because CALGRID is an Eulerian model, inherent problems exist for situations when the horizontal grid cell size is small and the wind speed is large, as material may be transported through more than one grid cell in a single time step. To minimize this possible issue, 20 nodes in the X and Y directions are recommended and are set as the default. For example, the cell size (and receptor spacing) for a 100-km grid should be 5 km. The number of nodes in the primary grid can be changed within the Cal.par file (see Section A.2.1).

It should be noted that the outer band of grid cells in CALGRID serve to initialize the inner grid cells within the domain. These cells are considered boundary cells and serve as storage locations for the lateral boundary conditions of the grid; no calculations (e.g., transport, diffusion, or deposition) are performed within these cells, and so no values are available for contouring. Therefore, the number of receptors in the X and Y directions available for contouring will always be two less than the actual number of nodes.

## 2.2.4 CALPOST

CALPOST is designed to interface with and summarize the output from the CALPUFF or CALGRID models. In DUSTRAN, the CALPOST post-processing module is used to create user-specified time-averaged values from standard hourly outputs generated by the models. In addition, CALPOST is used to create Top 50 tables, which are tabular values of the highest 50 concentration and deposition values during a simulation for the averaging period of interest. The averaging periods are set within the DUSTRAN interface (i.e., currently 1-, 3-, 8-, and 24-hour averages are available) and calculated for the length of the run.

## 2.3 Dust-Emission Modules

Dust is injected into the atmosphere through active and natural processes. Active processes primarily involve human activity that directly disturbs the surface (e.g., vehicle activity on dirt roads and other unpaved areas or from re-suspension of loose material covering paved roads). Natural processes include wind erosion, which occurs primarily in arid or semiarid environments and may be enhanced by soil disturbance following recent human activity or following natural disasters (e.g., range fires). The dust-emission modules incorporated into DUSTRAN account for both vehicular and wind-blown dust-generation processes.

### 2.3.1 Emission by Vehicular Activity

The vehicular dust-emission module represents dust emissions as the product of an empirically formulated emission factor and the vehicle activity, the latter taken as the total vehicle distance traveled (summed if there are multiple vehicles) in a given period of interest. Explicitly, it can be written as

$$F_j = E_j \cdot A \quad (2.11)$$

where

- $F_j$  = dust emission due to vehicle activity for particulate size class j [g]
- $E_j$  = emission factor for particulate size class j [g/VKT]
- $A$  = vehicle activity [VKT]
- $VKT$  = vehicle kilometers traveled.

The relations used to determine  $E_j$  are entirely empirical and are usually available for only some of the standard particulate size classes (e.g.,  $PM_{2.5}$ ,  $PM_{10}$ ,  $PM_{15}$ , and  $PM_{30}$ ). Variables on which various authors have expressed an  $E_j$  dependency include the silt content of the surface, the number of vehicle axles,

vehicle weight, vehicle speed, and soil moisture. The emission factor,  $E_j$ , is determined as a product of some combination of these variables, each raised to an empirically determined power and a fitted constant. The paved and unpaved road-emission factors in EPA's AP-42 (EPA 2005) are based on this approach and are available for use in DUSTRAN.

Emission factors have been measured for specific vehicles or classes of vehicles. The particulate emission factors for wheeled and tracked military vehicles used in DUSTRAN were provided through SERDP research projects. In observations carried out using a variety of wheeled vehicles (primarily military) at Ft. Bliss, Texas, Gillies et al. (2005a, 2005b) found that the only two variables that matter significantly in calculating the  $PM_{10}$  emission factor for unpaved roads are vehicle weight and vehicle speed. Moreover, when weight and speed are properly accounted for, a single empirically derived functional form may be used to calculate a vehicle-specific emission factor. This function may be expressed using

$$E_{PM_{10}} = 0.003 \cdot W \cdot S \quad (2.12)$$

where  $W$  = vehicle weight (kg)  
 $S$  = mean vehicle speed (km/h).

Combining Equations 2.11 and 2.12 and summing over the types of wheeled vehicles operating on an unpaved road of length,  $L$ , during time period,  $T$ , gives the total emission from the road for that time period as:

$$F_{PM_{10}} = 0.003 \cdot \sum_{i=1}^k W_i \cdot S_i \cdot A_i \quad (2.13)$$

where  $i$  = vehicle type (e.g., Humvee; specifies vehicle weight)  
 $k$  = total number of vehicle types  
 $A_i$  =  $L \cdot N_i$   
 $N_i$  = total number of vehicles of type  $i$ .

Similarly, using results from Kuhn et al. (2010), the total emission from an unpaved road from tracked military vehicles for a given time period can be expressed as:

$$F_{PM_{10}} = 0.0014 \sum_{i=1}^k W_i \cdot S_i \cdot A_i \quad (2.14)$$

where  $F$ ,  $W$ ,  $S$ ,  $A$ ,  $i$  and  $k$  are defined as above.

The DUSTRAN vehicle-activity dust-emission module produces total emissions for each road segment over the time period,  $T$ . Vehicular dust emissions are then passed to the CALPUFF dispersion model where they are released into the modeling domain uniformly along each road segment in both space and time for the duration of the activity.

The vehicle emissions module requires the Universal Transverse Mercator (UTM) easting and northing coordinates to describe the starting and ending points of each road segment as well as the activity duration. Within DUSTRAN, the roadways are created graphically by drawing each segment within MapWindow. For a given line segment, DUSTRAN prompts the user to enter the weight and mean speed for various vehicle types traveling on the roadway. For paved surfaces, emission factors are based on EPA AP-42 recommended values (EPA 2005) and are available for  $PM_{2.5}$ ,  $PM_{10}$ ,  $PM_{15}$ , and  $PM_{30}$ . For unpaved road surfaces, the user has the option of specifying whether to use emission factors derived from

EPA AP-42 (EPA 2005) or from Gillies et al. (2005a, 2005b) and Kuhn et al. (2010). Because the Gillies et al. (2005a, 2005b) and Kuhn et al. (2010) work is specifically for  $E_{PM_{10}}$ , emission factors for other size classes under this option are estimated by computing the ratio of Gillies et al.  $E_{PM_{10}}$  to EPA AP-42  $E_{PM_{10}}$  and applying this ratio to values for EPA AP-42 unpaved road  $E_{PM_{2.5}}$  and  $E_{PM_{30}}$  particle class sizes. As of this writing, AP-42 does not include recommendations for unpaved road  $PM_{15}$  emission factors;  $PM_{15}$  emissions under both options are thus estimated via a linear interpolation between  $PM_{10}$  and  $PM_{30}$  emissions. Average fleet weight and average fleet speed, required for AP-42 formulations, are calculated automatically from information input by the user in the DUSTRAN interface.

During military training exercises, off-road activities can occur within specific training areas where numerous vehicles can move around the area (both on- and off-road) during a period of time where the specific paths of the vehicles are not known. DUSTRAN treats this area-wide training activity as an area source (see Section 4.6.3.1). The total area-wide dust emissions for each particle size range during the period of the training are determined using the same method as for roads described above. Knowing the total distance traveled by each vehicle type during the training period, the total dust emissions for each particle size range are determined using the emission factors described above for unpaved roads. No distinction is made between dust emissions from vehicles operating on unpaved roads versus vehicles operating during off-road maneuvers. At this time, dust-emissions factors for off-road activities are not available; however, emission factors for unpaved roads should be a reasonable surrogate for off-road vehicular activities.

### 2.3.2 Windblown Dust

The windblown dust formulation in DUSTRAN provides a measure of the dust emission from the modeling domain caused by wind erosion of the surface. These emissions are a function of the surface wind stress, vegetation class, and soil texture across the modeling domain. The surface wind stress, as approximated by the friction velocity, is calculated as a function of time and location from the CALMET meteorological model. Vegetation class and soil texture coverage come from well-established global databases and are discussed further in Sections 2.3.2.3 and 2.3.2.4, respectively. An evaluation of the wind-erosion model described in this section has been reported by Shaw et al. (2008).

The “Add Site Wizard” (see Section 7.0) in DUSTRAN automatically creates vegetation class and soil texture files for use in a wind-blown dust simulation whenever a new site is created. These characteristic files, which are a subset of the original global datasets, can be used for any domain specified within a site and are the default files used for generating dust emissions in a wind-blown dust simulation. In addition, the user has the option of specifying finer-resolution characteristic files (see Section 4.6.9) that can be ranked by order of use in a given simulation. When used in this way, high-resolution files can provide detailed information in user-specific regions within the domain and the default files provide information where there is no user-specified information. High-resolution files can be created using the “Polygon Layer Creator” (see Section 5.0), which is an easy way to build vegetation class and soil texture files or to explore the effects of vegetation removal or soil disruption (e.g., off-road vehicle traffic disturbing soils in new areas or field plowing) on dust emissions.

The general approach in DUSTRAN for computing  $PM_{10}$  concentrations resulting from wind-blown dust is to first calculate gridded fields of wind-generated dust emissions over the modeling domain for each model time step. The time- and space-varying dust emission is then provided to the CALGRID dispersion model, which uses winds from CALMET for transporting, dispersing, and depositing the emitted dust throughout the modeling domain. The wind-blown dust emissions for each model grid cell are calculated using the method given in Sections 2.3.2.1 through 2.3.2.4. The principal information needed to calculate the dust emissions for each model grid cell is the time-varying friction velocity (from

CALMET), the area-weighted average vegetation mask, and the area-weighted average fraction of total dust emissions by particle size category for each grid cell. Section 2.3.2.5 gives the method for calculating the fractional distribution of vegetation class and soil texture for each grid cell.

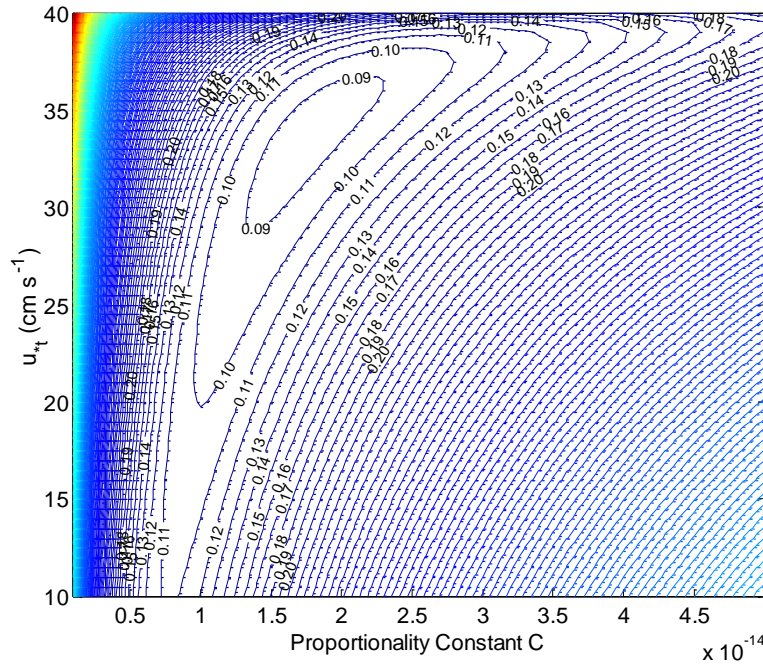
### 2.3.2.1 Dust Flux as a Function of Friction Velocity

Numerous authors over the past three decades have made laboratory and field measurements of dust flux from wind erosion and empirically related those measurements to the friction velocity,  $u_*$ , which is a measure of wind stress on the surface. Some efforts have been made to provide a theoretical foundation for the functional form of the flux in terms of friction velocity, but observations continue to have a great deal of scatter and do not yet validate particular theoretical results. The primary difference among published relations is whether the flux depends on  $u_*$  raised to the third or fourth power. Because of their field measurements of dust flux,  $G$  ( $\text{g cm}^{-2} \text{s}^{-1}$ ) under a variety of conditions, DUSTRAN uses the formulation of Gillette and Passi (1988):

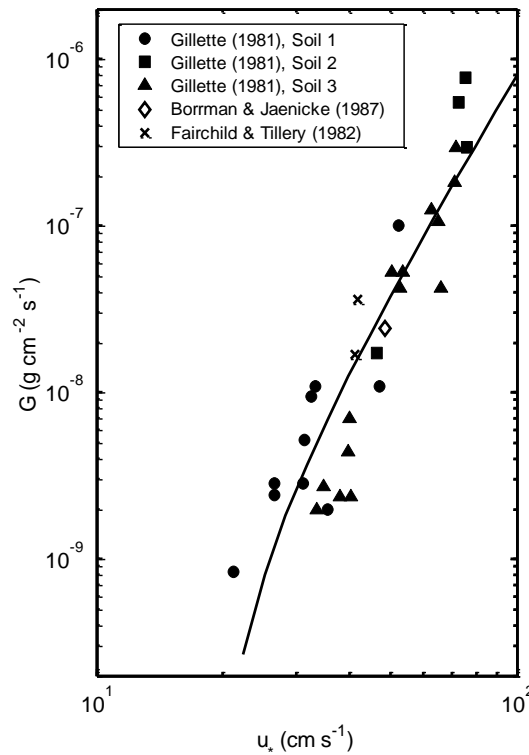
$$G = Cu_*^4 \left( 1 - \frac{u_{*t}}{u_*} \right) \quad (2.15)$$

where  $u_{*t}$  ( $\text{cm s}^{-1}$ ) is a threshold friction velocity below which dust emission does not occur. In addition to the uncertainty in the exponent of  $u_*$ , there has also been significant experimental variation in the values of  $u_{*t}$ .

Gillette and Passi did not actually publish values of  $C$  and  $u_{*t}$  in the above relation. However, they did graphically present a variety of observations of  $G$  versus  $u_*$ . Data digitized from their graph was used to compute the root-mean-square (rms) difference between the function above and the data for a variety of combinations of  $C$  and  $u_{*t}$ . Those results are shown as a contour plot in Figure 2.5, which shows a broad region over which the rms differences are not much different from the absolute minimum value that occurs near a fitted threshold friction velocity of about  $33 \text{ cm s}^{-1}$ . Compromise values of  $C = 1.0 \times 10^{-14} \text{ g cm}^{-6} \text{ s}^3$  and  $u_{*t} = 20 \text{ cm s}^{-1}$  were selected, which place the threshold friction velocity below the lowest reported value of  $u_*$ , because some of the observations of Gillette and Passi showed dust flux occurring for values of  $u_* < 30 \text{ cm s}^{-1}$ . Figure 2.6 shows the fit using PNNL's coefficients.



**Figure 2.5.** Contour Plot of RMS Differences Between Equation (2.15) and Observations of Dust Flux  $G$  Discussed by Gillette and Passi (1988)



**Figure 2.6.** Observations of  $G$  Versus  $u^*$  after Gillette and Passi (1988). The solid line is Equation (2.15) with  $C = 1.0 \times 10^{-14} \text{ g cm}^{-6} \text{ s}^3$  and  $u_{*t} = 20 \text{ cm s}^{-1}$ .

### 2.3.2.2 Effect of Soil Moisture

Soil moisture, if a measure is available, is taken into account in our approach using the method of Fecan et al. (1999) as cited by Nickovic et al. (2001). Basically, soil moisture is incorporated through a wetness factor,  $f_w$ , that multiplies the threshold friction velocity to increase it. Consequently, the total dust flux from the surface accounting for soil moisture is

$$G = Cu_*^4 \left( 1 - \frac{f_w u_{*t}}{u_*} \right) \quad (2.16)$$

where the soil wetness factor is given as

$$f_w = \begin{cases} \left[ 1 + 1.21(w - w')^{0.68} \right]^{1/2} & w > w' \\ 1 & w \leq w' \end{cases} \quad (2.17)$$

$w$  is the gravimetric soil moisture (i.e., mass of water/mass of soil; %), and  $w'$  is the maximum amount of water that can be adsorbed by the soil (%), given as a function of the fraction of clay in the soil,  $\beta_1$  (see Section 2.3.2.4).  $w'$  is given as

$$w' = 14\beta_1^2 + 17\beta_1 \quad (2.18)$$

At this time, soil moisture,  $w$ , is not a function of time or location in DUSTRAN, but is currently specified as a constant value in the Cal.par model static file described in Section A.2.1.1. The default value is zero, leading to a wetness factor of one, which is dry soil.

### 2.3.2.3 Vegetation Cover Effects on Dust-Emitting Potential

Equation 2.8 gives the maximum wind-generated dust flux from the surface not accounting for the effects of different types of vegetation cover on dust-emitting potential. Essentially, more vegetation cover results in less wind-blown dust generated from the surface. This effect of vegetation cover on wind-blown dust is treated by simply multiplying the dust flux from Equation 2.16 by a vegetation mask,  $\alpha$ , that ranges from zero to one. The total dust flux from the surface accounting for vegetation is then given as

$$G = \alpha Cu_*^4 \left( 1 - \frac{f_w u_{*t}}{u_*} \right) \quad (2.19)$$

The vegetation mask is determined using the Olson World Ecosystem (Olson 1992) that defines 59 distinct classes of vegetation. Of the 59 classes, only 4 have been sufficiently exposed to soil to allow for wind erosion, and they include two desert categories and two semi-desert categories. Because of the sparseness of vegetation in deserts,  $\alpha$  for those categories has a value of 1.0. Because of the more widespread presence of shrubs and grasses in the semi-desert categories,  $\alpha$  is assigned a value of 0.5. Table 2.6 lists the Olson identification number, vegetation class description, and  $\alpha$  for these four classes. All other Olson categories are assigned a value of zero for  $\alpha$  and, therefore, do not contribute to wind-blown dust emissions.

Within DUSTRAN, the default Olson vegetation class file is derived from the original 10-minute resolution global database at the time of the sites creation (see the “Add Site Wizard” in Section 7.0).

The default dataset can be supplemented with higher-resolution, Olson-based vegetation class files created by the user using the “Polygon Layer Creator” (see Section 5.0).

**Table 2.6.** Olson Vegetation Classes Used in the Wind-blown Dust-Emission Model

ID #	Olson Vegetation Class Description	$\alpha$
8	Desert, mostly bare stone, clay and sand	1.0
50	Sand desert, partly blowing dunes	1.0
51	Semi-desert/desert, scrub/sparse grass	0.5
52	Cool/cold shrub, semi-desert/steppe	0.5

The value of  $\alpha$  actually used in Equation 2.19 to calculate the dust emissions for a model grid cell is the area-weighted average of  $\alpha$  's for all the vegetation categories that fall within the grid cell. The area-weighted average vegetation mask,  $\bar{\alpha}$ , is calculated as

$$\bar{\alpha} = \sum_{i=1}^4 f_i^V \alpha_i \quad (2.20)$$

where  $\alpha_i$  is the vegetation mask for the  $i^{\text{th}}$  Olson vegetation class (Table 2.6), and  $f_i^V$  is the area fraction of the  $i^{\text{th}}$  Olson vegetation class in a grid cell. The area fractions for the four Olson vegetation classes will sum to one or less. The sum may be less than one because, as noted previously, many other Olson vegetation classes exist that have  $\alpha$  's equal to zero. See Section 2.3.2.5 for the determination of the area fractions.

### 2.3.2.4 Approximating the Size Distribution of Windblown Dust

The formulation given above estimates the total mass of dust produced by wind. However, it is also useful to know the size distribution and in particular how much of the dust consists of particles smaller than 10  $\mu\text{m}$  in diameter. To do this, global databases of soil texture class have been used to estimate the fraction of the emitted dust in four separate particle size ranges. Soil textures are typically defined in terms of their fractions of clay, small silt, large silt, and sand (Tegen and Fung 1994). Table 2.7 gives typical properties of particles for each soil texture class.

**Table 2.7.** Features of Typical Dust Particles (after Nickovic et al. 2001)

k	Soil Texture Class	Range of Particle Diameters ( $\mu\text{m}$ )	Typical Particle Diameter ( $\mu\text{m}$ )	Particle Density ( $\text{g cm}^{-3}$ )	$\gamma_k$
1	clay	1–2	1.5	2.50	0.08
2	small silt	2–20	12	2.65	1.00
3	large silt	20–50	36	2.65	1.00
4	sand	50–100	76	2.65	0.12

The approach for determining the soil texture class (and thus the particle size distribution) follows from Nickovic et al. (2001) using a Zabler soil categories database. Table 2.8 lists the fractions,  $\beta_{j,k}$ , of the four (k-index) soil texture classes within each of the seven (j-index) Zabler soil categories. Note that the fractions of soil texture classes for each Zabler category sum to one. In addition, note that the size fractions for small and large silt given by Nickovic et al. (2001) were too large by a factor of two. The values in Table 2.8 are corrected.

**Table 2.8.** Fractions,  $\beta_{j,k}$ , of the Soil Texture Classes in each Zobler Soil Category

j	Zobler Soil Categories	k=1	2	3	4
		Clay	Small Silt	Large Silt	Sand
1	coarse	0.12	0.04	0.04	0.80
2	medium	0.34	0.28	0.28	0.10
3	fine	0.45	0.15	0.15	0.25
4	coarse-medium	0.12	0.09	0.09	0.70
5	coarse-fine	0.40	0.05	0.05	0.50
6	medium-fine	0.34	0.18	0.18	0.30
7	coarse-medium-fine	0.22	0.09	0.09	0.60

Currently, the soil texture category for a desired location in the modeling domain is being read from an ASCII, comma-delimited text file that was derived from the Zobler raster image with a 1-degree resolution (Staub and Rosenzweig 1992). Sources for higher-resolution soil textures that are spatially complete (e.g., cover the continental U.S.) are being investigated for possible inclusion in a future version of DUSTRAN. In addition, the user has the option of creating high-resolution Zobler soil texture files using the “Polygon Layer Creator” (see Section 5.0). The user-specific files can be associated with a given simulation (see Section 4.6.9) to supplement or replace the soil textures derived from the default Zobler global file.

To accomplish the size partitioning of the dust flux from each model grid cell, DUSTRAN uses the dust-productivity factor as defined by Nickovic et al. (2001). For each of the four particle size classes, DUSTRAN defines a dust-productivity factor  $\delta_k$  so that the dust flux in the  $k^{\text{th}}$  particle size class,  $G_k$ , is

$$G_k = \delta_k G \quad (2.21)$$

where  $G$  is from Equation 2.19. The dust-productivity factor for a grid cell is determined by

$$\delta_k = \gamma_k \sum_{j=1}^7 f_j^Z \beta_{j,k} \quad (2.22)$$

where  $\gamma_k$  = the ratio of mass available for uplift to total mass in that soil texture class (size range)  
 $\beta_{j,k}$  = from Table 2.8  
 $f_j^Z$  = the area fraction of the  $j^{\text{th}}$  Zobler soil category in a grid cell.

The area fractions for the seven Zobler categories sum to one. See Section 2.3.2.5 for the determination of the area fractions. Table 2.7 lists the values of  $\gamma_k$ , which are those used by Nickovic et al. (2001). Because the values of  $\delta_k$  represent a partitioning of the total flux,  $G$ , they should sum to unity. However, the values of  $G$  used by Gillette and Passi (1988) to develop Equation 2.15 were for particle sizes  $<40 \mu\text{m}$  in diameter. This essentially excludes the larger sand category. This exclusion of the larger sand category is accounted for by actually using an “enhanced” total dust flux,  $G'$ , in Equation 2.21. Therefore, the “actual” dust flux for each particle size (soil texture class) within a grid cell is

$$G_k = \delta_k G' \quad (2.23)$$

where  $G'$  is determined as

$$G' = \frac{\sum_{k=1}^4 \delta_k}{\sum_{k=1}^3 \delta_k} G \quad (2.24)$$

Substituting Equation 2.24 into 2.23 gives the actual dust flux by particle size category as

$$G_k = \delta_k \frac{\sum_{i=1}^4 \delta_i}{\sum_{i=1}^3 \delta_i} G \quad (2.25)$$

Currently in DUSTRAN, only the PM<sub>10</sub> size particles from wind-blown dust are provided as a gridded output. The emission flux of PM<sub>10</sub> for each grid cell is the sum of the first two particle size categories, or

$$G_{PM10} = \sum_{k=1}^2 G_k \quad (2.26)$$

### 2.3.2.5 Calculating Soil and Vegetation Types for Use in Wind-Blown Dust Simulations

This section provides specific information on how the Olson vegetation class and Zobler soil-texture values are sampled and mapped to model grid cell average values in DUSTRAN. Mapping is necessary because the characteristic files provide vegetation and soil-texture information as a series of polygon shapes whereas CALGRID requires emissions from a regular array of cells within a Cartesian grid. This section is not necessary to understand how wind-blown dust is determined, but is given here for completeness of the calculations and operations performed within DUSTRAN.

For calculating wind-blown dust emissions, DUSTRAN requires the fractional area coverage of the four Olson vegetation classes and seven Zobler soil texture categories for all the model grid cells within the model domain. The fractional area coverage of either the vegetation or soil textures class for each model grid cell is calculated by “sampling” the respective base characteristic file. The default base characteristic files are created automatically at the time of the site’s creation (using the “Add Site Wizard,” Section 7.0) and are derived from the original Olson World Ecological and Zobler soil textures global database files. The default files are assigned automatically to a given wind-blown dust scenario using the “Sources” tab (see Section 4.6) within DUSTRAN and can be supplemented with higher-resolution, user-specific characteristic files created using the “Polygon Layer Creator” (see Section 5.0).

The format of the two base data files includes headers containing the number of data columns and rows found in the two site-wide files as well as headers detailing the UTM coordinates of the lower left and upper right corners of the site extent. Typically, site extents are greater than 600 km square to accommodate modeling domains centered at various locations and of various sizes. Following the headers are data records containing the soil or vegetation data. Each data record contains five fields separated by commas that represent one grid point in the base file. The first two fields of each record contain the column and row indices of the data’s location in the data file. The third element contains the soil or vegetation type ID. A 9999 in the type field represents a grid point that does not contain any soil or vegetation data. Lastly, the fourth and fifth elements are the UTM easting and northing coordinates of the grid point. The [0,0] indices in the file represent the X and Y values of the lower left (southwest) corner of the site extent. X indices increase to the right (east), and Y indices increase to the top (north).

The fractional area coverage,  $f_k^A$ , within a model grid cell for the  $k^{\text{th}}$  category of surface property A (e.g., soil texture) calculates as

$$f_k^A = \frac{N_k}{N_G N_G} \quad (2.27)$$

where  $N_k$  is the number of occurrences of the  $k^{\text{th}}$  category of property “A,” and  $N_G$  is the number of sampling points in the x- and y-directions in a square model grid cell. Currently in DUSTRAN,  $N_G$  is equal to 5 for a total of 25 sampling points per model grid cell.

The desired property value for each model grid cell sampling point is read from the appropriate site-wide file containing the specific property (e.g., soil texture or vegetation cover) of interest. The property value at a grid cell point located at  $[X_m, Y_n]$ , where  $m = 1$  to  $N_G$  and  $n = 1$  to  $N_G$ , is determined by knowing the nearest site-wide data point to the sampling point. The indices  $[i_m, j_n]$  of the nearest site-wide point to the  $[m, n]$  grid cell point are determined as

$$i_m = NINT \left[ \frac{X_m - X_0}{X_d - X_0} (N_x - 1) \right] \quad (2.28)$$

$$j_n = NINT \left[ \frac{Y_n - Y_0}{Y_d - Y_0} (N_y - 1) \right] \quad (2.29)$$

where

- $i_m$  = 0 to  $N_x-1$ ; X-direction index of  $m^{\text{th}}$  grid cell sampling point in site-wide file
- $j_n$  = 0 to  $N_y-1$ ; Y direction index of  $n^{\text{th}}$  grid cell sampling point in site-wide file
- $X_m$  = UTM Easting coordinate of the model grid cell sampling point
- $Y_n$  = UTM Northing coordinate of the model grid cell sampling point
- $X_0$  = UTM Easting coordinate of the southwest corner of the site-wide file
- $Y_0$  = UTM Northing coordinate of the southwest corner of the site-wide file
- $X_d$  = UTM Easting coordinate of the northeast corner of the site-wide file
- $Y_d$  = UTM Northing coordinate of the northeast corner of the site-wide file
- $N_x$  = Number of data points in the X-direction in the site-wide file
- $N_y$  = Number of data points in the Y direction in the site-wide file
- $NINT$  = get nearest integer of quantity in brackets.

The  $X_m$  and  $Y_n$  coordinates for each of the grid cell sampling points are determined as

$$X_m = X_0^G + \frac{\Delta}{2N_G} [1 + 2(m-1)] \quad (2.30)$$

$$Y_n = Y_0^G + \frac{\Delta}{2N_G} [1 + 2(n-1)] \quad (2.31)$$

where

- $\Delta$  = Length of square grid cell along one side
- $X_0^G$  = UTM Easting coordinate of the model grid cell southwest corner
- $Y_0^G$  = UTM Northing coordinate of the model grid cell southwest corner

As mentioned previously, the spatial resolution of the Olson vegetation class database is 10 minutes (roughly 15 km at mid-latitudes) and the Zobler soil texture database is 1 degree (roughly 80 km at mid-latitudes). In general, these data are at a much coarser resolution than the grid resolution that will be likely used in a windblown dust simulation. For example, a 200 km domain with 20 grid cells in the X and Y direction will have a 10 km resolution, which is a finer resolution than either the default vegetation class or soil texture database files. Nevertheless, the 25 (5 by 5) sampling points per grid cell method is not computationally expensive and is employed for situations where the user may supplement a simulation with higher-resolution characteristic files.

## 3.0 DUSTRAN Installation Instructions

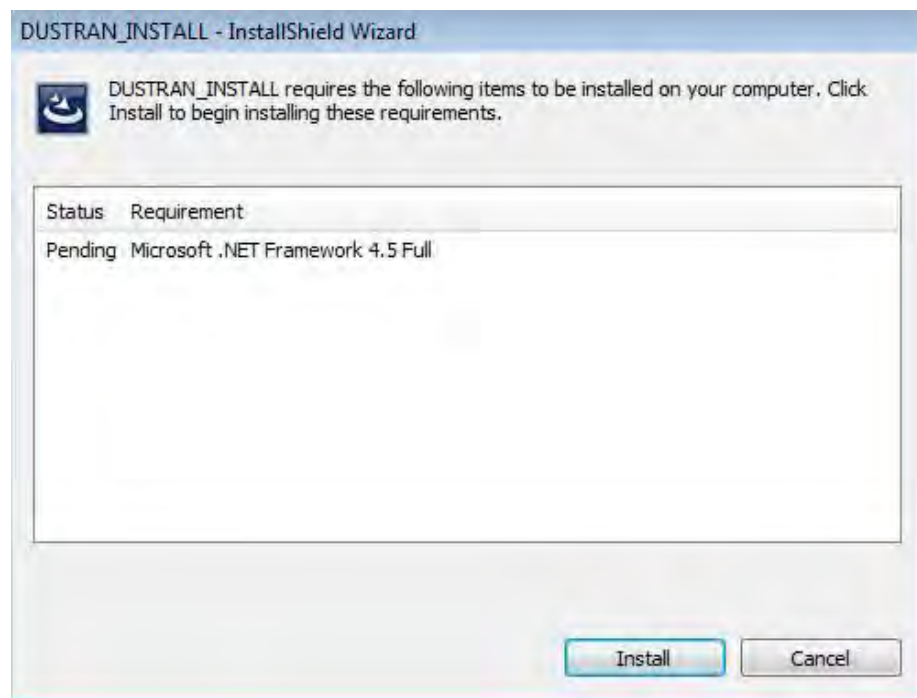
DUSTRAN requires that both the Microsoft .NET 4.5 framework and the MapWindow GIS be installed on the system. The installation instructions below explain how to install these if they are not already present. These instructions will cover installing DUSTRAN and setting up access to DUSTRAN from within MapWindow.

### 3.1 Installing DUSTRAN

- DUSTRAN V2.0 runs within the MapWindow Version 4.7 application.
- Note that the installation of this software requires that the user has administrative privileges on the machine in which it is being installed.
- Before installing DUSTRAN, be sure all other applications are closed.
- If a prior version of DUSTRAN has been installed, it will need to be removed prior to installation of the new version.

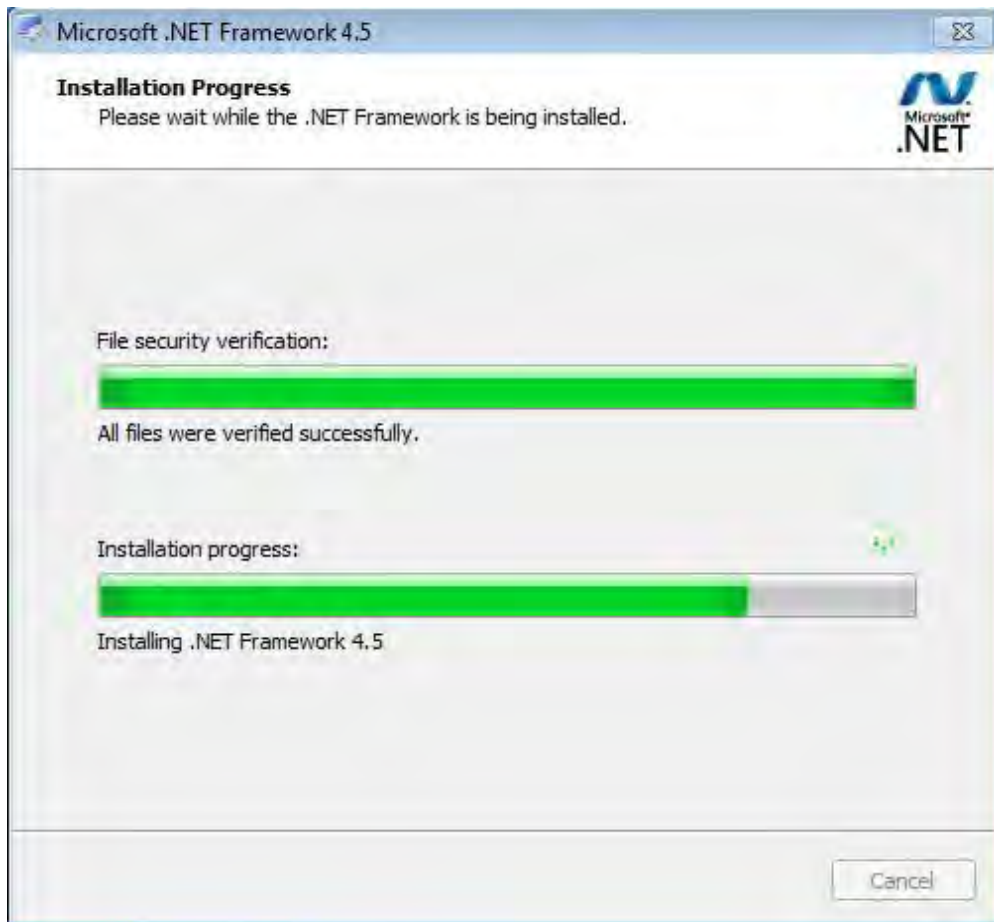
### 3.2 Installing DUSTRAN and Setting Up Access to DUSTRAN from Within MapWindow.

1. Start the installation of the DUSTRAN modeling system by double-clicking on the “Dustran\_Installer.exe” executable file.
2. If the Microsoft .NET 4.5 framework is not currently installed on the machine, the DUSTRAN installation will prompt for the start of the .NET 4.5 installation process. Click the “Install” button to start the installation.



**Figure 3.1.** .NET Framework 4.5 Installation Start

3. During the installation of the .NET framework, a number of dialog windows will be displayed showing the extracting and installation progress. These windows will close on their own and do not require user action.



**Figure 3.2.** .NET 4.5 Installation Progress

4. Once the .NET framework has been installed, the DUSTRAN install wizard will start. Click the “Next” button to continue with the installation.



**Figure 3.3.** DUSTRAN Install Start

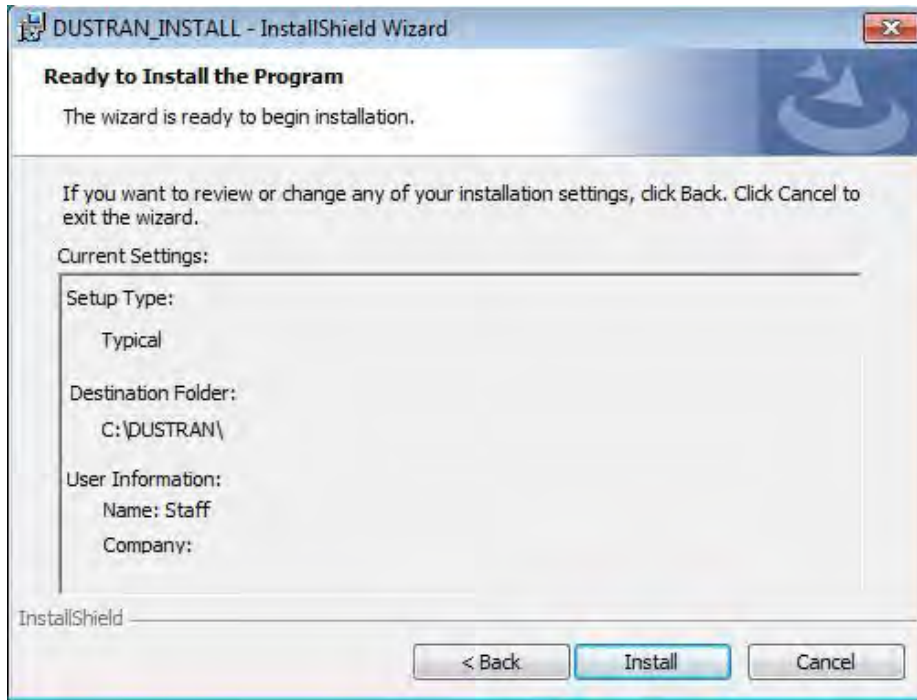
5. A “Destination Folder” prompt will be displayed showing a default path of “C:\DUSTRAN\” as the installation path.



**Figure 3.4.** DUSTRAN Destination Select

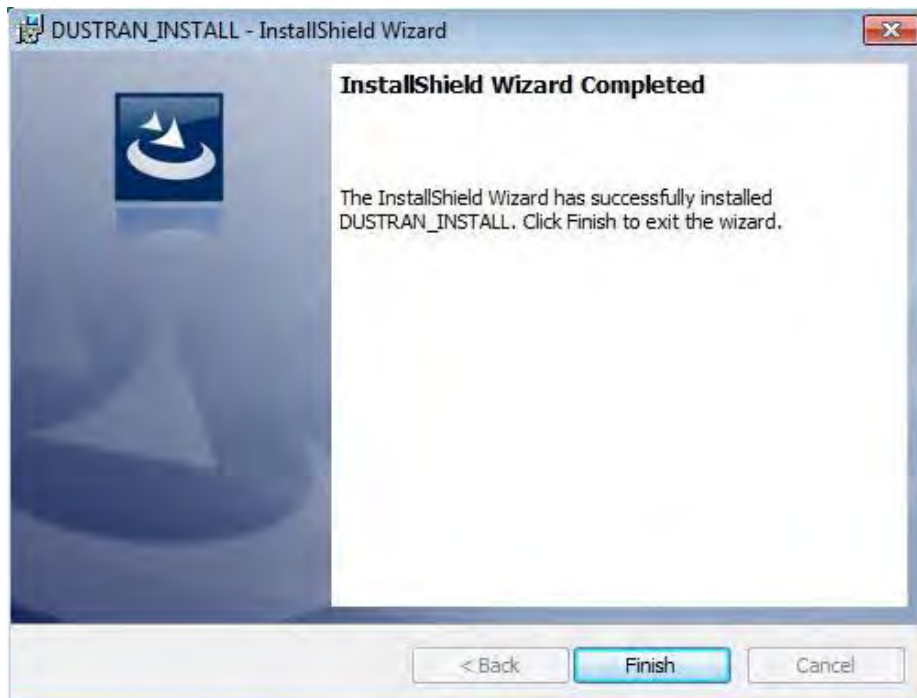
6. Click the “Change...” button to select a different destination folder or click on the “Next” button to select the default path and continue the installation.

7. The “Ready to Install the Program” dialog window will be displayed. Click the Install button to start the installation process.



**Figure 3.5.** Start DUSTRAN Installation

8. When “InstallShield Wizard Completed” is displayed, the DUSTRAN portion of the install has completed, click on the “Finish” button to start the “DUSTRAN Configuration Manager.”



**Figure 3.6.** DUSTRAN Install Finished

9. Following the DUSTRAN install, the installer will start an install of Microsoft Chart Controls.

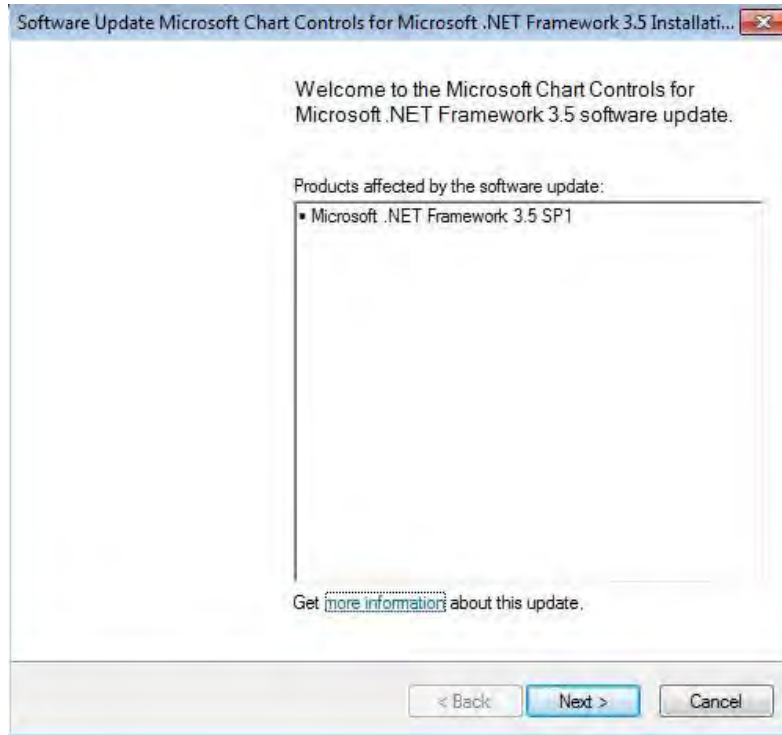


Figure 3.7. Microsoft Chart Control Installation Start Window

10. Review and accept license terms for the chart control software and then click “Next.”

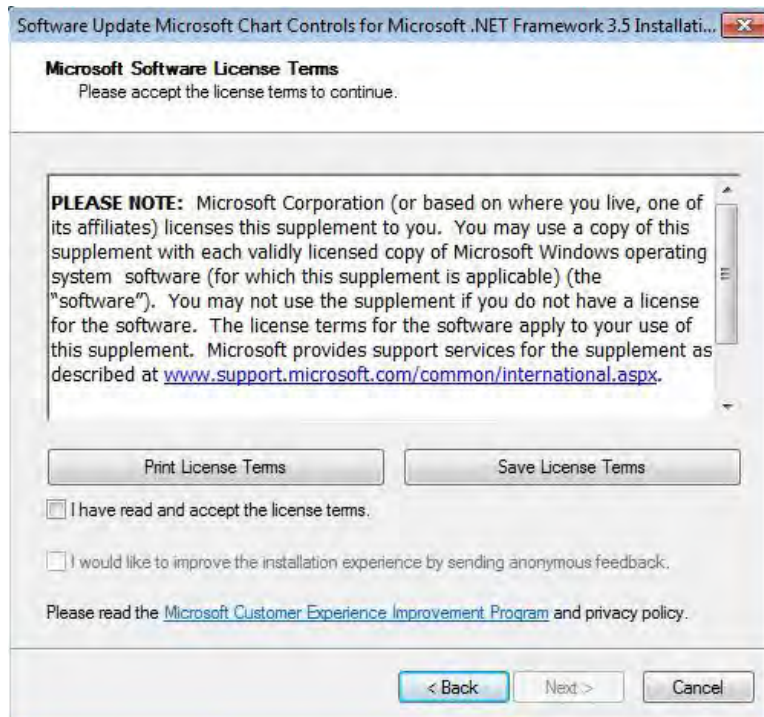
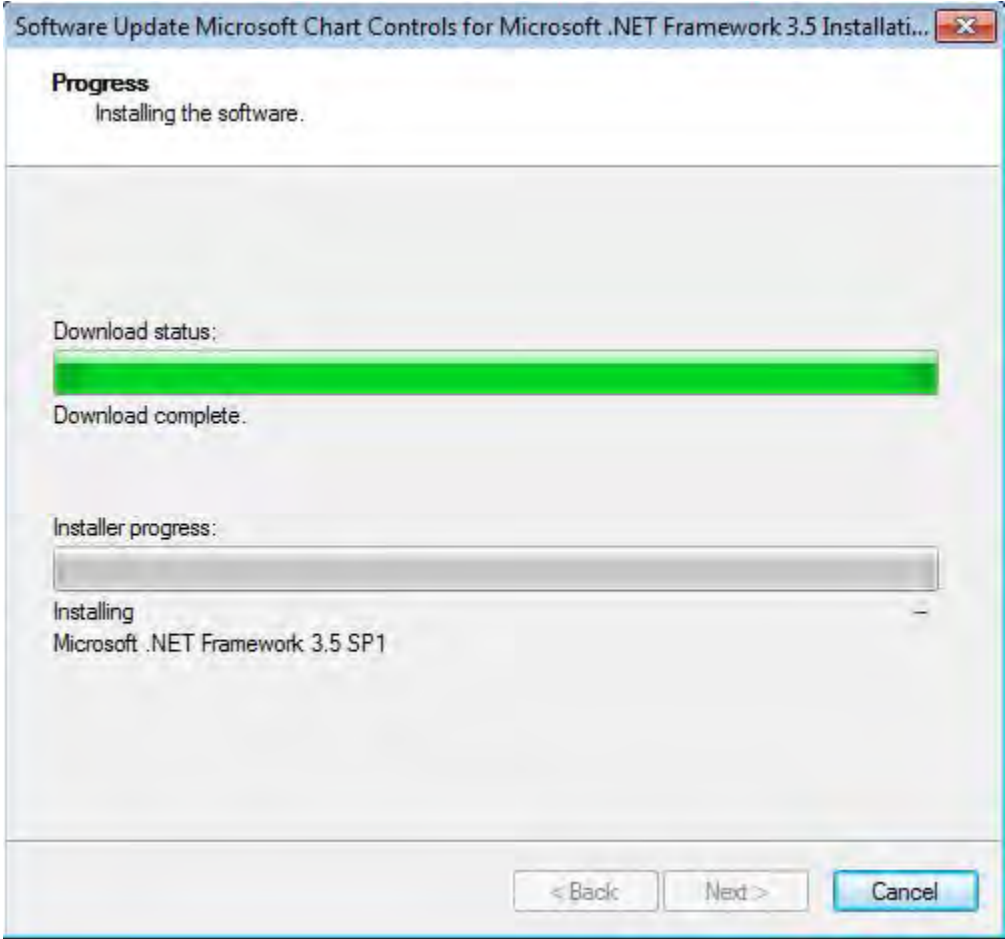


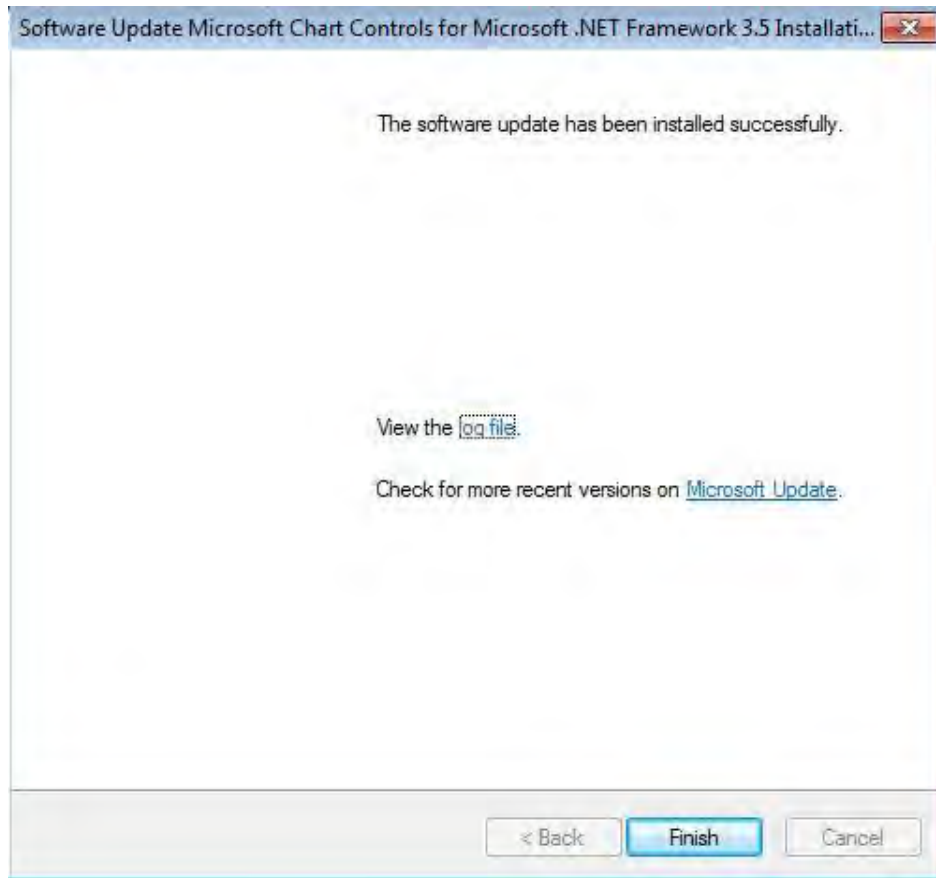
Figure 3.8. Chart Control License Agreement

11. During the installation of the chart control a progress dialog window will be displayed and then shut down once the files have been installed.



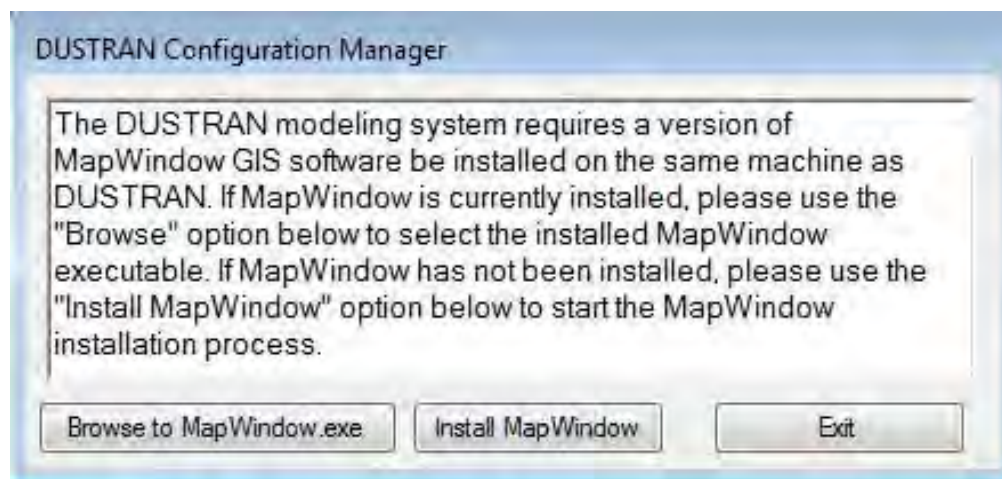
**Figure 3.9.** Chart Control Installation Progress Window

12. Upon completion, the installer will display a finish dialog. Click on the “Finish” button to close the window and complete the chart control install.



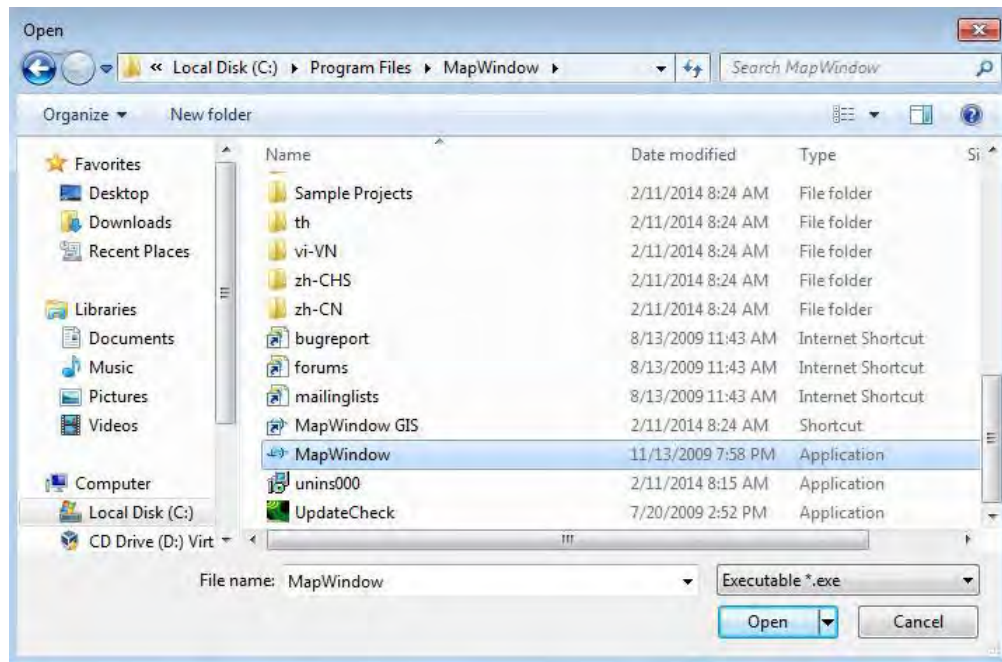
**Figure 3.10.** Chart Control Installation Complete Window

13. In order to use DUSTRAN there must be a copy of MapWindow GIS software present on the installation machine.
14. If MapWindow has not been previously installed, click on the “Install MapWindow” button of the configuration manager which will start the MapWindow installation wizard.



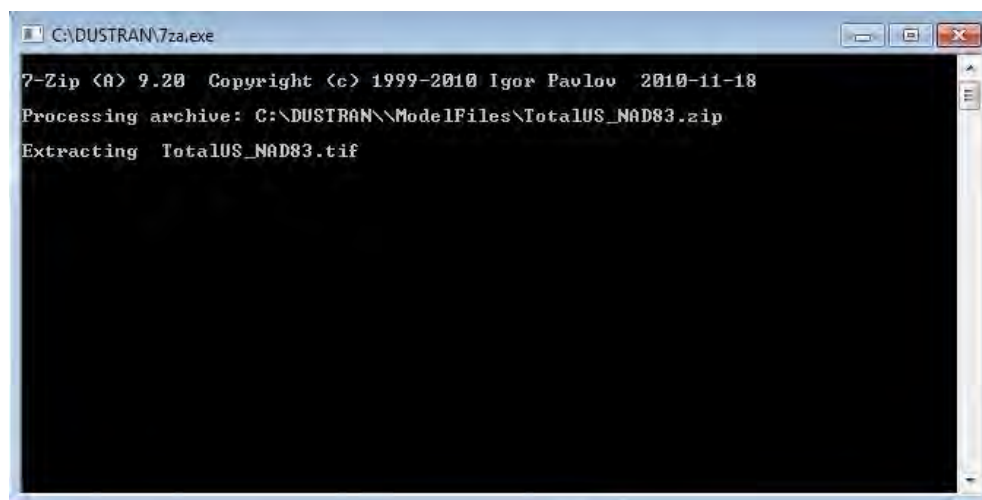
**Figure 3.11.** DUSTRAN Configuration Manager

15. Once started, the MapWindow installation wizard will walk through the steps required to install the software.
16. Once the MapWindow installation has finished, return to the DUSTRAN Configuration Manager dialog window and click on the “Browse to MapWindow.exe” button.
17. Use the Open dialog window to browse to and select the MapWindow.exe. When the file has been selected click the “Open” button to close the browse window.



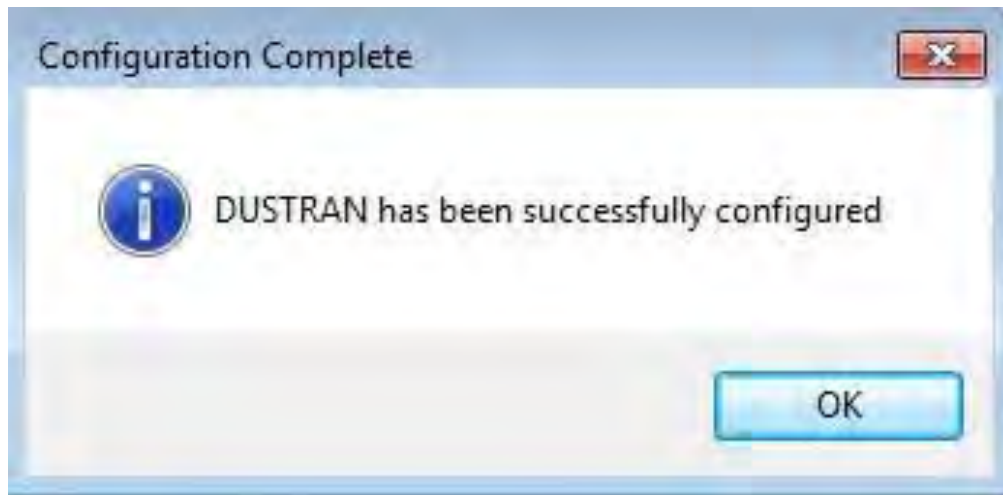
**Figure 3.12.** Select MapWindow.exe File

18. Once the MapWindow.exe has been selected, a command prompt window will be displayed showing the extraction of the .tif raster file used in the creation of new sites. The extraction will take a few minutes to complete.



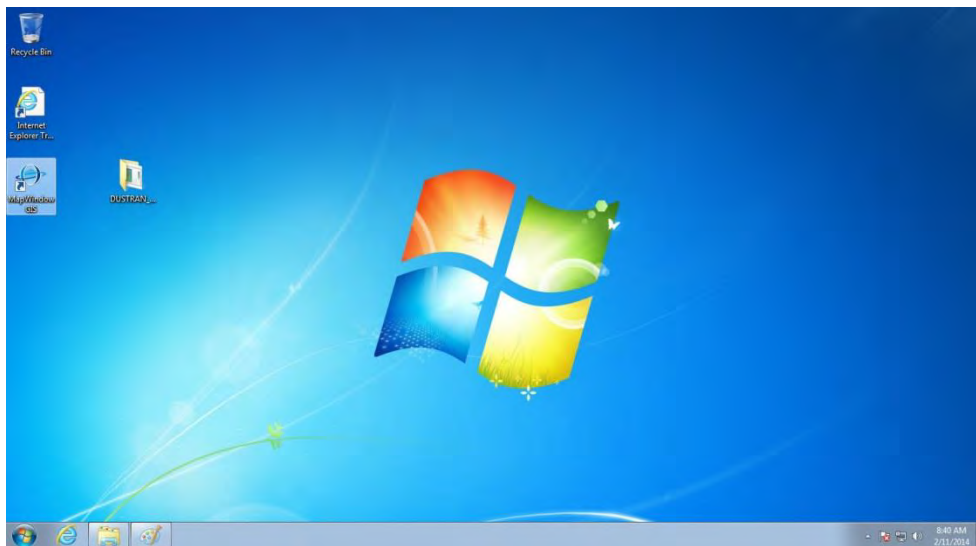
**Figure 3.13.** .tif File Extraction Window

19. When the extraction completes, “Configuration Complete” will be displayed. Click on the OK button to close the install application.



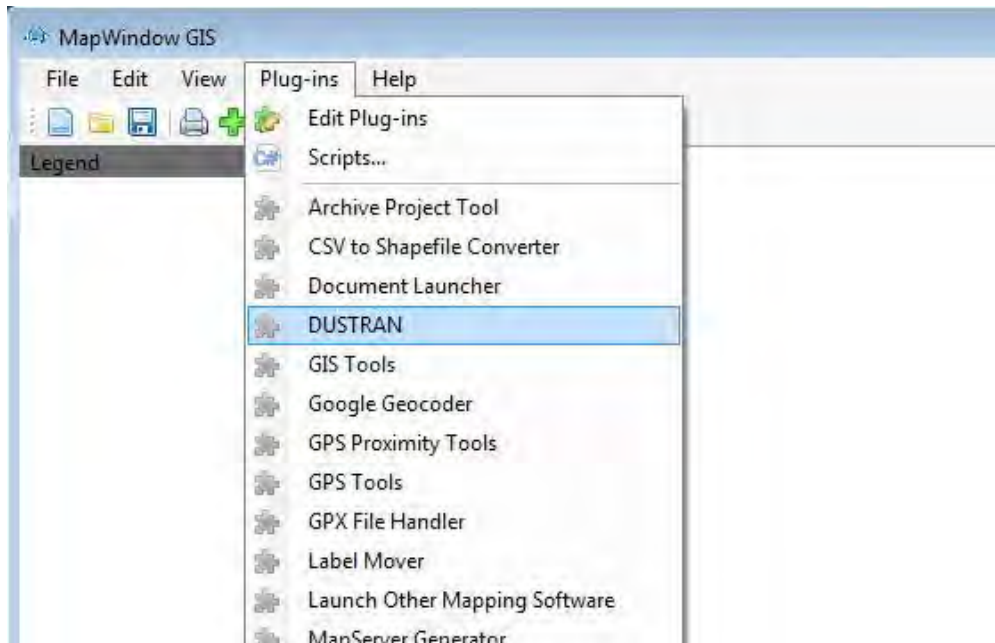
**Figure 3.14.** DUSTRAN Configuration Complete

20. Double-click on the “MapWindow GIS” desktop icon to start the MapWindow application after the installation has successfully completed.



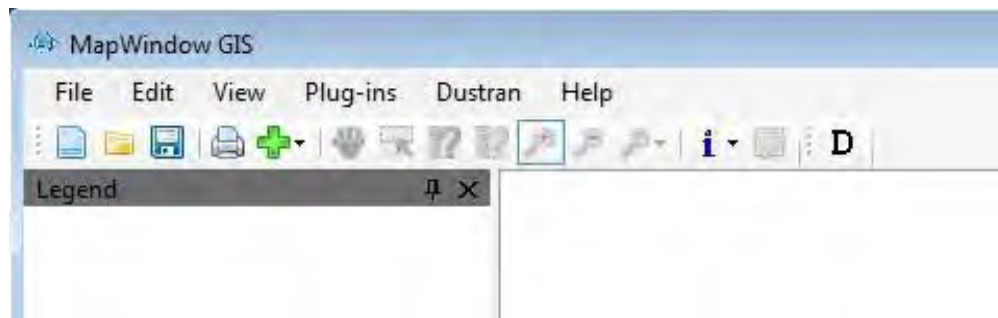
**Figure 3.15.** MapWindow Desktop Icon

21. Under the “Plug-ins” menu inside of the MapWindow application, select “DUSTRAN.”



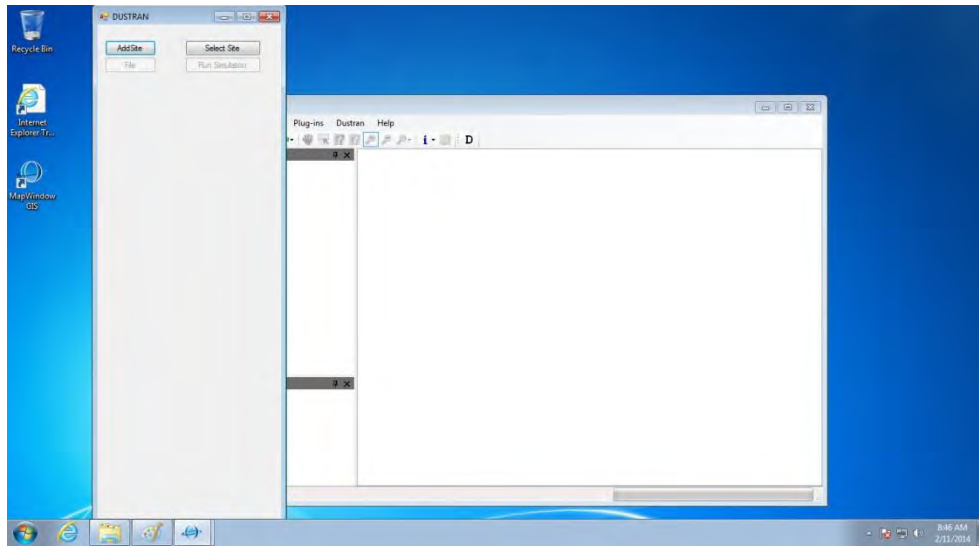
**Figure 3.16.** Selecting DUSTRAN Plug-in

22. Once the plug-in has been loaded, select the “DUSTRAN” menu item, the “D” icon on the toolbar, or press “alt-d” to open the DUSTRAN user interface.



**Figure 3.17.** MapWindow DUSTRAN Menu Items

23. To add a site, click on the “Add Site” button in DUSTRAN and follow the steps outlined in Chapter 6 of this user’s guide to create a new simulation site.



**Figure 3.18.** DUSTRAN Startup

## 4.0 DUSTRAN User Interface

DUSTRAN functions as a plug-in within the MapWindow GIS application. To perform a simulation in DUSTRAN, several fields within the interface must be selected, entered, or completed. This section details the various user-entry fields within the interface and is intended as a reference guide for the application. This section assumes that both MapWindow and DUSTRAN are already installed, and the user has some familiarity with the MapWindow application.

### 4.1 Starting DUSTRAN and Loading a Site

DUSTRAN functions as a plug-in within the MapWindow application and is accessible through the MapWindow toolbar (see Section 3.0, “DUSTRAN Installation Instructions”). To start DUSTRAN, first start the MapWindow application and then start DUSTRAN by clicking on the “D” button located on the MapWindow toolbar.

Once the DUSTRAN interface has been opened, click on the “Select Site...” button to open a dialog box that contains a list of available sites. Select a site from the “Current Site” list and click “Open” to open the site in DUSTRAN. The GIS map files associated with the site are automatically loaded and displayed in the map window. For example, Figure 4.1 shows the Yakima site loaded into the DUSTRAN modeling system showing the Hanford site within Washington State.

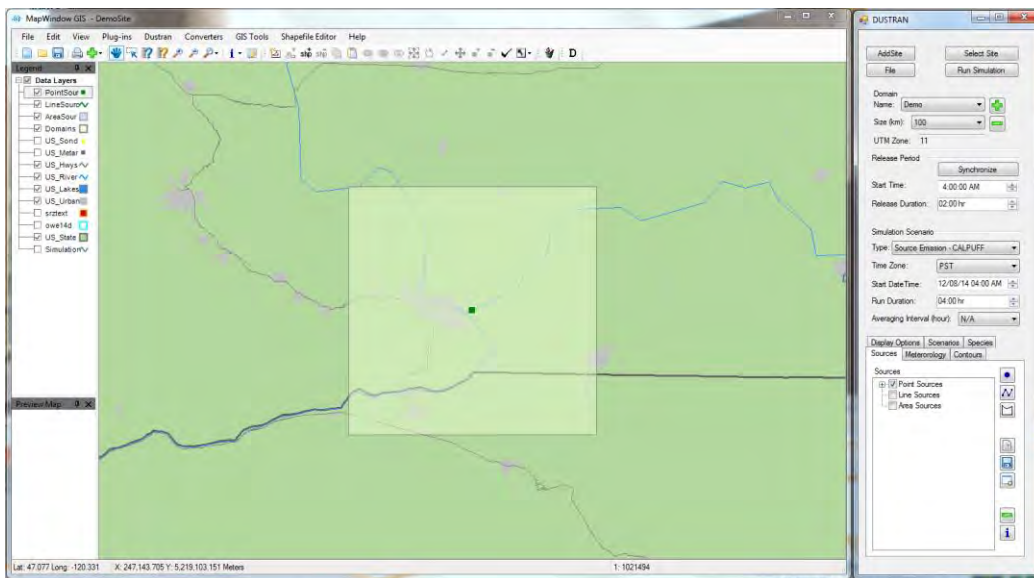


Figure 4.1. Site Loaded into the DUSTRAN Modeling System

### 4.2 Domain Panel

The “Domain” panel within the DUSTRAN interface is used to set the location and size of the modeling domain that will be used in a model simulation. The modeling domain is the area where both the meteorological and dispersion calculations are performed.


The “Domain” panel allows for domains to be selected, added, and deleted. Figure 4.2 displays an example of the “Domain” panel with an existing domain name and size selected.



**Figure 4.2.** Example Domain Panel with Controls Labeled

### 4.2.1 Creating a New Domain

Multiple model domains can be created for a site, but only one model domain can be used in a given simulation. Use the following steps to create a model domain:

1. Within the “Domain” panel, click on the “Add Domain”  button.
2. Select the location of the center of the new domain by clicking on a map location within MapWindow.
3. When prompted, enter a name for the domain. This name will be added to the list of domains that are stored within the “Name” list; these domains are available for use in a given simulation.
4. Set the domain size by selecting a size from the “Size” list. Domain sizes available for use within DUSTRAN include square areas that are 20, 50, 80, 100, 150, 200, 250, 300, 350, and 400 km on a side.
5. Following the selection of a domain size, MapWindow’s map display will refresh automatically to the selected domain location, and the domain boundary will be sized appropriately.


### 4.2.2 Selecting an Existing Domain

Domains that currently exist for a site are available for selection under the “Name” list. To select an existing domain:

1. Within the “Domain” panel, select a desired domain from the “Name” list.
2. The domain will automatically display in MapWindow. To change the size of the domain, select a size from the “Size” list.
3. Following the selection of a domain size, MapWindow’s map display will refresh automatically to the selected domain location, and the domain boundary will be sized appropriately.

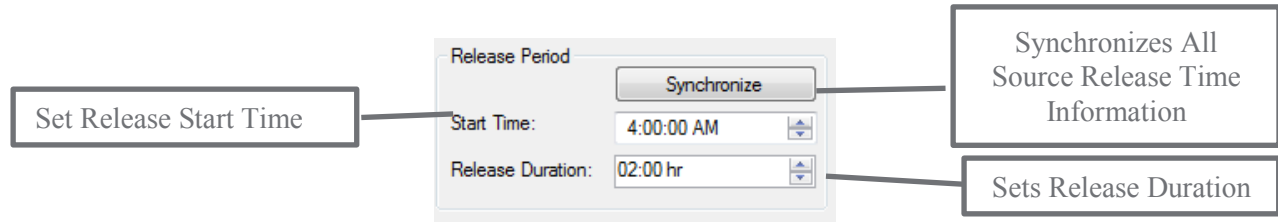
### 4.2.3 Deleting a Domain from a Site

A previously created domain can be deleted from a site so that it no longer appears as an available domain under the “Name” list. To delete a domain:

1. Within the “Domain” panel, select the name of the domain to delete from the “Name” list.
2. Click on the “Delete Domain”  button to permanently delete the domain from the site.

## 4.3 Release Period Panel

The “Release Period” panel is used to set a default start time and duration for all newly created sources. The start time and duration for a given source can be set independently of the default value at the time of the source’s creation (see the Section 4.6 for information on creating sources). In addition, the “Release Period” panel can be used to synchronize each selected source’s start and end times. Source synchronization is normally performed after all sources have been created and is a convenient method for assigning sources the same release time and duration, if desired. Figure 4.3 displays an example of the “Release Period” panel with the input controls labeled.



**Figure 4.3.** Example Release Period Panel with Controls Labeled

### 4.3.1 Setting the Default Release Start Time and Duration

A default “Start Time” and “Release Duration” can be set for sources on the “Release Period” panel. The “Start Time” is the default starting time in which sources begin releasing material. The “Release Duration” is the default period for which material is released. These values are used as defaults whenever a source is created and can be changed specifically for each source on the “Release Parameters” form for that source.

- To change the default start time, enter an hour value or click the increase or decrease arrow buttons for the “Start Time” input box. Clicking the up-arrow (down-arrow) will increase (decrease) the time by 1 hour. Note, start times are limited to hour increments, and any minutes entered will be ignored by the simulation.
- To change the default release duration, enter an hour value or click the increase or decrease arrow buttons for the “Release Duration” input box. Clicking the up-arrow (down-arrow) will increase (decrease) the time by hourly increments.

### 4.3.2 Synchronizing the Release Start Time and Duration for All Sources

All start times and durations can be synchronized to the same time and duration for all selected sources. However, synchronization should be used with caution to avoid inadvertently resetting release start times and durations to unintended values. Synchronization is typically performed after all sources have been created via the “Source” tab, but only if the user wants all source start times and release durations to be the same. To synchronize source times:

- Set the default “Start Time” and “Release Duration” on the “Release Period” panel.
- Click on the “Synchronize” button. A dialog box will be displayed asking the user to confirm changing the time data for all of the sources. Selecting the “OK” option will result in the time data for all sources to be changed to the default values found in the “Release Period” panel. Selecting the “Cancel” option will cancel the synchronize operation, and no changes will occur.

## 4.4 Simulation Scenario Panel

The “Simulation Scenario” panel is used to set the simulation type, start date, time, and run duration. The start date, time, and run duration correspond to the time that the AERMOD, CALPUFF, or CALGRID models are run and do not need to correspond with source release start times or durations. Often, the run duration is chosen so that it is longer than the release duration to continue simulating the plume movement and diffusion on the domain after all sources have finished releasing material. Figure 4.4 shows an example of the “Simulation Scenario” panel with sample entries.

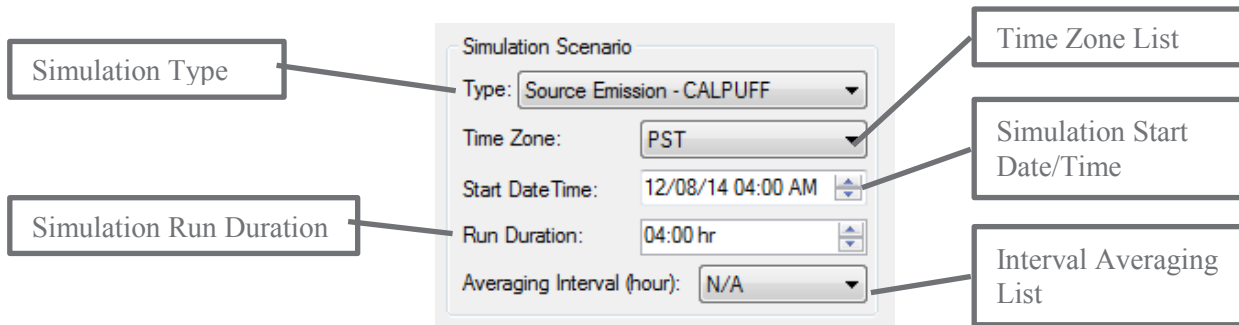


Figure 4.4. Example Simulation Scenario Panel with Controls Labeled

### 4.4.1 Setting the Simulation Type

The simulation type is used to distinguish between which dispersion model (AERMOD, CALPUFF, or CALGRID) is used to run a given simulation. AERMOD and CALPUFF are used to model standard “Source Emissions” and includes emissions that can be quantified using point-, area-, or line-source types. Vehicular dust emissions, which can be quantified using area- or line-source configurations, is an example source type that should be run using this mode. CALGRID is used to model wind-blown dust dispersion over the modeling domain. A qualitative overview of the models is provided in Sections 2.2.2 and 2.2.3, respectively.

To set the dispersion model to use for the current simulation type, click on the “Type” field and select one of the following:

- “Source Emissions – CALPUFF” to use an EPA version of the CALPUFF dispersion model for the current simulation. CALPUFF is ideal for modeling discrete sources that can be quantified using point-, area-, or line-source types. Emissions from stacks or roadways are example sources that would normally be run using this simulation type.
- “Source Emissions – CALPUFF (DRI)” to use the CALPUFF dispersion model with dry-deposition factors developed by DRI for the current simulation. CALPUFF is ideal for modeling discrete sources that can be quantified using point-, area-, or line-source types. Emissions from stacks or roadways are example sources that would normally be run using this simulation type.
- “Source Emissions – AERMOD” to use the EPA-approved version of the AERMOD dispersion model for the current simulation. AERMOD is ideal for modeling discrete sources that can be quantified using point-, area-, or line-source types. Emissions from stacks or roadways are example sources that would normally be run using this simulation type.
- “Source Emissions – AERMOD (DRI)” to use the AERMOD dispersion model with dry-deposition factors developed by DRI for the current simulation. AERMOD is ideal for modeling

discrete sources that can be quantified using point-, area-, or line-source types. Emissions from stacks or roadways are example sources that would normally be run using this simulation type.

- “Wind-blown Dust” to use the CALGRID dispersion model for the current simulation. The wind-blown dust emissions provided to CALGRID are automatically calculated for each model grid cell within the modeling domain using the approach described in Section 2.3.2.

#### 4.4.2 Setting the Time Zone

The time zone is set through the “Time Zone” listbox within the “Simulation Scenario” panel. Available time zones include: Pacific Standard (PST), Central Standard (CST), Mountain Standard (MST), and Eastern Standard (EST). “Time Zone” is used to correct upper-air soundings to local time and is also used by the CALMET meteorological model to calculate sunrise and sunset for sensible heat flux calculations.

#### 4.4.3 Setting the Start Date

The start date for the simulation is entered in the “Start Date” textbox within the “Simulation Scenario” panel.

- To enter the date manually, click on the month, day, or year portion of the date displayed in the control. Once the appropriate portion of the date has been selected, the new value can be entered. All values should be entered as integers and are automatically checked for correctness. In the case of the month, it will convert the integer to the appropriate month name abbreviation.
- To enter the date using the calendar control, first click on the dropdown arrow. A calendar will be displayed for the date that is currently entered in the “Start Date” control. To change years, click on the year label within the calendar and click on the up (down) arrows to increment (decrement) by one year. To change months, click on the right or left arrow buttons located at the top of the calendar control. Clicking on the left (right) arrow buttons decreases (increases) the month by one. To select a day, click on the desired day within the calendar, and the calendar control will then close with the “Start Date” input box automatically updating to the new date.

#### 4.4.4 Setting the Start Time

The start time for the simulation is entered in the “Start Time” textbox within the “Simulation Scenario” panel. The simulation start time can begin *before* any sources begin releasing material. In fact, the meteorological model, CALMET, requires the simulation to begin *before* sunrise, which for most of the year generally occurs after 05:00 a.m. local time at most continental U.S. locations. This requirement exists because the CALMET-derived boundary-layer parameters and mixing height are a function of the sensible heat flux, which in turn is function of sunrise. For most simulations, setting the “Start Time” to 04:00 a.m. adequately meets CALMET requirements.

To set the start time, click the “Start Time” textbox and enter the hour value manually or by clicking on the increase or decrease arrow buttons found to the right of the input box. Clicking the up-arrow (down-arrow) will increase (decrease) the time by one hour. Start times are currently limited to hour increments and minutes are ignored.

#### 4.4.5 Setting the Run Duration

The run duration for the simulation is entered in the “Run Duration” textbox within the “Simulation Scenario” panel. For CALPUFF or CALGRID, the run duration is typically longer than any source release duration to allow for the dispersion models to continue calculating concentration and deposition values for any residual plume material in the modeling domain.

To set the run duration, click the “Run Duration” textbox and enter an hour value manually or by clicking on the increase or decrease arrow buttons found to the right of the input box. Clicking the up-arrow (down-arrow) will increase (decrease) the time by 15-minute intervals. Currently, the models simulate hour increments, and any minutes are ignored.

#### 4.4.6 Setting the Averaging Interval

The averaging interval of a simulation is the number of hours to use when processing the average of the results generated by the CALPUFF or CALGRID dispersion models. The following averaging intervals are available:

- N/A: No averaging will be performed for the simulation. **Note:** the “N/A” interval corresponds to a model-default, 1-hour average
- 3 Hours: 3-hour averaging will be used for the processing of results
- 8 Hours: 8-hour averaging will be used for the processing of results
- 24 Hours: 24-hour averaging will be used for the processing of results
- Run Length: Averages will be calculated using the entire length of the simulation run

To set the averaging interval, select the desired interval from the “Averaging Interval” list found in the “Simulation Scenario” panel. If the averaging interval selected is greater than the “Run Duration,” a message box will be displayed explaining the time mismatch.

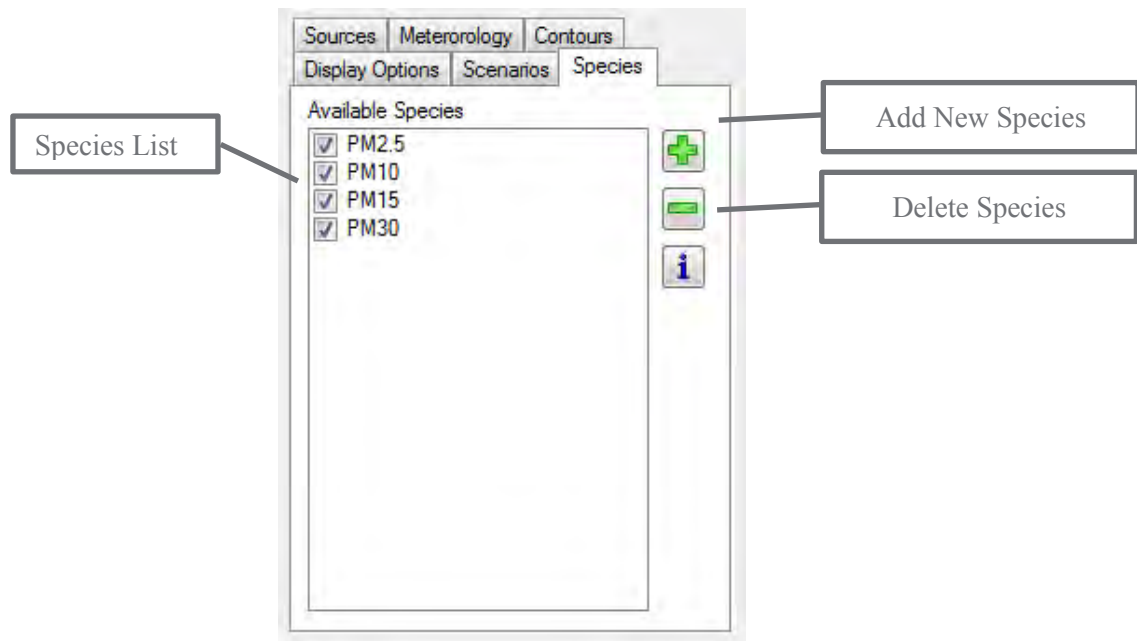
### 4.5 Species Tab

The “Species” tab is used to view, add, and delete species from the current model scenario. Species can be either particles or gases and their properties (diameter or molecular weight) can be set to allow for deposition calculations. Species that are “checked” are available for selection on all source forms when creating new or editing existing sources. Figure 4.5 shows an example of the “Species” tab with four species selected and the controls labeled.

#### 4.5.1 Selecting an Existing Species

Existing species that are available for selection in a simulation are shown in the “Available Species” list on the “Species” tab. Species that are selected will appear on each source’s “Release Parameter” form.

To select an existing species, check the box located to the left of the species. There are four default PM species—PM10, PM2.5, PM15, and PM30. The number after the PM designation represents the mean particle diameter, in microns. Emissions for these four particle size categories are calculated automatically by the dust-emission module within DUSTRAN. However, emission rates for user-specified species are not determined by DUSTRAN and must be entered directly for each source.



**Figure 4.5.** Example Species Tab


#### 4.5.2 Modifying an Existing Species

Existing species data can be modified. For example, the mean diameter for a particle or the molecular weight for a gas can be changed. To modify an existing species:

- Double-click on the name of the species in the “Available Species” list on the “Species” tab. The “Species Input Data” window will appear.
- To change the existing species, click “Yes.”
- Indicate whether the species is a gas by clicking “Yes” or particle by clicking “No.”
- If deposition calculations are desired, click “Yes”; otherwise click “No.” For deposition, the program will prompt for the species’ mean diameter (particle) or molecular weight (gas).

#### 4.5.3 Adding a New Species


New species, either particles or gases, can be added to a simulation. The species will then be available on each source’s “Release Parameter” form. To add a new species:

- Click the “Add”  button located on the “Species” tab. When prompted, enter a name for the new species.
- Next, indicate whether the species is a gas by clicking “Yes” or particle by clicking “No.”

If deposition calculations are desired, click “Yes”; otherwise click “No.” For deposition, the program will prompt for the species’ mean diameter in  $\mu\text{m}$  (particle) or molecular weight (gas).

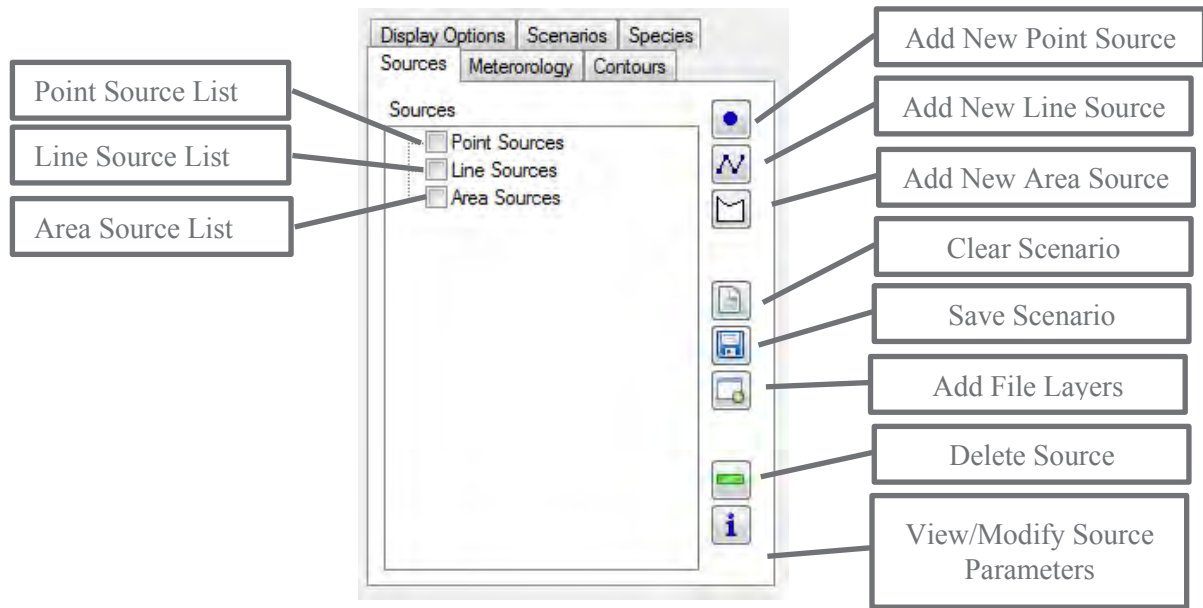
#### 4.5.4 Deleting an Existing Species

Existing species can be deleted from a simulation. Release information from existing sources for that species will also be deleted.

To delete a species, select the species from the list and click the “Delete”  button located on the “Species” tab.

#### 4.6 Sources Tab


The “Sources” tab is used to add, edit, and delete sources within DUSTRAN. In addition, the sources tab is used to associate characteristic data files, such as vegetation and soil texture layers, which are used by the DUSTRAN modeling system to generate gridded dust emissions for a model domain when simulating wind-blown dust. Various source types are available, including point, area, and line sources. Once a source has been created, it will appear on the source list within the “Sources” tab; each source appearing on the list can be edited and can be selected or deselected for use in the current simulation. Figure 4.6 shows an example “Sources” tab with the controls labeled and existing sources populated in the source list.



**Figure 4.6.** Example Sources Tab with Point, Line, and Area Sources Entered

##### 4.6.1 Adding a New Point Source

A point source, such as a stack emission, is modeled as a discrete point that can include the effects of plume rise due to buoyancy and momentum. A new point source can be added to a DUSTRAN simulation by doing the following:

- Click on the “Add New Point Source”  button. A prompt will appear directing the user to select a location in the MapWindow map display for the point source. Click “OK.”

- The mouse cursor will change to a crosshair; move the crosshair to the desired location for the point source on the map within MapWindow and click. Enter a name for the point source in the dialog box that appears and click “OK.”
- The point source will appear in the source list under “Point Sources” and will also be displayed within MapWindow.

A “Source Input” window will appear with two tabs—“Release Parameters” and “Coordinates.” “Release Parameters” are editable parameters that describe the release for the point source. “Coordinates” are the UTM easting and northing coordinates for the source and are not editable.

#### 4.6.1.1 Setting Point-Source Release Parameters

Once a new point source has been added or the name of an existing point source has been double-clicked on the “Sources” tab, the point “Source Input” window will be displayed. The “Release Parameters” tab is selected by default and is used to enter the characteristics of the point source, such as the stack diameter, release time period, and the emission rates of species emitted by the source. Figure 4.7 displays an example “Release Parameters” form for a point source.

The screenshot shows a dialog box titled "Source Input - Demo" with two tabs: "Release Parameters" (selected) and "Coordinates". The main content area is titled "Demo Source Parameters".

Parameters and their values:

- Height of release: 0 m
- Enable Stack Release Parameters
- Stack gas exit velocity: 0 m/s
- Stack gas exit temperature: 25 C
- Stack diameter: 1 m
- Building cross section: 0 m<sup>2</sup>
- Initial horizontal plume size: 1 m
- Initial vertical plume size: 1 m
- Start DateTime: 12/08/2014, 04:00 AM
- Duration: 2 Hours

Emission rates (g/s) table:

Specie	Emission Rate
PM2.5	0
PM10	0
PM15	0
PM30	0

Buttons: Ok, Cancel

**Figure 4.7.** Example Point-Source Input Window

The following input parameters are available on the “Release Parameters” tab for a point source:

- Height of release
- Stack gas exit velocity
- Stack gas exit temperature
- Stack diameter
- Building cross section
- Initial horizontal plume size
- Initial vertical plume size.

Default values are provided for each parameter. To change a parameter's value, click on the textbox and enter a value. For quality assurance, valid textbox entries will appear green and invalid textbox entries will appear red. A range of valid entries appears in the yellow label at the bottom of the form for a given textbox entry.

The point-source "Start Date," "Start Time," and "Duration" must also be entered on the "Release Parameter" tab. This is the date, time, and total period the source emits material in the simulation.


- Setting the point-source start date:
  - To enter the date manually, click on the month, day, or year portion of the date displayed in the control. Once the appropriate portion of the date has been selected, the new value can be entered. All values should be entered as integers and are automatically checked for correctness. In the case of the month, it will convert the integer to the appropriate month name abbreviation.
  - To enter the date using the calendar control, first click on the dropdown arrow. A calendar will be displayed for the date that is currently entered in the "Start Date" control. To change years, click on the year label within the calendar and click on the up (down) arrows to increment (decrement) by one year. To change months, click on the right or left arrow buttons located at the top of the calendar control. Clicking on the left (right) arrow buttons decreases (increases) the month by one. To select a day, click on the desired day within the calendar, and the calendar control will then close with the "Start Date" input box automatically updating to the new date.
- Setting the point-source start time:
  - Click the "Start Time" textbox and enter the hour value manually or by clicking on the increase or decrease arrow buttons found to the right of the input box. Clicking the up-arrow (down-arrow) will increase (decrease) the time by one hour. Start times are currently limited to hour increments, and any minutes are ignored.
- Setting the point-source duration:
  - Click the "Duration" textbox and enter an hour value manually or click on the increase or decrease arrow buttons found to the right of the input box. Clicking the up-arrow (down-arrow) will increase (decrease) the time by hourly intervals.

Emission rates for material being released from the point source are also entered on the "Release Parameters" tab. Emission rates can be set for several species (Note: Species are added in DUSTRAN through the "Species" tab [see Section 4.5].)

To set the point-source emission rates, click on the "Emission Rate" cell for a given "Species" and enter its emission rate. If an "Emission Rate" is labeled "Not Selected," the species must be activated on the "Species" tab in DUSTRAN. All emission rates are validated before closing the form.

#### 4.6.2 Adding a New Line Source

A line source, such as emissions from roadways, is modeled as a series of line segments in DUSTRAN. Line-source emissions can be entered explicitly or calculated automatically when using the vehicular dust-emissions module for simulating dust emission from paved or unpaved roadways. A new line source can be added to a simulation by doing the following:

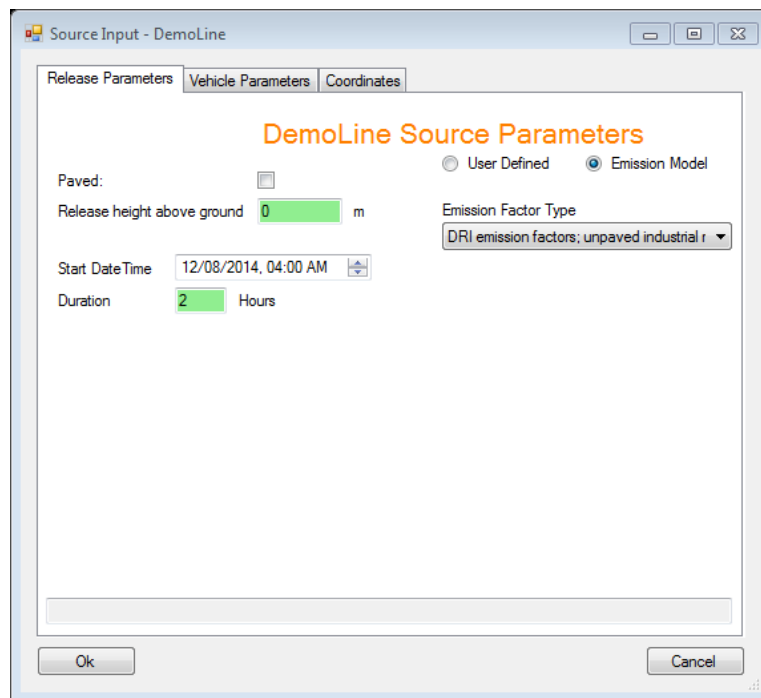
- Click on the "Line Source"  button. A prompt will appear directing the user to select a location in the MapWindow map display for the line source. Click "OK."

- The mouse cursor will change to a crosshair. The line source is drawn as a series of line segments. To create a line segment, click the mouse on the beginning and ending points of the segment. To complete the line source, double-click the mouse on the ending point of the last line segment. Enter a name for the line source in the dialog box that appears and click “OK.”
- The line source will appear in the source list under “Line Sources” and will also be displayed within MapWindow.

A “Source Input” window will appear with two tabs—“Release Parameters” and “Coordinates.” The “Release Parameters” tab contains editable parameters that describe the release for the line source. “Coordinates” are the UTM easting and northing coordinates for the source and are not editable. A third tab, called “Vehicle Parameters,” is available if the “Emission Model” option is selected on the “Release Parameters” tab. The “Vehicle Parameters” tab is used to enter characteristic vehicle information for the line-source dust-emissions model.

#### 4.6.2.1 Setting Line-Source Release Parameters

Once a new line source has been added or the name of an existing line source has been double-clicked on the “Sources” tab, the line “Source Input” window will be displayed. By default, the “Release Parameters” tab is selected and is used to enter characteristics of the line source, such as the release height above ground level. Figure 4.8 displays an example “Release Parameters” form for a line source with the “Emission Model” option selected.



**Figure 4.8.** Example Line-Source Input Window Using the User-Defined Emission Option

The “Release height above ground” setting is required for each line source and can include heights to accommodate elevated releases. For road emissions, the release height should be zero. To change the parameter’s value, click on the textbox and enter a value.

The line-source “Start Date,” “Start Time,” and “Duration” must also be entered on the “Release Parameter” tab. This is the date, time, and total period the source emits material in the simulation.

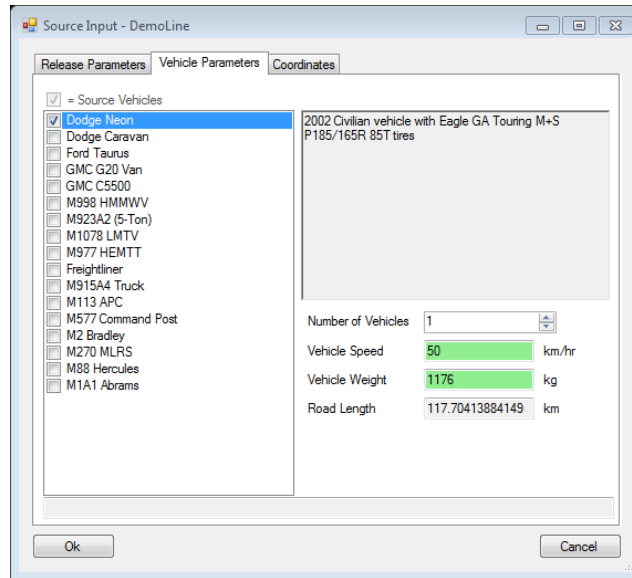
- Setting the line-source start date:
  - To enter the date manually, click on the month, day, or year portion of the date displayed in the control. Once the appropriate portion of the date has been selected, the new value can be entered. All values should be entered as integers and are automatically checked for correctness. In the case of the month, it will convert the integer to the appropriate month name abbreviation.
  - To enter the date using the calendar control, first click on the dropdown arrow. A calendar will be displayed for the date that is currently entered in the “Start Date” control. To change years, click on the year label within the calendar and click on the up (down) arrows to increment (decrement) by one year. To change months, click on the right or left arrow buttons located at the top of the calendar control. Clicking on the left (right) arrow buttons decreases (increases) the month by one. To select a day, click on the desired day within the calendar, and the calendar control will then close with the “Start Date” input box automatically updating to the new date.
- Setting the line-source start time:
  - Click the “Start Time” textbox and enter the hour value manually or by clicking on the increase or decrease arrow buttons found to the right of the input box. Clicking the up-arrow (down-arrow) will increase (decrease) the time by one hour. Start times are currently limited to hour increments, and any minutes are ignored.
- Setting the line-source duration:
  - Click the “Duration” textbox and enter an hour value manually or click on the increase or decrease arrow buttons found to the right of the input box. Clicking the up-arrow (down-arrow) will increase (decrease) the time by 15-minute intervals. Currently, the models simulate hour increments, and any minutes are ignored.

Emissions for line sources can either be “User Defined” or calculated by the “Emissions Model” using EPA AP-42 (EPA 2005) or DRI (Gillies et al. 2005a, 2005b) emission factors. Selecting “Emissions Model” causes the “Vehicles Parameters” tab to appear on the “Source Input” form (see “Setting Line Source Vehicle Parameters” for this option). If “User Defined” is selected, the emission rates can be entered directly on the “Release Parameters” tab. Emission rates can be set for several species (Note: species are added in DUSTAN through the “Species” tab [see Section 4.5].)

To set the line-source emission rates, click on the “Emission Rate” cell for a given “Species” and enter its emission rate. If an “Emission Rate” is labeled “Not Selected,” the species must be activated on the “Species” tab in DUSTAN. All emission rates are validated before closing the form.

#### **4.6.2.2 Setting Line-Source Vehicle Parameters**

The line-source “Vehicle Parameters” tab is activated on the line “Source Input” form by selecting “Emission Model” on the “Release Parameters” tab. The “Vehicle Parameters” tab is used to enter information about vehicles that will be traveling along the path of the line source. This information, which is used to calculate road dust emissions generated by vehicle traffic, includes the types of vehicles as well as their speed, weight, and the distance traveled. The particulate emission factors for wheeled vehicles operating on unpaved roads are empirically derived functions described in Section 2.3.1. Two calculation options are available: emissions using factors formulated by DRI (Gillies et al. 2005a, 2005b), or emissions using factors calculated using EPA AP-42 recommendations (EPA 2005). Figure 4.9 shows the “Vehicle Parameters” form for a sample line source with vehicles selected.



**Figure 4.9.** Example Vehicle Input Window for a Line Source

A vehicle is used as an emission source by checking the box next to the vehicle’s name. By clicking on a vehicle’s name, a description of the vehicle is given in the “Vehicle Description” box and a set of input parameters for the vehicle is displayed. The vehicle-specific input parameters include:

- Number of Vehicles
- Vehicle Speed
- Vehicle Weight
- Road Length (non-editable—calculated by the interface).

As discussed in Section 2.2.2.5, DUSTRAN does not treat the motion of individual vehicles. Instead, a bulk approach is used to quantify dust emissions from vehicle activities. That is, the dust emissions from all vehicles active on a road over a specified time are assumed to be released uniformly from the road at a constant rate throughout the duration of the activity. Therefore, the input fields on the “Vehicle Parameters” form (Figure 4.9) should not be interpreted as the specific motion of individual vehicles; the form is simply an approach for providing the information needed by DUSTRAN in a bulk sense.


The approach for determining the input required on the “Vehicle Parameters” form (Figure 4.9) is to first estimate the total distance traveled along the road for all vehicles within a given vehicle type throughout the duration of the activity and then divide this total distance traveled by the road length to get the total effective “Number of Vehicles” on the form (Figure 4.9). Since the number of vehicles must be entered as a whole number, it is recommended that any fractional vehicles be rounded up to err on the side of conservatism in the dust emissions estimated from the vehicle activities. The only constraint on the inputs on the form is that the effective number of vehicles  $\times$  vehicle speed  $\times$  activity duration be greater than the road length.

As described in Section 2.3.1, the dust emissions from a moving vehicle are proportional to the vehicle momentum (i.e., vehicle weight  $\times$  vehicle speed). Therefore, if some vehicles of one type travel at significantly different speeds than other vehicles of the same type, another vehicle type will need to be added to the list such that the other speed(s) can be specified.

For quality assurance, valid textbox entries will appear green and invalid textbox entries will appear red. A range of valid entries appears in the yellow label at the bottom of the form for a given textbox entry.

### 4.6.3 Adding a New Area Source

An area source, such as emissions from vehicles randomly crossing an off-road region, is modeled as a three- or four-sided polygon in DUSTRAN. Area-source emissions can be entered explicitly or calculated automatically when using the vehicular dust-emissions module for simulating dust emissions from paved or unpaved roadways. A new area source can be added to a simulation by doing the following:

- Click on the “Area Source”  button. A prompt will appear directing the user to select a location in the MapWindow map display for the area source. Click “OK.”
- The mouse cursor will change to a crosshair. To create the area source, click the mouse at three or four points, depending on whether you want a triangle or a four-sided polygon. On the last point, double-click the mouse to complete the area source. Enter a name for the area source in the dialog box that appears and click “OK.”
- The area source will appear in the source list under “Area Sources” and will also be displayed within MapWindow.

A “Source Input” window will appear with two tabs—“Release Parameters” and “Coordinates.” The “Release Parameters” tab contains editable parameters that describe the release for the area source. “Coordinates” are the UTM easting and northing coordinates for the four corners of the area source and are not editable. A third tab, called “Vehicle Parameters,” is available if the “Emissions Model” option is selected on the “Release Parameters” tab. The “Vehicle Parameters” tab is used to enter characteristic vehicle information for the area-source dust-emissions model.

#### 4.6.3.1 Setting Area-Source Release Parameters

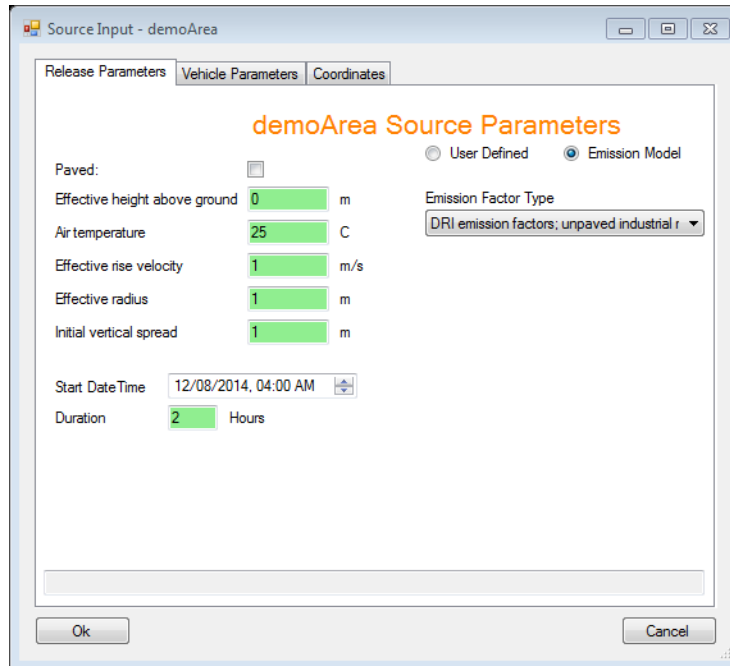
Once a new area source has been added or the name of an existing area source has been double-clicked on the “Sources” tab, the area “Source Input” window will be displayed. By default, the “Release Parameters” tab is selected and is used to enter characteristics of the area source, such as the effective release height above ground level. Figure 4.10 displays an example “Release Parameters” form for an area source with the “User-Defined” emissions option selected.

The following input parameters are available on the “Release Parameters” tab for an area source:

- Effective height above ground
- Air temperature
- Effective rise velocity
- Effective radius
- Initial vertical spread.

Default values are provided for each parameter. To change a parameter’s value, click on the textbox and enter a value. For quality assurance, valid textbox entries will appear green and invalid textbox entries will appear red. A range of valid entries appears in the yellow label at the bottom of the form for a given textbox entry.

The area-source “Start Date,” “Start Time,” and “Duration” must also be entered on the “Release Parameter” tab. This is the date, time, and total period the source emits material in the simulation.



**Figure 4.10.** Example Area-Source Input Window Using the User-Defined Emission Option

- Setting the line-source start date:
  - To enter the date manually, click on the month, day, or year portion of the date displayed in the control. Once the appropriate portion of the date has been selected, the new value can be entered. All values should be entered as integers and are automatically checked for correctness. In the case of the month, it will convert the integer to the appropriate month name abbreviation.
  - To enter the date using the calendar control, first click on the dropdown arrow. A calendar will be displayed for the date that is currently entered in the “Start Date” control. To change years, click on the year label within the calendar and click on the up (down) arrows to increment (decrement) by one year. To change months, click on the right or left arrow buttons located at the top of the calendar control. Clicking on the left (right) arrow buttons decreases (increases) the month by one. To select a day, click on the desired day within the calendar, and the calendar control will then close with the “Start Date” input box automatically updating to the new date.
- Setting the line-source start time:
  - Click the “Start Time” textbox and enter the hour value manually or by clicking on the increase or decrease arrow buttons found to the right of the input box. Clicking the up-arrow (down-arrow) will increase (decrease) the time by one hour. Start times are currently limited to hour increments, and any minutes are ignored.
- Setting the line-source duration:
  - Click the “Duration” textbox and enter an hour value manually or click on the increase or decrease arrow buttons found to the right of the input box. Clicking the up-arrow (down-arrow) will increase (decrease) the time by 15-minute intervals. Currently, the models simulate hour increments, and any minutes are ignored.

Emissions for area sources can either be “User Defined” or calculated by the “Emissions Model” using EPA AP-42 (EPA 2005) or DRI (Gillies et al. 2005a, 2005b) emission factors. Selecting “Emissions Model” causes the “Vehicles Parameters” tab to appear on the “Source Input” form (see “Setting Area

Source Vehicle Parameters” for this option). If “User Defined” is selected, the emission rates can be entered directly on the “Release Parameters” tab. Emission rates can be set for several species (Note: Species are added in DUSTRAN through the “Species” tab [see Section 4.5]).

To set the area-source emission rates, click on the “Emission Rate” cell for a given “Species” and enter its emission rate. If an “Emission Rate” is labeled “Not Selected,” the species must be activated on the “Species” tab in DUSTRAN. All emission rates are validated before closing the form.

#### 4.6.3.2 Setting Area-Source Vehicle Parameters

The area-source “Vehicle Parameters” tab is activated on the area “Source Input” form by selecting “Emission Model” on the “Release Parameters” tab. The “Vehicle Parameters” tab is used to enter information about vehicles that will be traveling within the area source. This information, which is used to calculate road dust emissions generated by the vehicles, includes the types of vehicles as well as their speed, weight, and the distance traveled. The particulate emission factors for wheeled vehicles operating on unpaved roads are empirically derived functions described in Section 2.3.1. Two calculation options are available: emissions using factors formulated by DRI (Gillies et al. 2005a, 2005b) or emissions using factors based on EPA’s AP-42 recommendations (EPA 2005). Figure 4.11 shows the “Vehicle Parameters” form for a sample area source with vehicles selected.

Vehicle	Description	Number of Vehicles	Vehicle Speed	Vehicle Weight	Polygon Area	Distance Traveled
<input checked="" type="checkbox"/> Dodge Neon	2002 Civilian vehicle with Eagle GA Touring M+S P185/165R 85T tires	1	50 km/hr	1176 kg	274.105186267334 km <sup>2</sup>	0 km
<input type="checkbox"/> Dodge Caravan						
<input type="checkbox"/> Ford Taurus						
<input type="checkbox"/> GMC G20 Van						
<input type="checkbox"/> GMC C5500						
<input type="checkbox"/> M998 HMMWV						
<input type="checkbox"/> M923A2 (5-Ton)						
<input type="checkbox"/> M1078 LMTV						
<input type="checkbox"/> M977 HEMTT						
<input type="checkbox"/> Freightliner						
<input type="checkbox"/> M915A4 Truck						
<input type="checkbox"/> M113 APC						
<input type="checkbox"/> M577 Command Post						
<input type="checkbox"/> M2 Bradley						
<input type="checkbox"/> M270 MLRS						
<input type="checkbox"/> M88 Hercules						
<input type="checkbox"/> M1A1 Abrams						

**Figure 4.11.** Example Vehicle Input Window for an Area Source

A vehicle is used as an emission source by checking the box next to the vehicle’s name. By clicking on a vehicle’s name, a description of the vehicle is given in the “Vehicle Description” box, and a set for vehicle input parameters is displayed. The vehicle-specific input parameters include:

- Number of Vehicles
- Vehicle Speed
- Vehicle Weight
- Polygon Area (non-editable—calculated by the interface)
- Distance Traveled (by one vehicle during the duration of the release).

As discussed in Section 2.2.2.5, DUSTRAN does not treat the motion of individual vehicles. Instead, a bulk approach is used to quantify dust emissions from vehicle activities. That is, the dust emissions from all vehicles active in an area over a specified time are assumed to be released uniformly from the area at a constant rate throughout the duration of the activity. Therefore, the input fields on the “Vehicle Parameters” form (Figure 4.11) should not be interpreted as the specific motion of individual vehicles; the form is simply an approach for providing the information needed by DUSTRAN in a bulk sense.

The approach for determining the distance traveled by a vehicle within a specific vehicle type (specific weight and speed) is to estimate the total distance traveled for all vehicles within a vehicle type throughout the duration of the activity and then divide this total distance traveled by the total number of vehicles within a vehicle type to get the average distance traveled for one vehicle. This average value is the distance traveled specified in the input window (Figure 4.11). The only constraint on the inputs to the window is that the average distance traveled for one vehicle not be greater than the vehicle speed  $\times$  activity duration. It is probable that the distance traveled will be less than the vehicle speed  $\times$  activity duration because of the likelihood that not all vehicles of a particular type will be active during the entire period. For example, some vehicles may move intermittently (at their specified speed) during the period because of their particular function.

As described in Section 2.3.1, the dust emissions from a moving vehicle are proportional to the vehicle momentum (i.e., vehicle weight  $\times$  vehicle speed). Therefore, if some vehicles of one type travel at significantly different speeds than other vehicles of the same type, another vehicle type will need to be added to the list such that the other speed(s) can be specified.


For quality assurance, valid textbox entries will appear green and invalid textbox entries will appear red. A range of valid entries appears in the yellow label at the bottom of the form for a given textbox entry.

#### **4.6.4 Selecting Existing Sources to Use in a Simulation**

Multiple point, area, and line sources can be created for use in a simulation. After a source has been created, it will appear in a list on the “Sources” tab. To use the source in a simulation:


- Check the checkbox next to the name of the source. The source will be displayed in the MapWindow map display and will be used in the model simulation.
- Check the checkbox next to that source type to select all sources for a particular source type (i.e., point, line, or area).

#### **4.6.5 View and Edit Existing Source Information**


Existing point, line, and area sources appear in a source list on the “Sources” tab. To view and edit the input parameters for a particular source, double-click on the source’s name or highlight the source name and click on the “Information”  button. The “Source Input” form for that particular source will appear and can be reviewed and edited.

#### **4.6.6 Deleting an Existing Source**


Existing point, line, and area sources appear in the source list on the “Sources” tab. To permanently delete a source and its corresponding source information so that it is no longer available for use in a

simulation, highlight the source's name and click on the "Delete"  button. The source will be removed from the simulation and from the MapWindow map display.

#### 4.6.7 Clearing All Existing Sources

Existing point, line, and area sources appear in the source list on the "Sources" tab. To permanently delete all sources and corresponding source information so that they are no longer available in the current simulation, click on the "New Scenario"  button. The sources will be removed from the simulation and from the MapWindow map display.


#### 4.6.8 Saving Existing Sources as a Scenario

Sources can be saved to a scenario that allows for the sources to be added to a simulation at a later time using the "Scenario" tab. A scenario is usually created after all sources and source parameters have been entered. To save the sources as a new scenario, click the "Save Scenario"  button. The scenario will also be added to the scenarios list, indicating that it is available for selection at a later time.

#### 4.6.9 Adding Characteristic Files (Soil and Vegetation for Wind-blown Dust)

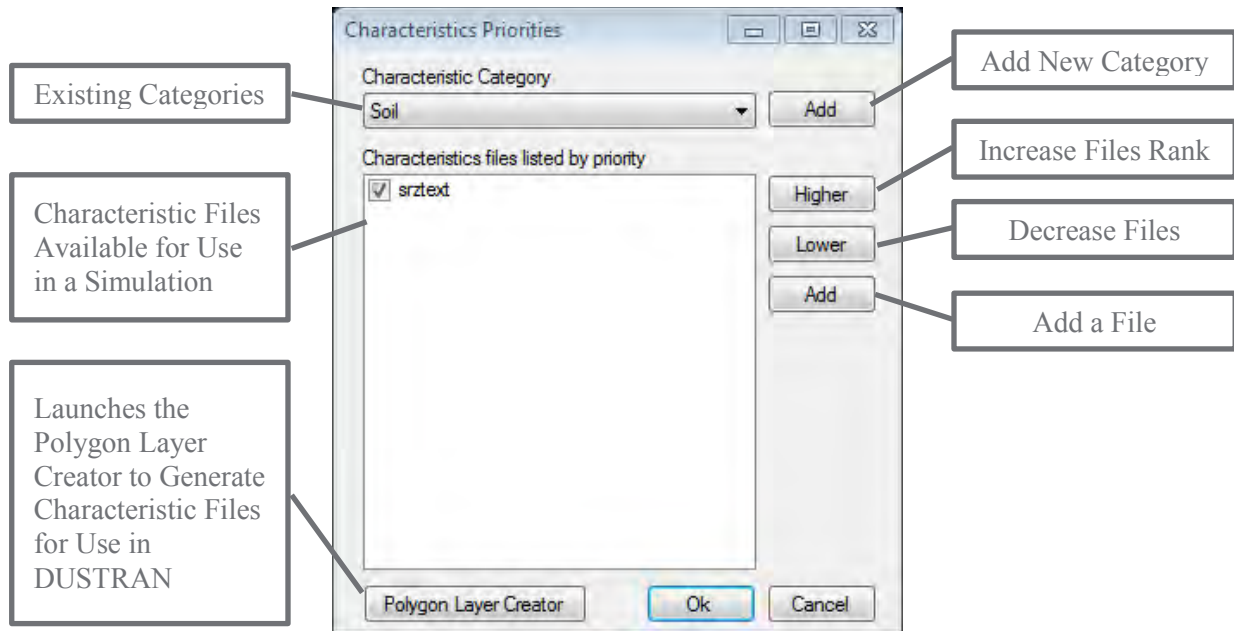
Soil and vegetation files that use the Zobler soil textures and Olson vegetation classes to characterize the underlying domain can be added to DUSTRAN for use in a "Wind-blown Dust" simulation. These files are created automatically at the time of the site's creation (see "Adding a New User Profile to DUSTRAN," Section 6.0) and must be associated with the scenario when performing a "Wind-blown Dust" simulation. Alternatively, high-resolution soil and vegetation data files can be generated from Environmental System Research Institute shape files using the "Polygon Layer Creator" discussed in Section 5.0. These detailed files can be used to more precisely define the underlying soil and vegetative surface characteristics for use in the wind-blown dust-emissions model.

To associate soil and vegetation characteristic files for use in a "Wind-blown Dust" simulation:

- Click the "Add Characteristic File"  button. The "Characteristics Priorities" form, as shown in Figure 4.12, will appear. This form allows for files from the "Polygon Layer Creator" (see Section 5.0, "Polygon Layer Creator") to be associated with the current scenario. Currently, two categories—Soils and Vegetation—are predefined and contain references to the standard Zobler soil texture and Olson Ecosystem class files created by the "Add Site" wizard within DUSTRAN.
- Click the "Add," "Higher," or "Lower" buttons for a given category to add a new characteristic file or to increase or decrease the file's usage priority. Generally, high-resolution files should be ranked higher in the list. A checkbox next to a file's name means the file will be used in the current simulation.
- Click "OK" to save the characteristic file selections or "Cancel" to ignore the most recent changes.

The "Polygon Layer Creator" button is used to launch the Polygon Layer Creator. This application allows for either manual or automatic (through Environmental System Research Institute shape files) creation of characteristic files for use in DUSTRAN (see Section 5.0, "Polygon Layer Creator"). Although the existing soils and vegetation classification files are sufficient for running a "Wind-blown Dust" simulation in DUSTRAN, higher-resolution files can be associated with each category to provide

better resolution. These files can be created within the “Polygon Layer Creator” tool, either manually or through user-specified shape files that use Zabler or Olson classification schemes.




**Figure 4.12.** Characteristics Priorities Dialog Box for Adding Files, such as Soil and Vegetation Classes, in DUSTAN

## 4.7 Scenarios Tab

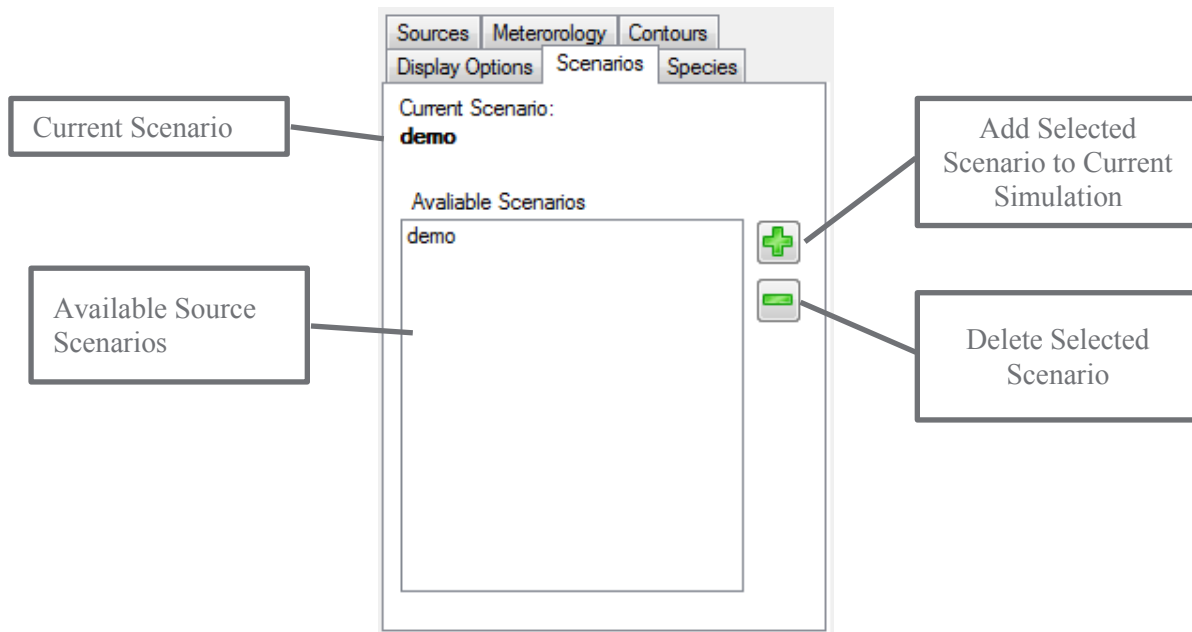
The “Scenarios” tab is used to open or delete an existing scenario from the simulation. A scenario contains previously saved source information, including each source’s location and parameter settings. A scenario gets created from the “Sources” tab (Note: To create a scenario, see Section 4.6, “Sources Tab”). When selected, the “Scenarios” tab displays the current scenario name as well as a list of currently available scenarios for the site. Figure 4.13 shows the “Scenarios” tab with an example scenario entered.

### 4.7.1 Adding an Existing Scenario

Previously saved sources (i.e., a scenario) can be opened for use in the current model simulation. To open a scenario:

- Click on the “Scenarios” tab. Highlight the scenario you wish to add by clicking on its name (Note: If no sources have been previously saved as a scenario, there will be no scenarios available in the list).
- Click the “Add Scenario”  button, and the scenario will be added to the simulation. All sources in the scenario will be listed on the “Sources” tab and displayed in MapWindow.


Multiple scenarios can be added to a simulation by following the steps above.



**Figure 4.13.** Example Scenario Tab with Controls Labeled

## 4.7.2 Deleting an Existing Scenario

Deleting a scenario permanently deletes all source and source-parameter information stored in that scenario from the site. Once the scenario is deleted from the site, it is no longer available for use in future simulations. To delete a scenario:

- Click on the “Scenarios” tab. Highlight the scenario you wish to delete by clicking on its name.
- Click the “Delete Scenario”  button, and the scenario will be deleted from the list.

## 4.8 Meteorology Tab

The “Meteorology” tab is used to select the surface and upper-air meteorological data sources for use in a simulation. Two options exist for specifying the meteorological data source in DUSTAN:

- Single Observation—for specifying meteorological conditions on a form within the DUSTAN interface. These observations are for a single location (center of the domain) and persist for the duration of the simulation.
- User Defined—for specifying preformatted CALMET surface and upper-air observation files for direct use in DUSTAN.

Each of these options is discussed further in the following sections.

### 4.8.1 Selecting Single Observation Meteorology

Single meteorological observation data can be used for any of the available simulation types by selecting “Single Observation” from the “Use” list on the “Meteorology” tab. A form will appear, allowing for the entry of standard meteorological parameters that apply to a single point on the domain (i.e., the center of the domain). The single observation data input form displayed will allow for the entry of meteorological

data for each hour of the simulation. Single observation data required by a simulation will vary depending upon the simulation type selected with AERMOD simulations requiring different inputs than the CALPUFF or CALGRID models. Figure 4.14 and Figure 4.15 provide examples of the meteorological input forms used for CALPUFF and AERMOD, respectively.

Simulation Hour	Year	Month	Day	Hour	Wind Direction (deg)	Wind Speed (m/s)	Temperature (C)	Relative Humidity (%)	Station Pressure (mb)	Mixing Height (m)	Stability
1	2014	12	9	5	270	2.2	10	50	1010	100	E - Slightly Stable
2	2014	12	9	6	270	2.2	10	50	1010	100	E - Slightly Stable
3	2014	12	9	7	270	2.2	10	50	1010	100	E - Slightly Stable
4	2014	12	9	8	270	2.2	10	50	1010	100	E - Slightly Stable

**Figure 4.14.** Example Meteorological Data Input Form for a CALPUFF simulation

Simulation Hour	Year	Month	Day	Hour	Wind Direction (deg)	Wind Speed (m/s)	Temperature (C)	Relative Humidity (%)	Station Pressure (mb)	Total Sky Cover (tenths)	Measurement Height (m)	Ceiling Height (ft)
1	2014	12	9	5								
2	2014	12	9	6								
3	2014	12	9	7								
4	2014	12	9	8								

**Figure 4.15.** Example Meteorological Data Input Form for an AERMOD simulation

To use a single observation in a DUSTRAN simulation:

- Select “Single Observation” from the “Meteorology” tab.
- Enter the meteorological observations on the “Specify Meteorological Data” form and then click “OK” to continue.
- Data entered into the form may be saved out to a .csv file using the “Save CSV” option.
- Data saved from an earlier simulation may be loaded into the form using the “Load CSV File” option.

For each simulation using the AERMOD model, surface characteristic data must be entered along with the meteorological data. Clicking on the “Surface Characteristics” tab of the “Specify Meteorological Data” form will display the “Surface Characteristics” input panel. Figure 4.16 is an example of the “Surface Characteristics” form with data entered. Segments within the form are used to define the different land-use surface characteristics associated with the simulation site. The number of segments that need to be filled depends on the site; the form allows for multiple segments or an individual segment that defines the entire simulation area. While the form allows any number of segments to be entered, enough segments must be entered to cover 360 degrees. The chart at the top of the form displays the segments and their degrees of coverage as they are entered by the user. Besides allowing the user to enter values directly into the form, data can also be entered by using lookup tables. The first method of accessing the lookup table is to click on the data box with the right button of the mouse, which brings up a menu version of the lookup table data. The second is to click on the “Lookup Tables” button, which will display the complete lookup tables in a separate form. Figure 4.17 shows an example lookup table. Clicking on a value in either of these lookup tables will automatically place the value in the input form.

Sector Name	Albedo	Bowen Ratio	Surface Roughness (m)	Start Degree	End Degree
one	0.18	1	0.2	0	180
two	0.16	0.3	1.3	180	270
three	0.14	0.3	1.3	270	360

**Figure 4.16.** AERMOD Surface Characteristics Input Form

Soil Parameter Lookup Tables

Albedo Bowen Ratio Surface Roughness

Class Number	Class Name	1	2	3	4	5
	Seasonal Albedo Values	1	2	3	4	5
11	Open Water	0.1	0.1	0.1	0.1	0.1
12	Perennial Ice/Snow	0.6	0.6	0.7	0.7	0.6
21	Low Intensity Residential	0.16	0.16	0.18	0.45	0.16
22	High Intensity Residential	0.18	0.18	0.18	0.35	0.18
23	Commercial/Industrial/Transp (Site at Airport)	0.18	0.18	0.18	0.35	0.18
23	Commercial/Industrial/Transp (Not at Airport)	0.18	0.18	0.18	0.35	0.18
31	Bare Rock/Sand/Clay (Arid Region)	0.2	0.2	0.2	NA	0.2
31	Bare Rock/Sand/Clay (Non-arid Region)	0.2	0.2	0.2	0.6	0.2
32	Quarries/Strip Mines/Gravel	0.2	0.2	0.2	0.6	0.2
33	Transitional	0.18	0.18	0.18	0.45	0.18
41	Deciduous Forest	0.16	0.16	0.17	0.5	0.16
42	Evergreen Forest	0.12	0.12	0.12	0.35	0.12
43	Mixed Forest	0.14	0.14	0.14	0.42	0.14
51	Shrubland (Arid Region)	0.25	0.25	0.25	NA	0.25
51	Shrubland (Non-arid Region)	0.18	0.18	0.18	0.5	0.18
61	Orchards/Vineyards/Other	0.18	0.18	0.18	0.5	0.14
71	Grasslands/Herbaceous	0.18	0.18	0.2	0.6	0.18
81	Pasture/Hay	0.2	0.2	0.18	0.6	0.14
82	Row Crops	0.2	0.2	0.18	0.6	0.14
83	Small Grains	0.2	0.2	0.18	0.6	0.14
84	Fallow	0.18	0.18	0.18	0.6	0.18
85	Urban/Recreational Grasses	0.15	0.15	0.18	0.6	0.15
91	Woody Wetlands	0.14	0.14	0.14	0.3	0.14
*	Emergent Herbaceous Wetlands	0.14	0.14	0.14	0.3	0.14

Close

Figure 4.17. Surface Characteristics Lookup Table

#### 4.8.2 Selecting User-Defined Meteorology

User-defined meteorological data can be used in a CALPUFF or CALGRID simulation by selecting “User Defined” from the “Use” list on the “Meteorology” tab. This option requires the surface and upper-air meteorological data to already exist and to be in the correct format for CALMET. Specifically, the user must have created the CALMET surface (SURF.dat) and upper-air (UP.dat) files using a processing utility exterior to the DUSTRAN interface. For more information on the format of the meteorological input files and processing utilities for CALMET, refer to “A User’s Guide for the CALMET Meteorological Model” (Scire et al. 2000b). **Note:** this option is not available for simulations using AERMOD.

To associate existing CALMET-ready meteorological data files with DUSTRAN, two files must be created—a .snf (surface) and a .unf (upper-air) file. These are DUSTRAN-specific files and contain station metadata, such as station name, ID, and coordinate location. To create a .snf and .unf to associate with existing CALMET SURF.dat and UP.dat files:

- Select “User Defined” from the “Meteorology” tab.
- Click the “Change Met Input Directory” to specify the directory where the CALMET-ready SURF.dat and UP.dat data files reside.
- Click on the “Edit Met Files” button. Select the “Surface Stations” tab and enter each station’s Name, ID, Longitude, Latitude, Elevation, and UTM Easting and Northing coordinates. Note that the station ID must agree with the station ID(s) specified in the CALMET-ready SURF.dat file.

- Select the “Upper Air Stations” tab and enter each station’s Name, ID, Longitude, Latitude, Elevation, and UTM Easting and Northing coordinates. Note that the station ID must agree with the station ID(s) specified in the CALMET-ready UP.dat file.
- Click “OK” on the “Edit Met Station Data” form.

Figure 4.18 shows a sample “Surface Stations” tab that is used to specify the station information that is associated with the CALMET-ready SURF.dat file. The “Upper Air Stations” tab (not shown) is a similar form for entering upper-air station information that is associated with the CALMET-ready UP.dat files.

ID	Name	Longitude (dec degrees)	Latitude (dec degrees)	Elevation (m)	UTM E (km)	UTM N (km)	Anem. Height (m)
K27U	K27U-Salmon	45.1833333	-113.9	1210	743.5463767	5007.9927245	10
K2U7	K2U7-Stanley- S	44.2083334	-114.9344445	1952	665.0245483	4897.086969	10
K4SV	K4SV-Strevell	42.0166667	-113.25	1612	810.5083939	4658.4333323	10
K77M	K77M-Malta	42.3166666	-113.3333333	1375	802.1739885	4691.4503698	10
KBOI	KBOI-Boise- Boi	43.5666667	-116.2405555	871	561.3292778	4824.025429	10
KBYI	KBYI-Burley- Bu	42.5425	-113.7713889	1265	765.1149966	4715.0655207	10
KCOE	KCOE-Coeur d	47.7666667	-116.8166667	707	513.737395	5290.3830002	10
KEUL	KEUL-Caldwell-	43.6333333	-116.6333334	741	529.5776149	4831.2145962	10
KIDA	KIDA-Idaho Fall	43.5208333	-112.0661112	1445	898.7655678	4830.4933417	10
KJER	KJER-Jerome- Je	42.7266666	-114.4572222	1234	708.1794794	4733.5977235	10

**Figure 4.18.** Sample “Surface Stations” Tab for Specifying CALMET-Ready Station Locations in DUSTAN

## 4.9 Contours Tab

The “Contours” tab is used to select the contours of interest to view for a given emission type and time period after completing a simulation in AERMOD, CALPUFF, or CALGRID. Various contour types can be displayed, including concentration, exposure (i.e., time-integrated concentration), deposition, and total deposition for the simulated averaging period. Contours can be animated over the simulated period to provide a dynamic perspective of the plume advection and diffusion pattern. Figure 4.19 displays an example of the “Contours” tab following a simulation run.

### 4.9.1 Setting the Contour Type

After completing a simulation, various contour types are available for display in the MapWindow map display. To display the contour type of interest, select the “Contours” tab and select the desired “Contour Type” from the listbox. The dispersion model that generated the contours precedes the contour type name. Contour types include:

- “Conc”—the average air concentration. If “Conc” is followed by “AVG” and an integer value, then the concentration is for the averaging period defined by the integer.
- “Dep”—the average deposition. If “Dep” is followed by “AVG” and an integer value, then the deposition is for the averaging period defined by the integer.
- “Exp”—the total exposure (i.e., time-integrated concentration).
- “TotalDep”—the total accumulated deposition.

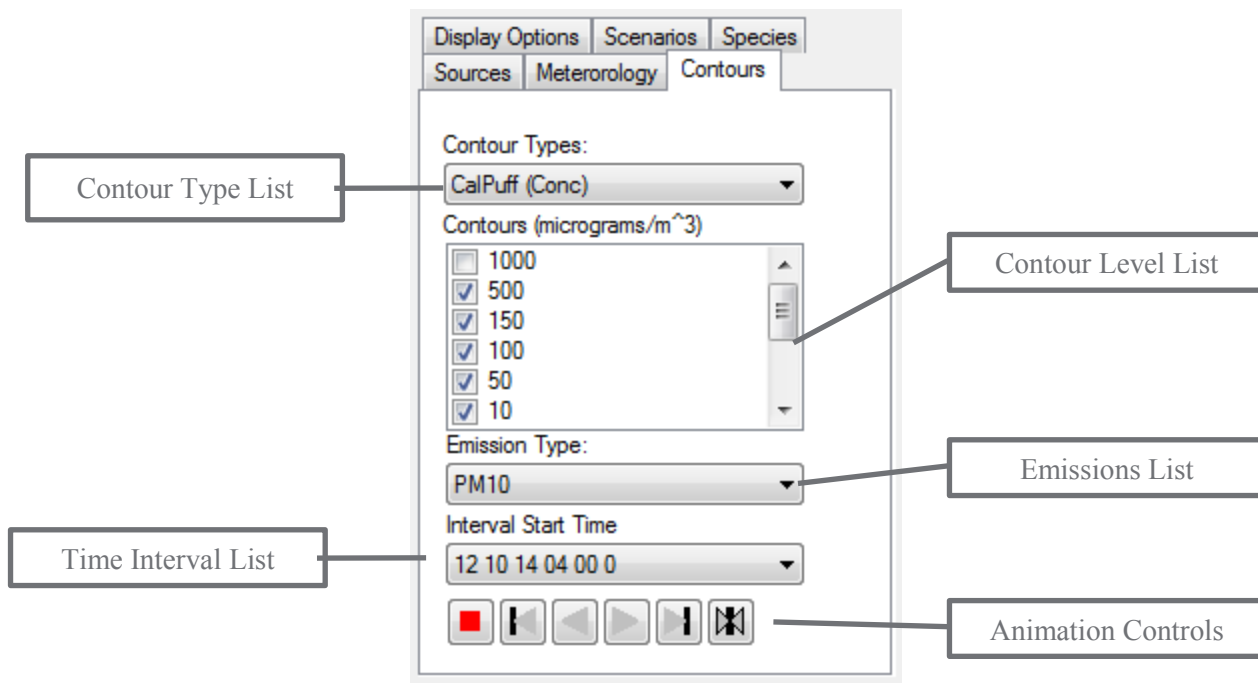


Figure 4.19. Example Contours Tab with Controls Labeled

#### 4.9.2 Selecting Contour Levels

After completing a simulation, various contour levels are available for display. In general, these levels span many orders of magnitude to allow the user to clearly define the concentration or deposition footprint for a given scenario. To view the contour levels, select the “Contours” tab and check the desired levels within the “Contours” list to be displayed in the MapWindow map display. Uncheck any levels to remove them from display in the MapWindow map display. Typically, a plume ground-level footprint can reasonably be described over a range of 3-to-5 orders of magnitude. Displaying more than 5 orders of magnitude is primarily used to evaluate the model computations rather than having any semblance to a real plume. The number of contour levels and values of contour levels computed by DUSTRAN are specified in the Cal.par file described in Section A.2. Currently, DUSTRAN is set up for computing a concentration range spreading 12 orders of magnitude, which reasonably brackets expected concentrations over a range of emission and dispersion rates.

#### 4.9.3 Selecting Emission Type

After completing a simulation, contours for a given emission type are available for display. The available emission type(s) correspond to the species selected on the “Species” tab before the model simulation. To set the emission type to display, click on the “Contours” tab and select a desired species from the “Emission Type” listbox. The contours for that particular emission type will be displayed in the MapWindow map display.







#### 4.9.4 Selecting Interval Start Time

After completing a simulation, concentration and deposition contours can be displayed for any hourly time interval in the simulated period. To view the results for a particular time interval, select the “Contours” tab and choose the desired time interval from the “Interval Start Time” listbox. The listed

times are in the following format: mm dd yy hh min sec, where mm is month, dd is day, yy is year, min is minutes, and sec is seconds. Averaged hourly results are referenced to the beginning of the “Interval Start Time.” For example, to view the 0900 to 1000 hourly average concentration, select 0900 from the interval listbox.

#### 4.9.5 Animating Contours

After completing a simulation, the displayed contours can be animated within the MapWindow map display to provide a dynamic perspective of the concentration or deposition pattern in time. The “Contours” tab contains a series of buttons to control the animation for the simulation. Figure 4.20 displays the animation control with each button labeled. The buttons (from left to right, in Figure 4.20) perform the following functions:

- Stop : Stops the current animation at a given interval time step.
- Reset : Resets the contour animation to the first time step in the simulation.
- Back : Steps the contour animation back one time interval.
- Forward : Advances the contour animation one time interval.
- Run Once : Runs contour animation once, sequentially displaying each interval in the simulation once.
- Loop : Continuously loops the contour animation.

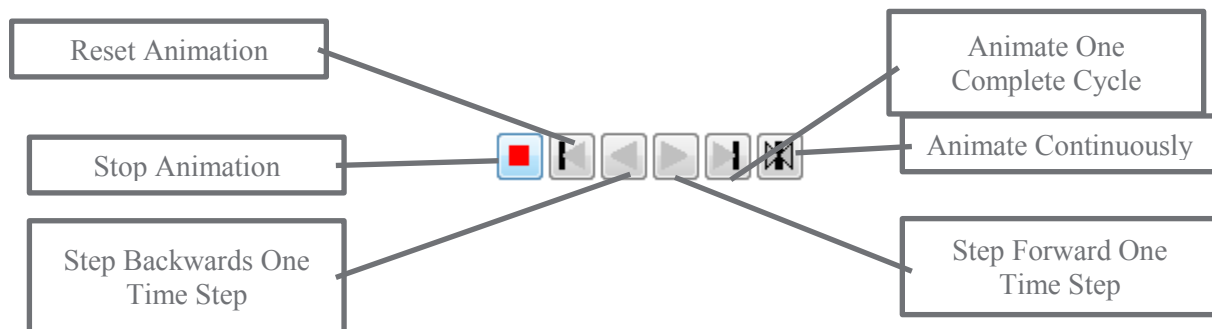
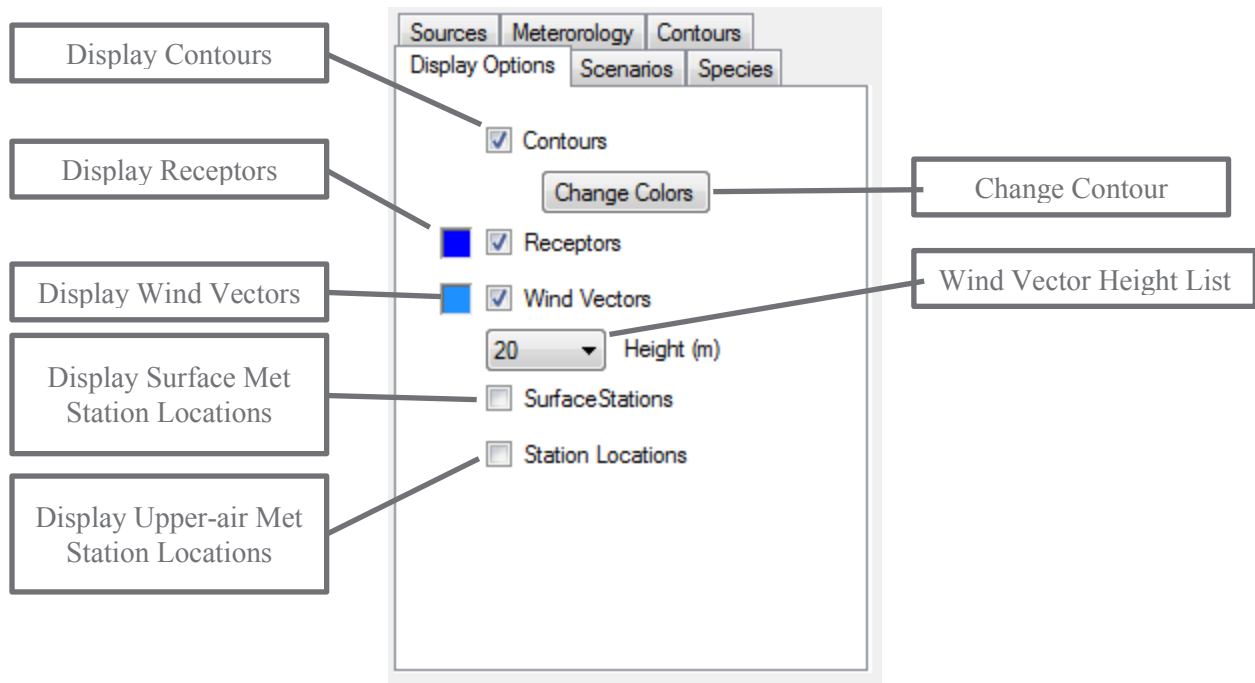


Figure 4.20. Animation Control with Buttons Labeled

#### 4.10 Display Options Tab

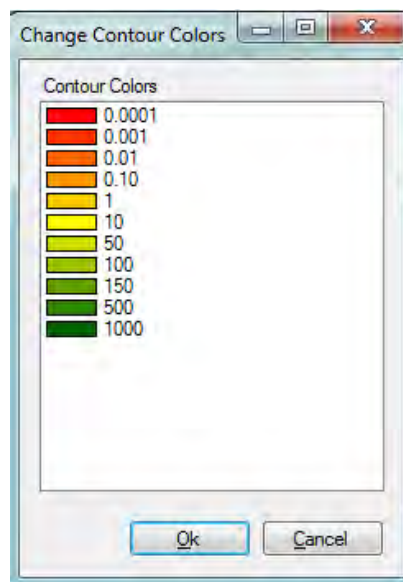
The “Display Options” tab allows for controlling the rendering of certain items within the MapWindow map display, including contours, receptors, wind vectors, surface meteorological stations, and upper-air station locations. In addition, the appearance, such as the symbol size, shape, or color, for some of the items can be adjusted. This tab is usually visited after making a DUSTRAN simulation to control which objects to display in the MapWindow map display. Figure 4.21 is an example of the “Display Options” tab showing the available items for displaying in MapWindow after completing a simulation. The various “Display Options” are described in the following sections.



**Figure 4.21.** Display Options Tab

#### 4.10.1 Displaying the Contour Results

The contours generated by the simulation can be viewed in the MapWindow map display by clicking on the checkbox labeled “Contours” on the “Display Options” tab. The colors used to display the different contouring levels can be changed by clicking on the “Change Colors” button which will bring up the “Change Contour Colors” form (See Figure 4.22). Clicking on the desired contour level will then cause a color selection form to appear which can be used to change the display color of the selected contour level.



**Figure 4.22.** Contour Color Selection Form

#### **4.10.2 Displaying the Receptor Network**

The receptor field—where concentration and deposition values are calculated—can be viewed in the MapWindow map display by clicking on the checkbox labeled “Receptors” on the “Display Options” tab. In addition, the color, size, and other properties of the displayed receptors can be adjusted by clicking on the colored box next to the checkbox.

#### **4.10.3 Displaying the Calculated Wind Vector Field**

The gridded wind vector field created by the CALMET meteorological model and used in the dispersion calculations can be viewed in the MapWindow map display by clicking on the checkbox labeled “Wind Vectors” on the “Display Options” tab. Wind vectors can be displayed for various heights above the ground (in meters) by selecting a height from the listbox beneath the “Wind Vectors” label. In addition, the color, size, and other properties of the wind vectors can be adjusted by clicking on the colored box next to the checkbox. The number of wind vectors plotted and the size (i.e., scale) of the vectors can be adjusted within the Cal.par file. By default, wind vectors are displayed at every other receptor location on the primary grid and are scaled such that a 3 m/s wind is exactly the distance between successive receptor locations.

#### **4.10.4 Displaying Surface and Upper-Air Meteorological Station Locations**

Surface and upper-air meteorological stations that were used in the CALMET meteorological model for creating the gridded meteorological fields can be displayed in the MapWindow map display by clicking on the checkbox labeled “Surface Stations” and “Station Locations,” respectively, on the “Display Options” tab. In addition, the color, size, and other properties of the stations can be adjusted by clicking on the colored boxes next to their respective checkboxes.

## 5.0 Polygon Layer Creator

The Polygon Layer Creator is a software application that can be used to create polygon-based GIS data for use in a DUSTRAN scenario. Using the .mwprj project file for a DUSTRAN site, a user can draw areas onto the map of the site and assign characteristic codes to each of the polygon areas through simple point-and-click operations. Once new areas have been drawn or existing areas have been modified, the utility can be used to generate a new shape file containing the changes as well as a .csv file. The text file can be used directly by the DUSTRAN modeling system for retrieving certain land-based characteristics, such as soil textures and vegetation classes, for use in wind-blown dust simulations. The interface for the Polygon Layer Creator consists of three parts: a map display, a table of contents for the layers displayed in the map, and a toolbar with buttons for use in controlling the map display and editing the polygons. Figure 5.1 displays an example of the Polygon Layer Creator interface with a sample site .mwprj file loaded.

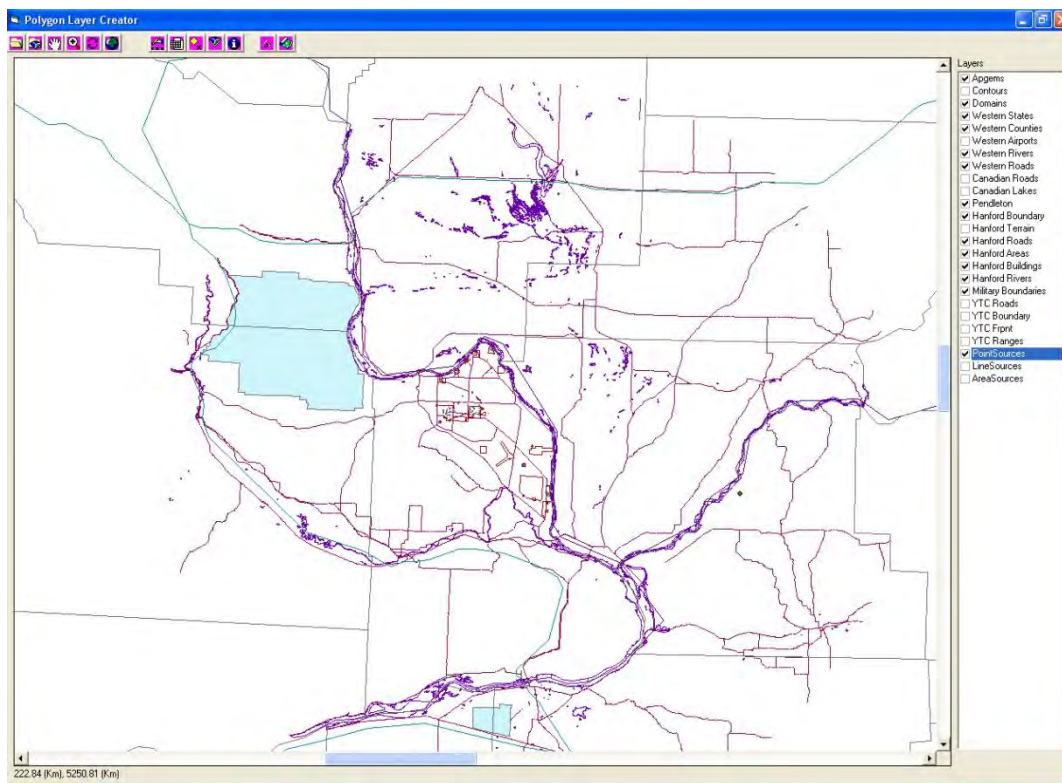



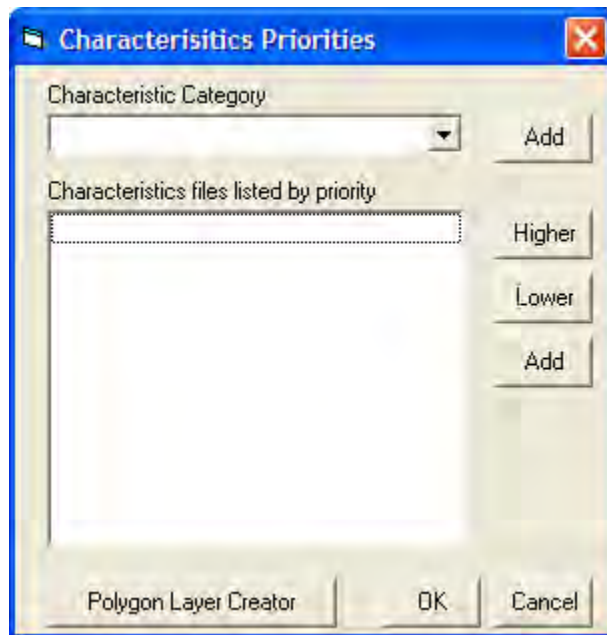
Figure 5.1. Polygon Layer Creator Interface

### 5.1.1 Starting the Polygon Layer Creator

The Polygon Layer Creator can be accessed from both within and outside of the DUSTRAN interface. To access the Polygon Layer Creator from within DUSTRAN:

- Select the “Sources” tab and click on the “Characteristic Files”  button. Characteristic files are .csv files created by the Polygon Layer Creator that describe certain characteristics of the domain, such as soil textures and vegetation classes. These files can be read directly by the DUSTRAN interface for calculation purposes, such as calculating gridded dust emissions for the model domain.


- The “Characteristic Priorities” (Figure 5.2) form will appear, from which the “Polygon Layer Creator” button can be clicked to launch the application. The “Characteristic Priorities” form is used to associate the files created in Layer Creator with the current scenario.



**Figure 5.2.** Launching Polygon Layer Creator from Within DUSTRAN


The Polygon Layer Creator can also be accessed outside of the DUSTRAN interface:

- To start the Polygon Layer Creator, double-click on the CreateLayer.exe file in the main DUSTRAN directory.

Once started, the application’s interface will be displayed with all buttons disabled except for the “Load shapefile”  button.


### 5.1.2 Loading a Shapefile

A GIS-based shapefile (.shp) can be loaded into the layer creator interface to provide a reference background on which to either create, add, or modify polygons representing the soil characteristics of the simulation site. To load a shapefile:

- Click on the “Load Shapefile file”  button.
- Using the browse window, navigate to the desired DUSTRAN site directory and select the .shp file representing the simulation site.
- Click on the “Open” button of the browse window to open the .shp file and close the browse window.
- Once the shapefile has been opened, the selected map layers will be automatically loaded into the map display and the layer names will be displayed in the “Layers” list.

### 5.1.3 Importing Polygons from an Existing Shape File

Shapefiles can be loaded into the “Polygon Layer Creator” utility to quickly create polygon shapes for use in DUSTRAN. These shape files typically describe characteristic features for a site, such as soil textures or vegetation classes. To import polygons from a shape file:

- Click on the “Import polygons from shape file”  button.
- Using the browse window, navigate to the directory folder that contains the desired shape file.
- Click on the shape file name and then click on the “Open” button to load the shape file and close the browse window.
- Once the shape file has been selected, a window will be displayed listing the field names available in the shape file.
- Select the primary field name that corresponds to the polygon values that will be used to describe the shapes. Figure 5.3 displays an example of the field selection window.
- Once opened, the shape file will be automatically loaded into the map display and its name added to the “Layers” list.

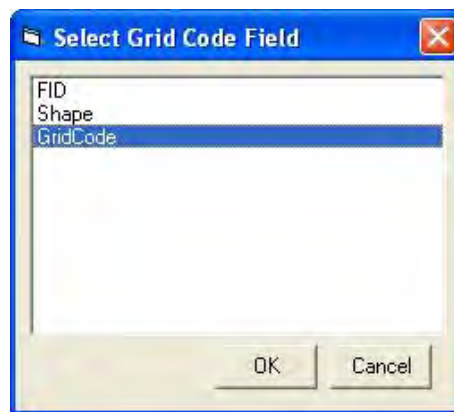



Figure 5.3. Select Grid Code Field Window

### 5.1.4 Starting a New Polygon Set

After a site’s .mwprj file has been loaded, polygons can be created to describe certain underlying characteristics of a site. To clear all existing polygons from a site and start a new polygon set:

- Click on the “Start new polygon set”  button to clear the current set of polygons and start a new set.
- Once the “Start new polygon set” button has been clicked, the previously selected polygons will be cleared, and new polygons can be entered.

### 5.1.5 Site Navigation Within Map Display Window


Standard navigation buttons are included within the Polygon Layer Creator for working with a site in the map display window. These navigation features include:

- Panning

- Zooming
- Reverting to Prior Extent
- Viewing the Full Extent.


### 5.1.5.1 Panning the Map Display

Panning is used to move around a site without changing the zoom. To pan the view in the map display:

- Click on the “Pan map image”  button.
- Click and hold on a point in the viewable map display.
- Move the mouse to move the map view displayed in the map control.


### 5.1.5.2 Zooming into the Map Display

Zooming is used to focus on a particular location within a site. To zoom on the map display:

- Click on the “Zoom into map image”  button.
- Using the mouse, click on a point in the map display and then drag a rectangle around the area you would like to zoom into.
- Release the mouse button, and this will zoom the extent of the viewable map to the rectangle drawn.


### 5.1.5.3 Reverting the Map Display to the Last Extent

Reverting the map display to the last extent is used to undo a particular zoom level. To revert to the extent for the map display:

- Click on the “Zoom to last extent”  button. The map display will automatically revert to the last extent used.

### 5.1.5.4 Returning the Map Display to the Full Extent

The full extent of the map display, as defined by the layers within the .mwprj file, is an efficient way to quickly view the entire extent of the site. To view the full extent:


- Click on the “Zoom to full map extent”  button. The map display will automatically adjust to the full extent of the map and refresh the display.

## 5.1.6 Working with Polygons

The Polygon Layer Creator allows for the creation of polygon areas that spatially represent a certain characteristic, such as soil textures or vegetation classes, for a site. Each polygon is assigned a value, called a grid code, which identifies it from surrounding polygons. For example, soil textures may be assigned a grid code ID, which identifies it by Zabler soil category (see Table 2.7). These grid codes can be read by DUSTRAN and used in certain calculations. Currently, DUSTRAN can read gridded Zabler soil texture IDs and Olson Ecosystem vegetation codes (see Section 2.3.2), both of which are used in the wind-blown dust-emissions module. The Polygon Layer Creator creates gridded values of these codes from the polygon shapes that are displayed in the map window and writes them to a text file for use in DUSTRAN. This section provides guidance on how to work with polygon shapes within the Polygon Layer Creator.

### 5.1.6.1 Adding Polygons to the Layer

Polygons can be manually drawn and added to a layer to create a collection, or set, of polygons. These polygons are used to represent a certain characteristic of the site, such as a specific soil texture or vegetation class. Polygons are differentiated by their grid code, which is a value that is entered after drawing the polygon shape. To add a new polygon to a polygon set:

- Click on the “Add polygons”  button.
- Draw the new polygon onto the map display using the mouse. Each corner of the polygon is created by a left-click of the mouse at the desired location.
- When finished drawing the desired polygon, double-click on the last point of the polygon. An input window will be displayed asking for the code value associated with the polygon. Figure 5.4 displays an example of the input window.
- Enter the value into the input window and click on the “OK” button.
- The new polygon will then be added to the map display.

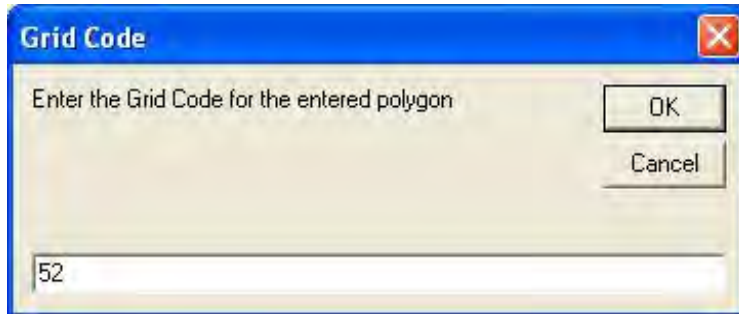



Figure 5.4. Grid Code Input Window


### 5.1.6.2 Editing the Value Associated with a Polygon

Each polygon has an associated value which identifies a particular attribute of the polygon. These values are assigned at the time the polygon is created, but can be edited. To edit a value associated with a particular polygon:

- Click on the “Edit layer polygon”  button.
- Double-click on the polygon whose value is to be changed.
- Once clicked, the polygon will flash, and an input window will be displayed showing the original value of the polygon.
- Enter the new value for the polygon and then select the “OK” button.

### 5.1.6.3 Deleting a Polygon

A single polygon shape and its associated value can be deleted from the map display. To delete a polygon:

- Click on the “Delete polygon”  button.

- Double-click on the polygon to be deleted.
- Once clicked, the polygon will flash, and then a message window will be displayed asking for confirmation of the deletion.
- Click on the “OK” button to delete the polygon.

#### 5.1.6.4 Changing the Color of the Polygon Boundaries

The boundaries that define a polygon area can have different colors to distinguish it from other polygons within the map display. Normally, colors are used for display purposes and visually represent values used to define each polygon layer. To change polygon boundary colors:


- Click on the “Change the color of the polygon boundaries”  button. Once the button has been clicked, the “Grid Code Color Select” window (See Figure 5.5) will be displayed.
- Within the “Grid Code Color Select” window, double-click on the code value that the color will be changed. Once the code has been clicked, a color selection window will be displayed.
- Select the desired color by clicking on the colored box and then click on the “OK” button.
- Once the colors have been selected for all polygons, click the “OK” button of the “Grid Code Color Select” window. The polygon boundary colors will be automatically updated in the map display.

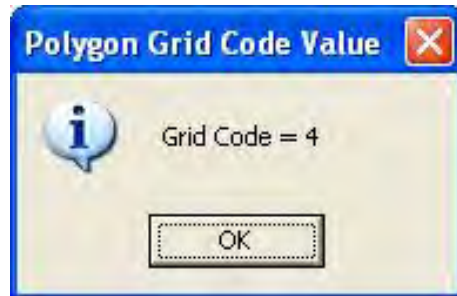


Figure 5.5. Grid Code Color Selection Window

#### 5.1.6.5 Viewing the Value of a Polygon

The grid code value that defines a polygon can be viewed within the map display window. To view the polygon value:

- Click on the “Show polygon grid code” button and then click on the polygon of interest.
- After clicking on a polygon, the polygon will flash, and the “Polygon Grid Code Value” window (see Figure 5.6) will be displayed with the value of the polygon.
- To close the “Polygon Grid Code Value” window, click on the “OK” button.

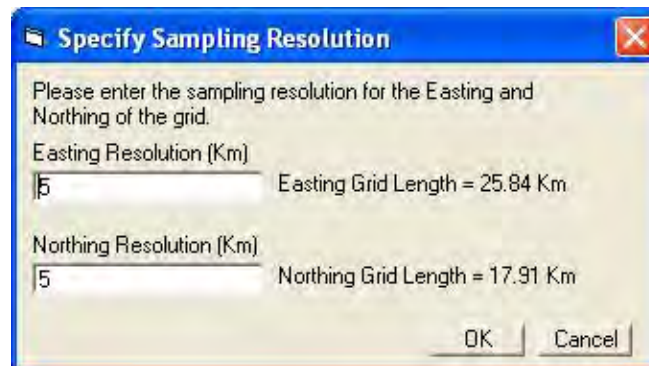


**Figure 5.6.** Polygon Grid Code Value Window

### 5.1.7 Setting the Resolution of the Output .csv File

The polygon areas and their associated values output a .csv file that can be read by DUSTRAN and used in certain calculations. Currently, DUSTRAN can read gridded Zobler soil texture IDs and Olson Ecosystem vegetation codes, both of which are used in the wind-blown dust emissions module. To set the resolution, or grid spacing, derived from the polygon shapes:

- Click on the “Modify the resolution of the output data” button; the “Specify Sampling Resolution” window will be displayed (Figure 5.7).
- Enter the desired “Easting” and “Northing” resolutions into the text boxes provided.
- Click on the “OK” button to accept the changes and close the window.



**Figure 5.7.** Specify Sampling Resolution Window

The output grid resolution should be commensurate with the average size of the polygons making up the data set. For example, if the various polygons making up the data set have an average dimension of roughly 10 km on a side, then the grid resolution should be on the order of 5 km to have roughly four grid points per polygon.

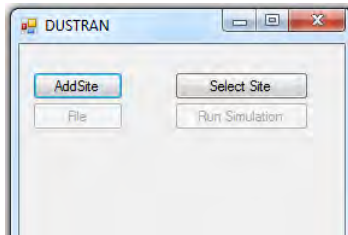
### 5.1.8 Creating the Output Shape File and .csv File

The polygons can be saved to a shape and text file for use in DUSTRAN. The shape file allows for the polygons to be displayed within the DUSTRAN map window; the text file can be interrogated by the DUSTRAN software for use in certain calculations. Currently, DUSTRAN reads gridded Zobler soil texture IDs and Olson Ecosystem vegetation codes, both of which are used in the wind-blown dust-emissions module. To create the files, click on the “Create shape file” button; a file browse window will be displayed. Enter a name for the output files and then click on the “Open” button to save the files.

## 6.0 Adding a New User Profile to DUSTRAN

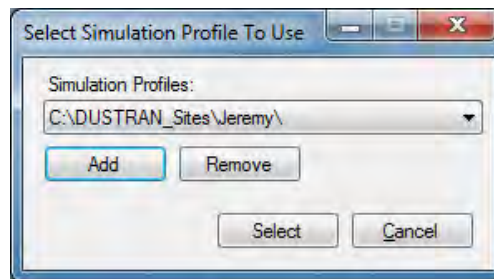
DUSTRAN V2.0 allows for the creation and use of multiple user profiles. These user profiles allow multiple users to use the same DUSTRAN software to run individual simulations using their own separate and distinct simulation sites. User profiles created using DUSTRAN V2.0 are no longer limited to being located within the DUSTRAN directory and can be created at any location the user desires as long as the machine on which DUSTRAN is installed has read/write access to that location. This allows users using the same machine to run their own instance of DUSTRAN without overwriting another user's site data. This section provides the step-by-step instructions for adding a new user profile to DUSTRAN.

1. To add a new user profile to DUSTRAN, both MapWindow and DUSTRAN must already be installed. Open MapWindow and click on the “D” button on the MapWindow toolbar. The DUSTRAN user interface will open and be displayed along with the MapWindow interface.
2. Within the DUSTRAN interface click on the “Add Site” button (see Figure 6.1).



**Figure 6.1.** DUSTRAN's “Add Site” Button

3. The “Select Simulation Profile To Use” window will be displayed.



**Figure 6.2.** “Select Simulation Profile To Use” Window

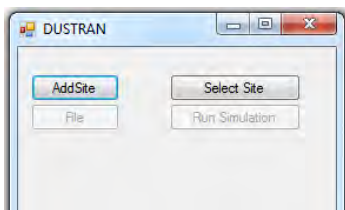
4. Click on the “Add” button to add a new profile.
5. Within the “Browse For Folder” window, either select an existing folder to locate the new profile or create a new folder.
6. In the “Simulation Profile Name” window, enter a name for the new user profile.
7. The profile name and path should now appear in the profile selection window. Click on the “Select” button to select the new profile. This profile will be used to run an instance of DUSTRAN without overwriting another user's site data.

## 7.0 Adding a New Site to DUSTRAN

A new site can be added to DUSTRAN using the “Add Site” wizard within the DUSTRAN interface. A new site contains all the geophysical data, such as terrain and land use/land cover, that is needed to run the AERMOD, CALPUFF, and CALGRID dispersion models. In addition, a new site contains base geospatial data that are used for displaying and analyzing the site within MapWindow. After a new site has been created, the user can add additional geospatial data to customize the map for a particular scenario or application.

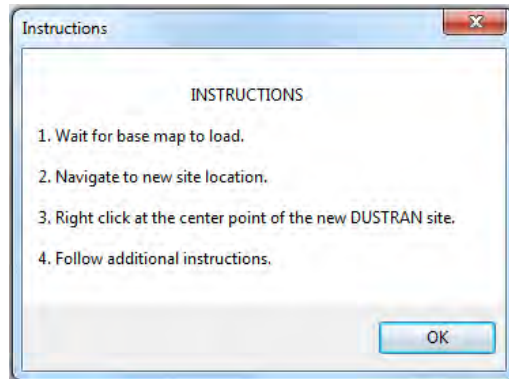
This section provides step-by-step instructions for adding a new site to DUSTRAN. Specifically, the “Add Site” wizard will guide the user through a series of forms that automate the following tasks:

- Specify the spatial range, or extent, of the new site.
  - Designate a name and UTM zone for the site.
  - Create a new site directory that contains all the necessary template files for performing a simulation in DUSTRAN.
  - Build DUSTRAN’s meteorological surface (.snf) and upper-air (.unf) station information files.
  - Build and save new GIS map files for display in MapWindow.
  - Register the site so that it can be opened within the DUSTRAN interface.
1. To add a new site, both MapWindow and DUSTRAN must already be installed. Open MapWindow and click on the “DUSTRAN” button on the MapWindow toolbar. DUSTRAN’s interface will open alongside the MapWindow application interface.
  2. Within DUSTRAN, click on the “Add Site” button (see Figure 7.1):

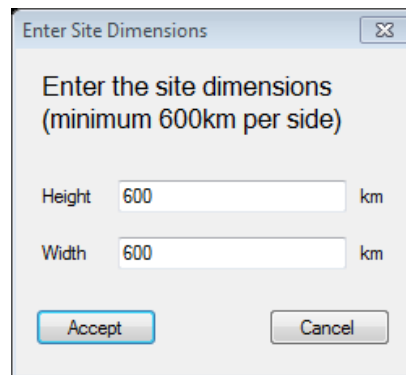


**Figure 7.1.** The DUSTRAN “Add Site” Button

3. After clicking “Add Site,” a set of instructions will appear that provides information on how to select the site location within MapWindow (see Figure 7.2). After reading the instructions, click “OK” to continue.
4. A map of the continental United States will be automatically loaded into the display of the MapWindow interface.
5. Use the MapWindow navigation tools (e.g., zoom and pan) to navigate to a desired location on the base map where the new site is to be located. Right-click on the general location of where the site is to be located. This sets a central point from which all geospatial data will be selected and clipped.
6. After right-clicking on the map, a dialog box will appear prompting for the geospatial site dimensions (see Figure 7.3). This affects the overall extent of the geospatial data and sets the clipping envelope for the data. The default values for the height and width are 600 km to verify that the spatial envelope is large enough to provide flexibility in siting the model domain in DUSTRAN. After setting the height and width for the geospatial envelope, click “OK” to continue.

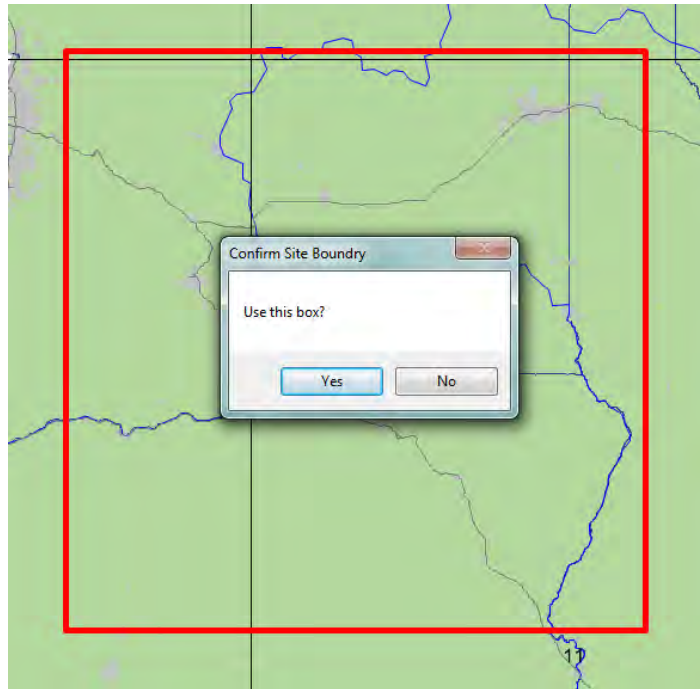


**Figure 7.2.** DUSTRAN’s Instructions for Selection of Site Location

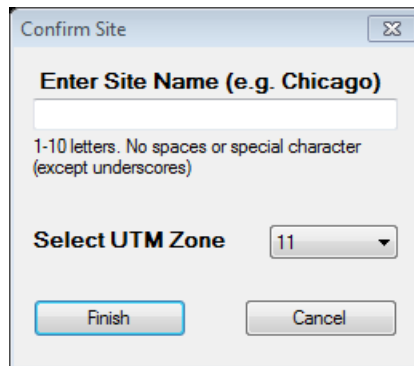


**Figure 7.3.** Prompt for Geospatial Site Dimensions

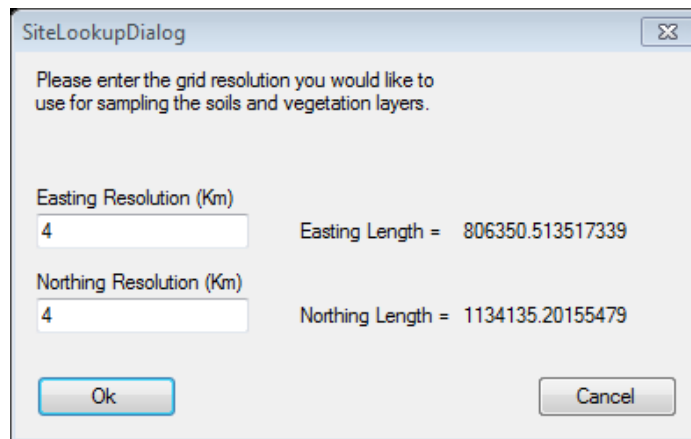
7. The base map will be displayed with a red box that represents the clipping envelope that will be applied to the geospatial data (see Figure 7.4). The box is used to intersect the “US\_States” layer. The envelope of the intersecting states serves as the actual clipping boundary for the geospatial data. Click “Yes” to accept or “No” to start again.
8. After accepting the clipping envelope, a dialog box will appear prompting for the site name and UTM zone (see Figure 7.5). The site name must be unique and cannot be the name of an existing site. The UTM zones are labeled on the base map (see image above for an example) and are used as the coordinate system in DUSTRAN. If the center of the site is in a UTM zone that is different than the UTM zone selected by the user, the selection must be confirmed before continuing.
9. Click “Finish” to finalize the site creation process. A progress bar and task list display the progress of the site creation. Because the utility must clip all of the base layers, loading the geodatabase may take several minutes, especially for sites located on the eastern coast of the United States.
10. A window will appear asking for the sampling resolution for the vegetation and soil texture files that are used in wind-blown dust simulations (see Figure 7.6). A default resolution of 4 km has been set.
11. Click the “OK” button, and the wizard will create four files: srztext.shp, srztext.csv, owe14d.shp, and owe14d.csv. The srztext files define the soil texture, and the owe14d files define the vegetation cover. The files with the extension .shp are shape files that are viewable within MapWindow and are stored within the site’s geodatabase; the .csv files are comma-delimited ASCII files that are interrogated by DUSTRAN when performing a wind-blown dust simulation and are stored within the TerData directory of the new site.



**Figure 7.4.** Red Box Enclosing Clipping Envelope

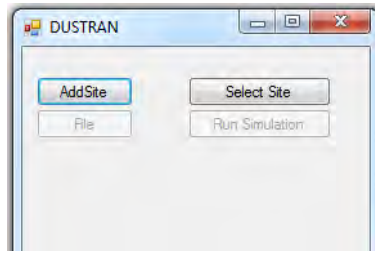


**Figure 7.5.** Prompt for Site Name and UTM Zone



**Figure 7.6.** Prompt for Sampling Resolution

12. Following the site's registration, the site may be opened by selecting the "Select Site" button on the main DUSTRAN interface.



**Figure 7.7.** Notification for Accessing the New Site

## 8.0 DUSTRAN Example Tutorials

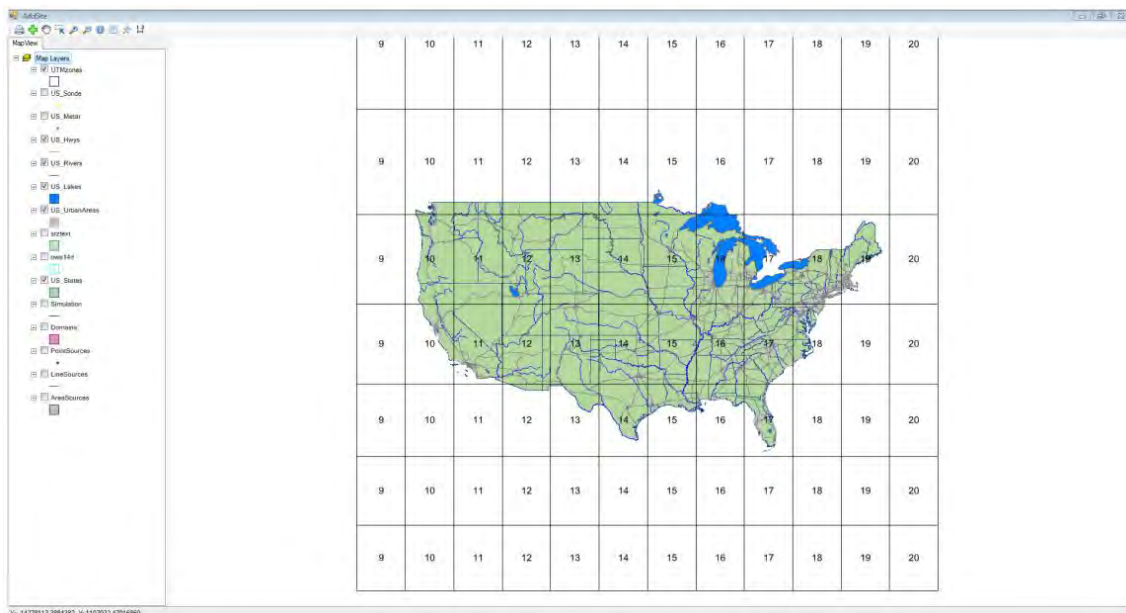
This section provides example tutorials for creating and running DUSTRAN simulations. Three tutorials are provided, all based on the sample Yakima site. The first tutorial simulates dust emissions from a point and area source using the CALPUFF model. The second tutorial simulates dust emissions from the same point and area source using the AERMOD model. The point-source emissions are prescribed explicitly; the area-source emissions are from vehicular activity and use the vehicular dust-emissions module intrinsic to DUSTRAN to generate the particulate emission rate. The third tutorial simulates a wind-blown dust event using the wind-blown dust-emissions module within DUSTRAN.

To run the examples detailed below, MapWindow and DUSTRAN must already be installed and at least one user profile created. Refer to the section entitled “DUSTRAN Installation Instructions, Section 3.0” in this user’s guide for detailed instructions on installing DUSTRAN and Section 6.0 for instructions on how to add a user profile.



### 8.1 Creating the Yakima Tutorial Site

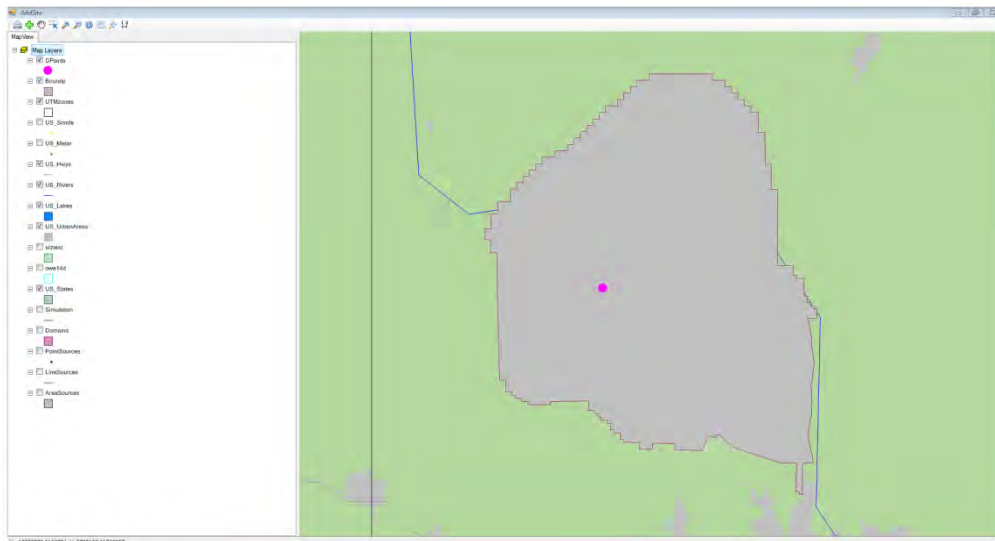
Each of the following DUSTRAN tutorials requires a simulation site named “Yakima”; Yakima is located in central Washington State. The following instructions provide the necessary steps to create a Yakima site for use in the DUSTRAN tutorials.

1. Start the MapWindow application and then click on the DUSTRAN “D” button located on its toolbar to start the DUSTRAN plugin.
2. Select the “Add Site” button on the DUSTRAN main interface.
3. Select one of the existing profiles using the “Select Simulation Profile To Use” form and click “Select”.
4. Once the add site instructions are displayed click the “Ok” button and wait for the map layers to be loaded into the MapWindow map display (Figure 8.1).



**Figure 8.1.** Add Site Map


5. Use the “Add Data” button (  ) on the “AddSite” toolbar to navigate and select the “Boundp.shp” shapefile located in the “Tutorial-Layers\WGS84-World-Mercator” folder in the DUSTRAN directory.
6. If a prompt is displayed asking to re-project the files to match the map projection select the “No” option.
7. Once the Boundp.shp shapefile is loaded, the map will automatically zoom to the Hanford boundary
8. Use the “Add Data” button (  ) on the “AddSite” toolbar to navigate and select the DPoints.shp shapefile located in the “Tutorial-Layers\WGS84-World-Mercator” folder in the DUSTRAN directory.
9. If a prompt is displayed asking to re-project the files to match the map projection select the “No” option.
10. At this time the Hanford boundary should be displayed on the map as well as a domain center point (Figure 8.2).

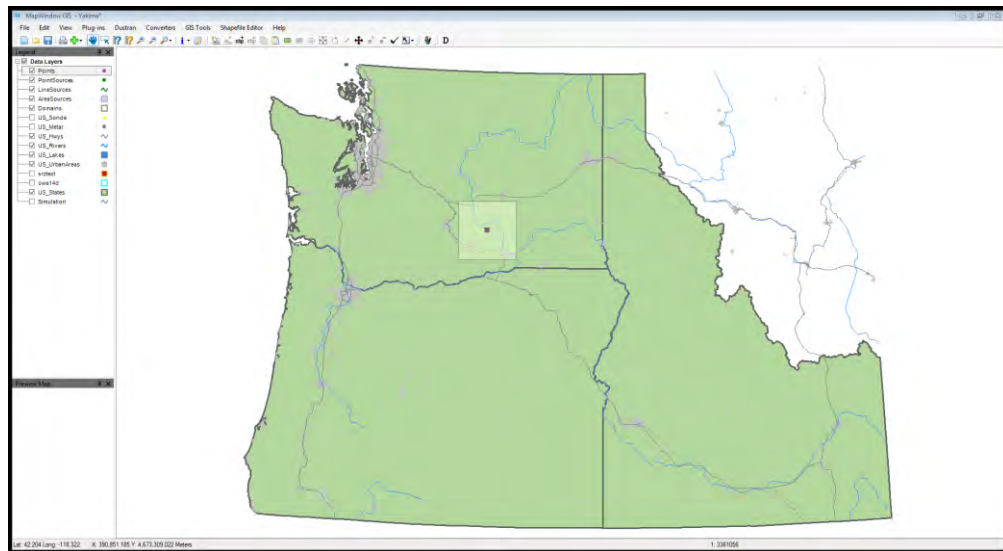


**Figure 8.2.** Add Site Map with Boundary and Point Data Loaded

11. *Right-click* on the domain point displayed on the map; the application will then walk through the “Add-Site” process detailed in Section 7.0.
12. When prompted to enter a site name, enter “Yakima” and leave the UTM Zone value at the default value of “11.”



18. Once the “Points.shp” shapefile has been loaded, click on the “Add New Domain Center” button (  ) from within the main DUSTRAN interface.
19. When prompted, click on the point displayed by the “Points.shp” shapefile.
20. When prompted, enter “Yakima” for the domain name, and click “Ok” to add a new model domain.
21. With the new model domain added, the “Yakima” site is now ready to be used with the DUSTRAN tutorials (Figure 8.5).



**Figure 8.5.** Completed Yakima Site

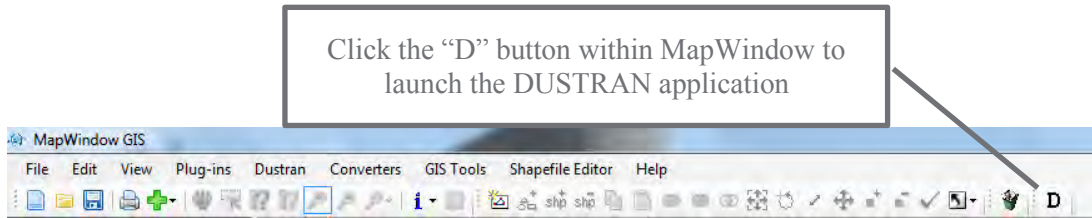
## 8.2 Simulating Dust Dispersion from Active Source Emissions Using CALPUFF

This tutorial steps through a dust-dispersion scenario from active source emissions for the “Yakima” site using the CALPUFF dispersion model. To perform this tutorial, the Yakima site must already exist before completing this tutorial; see Section 8.1 for instructions on creating the Yakima site.

In this example, a point source will be used to represent particle emissions from a stack; the emissions will be defined explicitly. An area source will also be created and it will represent a region of dust emissions from vehicular activity; these emissions will be calculated automatically by the DUSTRAN vehicular dust-emissions module. Both sources will be set to run for the same duration, and the downwind air-concentration and ground deposition will be simulated.

### 8.2.1 Starting DUSTRAN

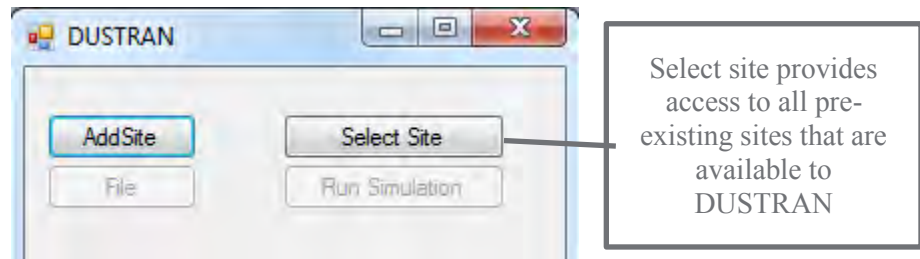
DUSTRAN is an integrated dispersion modeling application integrated with the MapWindow GIS application. To begin a DUSTRAN simulation, open MapWindow. On the MapWindow toolbar, click on the “D” button (Figure 8.6):



**Figure 8.6.** MapWindow Toolbar

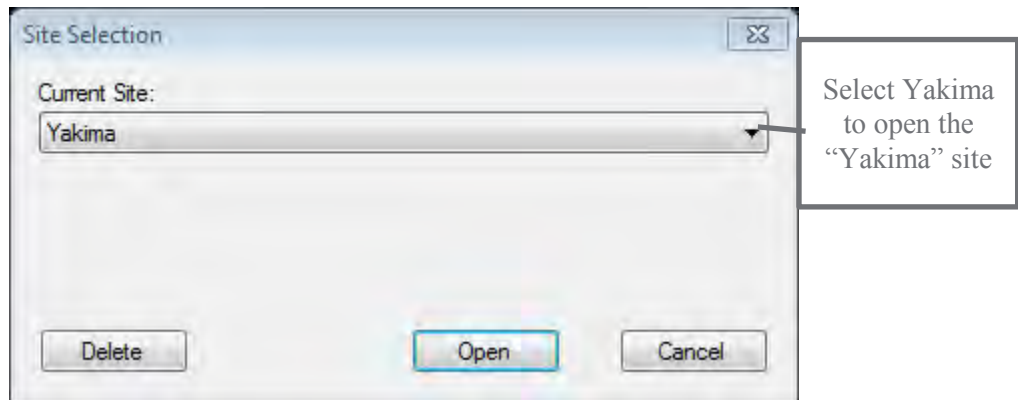
### 8.2.2 Selecting a Site

The user interface to the DUSTRAN model will appear alongside the MapWindow GIS application (Figure 8.7). Click the “Select Site...” button to open a dialog box that allows the user to select an existing site:



**Figure 8.7.** DUSTRAN User Interface

Select “Yakima” from the list of available model sites (Figure 8.8) and then click “Open” (Note: Section 8.1 provides instructions on how to create the “Yakima” site.):



**Figure 8.8.** Available DUSTRAN Sites

The “Yakima” site will open within MapWindow. A list of available GIS data layers will appear in the left frame, and DUSTRAN-specific input parameters will appear in the DUSTRAN frame (Figure 8.9).



The screenshot shows a 'Release Period' panel with a 'Synchronize' button at the top. Below it, there are two input fields: 'Start Time' set to '7:00:00 AM' and 'Release Duration' set to '03:00 hr'. Both fields have small up/down arrow icons to their right.

**Figure 8.11.** Release Period Panel

### 8.2.5 Setting the Simulation Scenario


This example will utilize the “CALPUFF” dispersion model to perform the atmospheric dispersion. Therefore, select the simulation “Type” as “Source Emission – CALPUFF”. Since the “Yakima” domain is being used, set the “Time Zone” to PST. Set the “Start Date Time” to the current date and the start time to 4 a.m. (Note: the simulation start time for a CALPUFF or CALGRID simulation must always begin before sunrise, as CALMET, the meteorological model used for these simulations, needs to calculate the hourly surface heat flux from sunrise until the end of scenario or sunset, whichever occurs first.) Finally, set the model “Run Duration” to 8 hours.

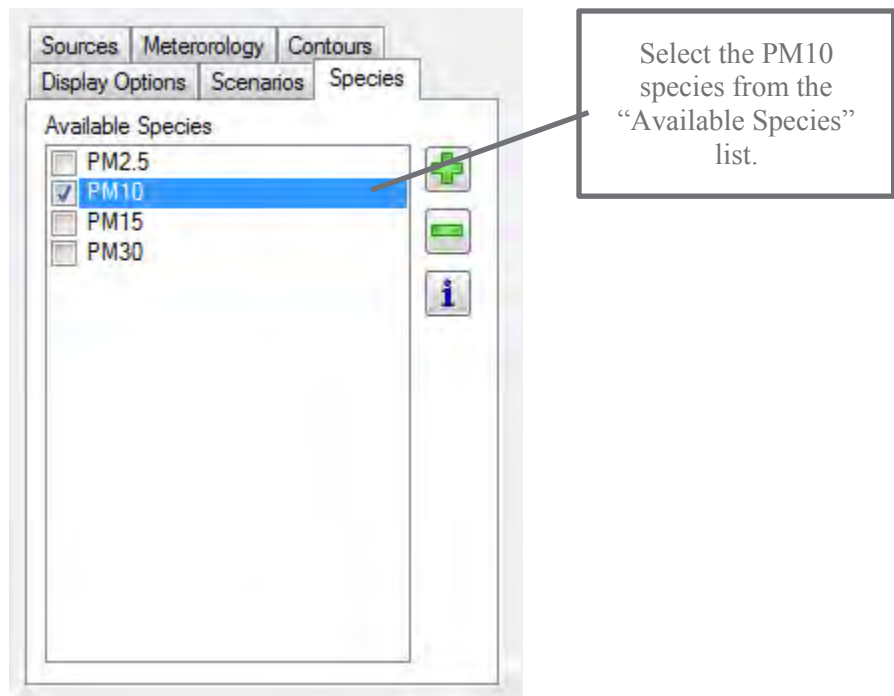
The screenshot shows a 'Simulation Scenario' panel. It contains five rows of controls: 'Type' is a dropdown menu set to 'Source Emission - CALPUFF'; 'Time Zone' is a dropdown menu set to 'PST'; 'Start DateTime' is a date-time picker set to '12/19/14 04:00 AM'; 'Run Duration' is a spinner set to '08:00 hr'; and 'Averaging Interval (hour)' is a dropdown menu set to 'N/A'.

**Figure 8.12.** Simulation Scenario Panel

### 8.2.6 Setting the Model Species

By default, there are four particulate matter (PM) species available to model in DUSTRAN (Figure 8.13). This tutorial will model the 10 micron (PM<sub>10</sub>) species; therefore, uncheck PM<sub>2.5</sub>, PM<sub>15</sub>, and PM<sub>30</sub>.


Additional species (particles and gases) can be added using the “Add Species”  button on the “Species” tab, but for this exercise, we will use the existing PM<sub>10</sub> species in the list.



**Figure 8.13.** Species Tab – “Available Species” List

### 8.2.7 Creating a Point Source

Click on the “Sources” tab. Note that there is already a point source called “Yakima” listed under “Point Sources”; this corresponds to the point that is used by DUSTAN to mark the center of the model domain. Uncheck the name, and the point will disappear from the center of the domain in the MapWindow map display.

To create a new point source, click on the “Point Source”  button on the “Sources” tab. Click on a location within the domain to place the point source. Call the source “Stack” and click “OK.”

The “Source Input” form for the point source will appear (Figure 8.14). Enter the “Release Parameters” as in Figure 8.14 and click “OK” to continue:

**Stack Source Parameters**

Height of release: 15 m

Enable Stack Release Parameters

Stack gas exit velocity: 2 m/s

Stack gas exit temperature: 25 C

Stack diameter: 1 m

Building cross section: 0 m<sup>2</sup>

Initial horizontal plume size: 1 m

Initial vertical plume size: 1 m

Start DateTime: 12/10/2014, 04:00 AM

Duration: 2 Hours

Building Cross Section >= 0.0


Emission rates (g/s)	
Specie	Emission Rate
PM2.5	0
PM10	1
PM15	0
PM30	0

Buttons: Ok, Cancel

**Figure 8.14.** Point Source Input Form – “Release Parameters” Tab

Notice that the new source shows up as a point in the MapWindow display and also appears in the “Point Source” list on the “Sources” tab.

### 8.2.8 Creating an Area Source

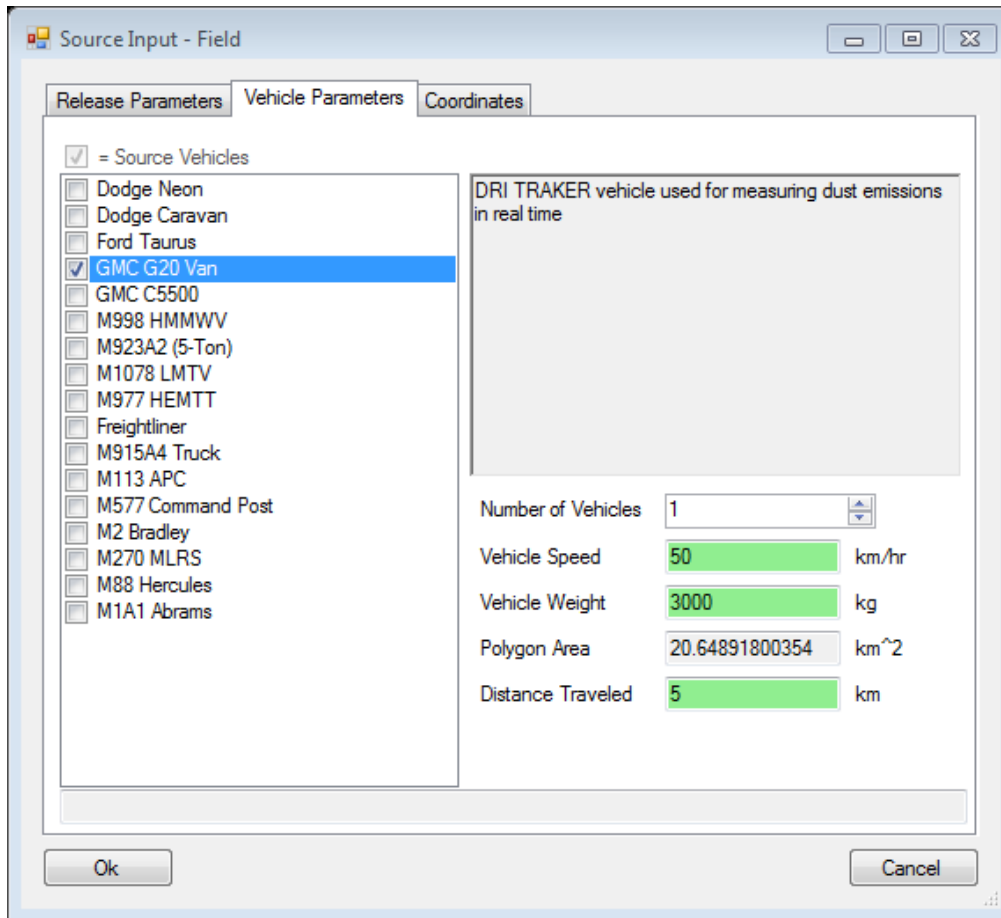
Next, create an area source by clicking on the “Area Source”  button on the “Sources” tab. An area source can be a triangle or four-sided polygon; it is created by clicking on three or four locations in the MapWindow map display. Note: the final corner should be a “right-clicked” to complete the polygon. Create the area source by drawing  $\approx 1$  km square polygon near the center of the domain, enter the source name “Field,” and click “OK.”

The “Source Input” form for the area source will appear (Figure 8.15):

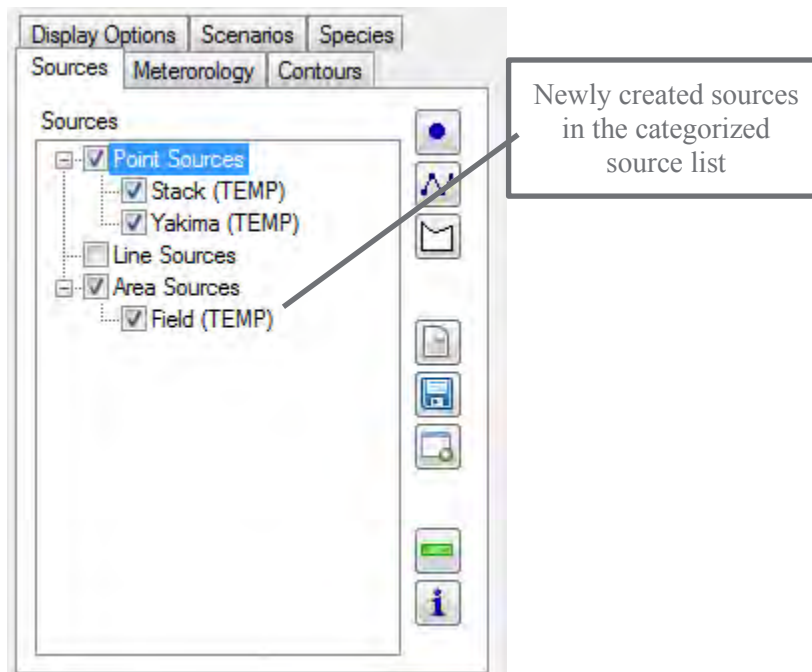
**Figure 8.15.** Area Source Input Form – “Release Parameters” Tab

For the area source, we will use the “Emission Model” to calculate dust emissions created by a single vehicle using the “DRI Factors” (Desert Research Institute). Vehicular dust emissions are a function of vehicle parameters, such as weight and speed. Click on the “Vehicle Parameters” tab (Figure 8.16) and specify the following vehicular information:

- The “Distance Traveled” is the total distance traveled by the vehicle within the area; enter a distance traveled of “5 km” (Figure 8.16). The emissions are assumed to be uniformly distributed over the area and constant for the duration of the release.
- Click “OK,” and the area source will appear in the MapWindow map display and also under the “Area Sources” list on the “Sources” tab (Figure 8.17).



**Figure 8.16.** Area Source Input Form – “Vehicle Parameters” Tab



**Figure 8.17.** Sources Tab – “Sources” List

### 8.2.9 Entering Meteorological Data

Next, click on the “Meteorology” tab within DUSTRAN and select “Single Observation” from the listbox. The “Specify Meteorological Data” form appears. Enter the meteorological observations as shown in the form below (Figure 8.18) shows the completed form.

Simulation Hour	Year	Month	Day	Hour	Wind Direction (deg)	Wind Speed (m/s)	Temperature (C)	Relative Humidity (%)	Station Pressure (mb)	Mixing Height (m)	Stability
1	2014	12	30	5	240	2.2	20	20	1005	200	E - Slightly Stable
2	2014	12	30	6	260	3	19	20	1007	200	E - Slightly Stable
3	2014	12	30	7	255	2.3	20	20	1003	200	E - Slightly Stable
4	2014	12	30	8	180	4	19	15	1000	200	E - Slightly Stable
5	2014	12	30	9	160	4.5	22	45	1005	300	D - Neutral
6	2014	12	30	10	157	4	23	55	1010	320	C - Slightly Unstable
7	2014	12	30	11	155	3.8	22	62	1011	500	C - Slightly Unstable
8	2014	12	30	12	160	2	23	60	1012	550	C - Slightly Unstable

Figure 8.18. Specify Meteorological Data Form – “Hourly Observations” Tab

### 8.2.10 Running DUSTRAN

After the sources, meteorology, and release duration information have been entered, a DUSTRAN simulation can be made. To run DUSTRAN, click on the “Run Simulation” button (Figure 8.19).

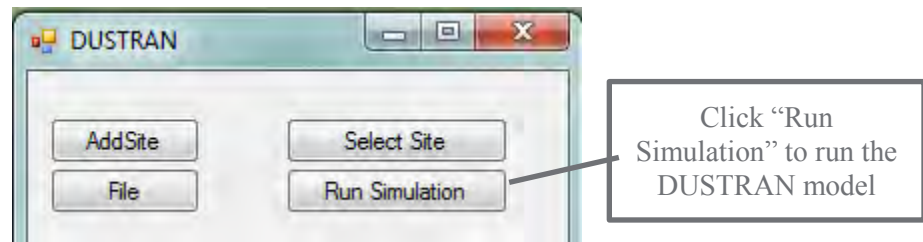
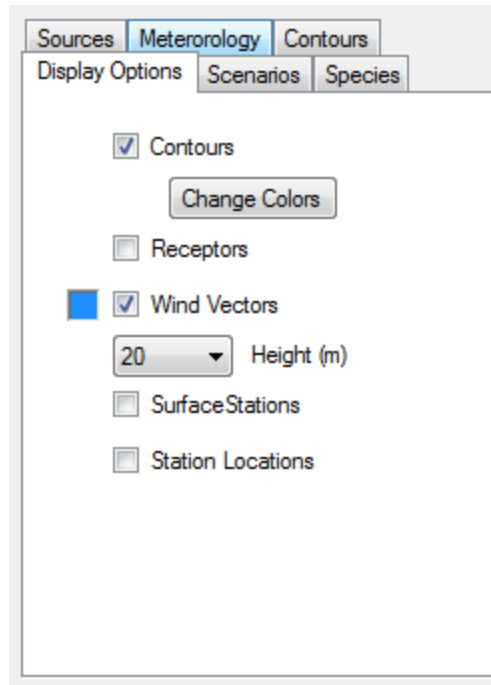


Figure 8.19. “Run Simulation” Button for Running DUSTRAN Simulation

### 8.2.11 Displaying Model Output

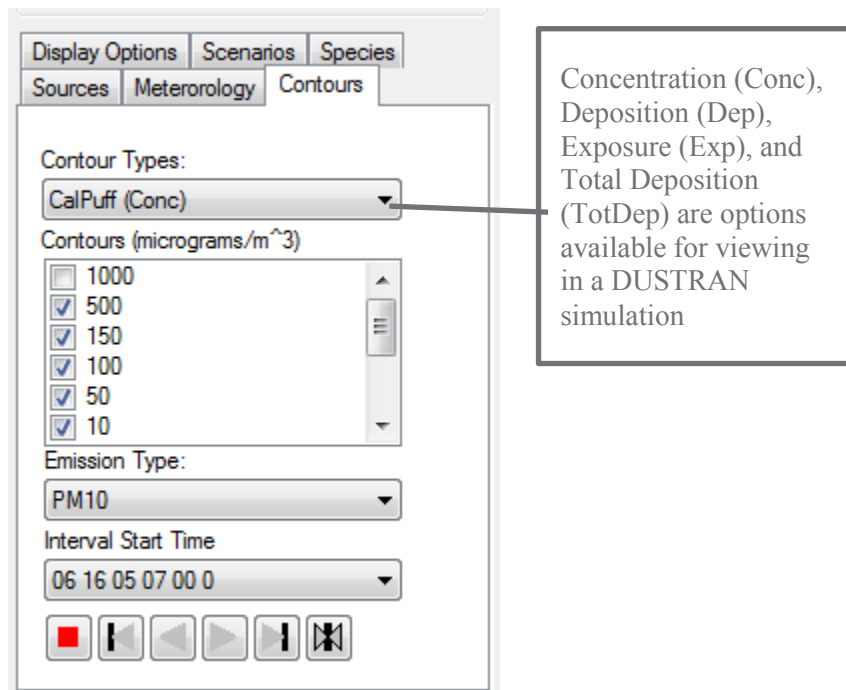
After the models finish running, click on the “Display Options” tab. Check “Contours” and “Wind Vectors” so that the plume contours and wind field will be displayed in the MapWindow map display (Figure 8.20). Wind vectors can be displayed for various layers throughout the domain; 20 meters is the top of the first layer, with mid-cell corresponding to 10 meters above ground level:



**Figure 8.20.** Display Options Tab – “Contours” and “Wind Vectors” options

### 8.2.12 Viewing Model Results

For each model time step, DUSTRAN calculates plume concentration and exposure as well as deposition and total deposition. To view a particular contour, click on the “Contours” tab and choose from the “Contour Types” listbox (Figure 8.21):

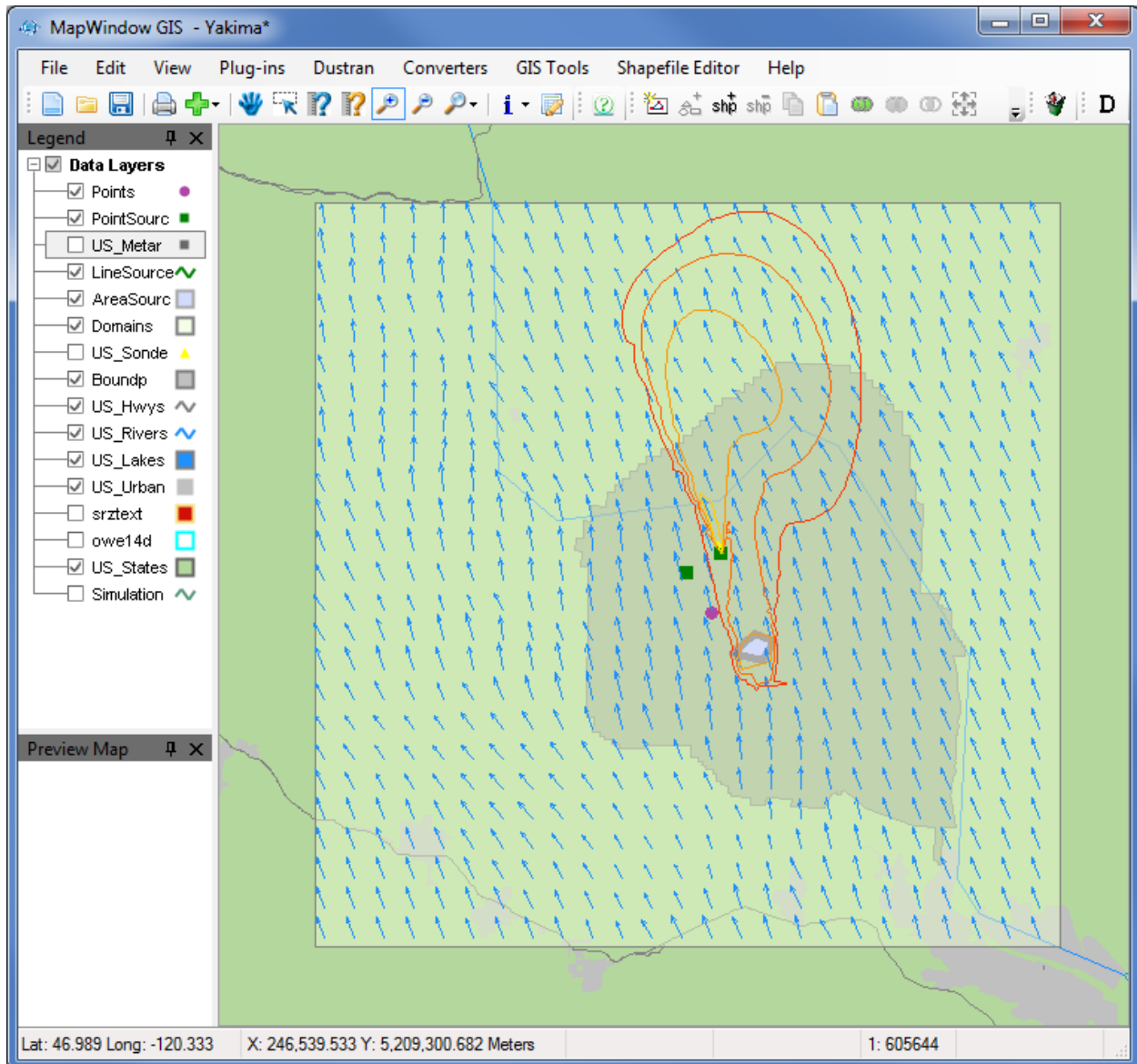


**Figure 8.21.** Contours Tab - “Contour Types” Listbox

In this example, select “Conc” to display hourly concentrations within MapWindow.

For a given contour type, numerous “Contours” are available for displaying. To display a particular contour interval, check the box next to the contour value. The default selection is normally adequate for displaying the maximum extent of the plume envelope.

To view a particular time step, select an interval from the “Interval Start Time” listbox. In this example, hourly time steps are available from the start of the release (7:00 a.m. local time) till the end of the run duration. Choose the 9:00 a.m. time step, which corresponds to the one hour (9:00 a.m. till 10:00 a.m.) average concentration (Figure 8.22):



**Figure 8.22.** Display of Concentration Contours and Wind Vectors for the Hour from 9-10 AM

Notice in the above image that the two plumes (point and area-source plumes) have merged. In addition, note the distortion to the wind field due to the local topography. The distortion is caused by terrain blocking because of the early-morning stability and slope flow due to cold-air drainage.

## 8.3 Simulating Dust Dispersion from Active Source Emissions Using AERMOD

This tutorial steps through a dust-dispersion scenario from active source emissions for the “Yakima” site using the AERMOD dispersion model. To perform this tutorial, the Yakima site must already exist before completing this tutorial; see Section 8.1 for instructions on creating the Yakima site.

In this example, a point source will be used to represent particle emissions from a stack; the emissions will be defined explicitly. An area source will also be created and it will represent a region of dust emissions from vehicular activity; these emissions will be calculated automatically by the DUSTRAN vehicular dust-emissions module. Both sources will be set to run for the same duration, and the downwind air-concentration and ground deposition will be simulated.

### 8.3.1 Starting DUSTRAN

DUSTRAN is an integrated dispersion modeling application integrated with the MapWindow GIS application. To begin a DUSTRAN simulation, open MapWindow. On the MapWindow toolbar, click on the “D” button (Figure 8.23):

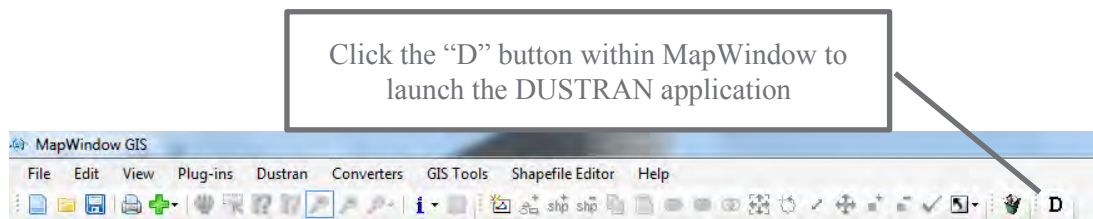


Figure 8.23. MapWindow Toolbar

### 8.3.2 Selecting a Site

The user interface to the DUSTRAN model will appear alongside the MapWindow GIS application (Figure 8.24). Click the “Select Site...” button to open a dialog box that allows the user to select an existing site:

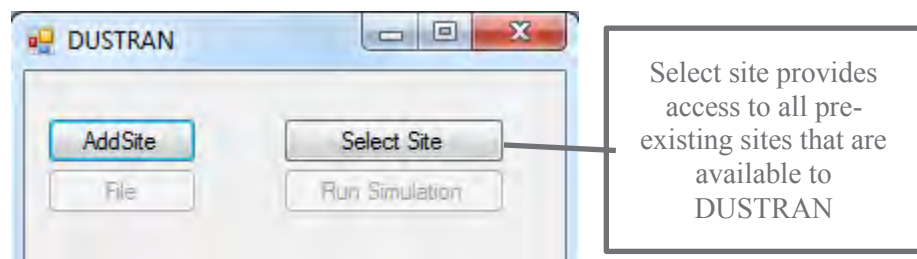
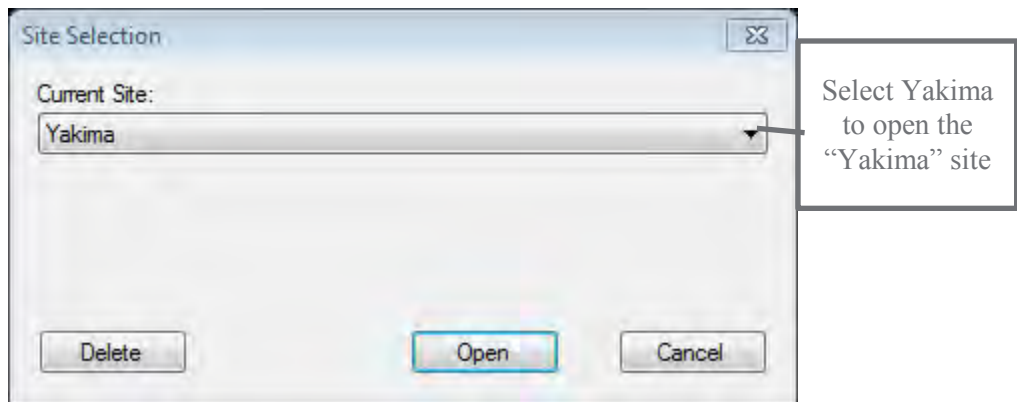


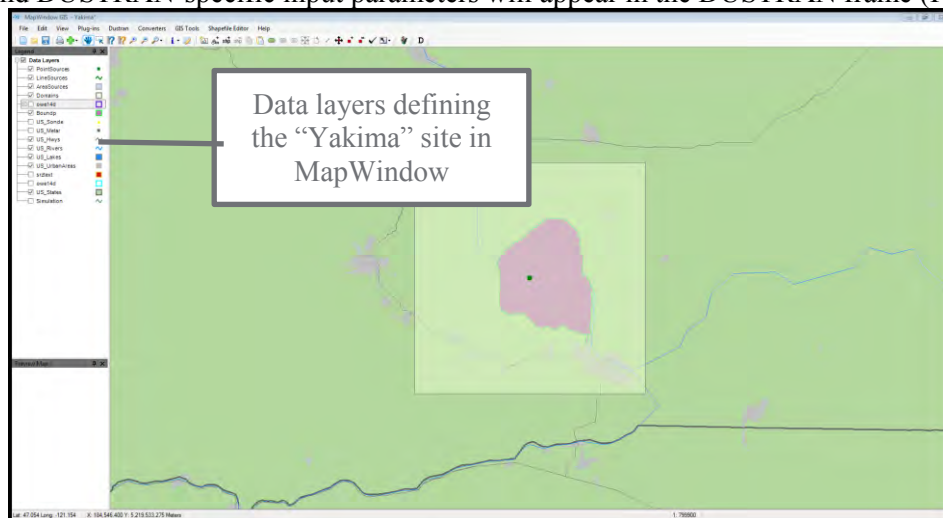
Figure 8.24. DUSTRAN User Interface

Select “Yakima” from the list of available model sites (Figure 8.25) and then click “Open” (Note: Section 8.1 provides instructions on how to create the “Yakima” site.):



**Figure 8.25.** Available DUSTAN Sites

The “Yakima” site will open within MapWindow. A list of available GIS data layers will appear in the left frame, and DUSTAN-specific input parameters will appear in the DUSTAN frame (Figure 8.26).





**Figure 8.26.** Yakima Site Displayed in DUSTAN

### 8.3.3 Creating a Domain

The first step in setting up a scenario in DUSTAN is to select a domain and set the domain size. A domain is a user-specified area where both meteorological and dispersion model calculations are performed.

Select the “Yakima” domain from the domain list in the “Domain” panel of the DUSTAN interface.

Since AERMOD is a plume model, it should only be used to model short-range dispersion (i.e., out to approximately 50 km). In this example, a domain size of 50 km will be used. Set the size from the “Size” listbox in the “Domain” panel to 50 km (Figure 8.27). The domain should appear as a shaded, rectangular region within MapWindows.

Domain  
 Name: Yakima   
 Size (km): 50   
 UTM Zone: 11

**Figure 8.27.** Domain Panel

### 8.3.4 Setting the Release Period

This example will simulate an early-morning release. Set the “Release Period” “Start Time” to 7 a.m. and the “Release Duration” to 3 hours (Figure 8.28).

Release Period  
 Synchronize  
 Start Time: 7:00:00 AM  
 Release Duration: 03:00 hr

**Figure 8.28.** Release Period Panel

### 8.3.5 Setting the Simulation Scenario


This example will utilize the “AERMOD” dispersion model to perform the atmospheric dispersion. Therefore, select the simulation “Type” as “Source Emission – AERMOD”. Since the “Yakima” domain is being used, set the “Time Zone” to PST. Set the “Start Date Time” to the current date and the start time to 7 a.m. Finally, set the model “Run Duration” to 3 hours (Figure 8.29).

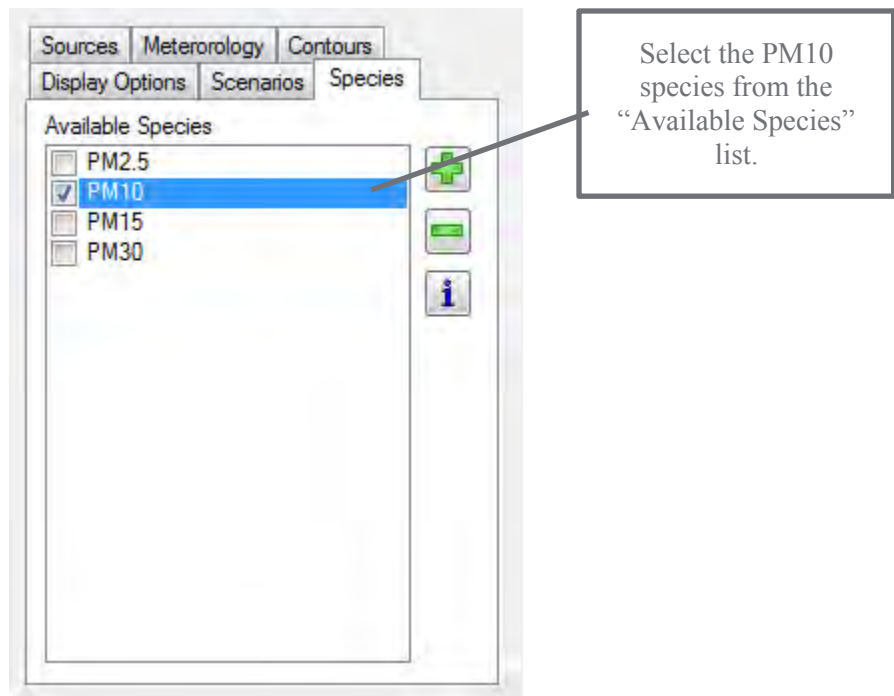
Simulation Scenario  
 Type: Source Emission - AERMOD  
 Time Zone: PST  
 Start DateTime: 01/09/15 07:00 AM  
 Run Duration: 03:00 hr  
 Averaging Interval (hour): N/A

**Figure 8.29.** Simulation Scenario Panel

### 8.3.6 Setting the Model Species

By default, there are four particulate matter (PM) species available to model in DUSTRAN (Figure 8.30). This tutorial will model the 10 micron (PM<sub>10</sub>) species; therefore, uncheck PM<sub>2.5</sub>, PM<sub>15</sub>, and PM<sub>30</sub>.


Additional species (particles and gases) can be added using the “Add Species”  button on the “Species” tab, but for this exercise, we will use the existing PM<sub>10</sub> species in the list.



**Figure 8.30.** Species Tab – “Available Species” List

### 8.3.7 Creating a Point Source

Click on the “Sources” tab. Note that there is already a point source called “Yakima” listed under “Point Sources”; this corresponds to the point that is used by DUSTRAN to mark the center of the model domain. Uncheck the name, and the point will disappear from the center of the domain in the MapWindow map display.

To create a new point source, click on the “Point Source”  button on the “Sources” tab. Click on a location within the domain to place the point source. Call the source “Stack” and click “OK.”

The “Source Input” form for the point source will appear (Figure 8.31). Enter the “Release Parameters” as in Figure 8.31 and click “OK” to continue:

**Stack Source Parameters**

Height of release: 15 m

Enable Stack Release Parameters

Stack gas exit velocity: 2 m/s

Stack gas exit temperature: 25 C

Stack diameter: 1 m

Building cross section: 0 m<sup>2</sup>

Initial horizontal plume size: 1 m

Initial vertical plume size: 1 m

Start DateTime: 01/09/2015, 07:00 AM


Duration: 3 Hours

Specie	Emission Rate
PM2.5	0
PM10	1
PM15	0
PM30	0

**Figure 8.31.** Point Source Input Form – “Release Parameters” Tab

Notice that the new source shows up as a point in the MapWindow display and also appears in the “Point Source” list on the “Sources” tab.

### 8.3.8 Creating an Area Source

Next, create an area source by clicking on the “Area Source”  button on the “Sources” tab. An area source can be a triangle or four-sided polygon; it is created by clicking on three or four locations in the MapWindow map display. Note: the final corner should be a “right-clicked” to complete the polygon. Create the area source by drawing  $\approx 1$  km square polygon near the center of the domain, enter the source name “Field,” and click “OK.”

The “Source Input” form for the area source will appear (Figure 8.32):

Source Input - Field

Release Parameters | Vehicle Parameters | Coordinates

### Field Source Parameters

Paved:

Effective height above ground: 0 m

Air temperature: 25 C

Effective rise velocity: 1 m/s

Effective radius: 1 m

Initial vertical spread: 1 m

Start DateTime: 01/09/2015, 07:00 AM

Duration: 3 Hours

Emission Model:  Emission Model  User Defined

Emission Factor Type: DRI emission factors: unpaved industrial r

Ok Cancel

**Figure 8.32.** Area Source Input Form – “Release Parameters” Tab

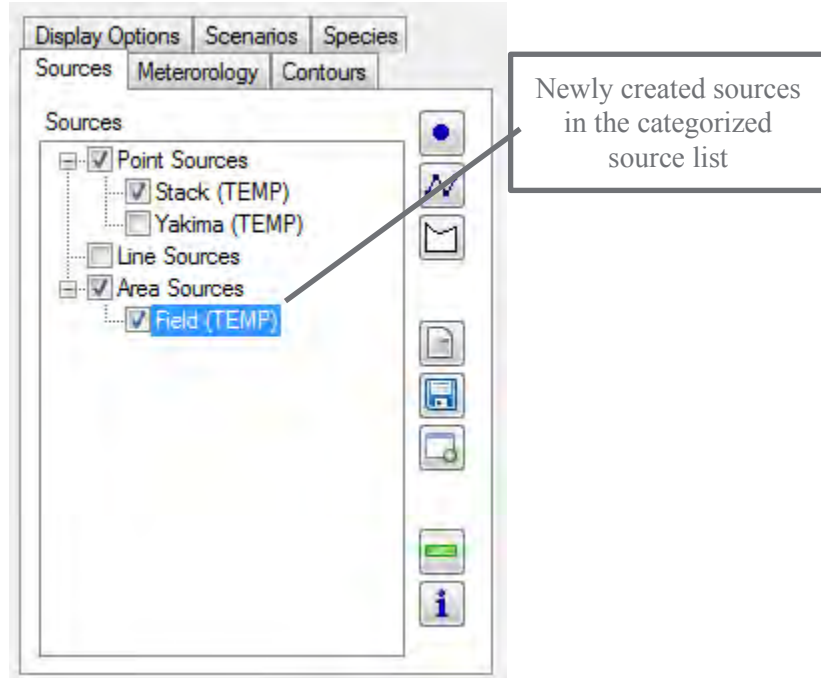
For the area source, we will use the “Emission Model” to calculate dust emissions created by a single vehicle using the “DRI Factors” (Desert Research Institute). Vehicular dust emissions are a function of vehicle parameters, such as weight and speed. Click on the “Vehicle Parameters” tab (Figure 8.33) and specify the following vehicular information:

- The “Distance Traveled” is the total distance traveled by the vehicle within the area; enter a distance traveled of “5 km” (Figure 8.33). The emissions are assumed to be uniformly distributed over the area and constant for the duration of the release.
- Click “OK,” and the area source will appear in the MapWindow map display and also under the “Area Sources” list on the “Sources” tab (Figure 8.34).

The screenshot shows a software window titled "Source Input - Field" with three tabs: "Release Parameters", "Vehicle Parameters", and "Coordinates". The "Vehicle Parameters" tab is active. On the left, there is a list of vehicle models, each with a checkbox. The "GMC G20 Van" is checked and highlighted in blue. To the right of the list is a text area containing the text "DRI TRAKER vehicle used for measuring dust emissions in real time". Below the text area are five input fields: "Number of Vehicles" (a spinner box set to 1), "Vehicle Speed" (a text box with "50" and "km/hr" unit), "Vehicle Weight" (a text box with "3000" and "kg" unit), "Polygon Area" (a text box with "20.64891800354" and "km^2" unit), and "Distance Traveled" (a text box with "5" and "km" unit). At the bottom of the window are "Ok" and "Cancel" buttons.

Parameter	Value	Unit
Number of Vehicles	1	
Vehicle Speed	50	km/hr
Vehicle Weight	3000	kg
Polygon Area	20.64891800354	km <sup>2</sup>
Distance Traveled	5	km

**Figure 8.33.** Area Source Input Form – “Vehicle Parameters” Tab



**Figure 8.34.** Sources Tab – “Sources” List

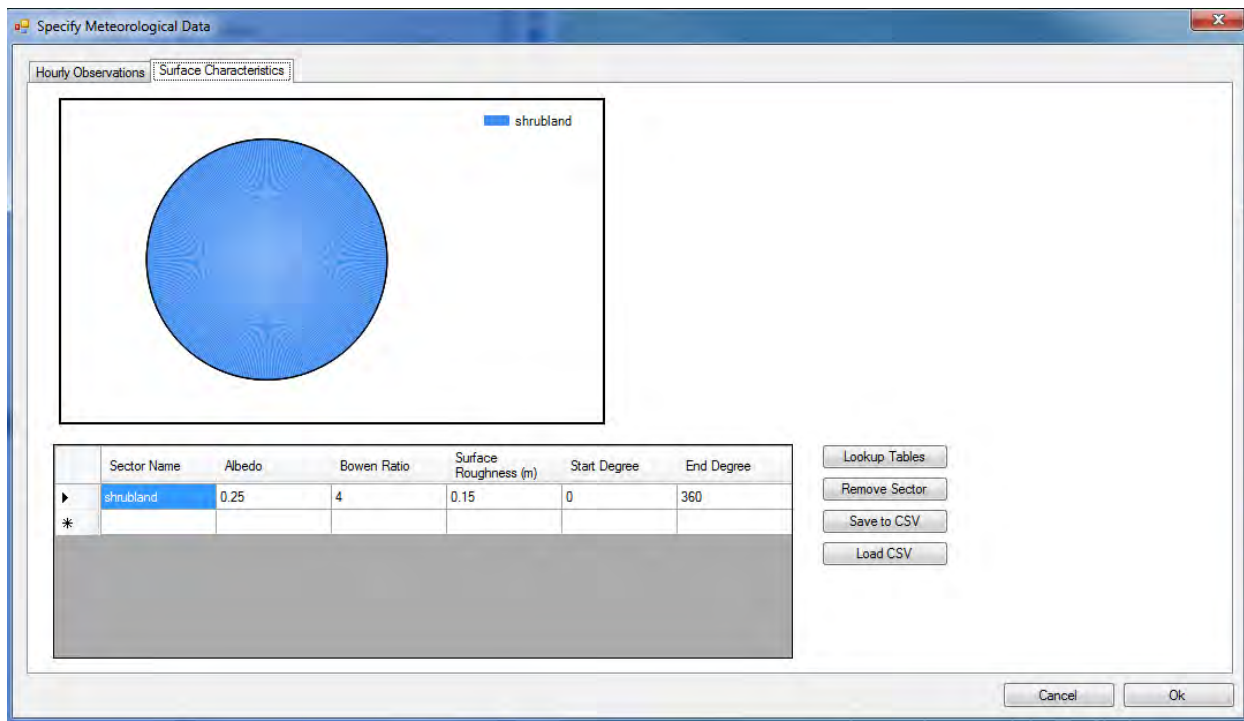
### 8.3.9 Entering Meteorological Data and Surface Characteristics

Next, click on the “Meteorology” tab within DUSTRAN and select “Single Observation” from the listbox. The “Specify Meteorological Data” form appears. Enter the meteorological observations as shown in the form below (Figure 8.35):

Simulation Hour	Year	Month	Day	Hour	Wind Direction (deg)	Wind Speed (m/s)	Temperature (C)	Relative Humidity (%)	Station Pressure (mb)	Total Sky Cover (tenths)	Measurement Height (m)	Ceiling Height (ft)
1	2015	1	9	8	255	2.3	20	20	1003	0	10	1000
2	2015	1	9	9	180	4	19	15	1000	0	10	1000
3	2015	1	9	10	160	4.5	22	45	1005	0	10	1000

**Figure 8.35.** Specify Meteorological Data Form – “Hourly Observations” Tab

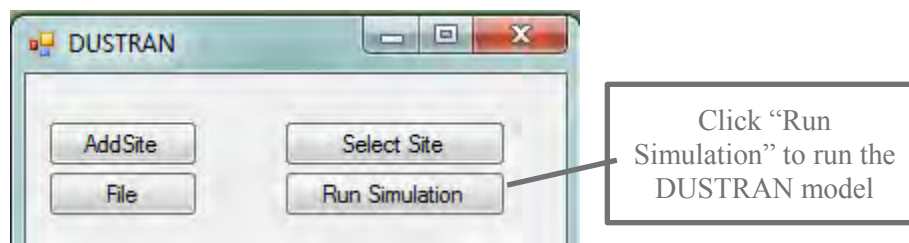
AERMOD’s meteorological preprocessor, AERMET, also requires information about the underlying model domain surface characteristics. Click on the “Surface Characteristics” tab to specify unique sectors and associated surface characteristics (i.e., albedo, Bowen ratio, surface roughness). Multiple sectors can be specified, and the resulting sectors should cover the entire model domain (i.e., 360 degrees). In this example, a single “Shrubland” sector is specified (0 to 360 degrees). Values for “Albedo”, “Bowen Ratio”, and “Surface Roughness” can be selected by right-clicking in a given cell and selecting a value or by using the “Lookup” button to list tables of common values. Enter the surface characteristics as shown in Figure 8.36:



**Figure 8.36.** Specify Meteorological Data Form – “Surface Characteristics” Tab

### 8.3.10 Running DUSTRAN

After the sources, meteorology, and release duration information have been entered, a DUSTRAN simulation can be made. To run DUSTRAN, click on the “Run Simulation” button (Figure 8.37).



**Figure 8.37.** “Run Simulation” Button for Running DUSTRAN Simulation

### 8.3.11 Displaying Model Output

After the models finish running, click on the “Display Options” tab. Check “Contours” so that the plume contours will be displayed in the MapWindow map display (Figure 8.38). Note: AERMOD is a plume model and uses a single, hourly wind direction to transport the plume. As a result, there is no wind vector field to display within AERMOD.

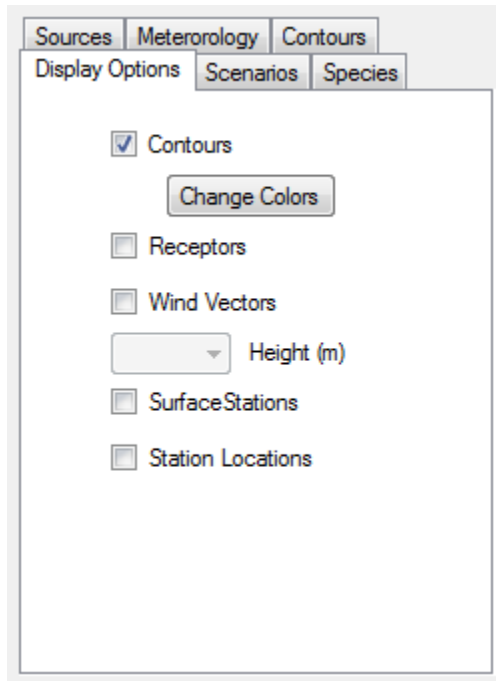


Figure 8.38. Display Options Tab – “Contours” options

### 8.3.12 Viewing Model Results

For each model time step, DUSTRAN calculates plume concentration and exposure as well as deposition and total deposition. To view a particular contour, click on the “Contours” tab and choose from the “Contour Types” listbox (Figure 8.39):

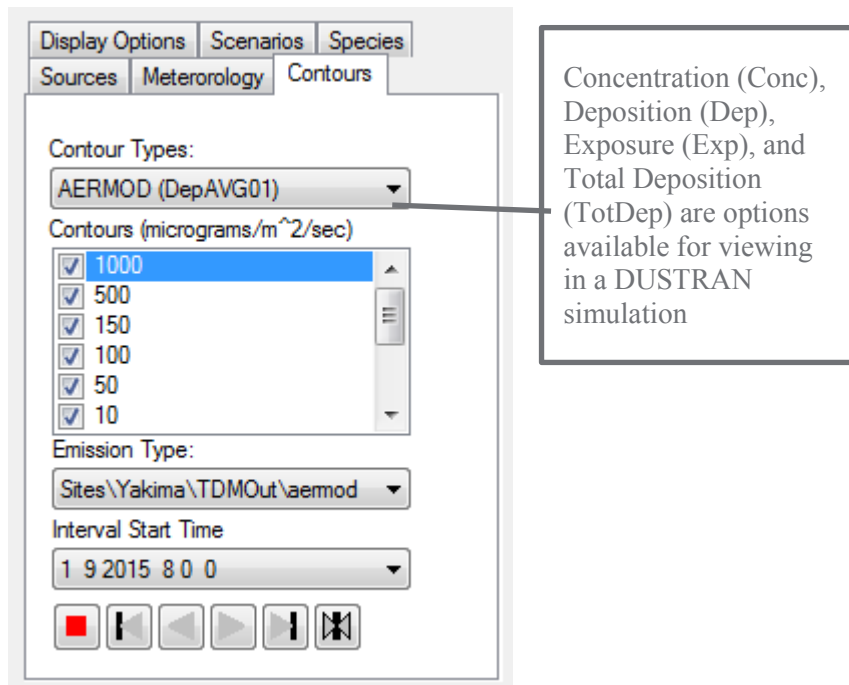
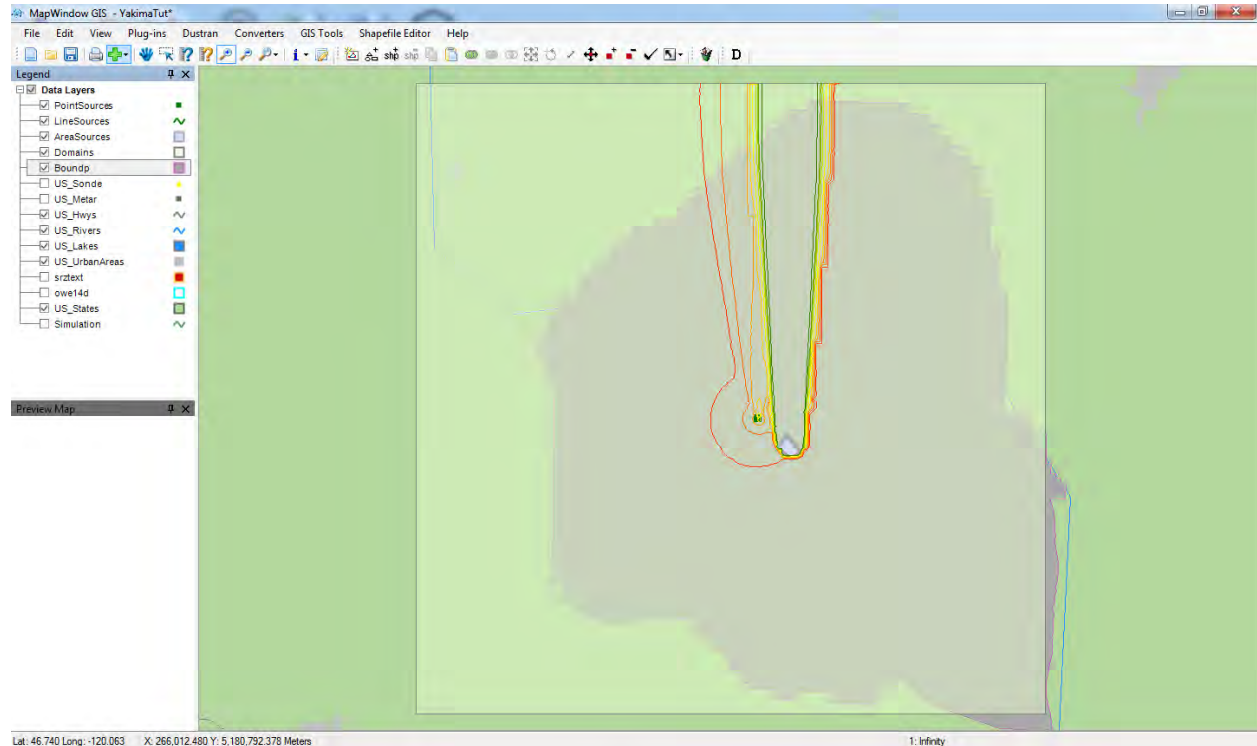


Figure 8.39. Contours Tab - “Contour Types” Listbox

In this example, select “Dep” to display hourly surface deposition values within MapWindow.

For a given contour type, numerous “Contours” are available for displaying. To display a particular contour interval, check the box next to the contour value. The default selection is normally adequate for displaying the maximum extent of the plume envelope.

To view a particular time step, select an interval from the “Interval Start Time” listbox. In this example, hourly time steps are available from the start of the release (7:00 a.m. local time) till the end of the run duration. Choose the 9:00 a.m. time step, which corresponds to the one hour (9:00 a.m. till 10:00 a.m.) average concentration and surface deposition (Figure 8.40):



**Figure 8.40.** Display of Deposition Contours for the Hour from 9-10 AM

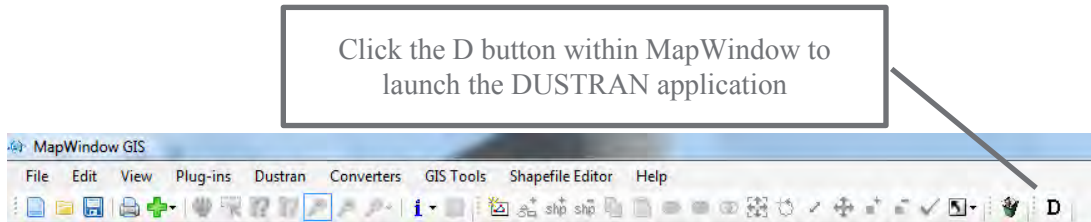
Notice in the above image that the deposition pattern from the two plumes (point and area-sources) are merged.

## 8.4 Simulating Wind-blown Dust Dispersion

This tutorial steps through the process of simulating a wind-blown dust scenario. Gridded dust emissions are created automatically by the emissions module and are a function of wind speed, soil texture, and vegetation class. In this scenario, a high wind event is assumed to occur over a 3-hour period, and the resulting wind-blown dust transport and diffusion is simulated.

### 8.4.1 Starting DUSTRAN

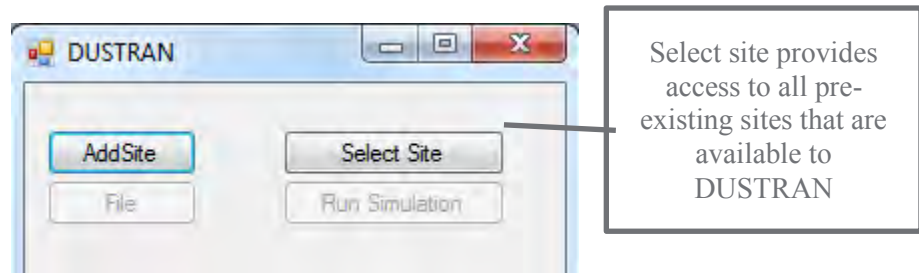
DUSTRAN is an integrated dispersion modeling application within the MapWindows GIS interface. To begin a DUSTRAN simulation, open MapWindows. On the MapWindow toolbar (Figure 8.41), click on the “D” button:



**Figure 8.41.** MapWindow Toolbar

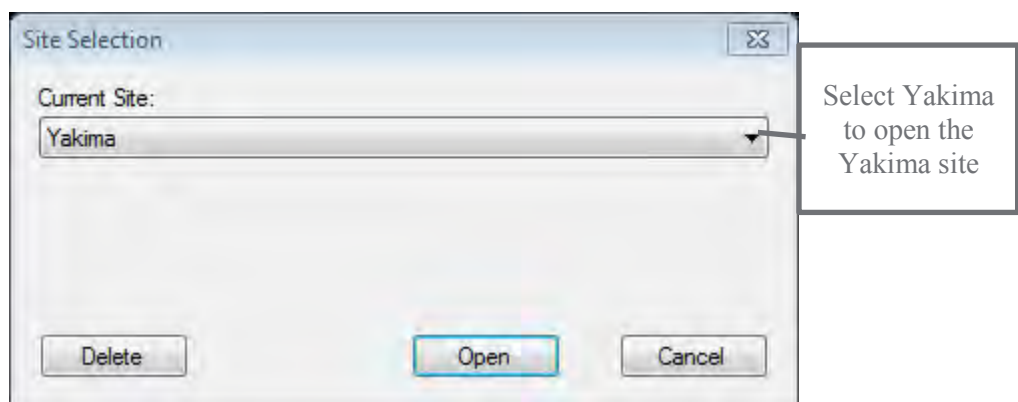
### 8.4.2 Selecting a Site

The user interface to the DUSTRAN model will appear alongside the interface of the MapWindow application (Figure 8.42). Click the “Select Site...” button to open a dialog box which allows the user to select an existing site:



**Figure 8.42.** Portion of User Interface to the DUSTRAN Model

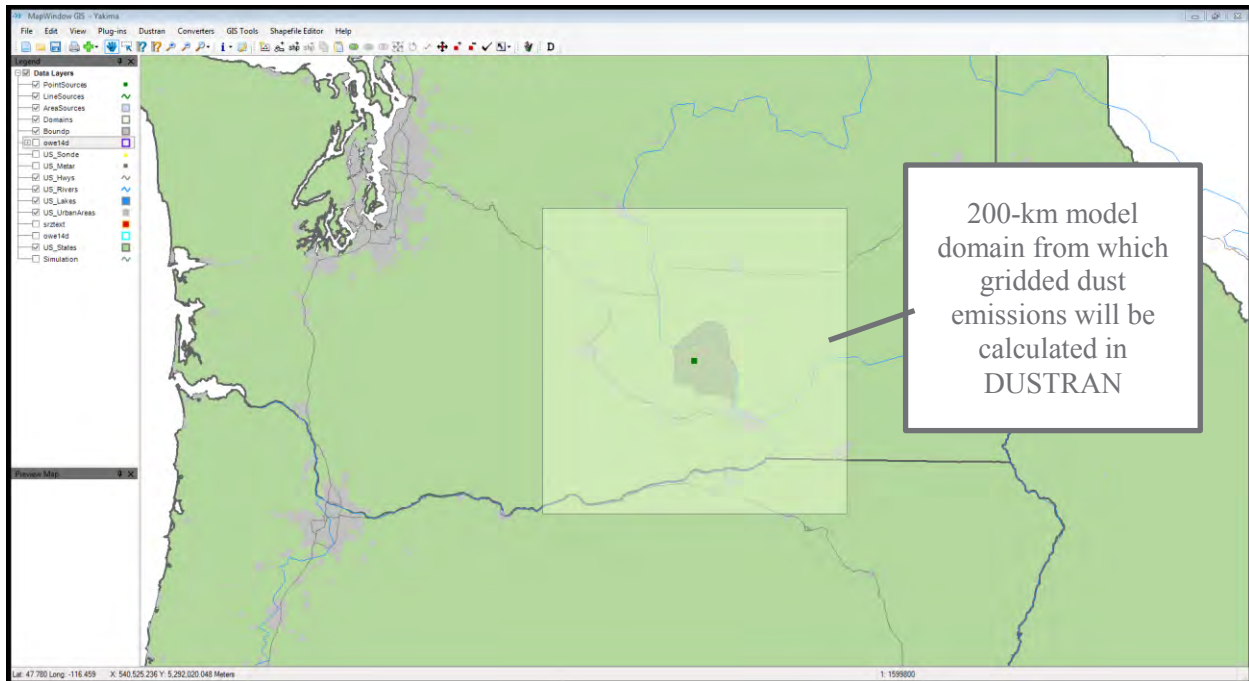
Select “Yakima” from the list of available model (Figure 8.43) sites and then click “Open”:



**Figure 8.43.** List of Available Model Sites

The Yakima site will open within the MapWindow map display. A list of available GIS data layers will appear in the layer list of the MapWindow application and DUSTRAN-specific input parameters will appear in the DUSTRAN user interface (Figure 8.44):

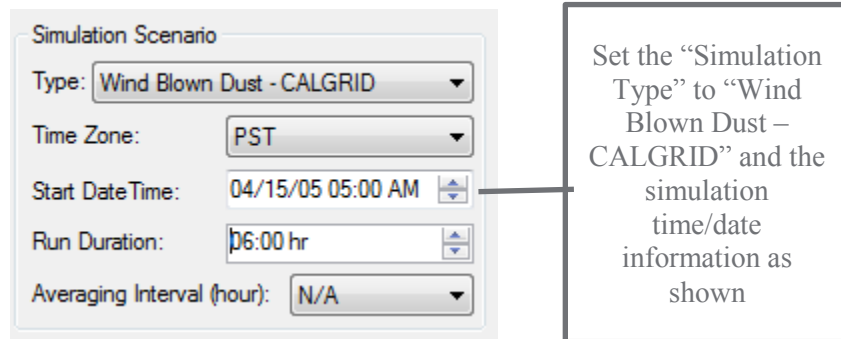




**Figure 8.46.** Display of 200-km-Square Yakima Domain within Yakima Site

#### 8.4.4 Setting the Simulation Scenario

This scenario will simulate wind-blown dust during a 3-hour wind event that occurs in the early morning hours of April 15, 2005. In the “Simulation Scenario” panel, set the “Simulation Type” to “Wind-blown Dust” and the “Time Zone,” “Start Date,” “Start Time,” and “Run Duration” as shown in Figure 8.47:

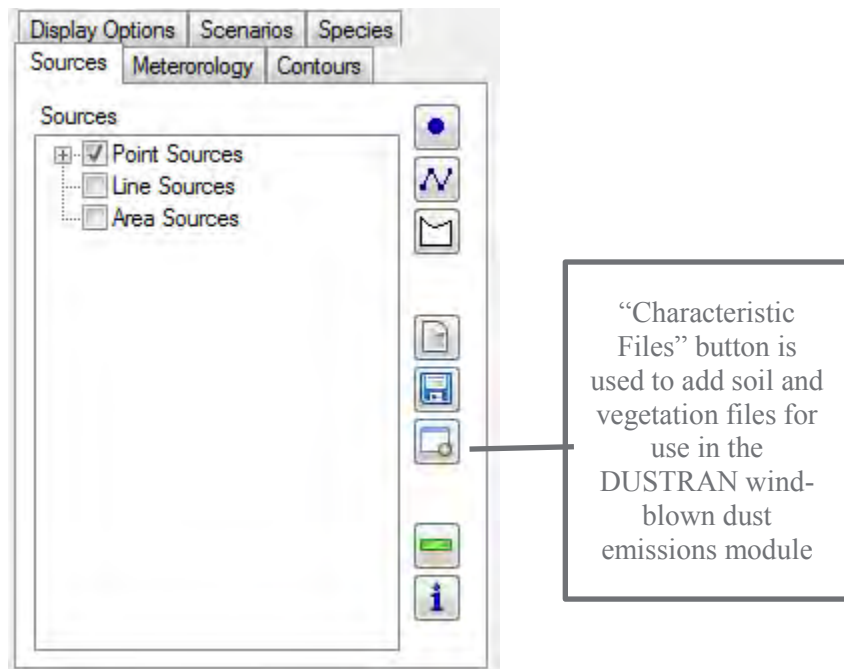


**Figure 8.47.** “Simulation Scenario” Panel

#### 8.4.5 Setting the Soil and Vegetation Characteristic Files

Zobler soil texture and Olson Ecosystem vegetation class files are generated whenever a site is created using the “Add Site” wizard within the DUSTRAN interface; these files are required to calculate dust emissions for the domain. In addition, the “Polygon Layer Creator” utility can be used to create high-resolution characteristic files for direct use in DUSTRAN (see Polygon Layer Creator, Section 5.0).

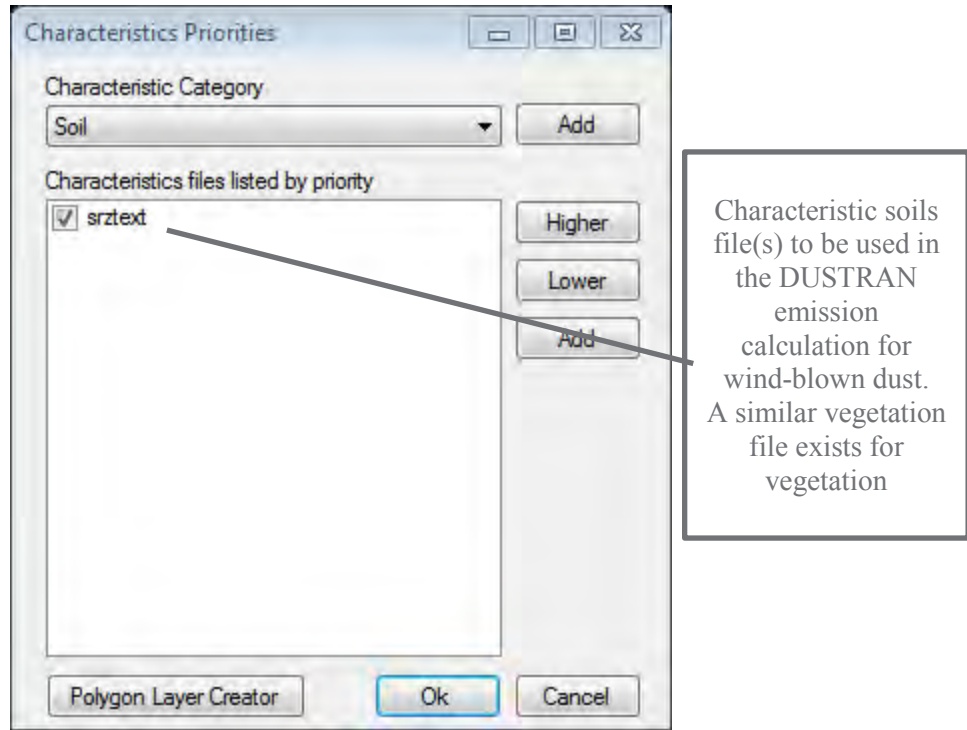
In this example, the characteristic files that are generated with the site will be used. To add soil and vegetation files, select the “Sources” tab and click on the “Characteristic Files” button (Figure 8.48):



**Figure 8.48.** Adding Soil and Vegetation Files from Dustran User Interface

After clicking the “Characteristics File” button, a form will appear that allows for the selection of both the “Soils” and “Vegetation” categories (Figure 8.49).

The standard soils file created for the site is called “srztext” and is selected by default. The file contains gridded values of Zobler soil textures for the site. Similarly, an Olson World Ecosystem gridded file, called “owe14d,” exists for the vegetation category and is selected by default. Site-specific soils and vegetation files can be added for use in the emissions calculations; however, they must use the Zobler or Olson identification system (see Windblown Dust, Section 2.3.2 for more information on these classifications).



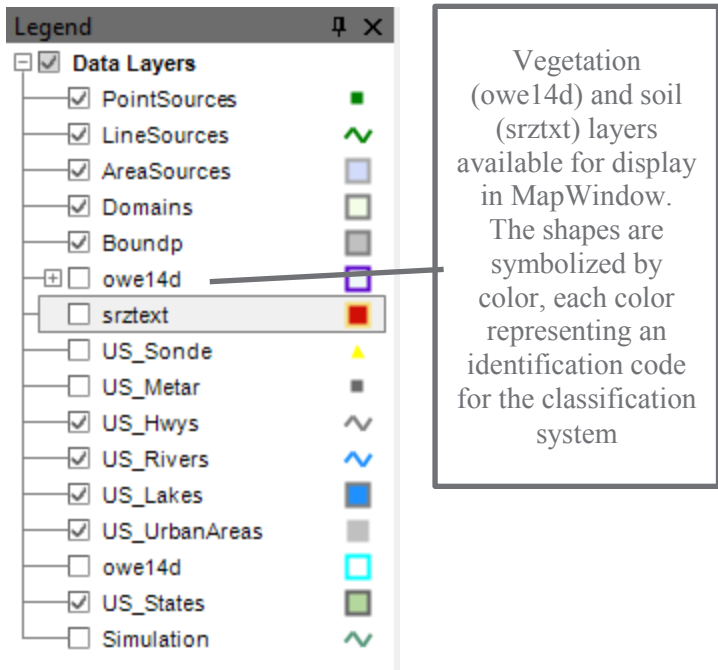
**Figure 8.49.** “Characteristics Priorities” Form

#### 8.4.6 Viewing the Soil and Vegetation Characteristic Files

Shape files, which represent the various soil and vegetation categories, can be displayed within MapWindow so that potential dust-emission regions within the domain can be readily identified. Default shape files are automatically created with the site and stored in the “TerData” directory for the site. These files can be added to MapWindow as “Layers” for display.

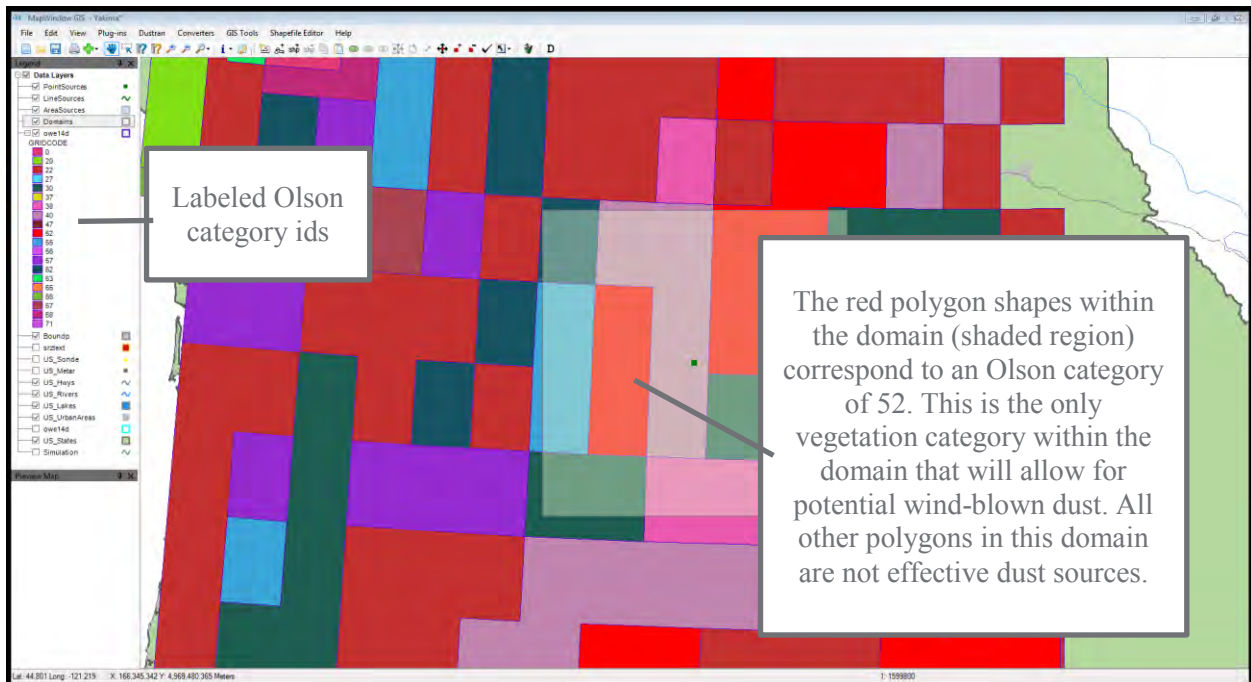
These Zobler soil and Olson World Ecosystem shape files should have already been added to the Yakima site during the creation of the tutorial site. The layers are turned off by default, but can be activated by “checking” the box next to each layer’s respective name.

To turn on the soil’s layer, “check” the layer called “srztxt” (Figure 8.50). Similarly, to turn on the vegetation layer, “check” the layer called “owe14d”:



**Figure 8.50.** Display Showing Choices for Soil and Vegetation Layers

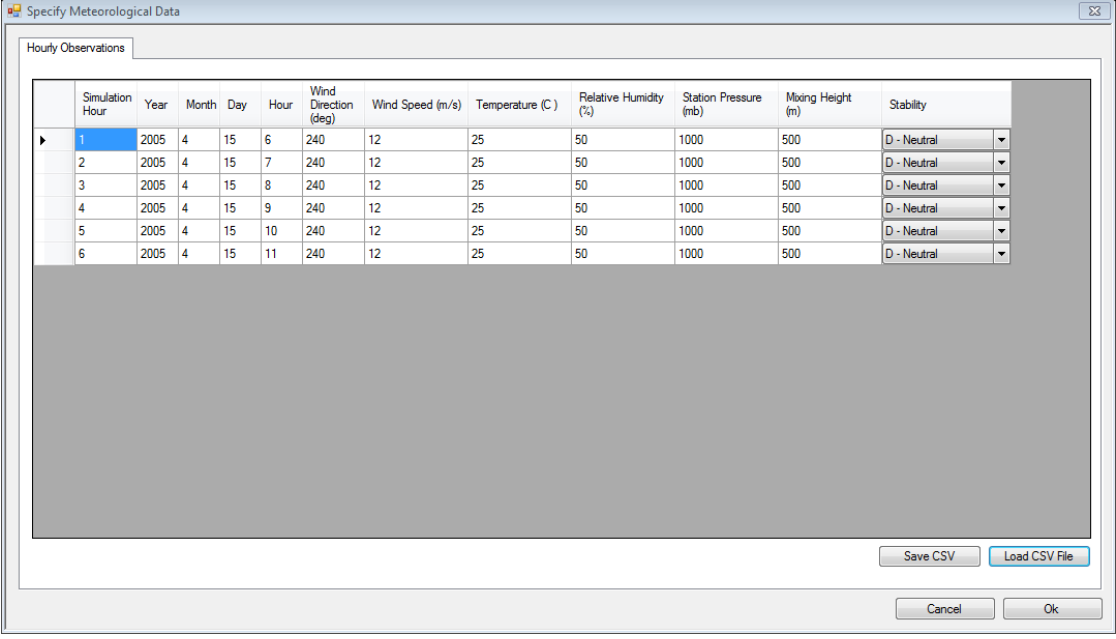
Figure 8.51 displays the Olson vegetation layer for the Yakima site. Each colored polygon represents an Olson World Ecosystem category ID, the values of which are displayed when the “Layer” is expanded. Of all the vegetation codes available, only four have been identified as allowing for effective wind-blown dust emissions. These categories, discussed in Section 2.3.2.4, include 8, 50, 51, and 52. For the Yakima site, only category 52—Cool/cold shrub, semi-desert/steppe exists within the domain; these are the red polygon regions and are the only potential source locations for wind-blown dust.



**Figure 8.51.** Display of Olson Vegetation Layer for the Yakima Site

### 8.4.7 Entering Meteorological Data

The final step before running the simulation is to set the meteorology. Click on the “Meteorology” tab within DUSTRAN and select “Single Observation” from the listbox. The “Specify Meteorological Data” form appears. Enter the meteorological parameters as shown in the form below. Select the “Atmospheric Stability” as “D – Neutral,” a wind speed of 10 m/s, and a wind direction from the southwest (240 degrees). The completed form will appear as shown in Figure 8.52:



The screenshot shows a window titled "Specify Meteorological Data" with a tab labeled "Hourly Observations". Below the tab is a table with 13 columns: Simulation Hour, Year, Month, Day, Hour, Wind Direction (deg), Wind Speed (m/s), Temperature (C), Relative Humidity (%), Station Pressure (mb), Mixing Height (m), and Stability. The table contains 6 rows of data, all with identical values. The first row is highlighted. Below the table are buttons for "Save CSV", "Load CSV File", "Cancel", and "Ok".

Simulation Hour	Year	Month	Day	Hour	Wind Direction (deg)	Wind Speed (m/s)	Temperature (C)	Relative Humidity (%)	Station Pressure (mb)	Mixing Height (m)	Stability
1	2005	4	15	6	240	12	25	50	1000	500	D - Neutral
2	2005	4	15	7	240	12	25	50	1000	500	D - Neutral
3	2005	4	15	8	240	12	25	50	1000	500	D - Neutral
4	2005	4	15	9	240	12	25	50	1000	500	D - Neutral
5	2005	4	15	10	240	12	25	50	1000	500	D - Neutral
6	2005	4	15	11	240	12	25	50	1000	500	D - Neutral

Figure 8.52. Completed “Specify Meteorological Data” Form

### 8.4.8 Running DUSTRAN

After the domain, simulation details, soil/vegetation categories, and meteorology have been entered, a wind-blown dust simulation in DUSTRAN can be made. To run DUSTRAN, click on the “Run Simulation” button (Figure 8.53).

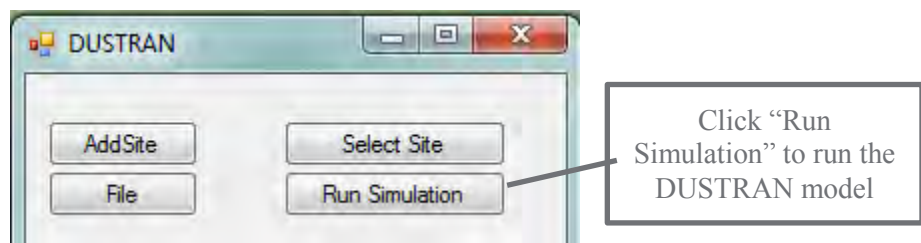
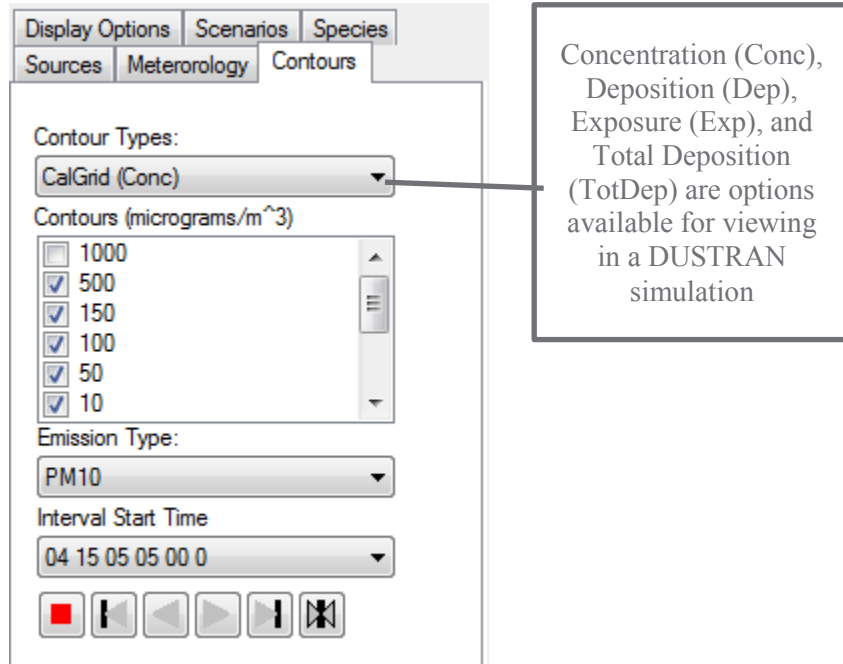


Figure 8.53. “Run Simulation” Button in DUSTRAN User Interface

### 8.4.9 Viewing Model Results

For each model time step, DUSTRAN calculates plume concentration and exposure as well as deposition and total deposition. To view a particular contour, click on the “Contours” tab and choose from the “Contour Types” listbox (Figure 8.54):



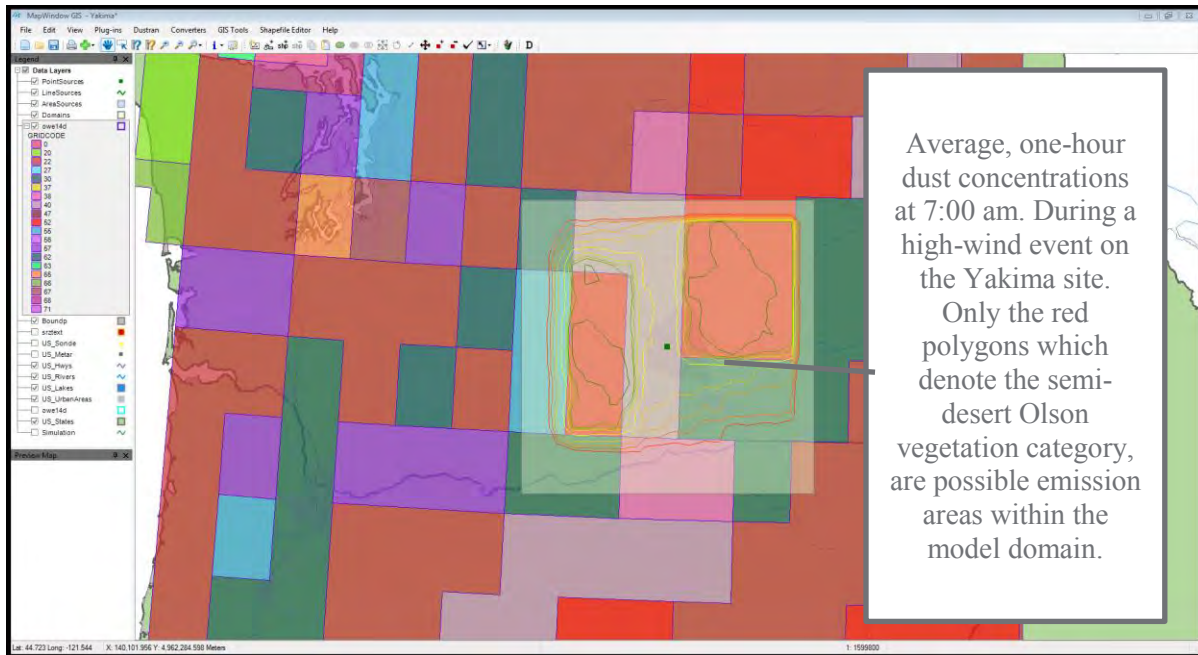
**Figure 8.54.** “Contours Types” Listbox

In this example, select “Conc” to display hourly concentrations within MapWindow.

For a given contour type, numerous “Contours” are available for display. To display a particular contour interval, check the box next to the contour value. The default selection is normally adequate for displaying the maximum extent of the plume envelope.

To view a particular time step, select an interval from the “Interval Start Time” listbox (Figure 8.55). In this example, hourly time steps are available from the start of the release (5:00 a.m. local time) till the end of the simulation. Choose the 7:00 a.m. time step, which corresponds to the one hour (7:00 a.m. till 8:00 a.m.) average concentration.

In the above image, the Olson vegetation coverage (colored polygons) and plume contours are displayed. Only the red polygons (Olson category 52—Cool/cold shrub, semi-desert/steppe) are potential source regions (as discussed previously) and are the only regions within the domain with plume contours.



**Figure 8.55.** Display of Concentration Contours for the Hour from 7-8 AM

## 9.0 References

- Allwine KJ Jr., FC Rutz, WJ Shaw, JP Rishel, BG Fritz, EG Chapman, BL Hoopes, and TE Seiple. 2006. "DUSTRAN 1.0 User's Guide: A GIS-Based Atmospheric Dust Dispersion Modeling System." PNNL-16055, Pacific Northwest National Laboratory, Richland, WA.
- Fecan F, B Marticorena, and G Bergametti. 1999. "Parameterization of the Increase of the Aeolian Erosion Threshold Wind Friction Velocity Due to Soil Moisture for Arid and Semi-arid Areas." *Annales Geophys.* 17:194-157.
- Gillette DA, and R Passi. 1988. "Modeling dust emission caused by wind erosion." *J. Geophys. Res.* 93:14233-14242.
- Gillies JA, V Etyemezian, H Kuhns, D Nikolic, and DA Gillette. 2005a. "Effect of Vehicle Characteristics on Unpaved Road Dust Emissions." *Atmos. Environ.* 39:2341-2347.
- Gillies JA, WP Arnott, V Etyemezian, H Kuhns, H Moosmuller, D DuBois, M Abu-Allaban, G Schwemmer, DA Gillette, WG Nickling, R Varma, T Wilkerson, and R Varma. 2005b. *Characterizing and Quantifying Local and Regional Particulate Matter Emissions from Department of Defense Installations*. Final report prepared for the Strategic Environmental Research and Development Program under Project CP-1191, March 2005.
- Gillies JA, V Etyemezian, H Kuhns, H Moosmuller, J Engelbrecht, J King, S Uppapalli, G Nikolich, JD McAlpine, D Zhu, M Skiba, DA Gillette, WJ Shaw, R Hashmonay. 2010. Particulate Matter Emissions Factors for Dust from Unique Military Activities. Report prepared for the Strategic Environmental Research and Development Program under Project SI-1399, June 2010.
- Irwin JS. 1998. *Interagency Workgroup on Air Quality Modeling (IWAQM) Phase 2 Summary Report and Recommendations for Modeling Long Range Transport Impacts*. EPA-454/R-98-019, Office of Air Quality Planning and Standards, Research Triangle Park, NC, 151 pp. (NTIS Accession Number PB 99-121089).
- Kuhns H, J Gillies, V Etyemezian, G Nikolich, J King, D Zhu, S Uppapalli, J Engelbrecht, and S Kohl. 2010. "Effect of Soil Type and Momentum on Unpaved Road Particulate Matter Emissions from Wheeled and Tracked Vehicles." *Aerosol Sci. Tech.* 44, 192-202.
- Nickovic S, G Kallos, A Papadopoulos, and O Kakaliagou. 2001. "A Model for Prediction of Desert Dust Cycle in the Atmosphere." *J. Geophys. Res.* 106, 18113-18129.
- Olson JS. 1992. "World Ecosystems (WE1.4). Digital Raster Data on a 10-minute Cartesian Orthonormal Geodetic 1080 × 2160 grid." In: *Global Ecosystems Database, Version 2.0*. Boulder, CO. Available at: [http://www.ngdc.noaa.gov/seg/cdroms/ged\\_ia/datasets/a05/ow.htm](http://www.ngdc.noaa.gov/seg/cdroms/ged_ia/datasets/a05/ow.htm) (accessed 08-15-2006).
- Scire JS, DG Strimaitis, and RJ Yamartino. 2000a. *A User's Guide for the CALPUFF Dispersion Model (Version 5)*. Earth Tech, Inc., Concord, MA.
- Scire JS, FR Robe, ME Fernau, and RJ Yamartino. 2000b. *A User's Guide for the CALMET Meteorological Model (Version 5)*. Earth Tech, Inc., Concord, MA.

Scire JS, RJ Yamartino, GR Carmichael, and YS Chang. 1989. *CALGRID: A Mesoscale Photochemical Grid Model Volume II – User’s Guide*. California Resources Board, Sacramento, CA.

Shaw WJ, KJ Allwine, BG Fritz, FC Rutz, JP Rishel, and EG Chapman. 2008. "An Evaluation of the Wind Erosion Module in DUSTAN." *Atmospheric Environment* 42(8):1907-1921.  
doi:10.1016/j.atmosenv.2007.11.022

Staub B, and C Rosenzweig. 1992. "Global Zobler Soil Type, Soil Texture, Surface Slope, and Other Properties. Digital Raster Data on a 1-degree Geographic (lat/long) 180 × 360 grid." In: *Global Ecosystems Database Version 2.0*. Boulder, CO, NOAA National Geophysical Data Center. Available at: [http://www.ngdc.noaa.gov/seg/cdroms/ged\\_jia/datasets/a11/sr.htm](http://www.ngdc.noaa.gov/seg/cdroms/ged_jia/datasets/a11/sr.htm) (accessed 08-15-2006).

Tegen I, and I Fung. 1994. "Modeling of mineral dust in the atmosphere: sources, transport, and optical thickness." *J. Geophys. Res.* 99:22987-22914.

Turner DB. 1994. *Workbook of Atmospheric Dispersion Estimates: An Introduction to Dispersion Modeling*. Second Edition. ISBN 1-56670-023-X. CRC Press, Inc. Boca Raton, FL, 33431.

U.S. Environmental Protection Agency (EPA). 2004a. "AERMOD: Description of Model Formulation." EPA-454/R-03-004.

U.S. Environmental Protection Agency (EPA). 2004b. "User’s Guide for the AMS/EPA Regulatory Model - AERMOD." EPA-454/B-03-001.

U.S. Environmental Protection Agency (EPA). 2004c. "User’s Guide for the AERMOD Meteorological Preprocessor (AERMET)." EPA-454/B-03-002.

U.S. Environmental Protection Agency (EPA). 2004d. "AERMOD Deposition Algorithms – Science Document." Available at: [http://www.epa.gov/scram001/7thconf/aermod/aer\\_scid.pdf](http://www.epa.gov/scram001/7thconf/aermod/aer_scid.pdf).

U.S. Environmental Protection Agency (EPA). 2005. "Compilation of Air Pollutant Emission Factors (AP-42) Fifth Edition, Volume 1: Stationary Point and Area Sources." U. S. Environmental Protection Agency, Research Triangle Park, NC. Available at <http://www.epa.gov/ttn/chief/ap42/>.

U.S. Environmental Protection Agency (EPA). 2008. "AERSURFACE User’s Guide." EPA-454/B-08-001.

U.S. Environmental Protection Agency (EPA). 2011. "User’s Guide for the AERMOD Terrain Preprocessor (AERMAP)." EPA-454/B-03-003.

U.S. Environmental Protection Agency (EPA). 2014a. "ADDENDUM: User’s Guide for the AMS/EPA Regulatory Model - AERMOD." EPA-454/B-03-001.

U.S. Environmental Protection Agency (EPA). 2014b. "ADDENDUM: User’s Guide for the AERMOD Meteorological Preprocessor (AERMET)." EPA-454/B-03-002.

## **Appendix A**

### **DUSTRAN Directory and File Documentation**

# Appendix A

## DUSTRAN Directory and File Documentation

This appendix provides detailed information about the DUSTRAN directory structure and the supporting files used within the modeling system. The section begins with an overview of the folders and files that are within the root DUSTRAN directory. Input files that are stored within each site's "StaticData" directory are then defined. These files may be edited by an advanced user who wishes to control certain options not available within the DUSTRAN interface or control the behavior of the CALMET, CALPUFF, and CALGRID models. An overview of DUSTRAN's geodatabase is then given and is provided as a reference for users who wish to interact with the model data within MapWindow. Lastly, detailed information about the structure of the dust emission input and output files (Ldustinp.txt and Ldustout.txt) are provided.

### A.1 DUSTRAN Directory

The DUSTRAN directory is the main directory used by the modeling system. This directory is normally a root directory on the machine's primary hard drive (e.g., c:\DUSTRAN). The main directory contains the executables used by the modeling system as well as the dynamic link library (DUSTRAN.dll) that integrates the modeling system with the MapWindow application. This directory also contains the individual site directories that are used within DUSTRAN simulations. The following table outlines the directories and files that are present in the DUSTRAN directory.

Name	Description
Aermap	Directory which contains the AERMAP executable.
Aermet	Directory which contain the AERMET executable.
Aemod	Directory which contains the AERMOD executable (EPA version [AERMOD.exe] and DRI version [AERMOD_DRI.exe]) and all files associated with a run including, the source emissions file, the AERMET generated surface (.sfc) and profile (.pfl) meteorological files, the AERMAP generated terrain files for receptors (.rec) and source (.src), and the AERMOD generated output file of concentration and deposition.
TerrFiles	Directory in which the land-use and terrain files used in the simulations are stored.
ModelFiles	Template model and processor input files are stored in this directory. The Add Site wizard uses these templates during the creation of a new site.
Site Directories	For each site present in the modeling system, a directory with the name of the site will be present. This directory is used to store all data that are specific to the site.
Areadust.exe	Wind-blown dust emission model executable.
CalConc.exe	Executable that processes the output of the CALPUFF and CALGRID models into the contours that are displayed in the map display of MapWindow.
Calgrid.exe	CALGRID dispersion model executable.
Calmet.exe	CALMET meteorological model executable.
Calpuff.exe	CALPUFF dispersion model executable.
Ctgproc.exe	Ctgproc land-use file processor executable.
LineDust.exe	Line and area dust-emission model executable.
Makegeo.exe	Makegeo land-use and terrain file processor executable.
Read62.exe	Upper air station meteorological data processor executable. This processor works with the Forecast System Laboratory (FSL) file format taken from the NOAA website.

<b>Name</b>	<b>Description</b>
Readmeviewer.exe	Executable that displays the readme.txt file before the first startup of DUSTRAN.
Terrel.exe	Terrain file processor executable.
Dustran.dll	DUSTRAN dynamic link library.
Calmet.inp	Input file used by the CALMET model. This file is generated by the modeling system before the execution of the model.
Calpuff.inp	Input file used by the CALPUFF model. This file is generated by the modeling system before the execution of the model.
Calgrid.inp	Input file used by the CALGRID model. This file is generated by the modeling system before the execution of the model.
Ctgproc.inp	Input file used by the Ctgproc processor. This file is generated by the modeling system before the execution of the processor.
Makegeo.inp	Input file used by the Makegeo processor. This file is generated by the modeling system before the execution of the processor.
Read62.inp	Input file used by the Read62 processor. This file is generated by the modeling system before the execution of the processor.
Terrel.inp	Input file used by the Terrel processor. This file is generated by the modeling system before the execution of the processor.
Calmet.lst	Output file generated by the CALMET model, which details the success or failure of the model run.
Calpuff.lst	Output file generated by the CALPUFF model, which details the success or failure of the model run.
Calgrid.lst	Output file generated by the CALGRID model, which details the success or failure of the model run.
Ctgproc.lst	Output file generated by the Ctgproc processor, which details the success or failure of the processor run.
Makegeo.lst	Output file generated by the Makegeo processor, which details the success or failure of the processor run.
Read62.lst	Output file generated by the Read62 processor, which details the success or failure of the processor run.
Terrel.lst	Output file generated by the Terrel processor, which details the success or failure of the processor run.
Convert.csv	Comma-separated text file containing the unit conversion factors used by the modeling system.
Apgemshelp.rtf	File that is displayed by the system when the Help option is selected.
Fileinstructions.rtf	File that is displayed by the system when the File Instructions option is selected.
Readme.rtf	File that is displayed by the “read me” viewer.
Baemarb.dat	Area-source input file used by the CALPUFF model. This file is generated by the modeling system based upon user inputs.
Lnemarb.dat	Line-source input file used by the CALPUFF model. This file is generated by the modeling system based upon user inputs.
Ptemarb.dat	Point-source input file used by the CALPUFF model. This file is generated by the modeling system based upon user inputs.
Ldustinp.txt	Line and area-source input file used by the line dust emission model. This file is generated by the modeling system based upon user input.
Ldustout.txt	Output file generated by the line dust emission model.

### **A.1.1 TerrFiles Directory**

The TerrFiles directory within the root DUSTRAN directory is used as a storage location for a default set of elevation and land-use files. These files are used by the TERREL and CTGPROC processors to generate the terrain and land-use input data required by the CALMET model. The default set of files

present in the directory represents data sets for North America. The following table details the default set of files that are present in this directory.

File Name	File Description
Nausgs2.img	U.S. Geological Survey (USGS) Land Use/Land Cover Scheme; used as input to the CTGPROC land-use processor for CALMET.
W100N40.dem	Global topographic digital elevation models with a horizontal grid spacing of 30 arc seconds (approximately 1 kilometer). Also known as GTOPO30 files, the files are tiled for ease-of-distribution. The four files listed in this directory spatially cover all of North America.
W100N90.dem	
W140N40.dem	
W140N90.dem	

### A.1.2 ModelFiles Directory

The ModelFiles directory within the root DUSTRAN directory is used to store default template input files that are used by the preprocessors, CALMET, CALPUFF, and CALGRID models. When a new site is added to DUSTRAN using the “Add Site” wizard, these files are automatically copied into the new site’s StaticData directory. The following table lists and describes the files that are stored in the ModelFiles directory.

File Name	File Description
Cal.par	Template copy of the default Cal.par file. The Cal.par file contains various model input controls that are not available from within the DUSTRAN interface. This template file is copied by the “Add Site” wizard and placed into the StaticData directory of the new site.
CalGeo.inp	CalGeo.inp is a template copy of the default input file for the TERREL, CTGPROC, and MAKEGO terrain and land-use preprocessing programs in DUSTRAN. The file is copied by the “Add Site” wizard and placed into the StaticData directory of the new site.
Calgrid.inp	Calgrid.inp is a template copy of the default input file for the CALGRID dispersion model in DUSTRAN. The file is copied by the “Add Site” wizard and placed into the StaticData directory of the new site.
Calmet.inp	Calmet.inp is a template copy of the default input file for the CALMET meteorological processor in DUSTRAN. The file is copied by the “Add Site” wizard and placed into the StaticData directory of the new site.
Calpuff.inp	Calpuff.inp is a template copy of the default input file for the CALPUFF dispersion model in DUSTRAN. The file is copied by the “Add Site” wizard and placed into the StaticData directory of the new site.
Calpost.inp	Calpost.inp is a template copy of the default input file for the CALPOST post-processor in DUSTRAN. The file is copied by the “Add Site” wizard and placed in the StaticData directory of the new site.
Pgems3.par	Template copy of the default Pgems3.par file used by the individual simulation sites. The file is copied by the “Add Site” wizard and placed into the StaticData directory of the new site.

### A.1.3 Site Directories

When a new site is added through the “Add Site” wizard in DUSTRAN, a new directory is created for the site and is located within the DUSTRAN root directory. The site directory is used to store site-specific model input and output files. In addition, the site directory stores site-specific data that are used by the models. Normally, the data are stored in sub-directories based upon the type of preprocessor or model that uses or generates the data. For example, data associated with the meteorological models and processors are stored in the MetData, MetOut, and MetRaw directories. The following table details the directories and files that are found within each site directory present in the modeling system.

Name	Description
------	-------------

MetData	Directory used to store the meteorological data that have been processed for use in a simulation.
MetOut	Directory used to store the output files generated by the CALMET meteorological model. The files contain the gridded meteorological fields used by the CALPUFF and CALGRID dispersion models.
MetRaw	Default directory used to store historic meteorological data for a site that may be used in a simulation.
RsData	Directory used to store the run-specification files that are generated by DUSTRAN for each simulation.
StaticData	Directory used to store the model-input template files as well as the data associated with the sources and domains entered into the modeling system.
TDMOut	Directory used to store the data generated by the dispersion models during a simulation run.
TerData	Directory that can be used to store terrain and land-use files that are specific to the site. These files can be used instead of the default files found in the root TerrFiles directory, providing the static Calgeo.inp file for the site is modified to reflect the type and path of the new terrain files.
TerOut	Directory used to store the data generated by the land-use and terrain processors.
*.mdb	Access database that stores information related to the site, such as source information.
*.mwprj	MapWindow project file that stores the settings of the map display for the site.
PGEMS3.ini	Text file that stores the physical path of all the site-specific subdirectories list above.

### A.1.3.1 MetData

The MetData directory within each site directory is used to store the data that are used as input by the meteorological model and processors. The data found in this directory include upper-air observations, surface observations, and files containing station characteristics.

File Name	File Description
Upn.dat	Upper air station meteorological data file used as input by the CALMET model. There will be one Upn.dat file present for each upper-air station selected for use during the simulation run.
Surf.dat	Surface-station meteorological data file used as input by the CALMET model.
*.upr	Upper-air-station meteorological data file generated from FSL data retrieved from the NOAA website.
*.unf	This text file contains a listing of the upper-air stations available for a site as well as descriptive information about each station. The station information found in this file includes station name, station ID, UTM coordinate location, and longitude and latitude of the station as well as the elevation.
*.snf	This text file contains a listing of the surface stations available for a site as well as descriptive information about each station. The station information found within this file includes station name, station ID, UTM coordinate location, and longitude and latitude of the station as well as the elevation of the station. The .snf file also contains the anemometer height used for the readings at the station.

### A.1.3.2 MetOut

The MetOut directory within each site directory is used to store the different output files generated from the results of the meteorological model.

<b>File Name</b>	<b>File Description</b>
*.vec	Comma-separated text file containing wind-vector data used to generate the wind fields that are displayed within the MapWindow map display.
WindBlownData.txt	Comma-separated text file containing meteorological grid data pulled from the output of CALMET. These data are required as input by the wind-blown dust-emission model.
*.dat	Binary output data file generated by the CALMET meteorological model.

### **A.1.3.3 MetRaw**

The MetRaw directory within each site directory is used to store the historical meteorological data that are available to the modeling system for a specific site. Currently, the modeling system is set up to process historical data for the Yakima and Fort Irwin simulation sites. While this directory is provided by default for each site, users are given the ability to store historical meteorological data in the directory of their choice whether they are located in the site or DUSTRAN directories. Historical data found in this directory are normally site specific and will not transfer across sites.

### **A.1.3.4 RsData**

The RsData directory within each site directory stores the run-specification file that is generated by DUSTRAN each time a site simulation is executed. Through this directory, each of the models is given access to the specification file to retrieve inputs entered by the user before the simulation starts.

<b>File Name</b>	<b>File Description</b>
*.rs	The run specification file is a comma-separated text file that contains the data entered by the user through the user interface.

### **A.1.3.5 StaticData**

The StaticData directory within each site directory contains the template input files that are used by the modeling system to create the actual input files used by the models and processors. The directory also contains the static parameter file Cal.par, which is used to hold model-run parameter data that are not accessible through the user interface. The Domain.dat and Sources.dat files are also stored within this directory and are used by the modeling system to track the characteristics of the domains and sources that have been entered for the site. The following table provides the details of the files that are stored within the StaticData directory.

<b>File Name</b>	<b>File Description</b>
Aermap.inp	Text file for the AERMAP model preprocessor. This file is used to retrieve the terrain and hill height scale factors for AERMOD model receptors and terrain heights for AERMOD sources. Terrain and hill height information is determined from a raster image, which is generated during site creation.
CalGeo.inp	Text file containing input sections for the Terrel, Ctgproc, and Makegeo processors. These input sections contain the default values for the individual processors and are used in the creation of the actual input file required for running the processors.
CALGRID.inp	Text file containing the default input parameters for the CALGRID model. This file is used in the creation of the actual input file for executing the CALGRID model for a simulation.
CALMET.inp	Text file containing the default input parameters for the CALMET model. This file is used in the creation of the actual input file for executing the CALMET model for a simulation.

<b>File Name</b>	<b>File Description</b>
CALPUFF.inp	Text file containing the default input parameters for the CALPUFF model. This file is used in the creation of the actual input file for executing the CALPUFF model for a simulation.
Cal.par	A static parameter file that contains inputs that are normally not changed (i.e., are considered static) for a modeling run, but can be modified for testing or fine tuning of the modeling system.
StationAlias.txt	Text file containing alias information for the National Training Center (NTC) surface station data. Currently, this file is only used for the Fort Irwin site.

### **A.1.3.6 TDMOut**

The TDMOut directory within each site directory is used to store the output data generated by the CALGRID and CALPUFF dispersion models. The directory also contains the contouring text files that are generated by the CalConc processor based on the results generated by the dispersion models. Data contained within the .ccn and .crd files are used by the modeling system to create the contours that are shown on the DUSTRAN map display following the successful execution of a simulation. The file types that are found within this directory are listed in the following table.

<b>File Type</b>	<b>File Type Description</b>
*.ccn	Text file containing the concentration contour data generated from the output files of the CALGRID or CALPUFF models.
*.CON	Binary output file generated by the CALPUFF model.
*.crd	Text file containing the contouring grid coordinates.
*.dat	Binary output file generated by the CALGRID model.
*.dep	Text file containing the deposition contour data generated from the output files of the CALGRID or CALPUFF models.
*.exp	Text file containing the exposure contour data generated from the output files of the CALGRID or CALPUFF models.
*.pst	Text file containing the AERMOD deposition and concentration results.
*.tdp	Text file containing the total deposition contour data generated from the output files of the CALGRID or CALPUFF models.

### **A.1.3.7 TerOut**

The TerOut directory within each site directory is used to store the output generated by the three terrain processors used by the modeling system. Output from the TERREL, CTGPROC, and MAKEGEO processors is stored within this directory following each successful simulation executed by the modeling system. The following table details the files that are stored within this directory.

<b>File Type</b>	<b>File Type Description</b>
*.out	Output file generated by the TERREL processor.
*.dat	Output files generated by the CTGPROC and MAKEGEO processors.

## **A.2 Site Directory Static Data Files**

### **A.2.1 Cal.par File**

Several parameters used by the DUSTRAN modeling system are not directly accessible through the DUSTRAN interface. Instead, these parameters are stored in a text file called “cal.par.” These

parameters change infrequently and were intentionally omitted from the interface to minimize screen clutter and accidental user revisions.

The cal.par file is an ASCII, comma-delimited text file and can be opened in any standard text editor. The file is stored in the “StaticData” directory for each site, and the values in the file apply to that site. For the most part, the file is self-describing; variable-specific comments are provided before or on the line of the actual variable.

A sample cal.par file is provided in the following section. For clarity, each line (excluding lines that wrap) is numbered within the {} brackets. The line numbers are used to reference the table in Section A.2.1.2, which provides a detailed description of each line in the sample file. The {} brackets and line numbers do not exist in an actual cal.par file. Items in bold are comments and are not used by the code.

### A.2.1.1 Example Cal.par File

```
{1} Meteorological parameters to construct profile from single observation and construct surface met file
{2} [WS, WD, Stability specified through single observation input window within DUSTRAN interface]
{3} A B C D E F G
{4} 0.07,0.07,0.10,0.15,0.35,0.35,0.35,Prural [Power Law exponents for wind profile; currently used]
{5} 0.15,0.15,0.20,0.25,0.30,0.30,0.30,Purban [Power Law exponents for wind profile]
{6} -0.025,-0.020,-0.015,-0.010,0.010,0.025,0.040,DtDz [Temperature lapse rate vs. stability]
{7} 0.,20.,50.,100.,500.,2000.,9000., zface heights used in the Calmet, Calpuff, and Calgrid models
{8} 10,0 Z0, ZTOP [Height of bottom and top sounding values (m agl)]
{9} 11,nHts [Number of heights in sounding]
{10} 100,ICEIL [Ceiling height (hundreds of feet)]
{11} 0,ICC [Opaque sky cover (tenths)]
{12} 25,TEMPK [Surface air temperature (Deg C)]
{13} 50,IRH [Relative humidity (percent)]
{14} 1000,PRES [Station pressure (mb)]
{15} 1000,WATDENSE [Density of water (g/m^3)]
{16} 0,IPCODE [Precipitation code (0=no precip; 1-18=liquid; 19-45=frozen)]
{17} T,WSPROF [T - Power law profile; F - Constant wind speed with height]
{18} F,MM5 data used check
{19} F,Advanced user Deposition flag; if T, then the ability to set deposition velocities is turned on
{20} 50,50, Number of x and y grid points for CALPUFF run
{21} 20,20, Number of x and y grid points for CALGRID run
{22} 100,100, Number of x and y grid points for AERMOD run
{23} T, Flag used to set if the Aermod simulation will or will not use polar grids
{24} Species names, molecular weight, particle mean diameter, particle standard deviation, default user-
defined deposition velocity
{25} 4,NumSpecs [Number of species present] Molecular weight does not appear to be used by Calpuff
{26} PM10,0.0,10.0,1.0,0.0
{26} PM2.5,0.0,2.5,1.0,0.0
{26} PM15,0.0,15.0,1.0,0.0
{26} PM30,0.0,30.0,1.0,0.0
{27} Point Source Parameter Units,8,
{28} Parameter,Release Height,Exit Velocity,Exit Temperature,Stack Diameter,Building Cross Section,Initial
Horizontal Plume Size,Initial Vertical Plume Size,Release Rate,
{29} Default Value,0,0,25,1,0,1,1,1,
{30} User Units,m,m/s,C,m,m^2,m,m,g/s,
{31} Model Units,m,m/s,C,m,m^2,m,m,g/s,
{32} Conversion Factor,1,1,1,1,1,1,1,1,
{33} Min Value,0,0,inf,0,0,1,1,0,
```

{34} Max Value,inf,inf,inf,inf,inf,inf,inf,inf,  
 {35} Range String,Release Height >= 0.0,Exit Velocity >= 0.0,No Boundaries,Stack Diameter >= 0,Building Cross  
 Section >= 0.0,Initial Horizontal Plume Size 0.0,Initial Vertical Plume Size > 0.0,Release Rate >= 0.0,  
 {36} Line Source Parameter Units,3,  
 {37} Parameter,HTL,ELEVL,QEMITL,  
 {38} Default Value,0,0,0,  
 {39} User Units,m,m,g/s/m,  
 {40} Model Units,m,m,g/s/m,  
 {41} Conversion Factor,1,1,1,  
 {42} Min Value,0,0,0,  
 {43} Max Value,inf,inf,inf,  
 {44} Range String,HTL >= 0.0,ELEVL >= 0.0,QEMITL >= 0.0,  
 {45} Area Source Parameter Units,7,  
 {46} Parameter,HT,ELEV,TEMPK,WEFF,REFF,SIGZ,QEMIT,  
 {47} Default Value,0,0,25,1,1,1,  
 {48} User Units,m,m,C,m/s,m,m,g/s  
 {49} Model Units,m,m,K,m/s,m,m,g/s  
 {50} Conversion Factor,1,1,1&0,1,1,1,1,  
 {51} Min Value,0,0,inf,1,1,1,0,  
 {52} Max Value,inf,inf,inf,inf,inf,inf,inf,  
 {53} Range String,HT >= 0.0,ELEV >= 0.0,No Boundaries,WEFF >= 1.0,REFF >= 1.0,SIGZ >= 1.0,QEMIT >= 0.0,  
 {54} Meteorology Parameter Units,3,  
 {55} Parameter,Wind Speed,Wind Direction,Mixing Height,  
 {56} Default Value,2.2,270,500,  
 {57} User Units,m/s,No Unit,m,  
 {58} Model Units,m/s,No Unit,m,  
 {59} Conversion Factor,1,1,1,  
 {60} Min Value,0,0,0,  
 {61} Max Value,inf,360,inf,  
 {62} Range String,Wind Speed >= 0.0,Wind Direction >= 0 and Wind Direction <= 360,Mixing Height >= 0.0,  
 {63} Line Source Vehicle Parameter,4,  
 {64} Parameter,Vehicle SpeedL,Vehicle WeightL,Road LengthL,Distance TraveledL,  
 {65} Default Value,50,3000,0.0,0.0,  
 {66} User Units,km/hr,kg,km,km,  
 {67} Model Units,km/hr,kg,km,km,  
 {68} Conversion Factor,1,1,1,1,  
 {69} Min Value,0,0,0,0,  
 {70} Max Value,inf,inf,inf,inf,  
 {71} Range String,Vehicle Speed >= 0.0,Vehicle Weight >= 0.0,Road Length >= 0.0,Distance Traveled >= 0.0,  
 {72} Area Source Vehicle Parameter,4,  
 {73} Parameter,Vehicle Speed,Vehicle Weight,Polygon Area,Distance Traveled,  
 {74} Default Value,50,3000,0.0,0.0,  
 {75} User Units,km/hr,kg,km^2,km,  
 {76} Model Units,km/hr,kg,km^2,km,  
 {77} Conversion Factor,1,1,1,1,  
 {78} Min Value,0,0,0,0,  
 {79} Max Value,inf,inf,inf,inf,  
 {80} Range String,Vehicle Speed >= 0.0,Vehicle Weight >= 0.0,Polygon Area > 0.0,Distance Traveled >= 0.0,  
 {81} 1.0E+6,Contours (micrograms/m^3),**Unit label and conversion factor for the concentration contour labels**  
 {82} 1.0E+6,Contours (micrograms/m^2/sec),**Unit label and conversion factor for the deposition contour labels**  
 {83} 1.0E+6,Contours (micrograms-sec/m^3),**Unit label and conversion factor for the exposure contour labels**  
 {84} 1.0E+6,Contours (micrograms/m^2),**Unit label and conversion factor for the total deposition contours**  
 {85} 1.0E-15,**Minimum contour level used by Calconc suggest 3 orders of magnitude smaller than the  
 smallest specified contour level**  
 {86} 11,**Number of contour levels to be calculated**

```

{87} 1.0E-10
{87} 1.0E-9
{87} 1.0E-8
{87} 1.0E-7
{87} 1.0E-6
{87} 10.0E-6
{87} 50.0E-6
{87} 100.0E-6
{87} 150.0E-6
{87} 500.0E-6
{87} 100.0E-5
{88} 17, NUMVEHCODES [Number of vehicle integer codes]
{89} 1,1176,Dodge Neon, 2002 Civilian vehicle with Eagle GA Touring M+S P185/165R 85T tires
{89} 2,1759,Dodge Caravan,2002 Civilian vehicle with GoodYear Integrity M+S 215/70R15 98S tires
{89} 3,1516,Ford Taurus,2002 Civilian vehicle with Firestone M+S P215/60R16 94T tires
{89} 4,3100,GMC G20 Van, DRI TRAKER vehicle used for measuring dust emissions in real time
{89} 5,5227,GMC C5500, 1999 Civilian vehicle 6 wheels with GoodYear and Michelin tires
{89} 6,2445,M998 HMMWV, Military Vehicle 4 wheels with tires
{89} 7,14318,M923A2 (5-Ton), Military Vehicle 2 front wheels and 8 rear wheels on dual axles
{89} 8,8060,M1078 LMTV, 2.5 Ton Military vehicle with 4 wheels and tires
{89} 9,20000,M977 HEMTT, Military vehicle with 8 wheels and tires
{89} 10,23636,Freightliner, Tractor trailer rig with 22 wheels and tires
{89} 11,8982, M915A4 Truck, Military line-haul wheeled tractor without trailer
{89} 12,10000,M113 APC,Tracked military vehicle armored personnel carrier
{89} 13,12727,M577 Command Post,Tracked military vehicle armored mobile command post
{89} 14,23636,M2 Bradley,Tracked military vehicle armored infantry fighting vehicle
{89} 15,25000,M270 MLRS,Tracked military vehicle armored multiple launch rocket system
{89} 16,50500,M88 Hercules,Tracked military vehicle armored heavy equipment recovery vehicle
{89} 17,60000,M1A1 Abrams,Tracked military vehicle battle tank
{90} Calpuff polar grid information
{91} 1
{92} POLAR_GRD
{93} 36,10,200.,400.,800.,1500.,2500.,3500.,4500.,5500.,6500.,7500.,
{94} 3,1000,number of grid spacings used to create area source grids - resolution of area source grid
(*** Note Calpuff will only accept up to 4000 discrete receptors ***)
{95} 2,2, Wind vector resolution, max windspeed
{96} 1.0E-20, Initial concentration value for CalGrid model
{97} 1,Model run flag 1=Calpuff run 2=Calgrid run 3=Both models run
{98} 1,Run Calgrid in wind blown dust mode 1=Run wind blown 0=Run without windblown dust
{99} 0.0,soil moisture (water mass / soil mass)
{100} http://www.irwin.army.mil/weather/WXdata.txt
{101}

```

[http://raob.fsl.noaa.gov/intl/GetRaobs.cgi?shour=All+Times&ltype=All+Levels&wunits=Knots&access=WBAN+Station+Identifier&view=NO&osort=Station+Series+Sort&offormat=FSL+format+\(ASCII+text\)](http://raob.fsl.noaa.gov/intl/GetRaobs.cgi?shour=All+Times&ltype=All+Levels&wunits=Knots&access=WBAN+Station+Identifier&view=NO&osort=Station+Series+Sort&offormat=FSL+format+(ASCII+text))

### A.2.1.2 Cal.par File Description

Line Number	Data Type	Description
1	String	Wind profile description header.
2	String	Wind profile description header.
3	String	Wind profile description header.
4	Floating Point	Rural Power Law exponents for wind profile. The wind profile is generated for simulations using the single observation meteorology option. (defaults Pr1=0.07, Pr2=0.07, Pr3=0.10, Pr4=0.15, Pr5=0.35, Pr6=0.35, Pr7=0.35)

Line Number	Data Type	Description
5	Floating Point	Urban Power Law exponents for wind profile. The wind profile is generated for simulations using the single observation meteorology option. (defaults Pu1=0.15, Pu2=0.15, Pu3=0.20, Pu4=0.25, Pu5=0.30, Pu6=0.30, Pu7=0.30)
6	Floating Point	Potential temperature lapse rate vs. stability for wind profile. The wind profile is generated for simulations using the single observation meteorology option. (defaults Pt1=-0.025, Pt2=-0.20, Pt3=-0.015, Pt4=-0.010, Pt5=0.010, Pt6=0.025, Pt7=0.40)
7	String	Comma-separated list of heights (meters above ground) for CALMET's vertical grid. The CALMET-derived parameters occur at the mid-point between successive heights. The number of heights is determined from the number of values listed minus one (the zero value).
8	Floating Point	Height (meters above ground level [agl]) of lowest observation in upper-air observation profile for "Single Observation" meteorology
8	Floating Point	Height (meters agl) of the top observation in the upper-air observation profile for "Single Observation" meteorology. If ZTOP equals 0.0, then the default value found in the static Calmet.inp file is used.
9	Integer	Number of heights in the upper-air observation profile, for "Single Observation" meteorology.
10	Integer	Default ceiling height (hundreds of feet), for "Single Observation" meteorology.
11	Integer	Default opaque sky cover (tenths), for "Single Observation" meteorology.
12	Floating Point	Default surface air temperature in (deg C), for "Single Observation" meteorology.
13	Integer	Default relative humidity (%), for "Single Observation" meteorology.
14	Floating Point	Default station pressure (mb), for "Single Observation" meteorology.
15	Floating Point	Density of water (kg/m <sup>3</sup> ). Used in the conversion of AGDISP output to emission rates.
16	Integer	Precipitation code (0 = no precipitation, 1 – 18 = liquid, 19 – 45 = frozen).
17	Character (True / False)	Power law profile flag (T = Power law profile, F = Constant wind speed with height). [(default T)]
18	Character (True / False)	Flag designating whether or not MM5 data are to be used by the modeling system.
19	Character (True / False)	Flag designating whether to turn on the advanced user parameters for the calculation of deposition. If this flag = T, then the user has the ability to enter geometric standard deviations and deposition velocities.
20	Integer	Grid spacing and number of receptor locations in the X and Y directions for a CALPUFF simulation.
21	Integer	Grid spacing and number of receptors locations in the X and Y directions for a CALGRID simulation.
22	Integer	Grid spacing and number of receptors locations in the X and Y directions for a AERMOD simulation.
23	Character (T/F)	Flag used to set if the AERMOD simulation will or will not use polar grids
24	String	Species data header.
25	Integer	Number of species available in DUSTRAN.
26	String	Name of the species, molecular weight, particle mean diameter, particle standard deviation, default deposition velocity
27	Integer	Number of parameters used by a point source
28	String	Label strings for point-source parameters separated by commas.
29	String	Default values for point-source parameters separated by commas.
30	String	User units for point-source parameters separated by commas.
31	String	Model units for point-source parameters separated by commas.
32	String	Conversion values for point-source parameters separated by commas.
33	String	Minimum values for point-source parameters separated by commas.
34	String	Maximum values for point-source parameters separated by commas.

<b>Line Number</b>	<b>Data Type</b>	<b>Description</b>
35	String	Strings giving the range of values that are appropriate for point-source parameters separated by commas.
36	Integer	Number of parameters used by a line source.
37	String	Label strings for line-source parameters separated by commas.
38	String	Default values for line-source parameters separated by commas.
39	String	User units for line-source parameters separated by commas.
40	String	Model units for line-source parameters separated by commas.
41	String	Conversion values for line-source parameters separated by commas.
42	String	Minimum values for line-source parameters separated by commas.
43	String	Maximum values for line-source parameters separated by commas.
44	String	Strings giving the range of values that are appropriate for line-source parameters separated by commas.
45	Integer	Number of parameters used by an area source.
46	String	Label strings for area-source parameters separated by commas.
47	String	Default values for area-source parameters separated by commas.
48	String	User units for area-source parameters separated by commas.
49	String	Model units for area-source parameters separated by commas.
50	String	Conversion values for area-source parameters separated by commas.
51	String	Minimum values for area-source parameters separated by commas.
52	String	Maximum values for area-source parameters separated by commas.
53	String	Strings giving the range of values that are appropriate for area-source parameters separated by commas.
54	Integer	Number of parameters used for meteorology input.
55	String	Label strings for meteorology input parameters separated by commas.
56	String	Default values for meteorology input parameters separated by commas.
57	String	User units for meteorology input parameters separated by commas.
58	String	Model units for meteorology input parameters separated by commas.
59	String	Conversion values for meteorology input parameters separated by commas.
60	String	Minimum values for meteorology input parameters separated by commas.
61	String	Maximum values for meteorology input parameters separated by commas.
62	String	Strings giving the range of values that are appropriate for meteorology input parameters separated by commas.
63	Integer	Number of parameters used for line-source vehicle input.
64	String	Label strings for line-source vehicle input parameters separated by commas.
65	String	Default values for line-source vehicle input parameters separated by commas.
66	String	User units for line-source vehicle input parameters separated by commas.
67	String	Model units for line-source vehicle input parameters separated by commas.
68	String	Conversion values for line-source vehicle input parameters separated by commas.
69	String	Minimum values for line-source vehicle input parameters separated by commas.
70	String	Maximum values for line-source vehicle input parameters separated by commas.
71	String	Strings giving the range of values that are appropriate for line-source vehicle input parameters separated by commas.
72	Integer	Number of parameters used for area-source vehicle input.
73	String	Label strings for area-source vehicle input parameters separated by commas.
74	String	Default values for area-source vehicle input parameters separated by commas.
75	String	User units for area-source vehicle input parameters separated by commas.
76	String	Model units for area-source vehicle input parameters separated by commas.
77	String	Conversion values for area-source vehicle input parameters separated by commas.
78	String	Minimum values for area-source vehicle input parameters separated by commas.
79	String	Maximum values for area-source vehicle input parameters separated by commas.
80	String	Strings giving the range of values that are appropriate for area-source vehicle input parameters separated by commas.

Line Number	Data Type	Description
81	Floating Point, String	Conversion factor for the concentration contour labels, Unit label for the concentration contour labels
82	Floating Point, String	Conversion factor for the deposition contour labels, Unit label for the deposition contour labels.
83	Floating Point, String	Conversion factor for the exposure contour labels, Unit label for the exposure contour labels
84	Floating Point, String	Conversion factor for the total deposition contour labels, Unit label for the total deposition contour labels
85	Floating Point	Minimum concentration level to be used in the processing of the contours from the generated results.
86	Integer	The number of contour levels to be processed from the generated results.
87	Floating Point	The individual contour levels to be used in the processing of the generated results.
88	Integer	Number of vehicles available in the modeling system.
89	Integer, Floating Point, String, String	Vehicle ID number, Vehicle weight, Vehicle name, Vehicle description
90	String	Polar grid header line.
91	Integer	Number of polar grids to be used in the simulation run.
92	String	Name of the polar grid to be used in the simulation run.
93	Integer, Integer, Floating Point	Number of radial distances used in the generation of the point-source polar grids, Number of arc distances (NARCS) used in the generation of the point-source polar grids, Comma-separated list of arc distances used in the generation of the point-source polar grids (there must be NARCS present in the file)
94	Integer, Integer	Parameters used to specify “sub-grid” Cartesian receptor grids. The first is the number of “main” Cartesian grid points extending beyond the area-source boundaries, and the second number is the spacing (m) between the “sub-grid” receptor points.
95	Integer, Floating Point	Two parameters for setting the resolution of the wind vector field displayed on the map and for setting the maximum wind speed used in the creation of the wind vector field. The first parameter indicates to display every “n <sup>th</sup> ” vector, and the second parameter is the magnitude of the vector spanning the distance between the vector output grid points.
96	Floating Point	Initial concentration value to be used by the CALGRID model.
97	Integer	Flag used to determine which dispersion model to execute for the simulation run. (1=CALPUFF run 2=CALGRID run 3=Both models run). Currently, model selection is being handled by the interface (i.e., Source Emissions = CALPUFF; Windblown Dust = CALGRID) and not through this flag.
98	Integer	Flag used to determine whether the CALGRID run is to be run in the windblown mode. (1=Run wind-blown model 0=Run CALGRID without windblown dust)
99	Floating Point	Soil moisture for each quadrant. (water mass/soil mass)
100	String	URL address of the website used to retrieve surface meteorological data for NTC.
101	String	URL address of the website used to retrieve upper air station data for NTC.

## A.2.2 Calmet.inp

The CALMET input file (Calmet.inp) is located in the “StaticData” directory for each site within DUSTRAN and is the template input file for CALMET. Its contents are merged with select-user input from the DUSTRAN interface for each simulation. Many of the parameters contained within Calmet.inp control certain aspects of the CALMET-derived gridded wind field and boundary-layer parameters. These parameters are not available from the DUSTRAN interface and can only be edited via the static file.

The static Calmet.inp file normally contains the most ideal parameter settings for a given site. However, there may be times when the user wants to examine the effects of modifying certain parameter settings. Extreme caution should be used when changing any parameter in the static Calmet.inp file, as it may cause unrealistic results. Each parameter in the Calmet.inp is documented in detail in the CALMET user's guide (Scire et. al. 2000b). The following discussion highlights those parameters that are generally considered the most important relative to affecting the gridded fields. Generally, these parameters are from the section "INPUT GROUP 5 – Wind Field Options and Parameters," and control the three-dimensional gridded wind field that is derived from surface and upper-air observations.

<b>CALMET Parameter</b>	<b>Allowed Values</b>	<b>Recommended Value</b>	<b>Description</b>
IWFCOD	0 (No) or 1 (Yes)	1 (Yes)	Wind Field Model Option—This parameter allows the CALMET model to be run as a diagnostic model and include the effects of terrain, or only perform objective analysis on the observations without regards to the underlying terrain. It is recommended the diagnostic model be used (IWFCOD = 1). The objective analysis might be considered if there are a high number of meteorological stations in an otherwise relatively flat domain.
IKINE	0 (No) or 1 (Yes)	0 (No)	Compute Kinematic effects—This parameter is intended to provide a characterization of terrain effects on vertical wind speed. CALMET then adjusts the horizontal wind speed components for mass continuity. This parameter has been found to cause unrealistic results in the horizontal wind field and so use of this parameter is discouraged.
IFRADJ	0 (No) or 1 (Yes)	1 (Yes)	Compute Froude number adjustment—This parameter is used to calculate the effects of terrain blocking on the horizontal wind field. A Froude number is calculated at each grid node in CALMET and if the value is below a certain criteria, the flow is considered blocked and is modified tangent to the terrain. The use of this parameter is recommended, particularly for domains in complex terrain.
ISLOPE	0 (No) or 1 (Yes)	1 (Yes)	Compute slope flow effects—This parameter calculates the wind flows created by sloping terrain, such as cold-air drainage flows. The use of this parameter is recommended, particularly for domains in complex terrain under calm, stable conditions.
IEXTRP	1 (-1) or 2 (-2) or 3 (-3) or 4 (-4)	-2 or -4	Extrapolate surface wind observations to upper levels—Surface winds can be extrapolated into the vertical to augment upper-air data when creating the three-dimensional gridded wind field in CALMET. This parameter allows the user to select the method of extrapolation: 1 (no extrapolation), 2 (power-law), 3 (user-factors), 4 (similarity theory). Out of the four methods, the power-law or similarity theory methods of extrapolation are recommended. Only experienced users should employ the user factors, as it requires a thorough understanding of the site to implement correctly. The negative sign preceding the value of IEXTRP has special meaning—it directs CALMET to ignore the first-level winds in the upper-air data when creating the surface layer wind field (i.e., use surface station data only).
ICALM	0 (No) or 1 (Yes)	0 (No)	Extrapolate surface winds even if calm— Under calm conditions, surface winds may not provide a realistic representation of the winds aloft, and extrapolation of the

CALMET Parameter	Allowed Values	Recommended Value	Description
			surface winds may not be desirable. It is recommended that the surface winds not be extrapolated under calm conditions.
RMAX1 RMAX2	User-specified (km)	RMAX1 (50 to 100 km)  RMAX2 (100 to 500 km)	Maximum radius of influence over land—This parameter is the radius of influence at the surface (RMAX1) and aloft (RMAX2) that observed winds have on derived winds at each grid node. CALMET uses a $1/r^2$ interpolation procedure when merging observations with the derived flow. These radii control the maximum extent to include observations at each node.
LVARY	T (True) or F (False)	F	Use varying radius of influence—This parameter increases the radius of influence parameters (RMAX1 and RMAX2) until an observation station is located and can be used in the $1/r^2$ interpolation procedure. This parameter is not recommended in general, especially in areas with complex terrain where the slope flow formulation should be relied on to estimate the wind field.
R1 R2	User-specified (km)	R1 (0.1 to 5 km)  R2 (0.1 to 10 km)	Radius for Equal Weighting of Observations with Node-derived Values—This parameter controls the radius in which observations are weighted equally with node-derived values at the surface (R1) and aloft (R2). For complex terrain with calm conditions, these radii should be set very small (0.1). For less complex terrain, or normal-to-high wind conditions, setting these to 1/20 of the domain width (i.e., 5 km for a 100-km domain) is recommended.
IOBR	0 (No) or 1 (Yes)	0 or 1	Use O'Brien procedure to adjust vertical velocity—This adjustment is used during the final step in the wind field formulation in CALMET and sets the vertical wind velocities to zero at the top layer of the model domain. This generally has the effect of dampening the vertical velocities at all layers of the model. Using this adjustment is recommended unless there is a known reason that vertical velocities should not be zero in the top layer of the domain (e.g., land-sea breeze present).
TERRAD	User-specified (km)	1 to 20 km	Radius of influence of terrain features—This value determines the relative impact terrain will have on the wind field. Under calm conditions and complex terrain, this parameter should be large ( $1/5$ of the domain width). If the terrain is not expected to have an effect, or modeling the terrain effects is not desirable, this value can be set lower.

### A.2.3 Calpuff.inp

The CALPUFF input file (Calpuff.inp) is located in the “StaticData” directory for each site within DUSTRAN and is the template input file for CALPUFF. Its contents are merged with select-user input from the DUSTRAN interface for each simulation. Many of the parameters contained within Calpuff.inp control certain aspects of the plume concentration and deposition calculations, including the dispersion processes. These parameters are not available from the DUSTRAN interface and can only be edited via the static file.

The static Calpuff.inp file normally contains the most ideal parameter settings for a given site. However, there may be times when the user wants to examine the effects of modifying certain parameter settings.

Extreme caution should be used when changing any parameter in the static Calpuff.inp file, as it may cause unrealistic results. Each parameter in the Calpuff.inp is documented in detail in the CALPUFF user's guide (Scire et al. 2000a). The following discussion highlights those parameters that are generally considered the most important relative to affecting CALPUFF results. Generally, these parameters are from the section "INPUT GROUP: 2 – Technical Options," and control the plume dispersion calculations.

CALPUFF Parameter	Allowed Values	Recommended Value	Description
MGAUSS	0 1	1	Vertical distribution used in the near field—The initial plume distribution in the vertical can be uniform (0) or have a Gaussian distribution (1). A uniform distribution most likely is not representative of an actual release, so a Gaussian distribution is recommended.
MCTADJ	0 1 2 3	0	No terrain adjustment (0) is recommended. The other options are an Industrial Source Complex model type adjustment (1), a simple CALPUFF-type adjustment (2), or a partial plume path adjustment (3). The model default is the partial plume path adjustment.
MCTSG	0 1	0	Subgrid-scale complex terrain flag—this parameter should be turned off (0).
MSLUG	0 1	1	Near-field puffs modeled as elongated—The slug model, which is used to elongate puffs near the source, is recommended (1) and appears to provide more accurate results near the source than no elongation (0).
MTRANS, MTIP, MSHEAR, and MSPLIT	0 1	0	There are several puff manipulation parameters including plume rise (MTRANS), stack-tip downwash (MTIP), vertical wind shear above stack height (MSHEAR), and puff splitting (MSPLIT) that can be employed in CALPUFF.
MCHEM, MAQCHEM	0 1	0	In DUSTRAN, particle concentrations are assumed to decrease rapidly from dispersion and deposition processes. Chemical mechanism (MCHEM) and aqueous phase transformation (MAQCHEM) are considered to be negligible, and the flags should be set to zero (not used).
MWET, MDRY	0 1	1	Deposition from wet and/or dry processes can be treated. It is recommended that deposition be activated.
MDISP	1 2 3 4 5	2	Method used to compute dispersion coefficients—CALPUFF allows the user a variety of ways to calculate dispersion coefficients. The authors recommend calculating the dispersion coefficients from micrometeorological values (2). This method uses similarity theory values, such as the Monin-Obukhov length and friction velocity, to estimate the dispersion parameters. Other options include calculating the dispersion coefficients from measured values of turbulence (1), and using different forms of the Pasquill-Gifford dispersion curves (3 through 5). If the meteorological data are not sufficient to allow the use of similarity theory, then one of the Pasquill-Gifford formulations is recommended.
MPARTL	0 1	0	Partial plume penetration of elevated inversion—This parameter will allow the plume to partially penetrate a temperature inversion if the calculated stack plume rise is higher than the temperature inversion (1). This parameter is not recommended for DUSTRAN (0) because it results in additional plume dilution.

## A.2.4 Calgrid.inp

The CALGRID input file (Calgrid.inp) is located in the “StaticData” directory for each site within DUSTRAN and is the template input file for CALGRID. Its contents are merged with select-user input from the DUSTRAN interface for each simulation. Many of the parameters contained within Calgrid.inp control certain aspects of the plume concentration and deposition calculations, including the dispersion processes. These parameters are not available from the DUSTRAN interface and can only be edited via the static file.

The static Calgrid.inp file normally contains the most ideal parameter settings for a given site. However, there may be times when the user wants to examine the effects of modifying certain parameter settings. Extreme caution should be used when changing any parameter in the static Calgrid.inp file, as it may cause unrealistic results. Each parameter in the Calgrid.inp is documented in detail in the CALGRID user’s guide (Scire et al. 1989). One general run control parameter in CALGRID that is not set by DUSTRAN is the number of time steps per hour (NTSUBTS). The model recommended default for this parameter is 3. In high wind conditions, CALGRID may produce the following error: “array bounds exceeded.” This error can be eliminated by increasing the value of NTSUBTS. It has been found that values of 20 and 30 are successful in preventing this error under high-wind-speed conditions.

## A.3 DUSTRAN Initialization File (DUSTRAN.ini)

An initialization file is used to store the configuration settings for the DUSTRAN modeling system. The file, called DUSTRAN.ini, is read upon launching the DUSTRAN application. The file is formatted text and primarily holds a list of variables that store available sites and directory path information. The following is an example of the DUSTRAN.ini file followed by a description of the parameters found in the file.

### A.3.1 Example DUSTRAN.ini File

```
[DUSTRAN]
Site_List= Yakima
GIS_exe=C:\Program Files\ArcGIS\Bin\MapWindow.exe
Install_dir=C:\DUSTRAN
GIS_dir=C:\DUSTRAN\Yakima\GISData
First_Run=False
InterfaceMode=Multiple
SystemName=DUSTRAN
AgDispName=SPRAYTRAN
Read_Me=False
Current_site=Yakima
APR_dir=
[Yakima]
CharCategories=Soil,Vegetation
Soil=srztext
SoilSel=yes
Vegetation=owe14d
VegetationSel=yes
Srztext=C:\DUSTRAN\Yakima\TerData\srztext.csv
Owe14d=C:\DUSTRAN\Yakima\TerData\owe14d.csv
```

### A.3.2 DUSTRAN.ini File and Parameter Description

<b>Parameter Name</b>	<b>Parameter Description</b>
Site_List	Comma-separated string containing the names of the sites currently registered with the modeling system.
GIS_exe	Directory path of the MapWindow executable.
Install_dir	Directory path in which the DUSTRAN modeling system has been installed.
GIS_dir	Directory path of the folder in which the .mwprj file for the current site is stored.
First_Run	Flag used to determine if the modeling system has been executed since being installed. If this is the first startup of the modeling system, the read me file will be displayed automatically.
InterfaceMode	Flag used to determine if the modeling system will be able to access multiple sites or only a single site.
SystemName	Name of the modeling system. This is the name that will be displayed on the toolbar button and the main interface form.
AgDispName	Flag used to determine if the modeling system is to be used to make DUSTRAN or SPRAYTRAN modeling runs.
Read_Me	Flag used to determine if the read me file is displayed automatically upon the start of the modeling system.
Current_site	Name of the last site opened in the modeling system.
APR_dir	Directory path of the folder used to store Avenue script files. (Currently not used)
CharCategories	Data characteristic categories that have been entered for the simulation sites. By default, each site will have the Soil and Vegetation categories present. Other categories can be entered for a site using the appropriate utility in the DUSTRAN interface.
Soil	Comma-separated string containing the file names of the soil characteristic files entered for the site. File names are listed in order of priority.
SoilSel	Comma-separated string containing the flags denoting whether a soil characteristic file is to be used in the simulation for the site.
Vegetation	Comma-separated string containing the file names of the vegetation characteristic files entered for the site. File names are listed in order of priority.
VegetationSel	Comma-separated string containing the flags denoting whether a vegetation characteristic file is to be used in the simulation for the site.
Srztext	Full file path to the location of the soil characteristic file for the site.
Owe14d	Full file path to the location of the vegetation characteristic file for the site.



**Pacific Northwest**  
NATIONAL LABORATORY

*Proudly Operated by **Battelle** Since 1965*

902 Battelle Boulevard  
P.O. Box 999  
Richland, WA 99352  
1-888-375-PNNL (7665)

U.S. DEPARTMENT OF  
**ENERGY**

---

[www.pnnl.gov](http://www.pnnl.gov)